HHS Public Access

Author manuscript

Chem Rev. Author manuscript; available in PMC 2021 May 27.

Published in final edited form as:

Chem Rev. 2020 May 27; 120(10): 4355–4454. doi:10.1021/acs.chemrev.9b00815.

Mass Spectrometry-Based Protein Footprinting for High Order Structure Analysis: Fundamentals and Applications

Xiaoran Roger Liu[†,*], **Mengru Mira Zhang**[†], **Michael L. Gross**[*]

Department of Chemistry, Washington University in St. Louis, St. Louis, MO, USA, 63130

Abstract

Proteins adopt different higher order structures (HOS) to enable their unique biological functions. Understanding the complexities of protein higher order structures and dynamics requires integrated approaches, where mass spectrometry (MS) is now positioned to play a key role. One of those approaches is protein footprinting. Although the initial demonstration of footprinting was for the HOS determination of protein/nucleic acid bonding, the concept was later adapted to MS-based protein HOS analysis, through which different covalent labeling approaches "mark" the solvent accessible surface area (SASA) of proteins to reflect protein HOS. Hydrogen deuterium exchange (HDX), where deuterium in D_2O replaces hydrogen of the backbone amides, is the most common example of footprinting. Its advantage is the footprint reflects SASA and hydrogen bonding, whereas one method drawback is the labeling is reversible. Another is slow irreversible labeling of functional groups on amino-acid side chains by targeted reagents with high specificity, probing structural changes at selected sites. A third footprinting approach is by reactions with fast, irreversible labeling species that are highly reactive and footprint broadly several amino-acid chains on the time scale of sub-milliseconds. All these covalent labeling approaches combine to constitute a problem-solving toolbox that takes mass spectrometry as the measurement tool for HOS elucidation. As there has been a growing need for MS-based protein footprinting in both academia and industry owing to its high throughput capability, prompt availability, and high spatial resolution, we present a summary of the history, descriptions, principles, mechanisms, and applications of these covalent labeling approaches. Moreover, their applications are highlighted according to the biological questions they can answer. This review is intended as a tutorial for MS-based protein HOS elucidation and as a reference for investigators seeking a MS-based tool to address questions in protein science.

Graphical Abstract

[*]**Corresponding Author** Xiaoran Roger Liu xliu167@wustl.edu, Michael L. Gross mgross@wustl.edu.

[†]X. R. Liu and M. M. Zhang contributed equally.

The authors declare no competing financial interests.

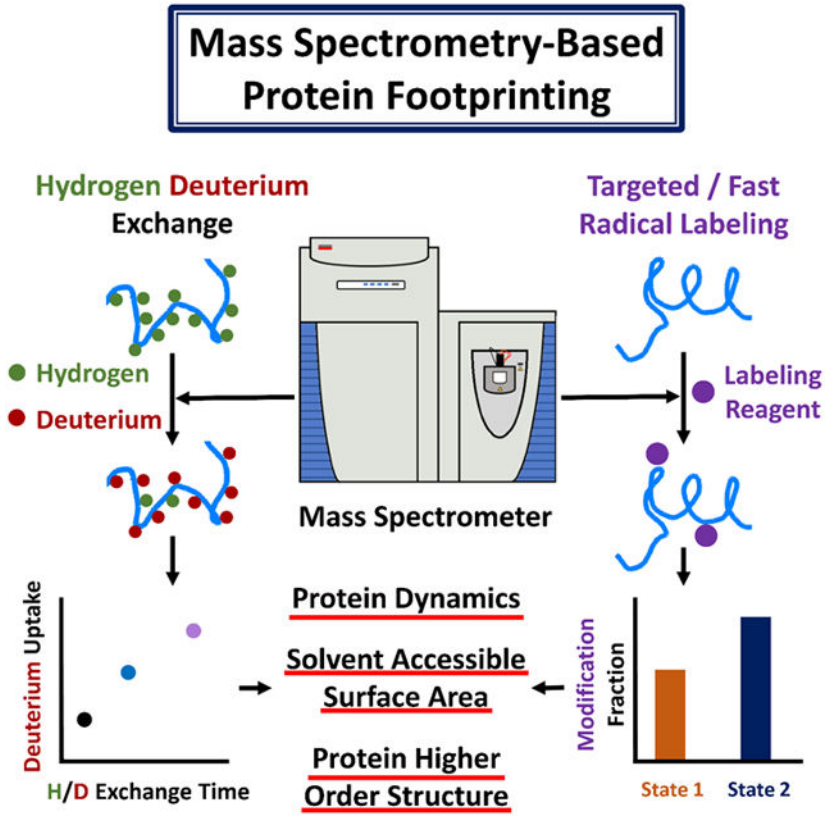

1. Introduction

Proteins carry out the programmed activities encoded by genes. Although constructed by the polymerization of only twenty distinct amino acids, their numerous biological functions require the high diversity arising from sequence variations and post-translational modifications. As living organisms evolve, proteins acquire specialized abilities that can be organized into different functional classes[1]: enzymes catalyze different intracellular and extracellular reactions; structural proteins provide support and maintain the structural rigidity of the cell; transport proteins facilitate trans-membrane flow of certain materials; regulatory proteins work as sensors and switches to regulate gene expression and protein activities; motor proteins facilitate macroscopic movements; and signaling proteins transduce messages to facilitate the communication of different cellular components. Despite high functionality and diversity, a protein's biological function and corresponding mechanisms of action are determined by their three-dimensional (3D) structure that is encoded in its primary sequence as demonstrated through the famous ribonuclease refolding experiment.[2] The exploration of protein structure-function relationship at the molecular level has developed into an independent subject named structural biology, for which characterization of protein high order structure (HOS) is the goal.

1.1. Protein Higher Order Structures

The understanding of protein HOS is a key topic in biology because the functional mechanisms of proteins are encoded in their 3D structures. Protein structure can be viewed as having four distinct orders (Figure 1).[1, 4] Primary structure refers to a linear combination of amino acids into a polymeric chain, which was first proposed in 1902.[5] Although originally heavily debated, its importance was settled after Sanger and coworkers[6-7] first sequenced insulin. The consensus is that protein **primary sequence** is determined by genetic information encoded in nucleic acids; that genetic information is translated into the order or sequence of the 20 common amino acids in a protein. The principal means of determining primary structure of proteins has become MS-based sequencing or proteomics analysis.

Upon forming linear polymeric chain, proteins fold to yield local structures including α-helices, β-sheets, β-turns, Ω-loop, etc. with the first two being most common. Such local ordering represents the **secondary structure** of proteins.

Tertiary structures of proteins are their overall 3D structures that result from the folding of the secondary structural components and other unstructured motifs. Although many proteins function individually, there are others that are not biologically active until they interact with other proteins or ligands, and these interactions give rise to **quaternary structure**. An overall 3D structure of a protein complex that contains multiple protein subunits comprises tertiary structure. The term “protein high order structure” often refers to the secondary, tertiary and quaternary structures of a protein. This is the subject of “structural proteomics”, and protein footprinting is a key component of the subject.

Besides the covalent peptide bonds that assemble amino acid building blocks into primary sequence, non-covalent interactions including hydrogen bonding,[8-9] charge-charge interactions (salt bridge),[10-11] hydrophobic interactions,[12-13] aromatic-aromatic interactions (π-π stacking),[14] cation-π interactions,[15] and Van der Waals forces[16] stabilize protein HOS. There is also a covalent contributor that stabilizes protein HOS, namely disulfide bonds.[17-18] All these forces work together to overcome the conformational entropy of protein folding (decrease in entropy from random coil to folded protein) and to stabilize a protein in its folded state.[19-21]

1.2. Biophysical Approaches for Characterizing Protein Higher Order Structure

In 1958, Sir John Kendrew[22] first reported the high-resolution structure of sperm whale myoglobin by X-ray crystallography, for which he shared the 1962 Nobel Prize in Chemistry with Max Perutz[23] for their studies of the structures of globular proteins. Their contributions are a milestone in the field of structural biology, opening the field to pursuits of protein HOS.

After decades of development, X-ray crystallography and nuclear magnetic resonance (NMR) became the “gold standard” for determining protein HOS. The interaction of an ordered protein crystal with X-ray radiation causes the incident beam to diffract. By measuring their diffraction angles and intensities, it is possible to obtain a 3D electron density map of a crystal, from which the protein 3D structure is constructed at atomic resolution.[25] X-ray crystallography provides atomic-level resolution of various protein sizes,

promoting it to be the most widely used spectroscopic approach in determining protein HOS to date. Its disadvantage is obvious as well; a crystalized protein sample is a must, and protein crystallization has always been challenging.[26-27] Moreover, X-ray crystallography provides a solid-state structure of proteins, posing concerns about whether proteins alter their structures upon crystallization as compared with their structures in solution or in vivo.[28-29]

NMR resolves protein structure by determining chemical shifts and structural restrains.[30-32] The development of multi-dimensional NMR (pioneered by Richard Ernst, who was awarded the 1991 Nobel Prize in Chemistry for his contributions to high resolution NMR) allowed protein structures to be determined with near-atomic resolution by employing structural restraints obtained from homo-nuclear and hetero-nuclear couplings.[33-34] Solution NMR for determining protein 3D structures was pioneered by Kurt Wüthrich,[35-36] who was later recognized with the 2002 Nobel Prize in Chemistry. Solution NMR determines the liquid-state protein structures, which should resemble native states in the absence of interactions with proteins, ligands, and salts. Although mainly applicable to small proteins, recent work demonstrates that in special cases, the approach can accommodate protein molecular weights up to 1 MDa.[37]

Another unique feature of solution NMR is its ability to measure protein dynamics in solution, which is not easily accessible at high resolution by other techniques.[38] For those proteins that are not readily soluble, membrane[39] and fibril[40] proteins for example, solid-state NMR contributes significantly.[41-42] The “dark side” of NMR-based protein structural elucidation is the sample amount, which is generally on the order of milligrams. The data acquisition and analysis are also time-consuming and labor intense. Some proteins cannot maintain their structure for long data-acquisitions and signal averaging.

X-ray crystallography and NMR have distinct advantages and drawbacks, but they complement each other.[43-44] As two of the most important pillars in protein HOS elucidation, the combination has contributed over 97 % of high resolution protein structures in Protein DataBank (PDB).[45]

Another emerging technique in high-resolution protein HOS elucidation is cryogenic electron microscopy (Cryo-EM), whose name is self-explanatory (EM at cryogenic temperature).[46-47] Upon snap-freezing the sample at cryogenic temperature, water molecules in the sample remain amorphous, thus minimizing distortion of the protein structure.[48] Damage by the electron beam to the sample is minimized by the cryogenic temperature.[49] The ability to average multiple randomly-aligned EM pictures accelerated the development of Cyro-EM.[50] These factors combined to enable structural determination of proteins with high-resolution. An early electron crystallographic study by Henderson and coworkers[51] demonstrates the capability of cryo-EM for determining membrane protein structure with near-atomic resolution (< 4 Å). Continued technical advances allow single-particle cryo-EM to characterize non-crystalline samples[52-53] and determine protein structures with atomic resolution (to 1.8 Å)[47, 54]. Cryo-EM is also capable of characterizing protein complexes[55-56] and membrane proteins[57]. As cryo-EM generally favors proteins with high molecular weights,[58] recent advances made possible the characterization of proteins with sizes < 100

kDa[54]. Its requirements of low sample amount, straightforward sample preparation, and high structural resolution make it the “rising star” in structural proteomics.[46-47] With X-ray crystallography and NMR, these three methods are the basis for determining protein structure with the highest resolution.

In addition to the high-resolution approaches, there are others including mass spectrometry (MS) that can characterize the proteins with lower resolution. Circular dichroism (CD)[59-60], Ultra-violet (UV) resonance Raman[61] and Fourier transform infrared spectroscopy (FT-IR)[62-63] can provide a general or overall characterization of protein secondary structure without providing atomic coordinates. UV at 280 nm is most commonly used in fast quantification of protein concentrations but contributes little to structure.[64] Fluorescence and Förster Resonance Energy Transfer (FRET) specialize in probing protein-protein interactions and protein conformational changes for regions of a protein.[65-67] There are other approaches that characterizes the protein from a global perspective, including dynamic light scattering[68-69] and its coupling with size exclusion chromatography[70] to focus on the hydrodynamic radius of proteins, negative staining electron microscopy[71-72] and atomic force microscopy, which examine the morphologies of proteins,[73] isothermal titration calorimetry, which discloses the thermodynamic properties of proteins,[74-75] surface plasmon resonance, which measures the kinetic properties of proteins upon interacting with others, [76-77] and many more. All these techniques combine to provide a biophysical toolbox for protein HOS elucidations; they are summarized schematically in Figure 2.

In addition to these biophysical approaches, computer modeling also plays a significant role in understanding protein HOS.[78-80] Early ideas of structural prediction were developed in the 1960s,[81-82] but it was not until 1974 that first structural prediction algorithm was actually developed.[83] These demonstrations were restricted to secondary structure predictions owing to limited computing power and mechanistic understanding of protein folding. Later on, with higher resolution, protein 3D structures could be resolved, template-based modeling (or homology modeling) became possible where available high-resolution structures serve as scaffolds when predicting HOS of unknown proteins.[79, 84-85] Free modeling (*ab initio*), on the other hand, predicts protein HOS from scratch,[86-87] and feasibility was first demonstrated in 2005.[88] Thanks to the development of computational approaches and bioinformatics, protein HOS prediction has developed into an independent research subject and is contributing more and more to the structural biology.[89-90]

1.3. Mass Spectrometry-Based Protein Structure Analysis

1.3.1. Historical Overview of Protein Mass Spectrometry

1.3.1.1. Ionization: To analyze a protein molecule in a mass spectrometer, ionization is the first step. The MS-based ionization methods were extensively developed in the 1960s to 1980s, key developments include chemical ionization,[91] electrospray ionization (ESI),[92] field desorption,[93] laser desorption,[94-95] Californium-252 plasma desorption,[96] secondary ion mass spectrometry,[97] fast atom bombardment,[98-99] matrix-assisted laser desorption ionization (MALDI)[100-101] and many more. Several of these techniques involved sample desorption; that is, MALDI and its precursor laser desorption, plasma desorption (PD), [102-103] and fast atom bombardment (FAB).[104] The latter was extensively used for over

nearly two decades (from 1980 to 2000) for studies of peptides and small proteins. Many of these approaches are vital steps in the long evolution of ionization methods, but none work as well as ESI or MALDI. PD preferentially ionizes the molecules on the surface of support, and its efficiency is low and affected by the homogeneity of the surface layer. FAB is a relatively hard ionization method with low ionization efficiency and a relatively high "chemical-noise" background and a propensity to fragment proteins upon desorption, limiting its use to small proteins.

Although FAB and PD convincingly demonstrated that proteins are amenable to MS analysis, the ionization scene improved significantly with two separate but complementary breakthroughs. In 1988, Tanaka and coworkers[105] improved MALDI by incorporating 30 nm cobalt particles to ionize successfully lysozyme and chymotrypsinogen and to obtain their masses while Hillenkamp and Karas[106] were simultaneously developing the MALDI protocol that is used today, moving systematically from peptides to proteins. Meanwhile, Fenn[107-108] developed ESI and successfully ionized various proteins, showing that multiple charging brings the *m/z* of the ions into a mass range of mass spectrometers where analysis was possible.

These two developments, particularly ESI, allow MS to become the enabling tool in the new field of proteomics and subsequently in protein HOS analysis, which further grow into one of the most important biophysical tools in structural biology nowadays. Their efforts led to awards of the 2002 Nobel Prize in Chemistry to Koichi Tanaka and John Fenn, shared with Kurt Wüthrich (in the field of protein NMR), for their contribution in "the development of methods for identification and structure analyses of biological macromolecules". Among these two methods, ESI (and later nano-ESI[109-110]) has become more extensively used in proteomics and HOS structure analysis owing to its capability to install multiple charges in the analyte, its ease in setup, and most importantly its compatibility with liquid chromatography (LC), uniting in a concatenated way separation and analysis.

1.3.1.2. Instrumentation: Besides development of ionization methods, development of MS instrumentation also greatly elevated the detection limit and resolving power, empowering MS to work with larger proteins and deliver protein structural information with high mass resolving power. The advances in mass analysis show an evolutionary thread that included quadrupole mass filters,[111] double-focusing sector mass spectrometers[112-113] that evolved into three[114] and four[115] (and even more[116]) sectors for tandem-MS (MS/MS). Time-of-flight (TOF) instruments profited developments of straight,[117] reflectron,[118] and orthogonal[119] TOF mass analyzers. Complementing and possibly exceeding them are quadrupole ion traps,[120] Fourier-transform ion cyclotron resonance (FTICR) instruments,[121] and more recently orbitrap mass analyzers[122-123]. Modern MS instruments are almost exclusively hybrid instruments that contain two or more different mass analyzers (represented by quadrupole-TOF[124] and quadrupole-orbitraps[125]), allowing rapid, accurate, and precise mass determination of both precursor and product ions, a long sought-after goal in MS.

1.3.1.3. Fragmentation: The use of MS in protein HOS analysis depends not only on the accurate measurement of mass to charge ratio (*m/z*) but also on fragmentation methods that

cleave the peptide backbone to provide sequence information that can locate sites of modification introduced as a protein footprint.[126] MS-based ion fragmentation required the introduction of collision induced dissociation (CID) and then tandem instruments, establishing the area of MS/MS.[126-128]

Owing to its rich history and high popularity at the time that peptides and proteins were first ionized, it is not surprising that CID was immediately developed as a method for to sequence peptides and to apply these ionization advances to unknowns.[129-131]

Over the years, different fragmentation methods including surface induced dissociation (SID),[132-133] electron transfer dissociation (ETD),[134] electron capture dissociation (ECD),[135] electron detachment dissociation (EDD),[136] ultraviolet photodissociation (UVPD),[137-138] infrared multiphoton dissociation (IRMPD)[139] were developed for studies of peptides and proteins. Their unique characteristics, advantages and limitations were reviewed in detail elsewhere.[126, 140]

1.3.2 Labeling-Based Protein Footprinting—MS contributes to peptide and protein determination at all four levels of structure.[141] The primary structure of a protein can be determined through MS/MS based *de novo* sequencing or partial sequencing and database searching.[142] Although protein sequencing was expedited mainly by sequencing its corresponding genome, there are still needs to sequence a protein when its corresponding genome is unknown or the sequence requires verification. MS/MS-based sequencing has become the nearly exclusive route to primary structure, replacing Edman degradation owing to its accuracy, certainty, and speed.[143] In addition to sequencing, the MS/MS approach also enables profiling of post translational modifications by following shifts in *m/z* that pinpoint the modification type.[144-148] Indeed, this capability is the basis for protein footprinting where finding the location of a chemical modification introduced purposely is the basis of determining protein footprints that are indicative of HOS.

Footprinting probes secondary and tertiary structure by mapping solvent-accessible surface area (SASA) through various covalent-labeling approaches including hydrogen/deuterium exchange (HDX). Quaternary structures are often characterized by differential footprinting that locates the contacting region by responding to changes in SASA for two different states (e.g., bound and unbound). Native spray MS, a gentle version of ESI that uses aqueous media, can maintain the non-covalent interactions in the gas phase to yield information on topology and stoichiometry but not on interface.[149-153] Ion mobility MS reports protein shape, a component of HOS, in the gas phase.[154-156] Chemical crosslinking, an in-solution approach, is now extensively used to provide some information on protein quaternary structures and to locate interfaces.[157-159] All these approaches are the analytical basis for MS-based structural proteomics and provide high order structure information, although not as detailed as that from NMR, X-ray crystallography, and Cryo-EM.

In this review, we have adopted a focus on the emerging role of MS-based protein HOS determination by different covalent labeling approaches, which is becoming one of the most informative MS-based structural proteomics tools. Covalent labeling with different reagents that react at solvent accessible surfaces of the protein leaves a “footprint”, serving as a

valuable probe for SASA that further reflects several aspects of protein HOS; thus, we term this workflow “protein footprinting”, a term that was initially proposed and demonstrated with HOS analysis of nucleic acids in 1978[160] and later adopted to analyze proteins[161]. We recommend wide adoption of “protein footprinting” as a key term to facilitate online literature searching. Early protein footprinting approaches were mostly cleavage-based, where protein SASA is revealed by limited proteolysis occurring at sites of the highest SASA[162-163] or by chemical cleavage by reactions with reactive radical species[164]. Because these approaches do not afford high spatial resolution, cleavage-based footprinting was soon replaced by labeling-based approaches.

Over the years two distinct categories of covalent labeling approaches have been developed and applied: reversible and irreversible. Reversible labeling is represented by HDX, which takes advantage of the hydrogen exchange between active hydrogens in the protein molecule and the hydrogen in the water solvent.[165] Upon dissolving protein in deuterium oxide (D_2O), solvent-accessible and weakly H-bonded hydrogen atoms in the protein will exchange with deuterium atoms in the solution, where mass differences between hydrogen (1.0078 Da) and deuterium (2.0136 Da) atoms serve as useful indicator for a mass spectrometer to report such exchanges. Although the exchanged H or D in backbone are covalently bonded in the protein, the exchange process is highly dynamic and reversible. Thus, for ex situ methods like MS, protein HDX needs to be performed under constrained conditions to prevent back exchange, which would quickly “erase” the footprint, and preserve the structural information from the labeling. Details about protein HDX will be covered in Section 2.

Another category is irreversible protein labeling. Labeling reagents generally react with solvent accessible amino acid side chains, leaving a chemical “mark” that can be identified in an upcoming analysis. Nature already does elegant protein labeling; that is, by post translational modifications (PTM).[144, 166-167] Mainly enzymatic processes introduce certain functional groups to incorporate proteins to modify them, often by adding or subtracting charges, so that new biological functions can be enabled by changing the conformation and the binding opportunities of a protein.[168]

Inspired by nature’s use of PTMs, investigators have developed different chemical reagents that irreversibly label solvent accessible surface areas of proteins. One sub-class of reagents are readily available today are targeted reagents that react with only certain amino acid residues with high specificity but low reaction rates.[169] An example is acetylation of lysine or esterification of aspartic acid. The second category includes fast labeling reagents, mostly radical species, which are highly reactive but have lower specificity.[170] The advantage of irreversible labeling is that sample handling and post labeling are simpler and can be slower than that of HDX, allowing to take full advantage of all the separation advances made in proteomics. The different labeling timescales allow irreversible labeling to address several biological questions that are not amenable to HDX.

1.3.3 Bottom-Up and Top-Down—With MS/MS, locating labels and determining the protein footprint that reflects HOS can be performed with either bottom-up or top-down approaches.[171-172] Bottom-up protein analysis requires proteolytic digestion of the proteins

prior to MS. Most approaches involving MS utilize a bottom-up approach as it has higher throughput, better compatibility with LC systems, greater sensitivity, and requires less advanced fragmentation technologies than top-down approaches. The key challenge for structural proteomics is to obtain high sequence coverage of the targeted protein, which is not a requirement for proteomics strategies that target proteins can be identified by using partial sequences determined for peptides that are “proxies” for the protein. Furthermore, PTMs are sometimes not accurately located owing to biased digestion efficiencies, as protease digestion efficiency is lower when its cleavage site is post translationally modified, as it may be in a footprint.[173]

Top-down MS has been extensively developed in the past 20 years thanks to advances in MS fragmentation methods.[172, 174] As the intact protein is submitted directly to the spectrometer, extensive fragmentation of the intact protein molecule must be induced to yield high spatial resolution. The major advantages of top-down is the capability of recovering different protein isoforms that are combinations of post-translational modifications and sequence variants. High fragmentation coverage is needed for footprinting, but today this is achieved mainly for small proteins. The approach is especially attractive when enzymatic cleavage sites are limited.[175] All these advantages make top-down a promising choice in proteomics.[176] Its drawbacks are primarily low throughput, limited sensitivity, and a lack of residue-level sequence coverage.[177] Reduced propensity for fragmentation in large proteins is due to the many modes or degrees of freedom for delocalizing energy in a big molecule, making it challenging to investigate proteins with high molecular weights.[178]

In the field of protein HOS elucidation by MS, there are fewer examples that couple protein footprinting with top-down MS,[179-181] than with bottom-up. The primary reason is that sequence coverage at residue-level is critical for high spatial resolution, for which top-down currently fails to deliver. Combined developments of instrumentation, fragmentation methods, and sample handling strategies may afford a brighter future in protein footprinting.

There has been a growing need for MS-based protein footprinting in both academia and industry owing to its high throughput, prompt availability, and high spatial resolution. In the coming sections, we will cover the history, principles, designs, and mechanisms of covalent labeling-based protein footprinting approaches. We will largely confine our attention to reports over the last ten years, emphasizing those that report advances in methodology, rather than routine adoptions, to highlight the biological questions that can be addressed. Our goal is to provide a review that will serve as both tutorial for MS-based protein HOS analysis and a reference for investigators seeking a MS-based tool to address their question in protein science.

2. “Unbiased” Protein Footprinting – Hydrogen Deuterium Exchange

2.1. An Historical Perspective

HDX is one of the most important and used covalent labeling protein footprinting approaches to date despite its reversible nature. Although HDX is usually distinguished from other irreversible footprinting approach by classifying the latter as covalent labeling or

covalent footprinting, HDX labeling also involves covalent bonds. The distinction is not covalent labeling as the exchange but rather that the exchange of N-H for N-D in HDX is a reversible process. We argue that the distinction between HDX and other footprinting is "reversible vs. irreversible" not covalent vs. an implied non-covalent bonding.

Protein HDX was first demonstrated in 1954 by Kaj Linderstrøm-Lang,[182] who was later recognized as "father of HDX"[183]. In the very first HDX experiment, Hvidt and Linderstrøm-Lang[182] incubated dried pork insulin into D_2O to allow exchange, followed by snap-freezing and lyophilization. The protein powder was then suspended in H_2O. The deuterium content was measured by the density of the newly obtained protein-H_2O solution in a gradient tube. Later, they studied the pH and temperature dependence of H/D exchange rates,[184-185] made a connection between H/D exchange rate and the dynamics of protein molecules,[186-187] and formulated equations that underpin the basis for protein HDX[185, 187-188]. Efforts by Linderstrøm-Lang and coworkers[183, 189] are part of the early history of protein HDX, but in a display of scientific insight, these investigators demonstrated an approach of tremendous potential, opening a new era of covalent labeling-based protein HOS elucidation.

To enhance spatial resolution, HDX was later coupled with other characterization approaches (e.g., UV spectroscopy,[190] IR spectroscopy,[191-192] neutron diffraction[193]), among which NMR was the most successful in early applications. The NMR applications began with a series of studies in late 1950s when Saunders and Wishnia[194-196] first demonstrated that the exchange of proteins and D_2O solvent can be measured by NMR with high spatial resolving power to give residue-level information at least for small proteins.[197] In 1976, these efforts were extended to the determination of individual amide proton exchange rates, as demonstrated by Wüthrich and coworkers.[30] Later, Wagner and Wüthrich[198] coupled two dimensional correlation spectroscopy (2D-COSY) NMR with H/D exchange rate measurements whereby exchange rates for every amino protons in a protein can be obtained in a single experiment. Recent development of fast 2D ^{1}H-^{15}N correlation NMR demonstrates measurement of fast HDX for amide bonds within a few seconds of acquisition time.[199] Along with these developments, NMR measurements also contributed significantly to the mechanistic understanding of protein HDX phenomena.[200-201]

The use of HDX-NMR in studying protein-protein interactions was first demonstrated by Roder and coworkers[202] in 1990. Although powerful and promising, HDX-based protein-protein interaction studies are not often made in NMR. Early protein NMR approaches suffered from limited spatial resolution, making it even more challenging to characterize large proteins by NMR.

As a complement to NMR, MS began to "pick up the baton" to extend HDX further to larger proteins at lower and lower concentrations. The demonstration of HDX followed by ESI MS was first by Katta, Chait, and Carr[203] in 1991 who showed that the mass spectrum of a small protein (ubiquitin) changed significantly when it was sprayed in deuterated solvent. As the mass of the deuteron (2.014) differs measurably from that of hydrogen (1.008), MS monitors HDX by tracking the centroid mass of the isotopic envelop of a specific protein or peptide.

As exchange-in continues, the centroid shifts to higher *m/z* and reports the average number of Hs that have exchanged with Ds.

The first example of off-line HDX and proteolytic digestion to reveal the regions of protein that exchanges was by Zhang and Smith.[204] They termed their approach as “the protein fragmentation method”, and they used fast atom bombardment (FAB) as their ionization method. This approach is the precedent for what is done today (except FAB is replaced by ESI).

2.2. Mechanism of Exchange

To provide a basic understanding of mechanism of HDX of the amide backbone, we will briefly discuss some fundamentals.[165, 200, 205] Among all hydrogens in a protein molecule, those that are part of O-H, S-H and N-H bonds exchange most rapidly with solvent water (D_2O) molecules. In a commonly executed “exchange-in” scenario, the protein is first solubilized in H_2O. Upon diluting with D_2O, labile Hs on the protein exchange with the surrounding solvent Ds, leading to an increase in mass that can be measured by a mass spectrometer. There is also an “exchange-out” mode where the protein is first incubated in D_2O, followed by addition of H_2O to cause a D-to-H exchange. Exchange-out is not as often used as “exchange-in,” and it will not be discussed further. Although HDX happens for both protein backbones and amino acid sidechains containing exchangeable Hs (e.g., NH_2, OH, SH), most experiments focus on backbone hydrogens. The hydrogens on the sidechains are weakly involved in hydrogen bonding, making their exchange fast and not easily followed with most experimental setups. These exchanges do not confuse the experimental outcome because, as fast exchangers, they return to an -XH state during workup and proteolysis that uses H_2O, as expected in an ex situ measurement.

Because the HDX of protein side chains is fast and not readily measurable, the total exchange is nearly only that of the amide N-H in peptide bonds, making HDX an “unbiased” labeling method because every amino acid residue (except Pro) has an N-H hydrogen that can be exchanged. The rate of exchange is fastest for amides that are solvent exposed and not involved in hydrogen bonding, for example, unstructured regions in a protein. HDX rates for these N-H hydrogens are represented by k_{ch}, which is a function of pD, the temperature of the solvent, and the nature of the side chains on neighboring amino acid residues. Previous studies reveal that HDX is both acid and base-catalyzed, and that k_{ch} minimizes at a pH around 2.5,[206-207] the pH that is chosen for quenching the reaction in a step that is essential for any ex situ measurement.

HDX for HOS determination is successful because the rate of HDX for backbone N-H hydrogen atoms is determined by local conformation. Protein local orders are stabilized by intramolecular N-H···O=C hydrogen bonding.[208] The breathing motion of these hydrogen bonds will alter the conformational states of the targeted hydrogens that comprise the N-H bonds from closed to open states with a rate constant of k_{op}. As the protein is highly dynamic, the open N-H bonds can also close with a rate constant of k_{cl}. A local view of HDX process for a backbone N-H, thus, can be represented by Eq. 1.

$$\text{N-H}_{\text{closed}} \underset{k_{cl}}{\overset{k_{op}}{\rightleftarrows}} \text{N-H}_{\text{open}} \xrightarrow{D_2O,\ k_{ch}} \text{N-D}_{\text{open}} \underset{k_{op}}{\overset{k_{cl}}{\rightleftarrows}} \text{N-D}_{\text{closed}} \quad (1)$$

In principle, every N-H possesses a unique combination of k_{op}, k_{ch} and k_{cl}. The observed rate constant for HDX, k_{HDX}, is determined mainly by two factors: the solvent accessibility and the local hydrogen bonding in the region of the amide bond. For regions that are highly flexible, the effect of these two factors is minimized so that $k_{HDX} = k_{ch}$. For regions that are structured, the HDX occurs under two limiting regimes, EX1 and EX2.[205, 209] EX1 is characterized by $k_{ch} >> k_{cl}$, for which $k_{HDX} = k_{op}$. In EX2, $k_{cl} >> k_{ch}$, so that $k_{HDX} = K_{op}k_{ch}$, in which $K_{op} = k_{op}/k_{cl}$. Practically, EX2 is more prevalent than EX1.[187, 201] There are also intermediate exchange regimes that are combinations of EX1 and EX2.[209]

2.3. Experimental Approach

Most HDX measurements compare two states of a protein (e.g., bound vs. unbound, wildtype vs. mutant); thus, this approach in footprinting is termed “differential”. In a differential experiment, HDX for a ligand-unbound protein is compared to the ligand-bound state, and the effects of local hydrogen bonding and back exchange cancel, leaving the differences in HDX to represent changes in solvent accessibilities and H-bonding for the two different states as the only factors determining the relative differences in HDX.[210]

Experimentally, HDX is most commonly executed in a “bottom-up” fashion,[207, 211] which originated from early experiments of tritium exchange.[212-213] Bottom-up HDX was first introduced by Zhang and Smith[204] in 1993. In the peptide mapping mode, the protein or peptide (in H_2O) is denatured and, following quenching at pH ~ 2.5 (in H_2O), is digested and made ready for LC-MS/MS analysis for peptide identification and m/z determination to establish the average number of D taken up in the exchange (Figure 3). One goal is to optimize the quenching condition to permit high sequence coverage to make available a peptide list comprised of peptide sequences, precursor masses, and their elution times under optimized quenching conditions. The quenching solution is usually composed of denaturant and an agent for disulfide bond reduction (if there are any) and is at pH = 2.5, where the rates of back-exchange (back exchange of deuterium in the protein to hydrogen) are minimized. The quenching conditions, once optimized, are then used in further HDX experiments.

In the actual HDX experiment, the protein of interest is initially dissolved in H_2O, and the solution diluted with D_2O and incubated for several different times to allow measurement of the HDX kinetics (Figure 4). Upon exchanging, solvent-accessible amide hydrogens become replaced by D. The exchange is then quenched by decreasing the solution pH to 2.5. Quenching is followed by fast protease digestion and then MS analysis. The digestion is usually carried out online by flowing the protein solution through a pepsin column. The solvents used in HPLC are at acidic pH. Good experimental design shortens the time prior to when the deuterated peptides are analyzed by MS to minimize back-exchange. The obtained data are analyzed by fitting the isotopic distribution for each peptide, from which a mass centroid is calculated, and the deuterium uptake is determined by the difference in peak centroids between the exchanged protein (or the peptides) and the unexchanged or control.

Measurement of HDX at the residue level with MS is challenging. Low-energy collisional activation found on orbitraps, ion traps, or Q-Tofs cannot be used because that activation induces deuterium scrambling,[214-215] erasing all the forward exchange that was scrupulous introduced. Novel fragmentation methods that minimize scrambling include ECD[135, 216] and ETD,[217] making possible, in some cases, measurement of residue-level deuterium uptake or of HDX in a "top-down" fashion[218-219].

2.4. Recent Advances and Applications

In this section, we will review several technical advances that increased the capabilities of HDX. One important goal is to increase its spatial resolution, ultimately to a single amino acid. Several approaches were developed to achieve a single-residue resolution, including vigorous proteolytic fragmentations to give overlapping peptides,[220-221] high-pressure on-line digestion to improve digestion efficiency,[222-223] incorporation of ETD and bottom-up HDX for enhanced spatial resolution,[224] and computation methods that facilitate processing the data from aforementioned methods[220, 225-226]. Novel digestion protocols give shorter peptides and more overlapping peptides. Single-residue HDX information can be obtained by considering the absolute deuterium uptake levels of two overlapping peptides that differ by a single amino acid residue.[220-223] This spatial resolution should also be achievable through fragmentation to give smaller peptides formed by ETD or ECD fragmentation that minimizes deuterium scrambling. Quantification of the resulting fragments will give data that resemble the deuterium uptakes for those fragments in solution.[224] Novel computation methods either facilitate the automatic processing of the overlapping peptides[225] or utilize novel algorithms to deconvolute the residue-level HDX behavior through a peptide-level HDX curve (by either close examination of isotopic envelope shape information[220] or a Bayesian approach for deconvolution[226]).

To shorten further the exchange time, investigators developed theta capillary spray[227] and gas-phase HDX[228-230] that allow exchange times as short as 20 μs to be followed. With further optimization, it should be possible to track deuterium uptake on the amino acid residue sidechains, which was not possible in conventional HDX (even with rapid mixing or stopped-flow) because the back-exchange of the active protons is rapid. It also allows HDX to capture fast dynamic processes that was not possible before.

To expand the capabilities of HDX to binding affinities, investigators developed titration-based HDX workflows including stability of unpurified proteins from rates of H/D exchange (SUPREX)[231] and protein–ligand interactions by mass spectrometry, titration, and H/D exchange (PLIMSTEX).[232] These approaches characterize ligand binding sites, binding orders (if there are multiple ligands that bind the protein of interest), and, most importantly, site-specific binding affinities. Both of these workflows were demonstrated at the peptide-levels,[233] showing that it is possible to carry out single-residue level with the combination of the efforts mentioned above (ETD or multiple proteolytic digestions).

To expand the ability of HDX to characterize membrane proteins, effective removal of detergent[234] and lipid,[235] optimization of HDX conditions for enhanced transmembrane domain sequence coverage,[236] and post-HDX deglycosylation[237] were developed. Post exchange detergent and lipid removal are based on either chromatographic separation and

organic solvent extraction[234] or on the interaction between zirconium(IV) oxide and phospholipids[235]. These advances make possible the characterization of HDX for membrane proteins without incurring extensive back-exchange. Post-HDX deglycosylation removes highly heterogenous glycans without compromising the deuterium labeling on the peptides, allowing an investigator to obtain a well-resolved, high coverage HDX analysis.[237] All these advances broaden the horizon of HDX.

Other than the experimental advances, we witnessed a burst of HDX data processing software in the past decade, some of the examples include HDExaminer,[238] DynamX (formerly HX-Express),[239] HDX Workbench,[240] AUTOHD,[241] Mass Analyzer, [242-243] HD Desktop,[244] HeXicon,[245] ExMS,[246] HDX-Analyzer,[247] HDX Finder,[248] and Mass Spec Studio[249]. There are also new HDX data visualization software include MSTools,[250] MEMHDX,[251] Deuteros,[252] and HDX-Viewer[253]. The development of these software tools contributes greatly to the broad application of HDX.

Undoubtedly, HDS-MS is now become relatively routine and is currently used in many applications in biochemistry and biophysics. The large number of these applications makes it challenging to cover them in this review. Instead, we will stick with our theme of protein footprinting and emphasize HDX as a footprinting method to provide HOS information. We will not review applications of HDX-MS because there are many specialized and comprehensive[165, 254-255] reviews that cover most applications including mapping epitopes and characterizing biotherapeutics,[256-259] monitoring protein folding dynamics,[260-261] locating protein binding sites,[210, 262-263] examining conformations of individual proteins or of large complexes,[264-266] probing allosteric effects,[267] monitoring protein-membrane interactions,[268] and developing methods to minimize deuterium scrambling during MS fragmentations[269]. A collaborative effort from 2018 summarizes the key aspects of performing HDX experiments, providing valuable recommendations on how to carry out an effective HDX study properly.[211] Lastly, for more details on HDX theory, the reader should consult early reviews by Englander et al.[200] and Smith et al.[207].

2.5. Conclusion

The union of HDX and MS launched MS into the field of protein HOS determination. Because HDX causes a minimal perturbation on protein structure, has a relatively simple setup and analysis, aided by a number of data processing packages, and requires no design or synthesis of reagents, the adoption by the biochemistry community has been rapid. HDX covalently “labels” all protein solvent-accessible backbone amide hydrogens (only amino acid without an exchangeable H is Pro). Unlike targeted- and the fast-labeling reagents whose labeling efficiencies are hugely variable and determined by residue-specific reactivities, HDX occurs across the whole protein, and its labeling efficiencies depend on local structure (solvent accessibility and hydrogen bonding). Thus, HDX footprints proteins in a relatively “unbiased” way. The advantages of HDX, as envisioned by early pioneers, have been realized, and new applications are being implemented, making HDX an important technology for HOS nearly three decades after its introduction.

3. Targeted-Labeling Reagents

The 20 amino acids have different kinds of functional groups on their side chains; most have functional groups (COOH, SH, NH_2, OH, $CONH_2$, aromatic ring) that can be labeled with chemical reagents that react specifically, usually with one or two amino acids. These modifying reactions can be used for footprinting provided the reactivity of these groups depends on SASA of the protein and the modifications in the early stages do not affect the protein structure, minimizing the biased report during the footprinting itself. Reagents react directly and usually slowly with specific solvent-accessible side chains in contrast to free radicals, which react rapidly. The product contains a characteristic mass tag that can be detected by MS analysis. Although numerous reagents have been developed to react with the amino acid side chains, a qualified protein footprinting reagent needs to label the protein under physiological conditions with reasonable efficiency and speed. The size and hydrophilicity of the reagent should be close to that of water to ensure its reactivity is an indicator of SASA. Most of these reagents developed to date are highly specific, targeting one or two side chains or functional groups although some can react with more than two.

In this section, we will review commonly used targeted protein footprinting reagents, starting with their history in protein labeling and then discussing their chemistry and the products resulting from labeling. Many of the protein labeling reactions were discovered and implemented some time ago but not as footprinting reagents. That had to await the development of MS methods for sensitive, specific, and effective analysis to locate the modified sites. Following the early work, MALDI was chosen for analysis, but more recently the combination of ESI and LC-MS/MS has become the mainstay analytical tool. Our purpose in this section is to organize the reagents and discuss original development. We will not cover all the applications of these reagents.[169, 270-274]

Because there are many reagents, this section is organized according to the target residues and the types of functional groups they contain. Cysteine is highly reactive owing to its highly nucleophilic thiol group. Tryptophan and tyrosine contain hydrophobic/aromatic side chains that are electron rich. Aspartic and glutamic acids are acidic residues for which many derivatization classic reactions are available. Arginine, histidine and lysine contain basic residues, and they are more difficult to footprint. Although some of the residues are preferentially charged under physiological conditions, their charge state depends on pH. All schemes in this section depict the charge neutral forms for simplicity.

Chemical crosslinkers, although bifunctional derivatives of targeted labeling reagents, are designed to afford information on protein/protein interfaces. They can be viewed as bifunctional footprinters, and, thus, we included them in a general discussion later in this section. Both footprinting and cross-linking have much in common and viewing them together provides an opportunity to compare and contrast.

A unique function for targeted protein labeling is covalent inhibition, where a bulky labeling reagent may inhibit a biochemical reaction. The covalent attachment of the labeling reagent may occupy a binding pocket and block a functional site, inhibiting measurably protein function. Although operationally similar to footprinting, this form of protein labeling will

not be covered here because this field was reviewed.[275-277] The covalent attachment of functional probes was also developed extensively during the past decade, as reviewed in a perspective by Tamura and Hamachi.[278]

3.1. Cysteine

Cysteine (Cys) is one of the most reactive amino acids owing to the high intrinsic reactivity of the nucleophilic thiol side chain. Cys fulfills a variety of protein biological functions including forming disulfide bonds to stabilize structure, binding metal ions, transferring hydrogen and oxygen atoms, electrons, and hydrides, catalyzing redox processes, and mediating hydrolysis.[279] Modifying Cys in a native protein, therefore, should be an informative footprinting goal as specific Cys groups throughout a protein are often important in biochemical processes.[280]

Cys labeling can be achieved through a large number of reagents, and many of them were developed as catalytic functional inhibitors (e.g., organomercurial compounds)[281] or affinity tags (e.g., functionalized biotin tag)[282]. The use of these reagents is not the primary goal of this review and, therefore, the reagents will not be discussed further. Interested readers should refer to a recent book by Lundblad.[271]

The thiol group in the Cys side chain becomes an even stronger nucleophile when it deprotonates to a sulfide anion. Therefore, most of the Cys labeling reactions take advantage of the nucleophilicity of -SH, or better, $-S^-$.

The first class of Cys-labeling reagents, α-haloketo compounds, represented by iodoacetamide (IAM),[283-284] label Cys by S_N2 nucleophilic substitution (Scheme 1, top). Other popular derivatizing reagents include iodoacetic acid,[285] iodoacetanilide[286] and iodoacetate[287]. Other than labeling Cys, IAM and its derivatives also modify Met, His, Lys, Tyr and Glu but with lower reactivity.[288-291] The reactivity of IAM not only depends on the solvent accessibilities of targeted residues but also on the local environments, a property that relates to most targeted labeling reagents.[292] The chloro- and bromo α-haloketo compounds are less reactive towards thiol groups (the leaving-group propensities for the halides are I > Br > Cl[293-294]) and, thus, chloro and bromo α-haloketo compounds are not commonly used in protein HOS analysis. These derivatizing agents, however, are more useful in affinity labeling as the reaction is facilitated because the reagent binds nearby, placing even an modestly reactive group in an appropriate position for reaction.[295]

Maleimide derivatives are more suitable footprinters by the introduction of bromomaleimides, which label Cys residues reversibly (Scheme 2).[296-298] In comparison to NEM, labeling by bromomaleimides involves nucleophilic substitution that preserves the double bond in the maleimide ring. Preservation of double bond allows a reaction with a second Cys residue (through Michael addition), which converts a bromomaleimide into a chemical cross-linker.[297-298] The reaction product, thiomaleimide, can be hydrolyzed to dehydroalanine or converted back to Cys by chemical reduction. Such versatility enables novel workflows in labeling or footprinting free Cys residues.

The other class of well-established Cys labeling reagents is *N*-alkylmaleimide that labels Cys through Michael addition (Scheme 1, bottom); a common example is *N*-ethylmaleimide (NEM).[299-301] Although NEM labels Cys residues with considerably higher reactivity and specificity than does IAM,[292] other nucleophiles including His and Lys can also be modified by NEM.[302-303] In the LC-MS analysis, however, the *N*-alkylmaleimide is prone to hydrolysis, forming an isomeric mixture of maleamic acid adducts.[291] The molar absorptivity of NEM is 620 $M^{-1}cm^{-1}$ at 302 nm,[299] enabling UV-Vis spectroscopy for analysis in NEM kinetic studies. The alkyl chain length in *N*-alkylmaleimide should be considered when the analysis is by MALDI as that group can be responsible a non-uniform effect on signal intensity.[304]

IAM and NEM are widely used not only in MS-based footprinting that takes advantage of their reactivity with Cys but also for protecting free Cys residues, a standard practice in almost all MS-based proteomics experiments. In a pioneering study that used IAM as a Cys footprinting reagent, Wu and coworkers[305] investigated the active sites of human type II inosine 5'-monophosphate dehydrogenase (IMPDH). 6-Chloropurine riboside 5'-monophosphate (6-Cl-IMP) is a structural analog of the IMPDH substrate and was used as an IMPDH inhibitor by modifying one of eight Cys residues in IMPDH. The results of IAM footprinting of IMPDH in its ligand-free and 6-Cl-IMP-bound states demonstrate that seven Cys residues show comparable IAM labeling, whereas Cys 331 was not labeled by IAM but by 6-Cl-IMP in the bound state, strongly suggesting that Cys 331 is critical in facilitating the enzymatic activity of IMPDH. IAM derivatives were also modified to serve as fluorescent probes for monitoring protein conformational changes in vivo with relatively good spatial resolution.[306-308] Chumsae et al.[309] incorporated Cys fluorescence labeling with MS-based peptide footprinting to study the unpaired Cys residues in human immunoglobulin G subclass 1 antibody; details will be discussed in section 4.5.

NEM labeling coupled with MS-based protein footprinting was pioneered by Reich and coworkers[310], who applied NEM to footprint the critical Cys residue in DNA methyltransferase. In the ligand-free state, Cys 25, 116 and 223 were modified by NEM, but upon incubation with DNA and sinefungin (a structural analog of cofactor *S*-adenosylmethionine), Cys 223 became essentially unmodified, demonstrating its critical role in preserving the enzymatic function of DNA methyltransferase. Notably, all the site-specific Cys labeling products were characterized by tandem MS with a magnet sector instrument, a demanding task at the time and now more readily accomplished with modern Q-ToF and orbitrap instruments.

Thiol groups in Cys residues can also be nitrosylated by active nitrogen compounds such as nitric oxide and tetranitromethane.[311-312] Reagents for Cys include cyanogen bromide[313] selenium reagents,[314] *N*-(phenylseleno) phthalimide,[315] 5,5'-dithiobis-(2-nitrobenzoic acid) (Ellman's reagent or DTNB) and its derivatives,[316] 2,2-dipyridyl disulfide and 4,4′-dipyridyl disulfide,[317] vinyl pyridine[318-319] and acrylamide.[320] These reagents will not be discussed further as their utility in MS-based Cys footprinting remains to be established.

The oxidized form of cysteine, cystine, exists with a disulfide bond. Cystine footprinting, interestingly, originates from the analysis of wool and its oxidation.[321-322] To label disulfide

bonds, cystine residues need to be reduced to cysteine. Many reducing reagents are available including cyanide,[323] phosphorothioate,[324] (2*S*)-2-amino-1,4-dimercaptobutane,[325] *bis*-(2-mercaptoethyl)sulfone and *N,N′*-dimethyl-*N,N′*-bis(mercaptoacetyl)hydrazine,[326] sodium borohydride,[327] and 2,3-dimercaptopropanol[328] that can deliver effective disulfide reduction. Three reagents, however, are commonly used to reduce disulfide bonds in proteins. Dithiothreitol (DTT), originally synthesized by Evans et al.[329] in 1949, is able to reduce disulfide bonds as was first demonstrated by Cleland[330] in 1964 (DTT is also known as Cleland's reagent). DTT is prone to oxidation when using in air, with a half-life of 10 h in neutral solution (pH = 7.5, 20 °C), decreasing to 1.4 h when the pH = 8.5,[331] making it critical to prepare a fresh DTT reagent solution. The oxidized form of DTT has an absorbance maximum at 283 nm, which can be utilized to determine the extent of disulfide bond reduction.[332]

Unlike DTT that only functions under near-neutral pH, *tris*(2-carboxyethyl)phosphine (TCEP)[333] reduces disulfide bonds rapidly under acidic conditions. TCEP is reasonably stable under acidic conditions, but its oxidation is significant at pHs greater than 7.[334] All these features led to broad acceptance and application of TCEP in HDX workflows.

The last reagent is 2-mercaptoethanol (β-mercaptoethanol, BME), which is stable and functions under alkaline pH.[335] With the development of DTT and TCEP, BME is less used in disulfide bond reduction, but it is also used in protein structural analysis.[271, 336] This and the other reducing reagents are usually used under denaturing conditions for better disulfide reduction, which is not appropriate for footprinting.

In addition to conventional reducing reagents, a novel approach is to utilize electrochemistry to reduce disulfide bonds.[337] This development may be particularly useful in HDX experiments, as it enables fast and effective on-line disulfide reduction.[338] The reduction converts cystine residues to cysteine residues that are ready for labeling or "capping" to avoid disulfide bond re-formation. MS-based disulfide mapping (cystine labeling) will be discussed in section 4.5.

3.2. Tryptophan

Tryptophan (Trp) is an electron-rich amino acid with a heterocyclic aromatic side chain; Trp is the lowest abundance amino acid in proteins.[339] As Trp is hydrophobic and rarely found on protein surfaces, its footprinting is not common. In the case of protein-protein and protein-membrane interactions, however, Trp contributes significantly,[340-343] motivating application of footprinting.

Trp and Tyr are responsible for most of the characteristic protein UV absorbance at 280 nm.[64] Trp is also responsible for most intrinsic protein fluorescence of proteins.[344-345] These unique features allow Trp residues to be photo-activated under UV irradiation.[346-351] In brief, Trp under irradiation by UV light results in a tryptophan radical and a hydrated electron.[346-347, 349] The formation of tryptophan radical-mediated reactive oxidative species leads to hydrogen peroxide as a product,[348, 352] which further oxidizes nearby residues[351]. A recent book by Lundblad[271] provides a detailed overview of Trp photoactivation.

The indole nitrogen atom in the side chain of Trp has a pK_a greater than 15,[271] making it difficult to activate for chemical modification. In limited demonstrations, Previero and Cavadore[353] developed formylation of Trp with hydrochloric acid and acetic acid, leading to *N*-formyl tryptophan as product. In another example, Linder and coworkers[354] employed 1,1,3,3-tetramethoxypropane to react with Trp residues under acidic conditions, producing a substituted acrolein with a free aldehyde. This chemistry was further developed by bringing together another immobilized hydrazide that reacts with the free aldehyde to afford chemical cross-linking.[355]

A better Trp labeling strategy is to target the C-H bond adjacent to the indole nitrogen, which is done by the three reagents as shown in the Scheme 3. 2-Hydroxy-5-nitrobenzyl-bromide (HNB) was first demonstrated to be an effective Trp labeling reagent by Koshland and coworkers[356-358]; HNB, therefore, is also known as Koshland's reagent (Scheme 3, top). Over the intervening years, many HNB derivatives were developed to label Trp, including dimethyl(2-hydroxy-5-nitrobenzyl)sulfonium bromide (HNSB),[359] 2-methoxy-5-nitrobenzyl bromide,[360] and 2-acetoxy-5-nitrobenzyl chloride.[361] The applicability of HNB in protein HOS analysis was first demonstrated by Strohalm et al.[362-363], where the investigators followed effective HNB labeling of Trp residues for the model proteins lysozyme, cytochrome *c,* and myoglobin by using MALDI-MS. Only solvent-accessible Trp residues were labeled under physiological conditions whereas all Trp residues did react in a denaturing environment, suggesting HNB to be a valuable Trp footprinter. Another widely used derivative of HNB is HNSB.[364-365] Unlike HNB, which must be prepared in an organic solvent (usually dry acetone), HNSB is a water-soluble sulfonium salt, which is an important factor that grants relevance in footprinting under physiological-like conditions.

The second Trp labeling reagent is *N*-bromosuccinimide (NBS),[366-367] which converts the indole ring to an oxindole (Scheme 3, middle). Among many successful demonstrations of NBS in footprinting Trp residues, the pioneering study by Takahashi et al.[368] adopted NBS labeling to footprint Trp residues of an α-amylase inhibitor PHA-I of *Phaseolus vulgaris*. PHA-I adopts a tetrameric conformation of $(\alpha\beta)_2$, and two of eight Trp residues (Trp 188 on each β subunit) show significant oxidation by NBS. When complexed with porcine pancreatic α-amylase, however, none of the Trp residues in the PHA-I were modified, suggesting that Trp 188 in the β subunit is critical for its inhibitory activity. This is a fine example that not only illustrates the effectiveness of NBS in assessing protein HOS but also shows the importance of Trp residues in assisting protein-ligand interactions.

The derivative of NBS, *N*-chlorosuccinimide (NCS), was also reported as an Trp labeling reagent.[369] In addition to Trp footprinting, all *N*-halosuccinimide reagents including NBS,[366] NCS[370] and *N*-iodosuccinimide[370] are capable of cleaving peptide bonds that occur upon further oxidation of oxindole. NCS is the most adopted reagent for this purpose.[371] This peptide bond cleavage served as an early Trp footprinting approach but has not been developed further because the development of proteomics capability with mass spectrometers has enabled other analytical approaches.

The third reagent that labels Trp residues is 2-nitrophenylsulfenyl chloride (Scheme 3, bottom), which was first reported by Scoffone and Rocchi[372] in 1968. The reagent, 2,4-

dinitrophenylsulfenyl chloride, was used together with 2-mercaptoethanol to attach covalently, on a Trp residue, a thiol group that can be further utilized for subsequent reactions.[373] The application of 2-nitrophenylsulfenyl chloride for MS-based Trp footprinting was first demonstrated by Simpson and coworkers[374] in 1993, where the investigators evaluated the effect of Trp derivatization on the biological activity and conformational stability of murine interleukin-6. Upon incubating with 2-nitrophenylsulfenyl chloride, Trp 36 and 160 showed significant labeling as identified by ESI-MS. The labeled interleukin-6 underwent a decrease in the biological activity in the murine-hybridoma growth-factor assay using 7TD1 cells and in binding affinity with its corresponding receptor. The overall conformation of labeled interleukin-6, however, remained unperturbed by CD measurements. They concluded that Trp 36 and 160 are critical in maintaining biological activity but not the structural integrity of interleukin-6. The derivative of 2-nitrophenylsulfenyl chloride, 2,4-dinitrophenylsulfenyl chloride has also been used as a TrP footprinting reagent as demonstrated by Zhang et al.[375] in 1997.

In summary, Trp labeling by targeted labeling reagents is less developed and used compared with footprinting of other residues, which is, in part, because all these labeling reagents favor acidic environments.[169] Under physiological pH, these reagents are either less specific (HNB[357] and NBS[367]) or less reactive (NBS[376-378]). Other than the reagents introduced above, other Trp labeling reagents including acetyl chloride,[379] hypothiocyanous acid,[380] and chloroform (under photo-activation)[381]. These reagents require harsher reaction conditions, and, thus, are less suitable as reagents for protein HOS analysis.

3.3. Tyrosine

Tyrosine (Tyr) is a phenol-containing hydrophobic amino acid that is often found on the protein surfaces.[382-383] Tyrosine is a critical target of several post translational modifications, including nitration,[384-387] sulfation[388-389] and phosphorylation[390-393]. These PTMs, especially phosphorylation, play an important role in cell signaling,[393] making Tyr an important target in protein footprinting.[391]

Among all the Tyr modification approaches, nitration has the richest history. Early demonstration of Tyr nitration dates back to 1910s when Johnson and Kohmann[394] determined the structure of nitrotyrosine and characterized Tyr nitration with nitric acid. Research over the years evolved to establish tetranitromethane (TNM) as the preferred Tyr nitration reagent, as was first reported by Wormall[395] in 1930 but not well established until the 1960s.[396-397] Tyr nitration by TNM is a representative of electrophilic aromatic substitution,[398] after which a nitro group is added to the electron-rich Tyr ring (Scheme 4, top). With excess amounts of TNM, a Tyr residue can be di-substituted as well. Although reaction between TNM and Tyr is reasonably specific, noticeable labeling of His,[397] Met,[397, 399] Trp,[397, 400] and Cys[401] at alkaline pH can also occur. Reactions between proteins and TNM will also induce intra- and inter-molecular chemical cross-linking via Tyr residues under acidic pH,[398, 402-403] providing a representative example of zero-length cross-linking[404] (see sections 3.9 and 4.3 for more information). A good illustration for TNM-facilitated zero-length chemical cross-linking is the dimerization of insulin, which was reported independently by several research groups.[403, 405]

TNM labeling coupled with MS analysis, as a footprinting platform has been used for protein HOS analysis. A pioneering study is by Ploug et al.[406], where they characterized the interactions between urokinase-type plasminogen activator and its glycolipid-anchored receptor. Using MALDI-MS, they identified Tyr 57 in the receptor and Tyr 24 in the isolated growth factor-like module of the activator as the key interacting residues. In another study, Šantrůček et al.[407] evaluated the correlation between TNM labeling extents and the SASA of the Tyr residues by using horse heart cytochrome *c*, hen egg-white lysozyme, and human serum albumin as model systems and MALDI-MS as the characterization tool. Surprisingly, they found only weak correlations between the TNM labeling extents and the SASA calculated from the crystal structure. For example, Tyr 148 and 341 in human serum albumin are highly reactive towards TNM but are poorly solvent-accessible. This study not only indicates that users be aware of other effects on footprinting by targeted labeling reagents and understand the importance of differential experiments when the factors that govern apparent reactivities are not fully understood. Method development studies are highly recommended.

Another Tyr nitration reagent is peroxynitrile, and it has become significant in the field of nitric oxide physiology and biological oxidations.[408-409] Its application in MS-based protein HOS analysis, however, is limited.[410] One possible reason is the low stability of peroxynitrile as compared with TNM. There are also reports demonstrating electrochemical[411] and copper-catalyzed[412] tyrosine nitration. Although promising, its application in protein HOS analysis remains to be established.

The second approach to label Tyr is iodination. As depicted in Scheme 4 (middle), iodination can lead to mono-iodotyrosine or di-iodotyrosine depending on reaction conditions. Although seldom used in protein footprinting, Tyr iodination is still valuable in protein radiolabeling (^{131}I has a radioactive decay half-life of 8 days[413]) and in pharmacokinetic studies.[414] To date there are several methods for Tyr iodination, including sodium iodide (NaI) coupled with *N*-chloro-4-methyl-benzenesulfonamide (chloramine T),[415-417] I_2 with iodine monochloride (ICl),[418-419] 1,3,4,6-tetra-chloro-3a,6a-diphenyl-glycouril (iodogen),[420] lactoperoxidase[421] and *N*-iodosuccinimide[422]. Iodination of Tyr by these reagents occurs as electrophilic aromatic substitutions, with iodonium ion or hypoiodous acid as the reactive species.[414] Other than Tyr iodination, oxidation of Met, Cys and Trp by these iodinating reagents should not be ignored.[423]

To utilize Tyr iodination for protein footprinting, Hobba et al.[424] in 1996 first demonstrated its efficacy by probing the insulin-like growth factor binding sites of bovine insulin-like growth factor protein-2. When the latter protein was footprinted by chloramine T-mediated iodination, Tyr 60 showed protection upon interacting with its binding partner. Confirmatory evidence is that iodinated bovine insulin-like growth factor protein-2 has a significantly lower binding affinity with its binding partner, consistent with the importance of Tyr 60 whose iodination perturbs binding. Note that Tyr iodination can also be achieved by a radical-mediated pathway,[181] which will be discussed in section 5.6.

The last Tyr labeling reagent for discussion is *N*-acetylimidazole (NAI), which was first demonstrated to be a protein labeling reagent in 1963.[425] Subsequent study by the same

group showed the applicability of NAI as a protein footprinting reagent by analyzing solvent accessible and buried Tyr residues in several proteins.[426] NAI acetylates phenolic hydroxyl groups through nucleophilic substitution, after which the Tyr residue becomes *O*-acetylated (Scheme 4, bottom). Acetylation of Ser and Lys also occurs occasionally.[427-428] Tyr labeling by NAI is optimized at a pH between 7.0 and 8.0 to minimize the hydrolysis of NAI and the product.[428-430] The application of NAI in mapping solvent accessible Tyr residues was nicely demonstrated by Pucci and coworkers[431] in 1997, where the surface topology of a small *de novo* designed β-protein minibody was mapped by MS-based peptide footprinting. The NAI footprint revealed that Tyr 35, 39 and 59 are exposed for NAI labeling whereas Tyr 15, 24 and 47 are silent. These results were further confirmed by TNM footprinting. Together with footprinting Lys (by acetic anhydride) and Arg (by 1,2-cyclohexanedione), the investigators obtained a comprehensive understanding of the minibody. Because NAI targets the hydroxyl group whereas iodination and TNM activate the C-H bond on the aromatic ring, this combination of Tyr footprinting will presumably provide different conclusions when a specific Tyr residue is involved in hydrogen bonding.[431] When Tyr is involved in hydrogen bonding, the hydroxyl group is not available for NAI footprinting whereas TNM is still capable of labeling the aromatic C-H bonds.

There have been two other acetylation reagents that are less specific as compared with NAI, 3-acetoxy-1-acetyl-5-methylpyrazole[432] and *N*-(2,2,5,5,-tetramethyl-3-carbonylpyrrolidine-1-oxyl)imidazole[433]. Both label aliphatic hydroxyl groups (Ser and Thr) as well.

Apart from the three major reagents introduced above, some other reagents for Tyr footprinting are acid anhydrides and acyl chlorides (target phenolic hydroxyl groups),[428, 434] cyanuric fluoride (targets phenolic hydroxyl groups),[435-436] various diazonium salts (target phenolic C-H bonds),[437-438] polyhalogenated quinones (target phenolic hydroxyl groups),[439] *p*-nitrobenzenesulfonyl fluoride (NBSF, targets phenolic hydroxyl group),[440-441] diisopropylphosphorofluoridate (targets phenolic hydroxyl groups),[442-443] *p*-nitrophenyl acetate (targets phenolic hydroxyl groups)[444] and hemin-activated luminol derivatives (target phenolic C-H bonds)[445]. Although this wide variety of reactive reagents demonstrates the importance of functional groups in footprinting, most await establishment in MS-based protein HOS elucidation.

3.4. Aspartic Acid and Glutamic Acid

Carboxylic acid functional groups in aspartic (Asp) and glutamic acid (Glu) residues are the targeted functional groups in Asp and Glu labeling. By incubating with methanol under acidic conditions, carboxyl acids can be esterified as first demonstrated for lysozyme in 1945.[446] Later on, IAM,[447-448] *N*-ethylphenylisoxazolium tetrafluoroborate[449] and various diazo derivatives[450-454] were also found to label Asp and Glu. These esterification reactions, however, are highly reversible and require methanol solvent and acidic conditions, making them inappropriate for footprinting under physiological conditions. Diazo reagents, although reactive under milder conditions, are not stable in aqueous solutions. For these reasons, the above reagents are less commonly used today in protein footprinting. Another class of reagent that was applied in Asp and Glu labeling is Woodward's reagent K (WRK).[455-457]

Despite its success in testing covalent inhibition,[458-459] it has not been used protein HOS interrogation because it may be too bulky and subject to steric hindrance to probe protein SASA effectively.

The emergence of carbodiimide-based reagents offers a welcome solution for footprinting acidic residues. The reagents are water-soluble and capable of labeling Asp and Glu residues under physiological conditions. Two early promising reagents are 1-cyclohexyl-3-(2-morpholinyl-(4)-ethyl) carbodiimide[460-463] and 1-ethyl-3-(3-dimethyl-aminopropyl) carbodiimide.[462] On the other hand, their reaction products have been poorly characterized, owing in part to limited characterization techniques at the time of study and to low yields.[463]

The breakthrough of carbodiimide Asp and Glu labeling was by Hoare and Koshland[464] in 1966, where carbodiimide serves as activating reagent, and a second reagent is incorporated to accomplish the labeling, affording an improved labeling efficiency and higher confidence in identification. In the original demonstration, *N*-benzyl-*N*′-3-dimethylaminopropylcarbodiimide (BDC) was the activating carbodiimide, and glycine methyl ester was the labeling reagent. Subsequent studies[465-466] revealed that the basis for quantification of Asp and Glu in proteins by carbodiimide-activated Asp and Glu labeling is activation of the carboxylic acid by carbodiimide to form an *O*-acylisourea intermediate (see Scheme 5). The intermediate then reacts rapidly with the nucleophilic labeling reagent to give a stable final product. In principle, any combination of water-soluble carbodiimide and a highly reactive nucleophile can facilitate such reactions. Currently, the activating carbodiimide used in Asp and Glu labeling is almost exclusively 1-ethyl-3-(3-(dimethylamino)propyl)carbodiimide (EDC), thanks to its high solubility and stability. The labeling in the early work, measured by amino acid analysis of the protein constituents, was motivated by analytical needs to “count” the number of Asp and Glu in a protein by quantifying by amino acid analysis the increase in glycine that occurs as a consequence of labeling.

The evolution of Asp and Glu footprinting from basic chemistry to application is typical for development of footprinting other amino acid residues. The extension of the labeling to footprinting and the study of protein HOS was not imagined in the early work, probably because complete analysis of the labeling was difficult in the absence of modern MS. Now, applications are not only facilitated by improvements in analysis technology but also extended by reagent development of several nucleophiles that couple with EDC, including glycinamide (GA), glycine ethyl ester (GEE) and benzhydrazide (BHD), providing for the field a new birth (pathways for these reagents are in Scheme 5).

Asp and Glu labeling by GA (and possibly by isotopic encoded GA for more reliable identification and quantification) and glycine methyl ester[466] was not applied to study protein HOS until decades later. The applicability of GA as a MS-based Asp and Glu footprinting reagent was first demonstrated by Akashi et al.[467] in 1993. Using a differential bottom-up footprinting workflow, the investigators identified Asp 101 as a key interacting residue in hen egg-white lysozyme when binding with its inhibitor, tri-*N*-acetylglucosamine. Moreover, the investigators utilized multiple MS-based techniques, where they measured intact mass of the protein by ESI-MS, the digested peptides by LC separation, UV detection

and Frit-FAB MS, and conducted tandem-MS for selected peptides to identify the modified residues by a sector mass spectrometer. Taken together, these systematic characterization steps prefigured the modern protein footprinting workflow. Although multiple mass spectrometers were used at that time, the analysis can now be accomplished by a single LC-MS/MS system.

In perhaps the first EDC-facilitated GEE footprinting of Asp and Glu, Sanderson and Mosbaugh[468] investigated how PBS2 uracil-DNA glycosylase inhibitor (Ugi) protein inactivates uracil-DNA glycosylase (Ung) by forming a protein-protein complex in which Ugi mimics duplex DNA bacteriophage PBS2 uracil-DNA glycosylase inhibitor protein. Electrophoresis was used to separate forms of the protein that differ in the amounts GEE adduction. Subsequent bio-functional assays determined their activities whereas protein cleavage by cyanogen bromide and analysis by MALDI MS and amino-acid sequencing localized the GEE modification sites. Because species that are heavily modified are biologically inactive, they were able to identify in systematic studies the key Asp and Glu residues that retain the protein's activity to be Glu-28 and Glu-31 in α2-helix.

As mentioned above, modern approaches utilize on-line LC in combination with MS and MS/MS for better separation and quantification with a single analytical system. In an example from 2009, Wen *et al.*[469] utilized GEE to footprint the Fenna-Matthews-Olson (FMO) antenna protein from *Chlorobaculum tepidum*. By LC separation and MS and MS/MS identification, locations and extents of labeling of FMO protein located in a native membrane as well as on a chlorosome-depleted membrane were compared. The differential footprinting reveals for the first time the orientation of the protein associated with the cytoplastic membrane as the Bchl *a* #3 side. Later on, isotopic encoded GEE was implemented for a better and more convenient identification.[470]

Although effective, GEE has its disadvantages. The ester group in the GEE molecule will undergo hydrolysis under both acidic and basic conditions. As the LC solvent usually contains acid to provide better ionization efficiency in MS, the hydrolysis problem can be significant.[469] Practically both the GEE modified species and its hydrolyzed species were quantified, which not only complicates the data analysis but also increases the errors in the quantification. To overcome these disadvantages, Guo *et al.*[471] developed BHD, which reacts with Asp and Glu under EDC activation (Scheme 5, bottom). Moreover, BHD labels the Asp and Glu residues with higher efficiencies than does GEE. BHD also requires lower reagent amounts, resembling better the native-like environment of the target protein molecule.

3.5. Arginine

Arginine (Arg) labeling draws significant attention owing to its participation in salt bridges.[472-473] Moreover, Arg residues can form up to five hydrogen bonds with other partners, facilitate hydrophobic interactions through its three methylene carbons, and interact with other aromatic functional groups via its guanidinium group.[383] All these interactions make Arg critical in the protein folding that gives functional structures for protein and protein complexes. Post translational modification of arginine residues is also critical in regulating protein-nucleic acid[474] and protein-protein interactions.[475] Its chemical labeling, however, is

challenging as the large pK_a (high basicity) of the guanidino group (greater than 12)[476] keeps Arg protonated at ~ pH = 7 and decreases its nucleophilicity.

Arginine residues are mostly labeled by vicinal dicarbonyl reagents, resulting in a cyclic product (summarized in Scheme 6). Arg labeling by phenylglyoxal and its derivatives was first demonstrated by Takahashi[477] in 1968, where the reactivities of phenylglyoxal and the Arg residues in peptides and bovine pancreatic ribonuclease A were systematically studied. The reaction between phenylglyoxal and an Arg residue is a two-step process, as shown in Scheme 6, and both steps are reversible. The final product to which two phenylglyoxal molecules are added, however, is stable under acidic conditions but readily decomposes at neutral and basic pH.[477-479] Other phenylglyoxal derivatives including *p*-hydroxyphenylglyoxal,[480] 4-hydroxy-3-nitrophenylglyoxal,[481] *p*-nitrophenylglyoxal,[482] *p*-azidophenylglyoxal[483] were also demonstrated to be valuable Arg labeling reagents. Given a deep understanding of the reactivity and appropriate reaction conditions, phenylglyoxal and its derivatives are the most extensively used Arg labeling reagents.[271]

As modern HPLC systems when coupled with MS analysis use acidic mobile phases (if working in the positive-ion mode of the mass spectrometer), stability of labeling product at acidic pH allow phenylglyoxal to be a MS-friendly Arg footprinter. The application of phenylglyoxal as an Arg footprinting reagent was pioneered in 1995 by Coggins and coworkers[484], who used ESI-MS to identify Arg 19 and Arg 23 as critical functioning residues for type II dehydroquinases in *Streptomyces coelicolor* and *Aspergillus nidulans*, respectively. Because MS instrumentation with ESI was beginning to emerge at the time of that study, key Arg residues had to be located by bottom-up MS analysis and confirmed by comparing the masses of resulting peptides with theoretical values instead of MS/MS. In a more sophisticated example later by McLafferty and coworkers,[485] phenylglyoxal Arg footprinting was coupled with tandem MS to allow confident identification of three key Arg residues that facilitate the function of rabbit muscle creatine kinase.

Another popular vicinal dicarbonyl reagent that labels Arg residues is 2,3-butanedione, which was first reported by Yankeelov and Crawford[486] in 1968. Upon reacting with Arg, a five-membered ring is the primary product (Scheme 6). The reaction between an Arg residue and 2,3-butanedione is highly reversible, and the labeling proceeds significantly slower than that of phenylglyoxal, limiting the application of 2,3-butanedione. In 1973, Riordan[487] discovered that borate has a dramatic effect on the reactivity of 2,3-butanedione with Arg residues, as borate stabilizes the initial diol product, thus pushing the reaction to a higher yield (Scheme 6). Similarly, Leitner and Linder[488-491] demonstrated that phenylboronic acid is also capable of stabilizing the initial adduct. This series of studies also represents the early applications of 2,3-butanedione as an Arg footprinting reagent in MS-based HOS analysis.[488-491] Currently, 2,3-butanedione labeling is mainly executed in borate buffers in the dark to minimize the photoactivation of 2,3-butanedione and to increase the labeling specificity and efficiency. 2,3-Butanedione is also capable of reacting with citrulline (the product of Arg residue upon reacting with peptidylarginine deiminase), as demonstrated in a few MS-based footprinting studies.[492-493]

The last vicinal dicarbonyl reagent for Arg labeling is 1,2-cyclohexanedione, which was first shown to modify Arg residues under basic conditions (pH > 12 for effective deprotonation) in 1967.[494] This pH is not biologically relevant and greatly limits its application in protein labeling and footprinting. In 1975, Patthy and Smith[495-496] discovered that borate can stabilize the diol product between 1,2-cyclohexanedione and an Arg residue under physiological pH, a similar phenomenon as Riordan[487] observed for 2,3-butanedione.

The application of 1,2-cyclohexanedione in MS-based Arg footprinting was first reported by Przybylski and coworkers[497] in 1992, when they found that four out of 11 Arg residues were modified in egg white lysozyme. By comparing the labeled Arg residues with those in a crystal structure, the investigators found an inverse correlation between labeling efficiency and solvent accessibilities. Upon closely examining the local environments of the labeled Arg residues, they were able to show that the proton acceptor groups are in close proximity. These neighboring proton acceptors assist deprotonation of Arg residues (first step in 1,2-cyclohexanedione labeling) and facilitate Arg labeling in an intramolecular catalytic fashion. All in all, this work is not only one of the pioneering studies that demonstrate protein footprinting by targeted labeling reagents but also is an early example that addresses effects of local environment on the labeling efficiencies of targeted labeling reagents.

An Arg labeling reagent that is not a vicinal dicarbonyl compound is represented by 3-ethoxy-1,1-dihydroxy-2-butanone (kethoxal), which is a popular RNA footprinting reagent that reacts with the guanine group.[498-499] Kethoxal was later demonstrated to react with Lys residues in proteins.[500-502] MS-based Arg footprinting by kethoxal was first demonstrated by Fabris and coworkers[502] in 2005, where they adopted Arg-containing protected amino acids, di- and tri-peptides, and model proteins to investigate the reaction product between kethoxal (structures depicted in Scheme 6) and an Arg residue and to demonstrate its capability as a Arg footprinting reagent. As the initial addition of kethoxal forms a diol product, the reaction can also include borate for higher yield.

Other than the reagents introduced above, there are other Arg footprinters including diphenylethanedione,[503] malondialdehyde,[504-506] methylglyoxal[507-508], ninhydrin[509-510]. These reagents, although they show potential for reacting with Arg, have found little application thus far in Arg footprinting.

3.6. Histidine

Targeted labeling of histidine (His) has drawn considerable attention owing to its high abundance in many enzyme active sites.[511] The two nitrogen atoms on the imidazole ring impart a unique character as an acid-base catalyst,[512] which further facilitates various enzymatic transformations. In general, His residues are not critical for structural stability of proteins,[513] and surface-accessible His residues are not involved in catalytic domains.[514] These general observations make His footprinting important for assessing structures of enzymes because buried His residues often play critical roles in bio-catalytic processes.

Early His modifications were achieved by using bromoacetic acid and bromoacetate.[288, 293, 515] Two nitrogen atoms on the imidazole are potential nucleophilic sites for modification. As halogen atoms are good leaving groups, many α-halo carboxylic acids and

amides were developed and utilized in His labeling, including but not limited to bromoacetate,[288, 516-521] chloroacetate,[288, 293, 517] iodoacetate,[517, 519, 522] bromoacetamide[523] and IAM[524]. Although effective, these reagents soon fell into disuse, primarily due to their lack in specificity. These reagents were later found to be reactive with other amino acid residues, most notably cysteine, which can be modified even more rapidly than histidine.[289] IAM today is one of the most widely used Cys alkylating reagent as mentioned in section 3.1. His labeling by bromoacetate, a reagent that can be used for Cys-free proteins, however, requires days to complete, greatly limiting broad application[516, 521] and causing concerns about structural change during the footprinting and misleading over-labeling. A similar situation applies to methyl-*p*-nitrobenzenesulfonate, which can label His residues but now principally serves as a alkylation reagent for Cys.[525-526]

Another reagent that is related to the α-halo carboxylic acid is 2-bromo-1-(4-bromophenyl)ethenone (*p*-bromophenacyl bromide), which irreversibly labels His residues; this reagent is similar to other α-halo carboxylic acids. *p*-Bromophenacyl bromide was first reported to react with carboxyl groups in Asp and Glu at the active sites of pepsin.[447] Subsequent studies demonstrated its capability for labeling His residues.[527-528] Although still being used today, *p*-bromophenacyl bromide has been almost exclusively used in labeling phospholipase A_2.[271, 529-530]

The most extensively used His labeling reagent to date is diethylpyrocarbonate (DEPC), whose reaction pathway with His is described in Scheme 7. Development of His labeling by DEPC reactions with intact proteins was pioneered by Fedorcsák and coworkers[531-533] in the 1960s. DEPC has advantages over the other reagents because it has relatively high specificity[271] and reactivity[534]. In the pH range between 5.5 to 7.5, DEPC primarily labels His residues, but it is also reactive with Arg, Cys, Lys, Ser, Thr, and Tyr residues.[535-538] As illustrated in Scheme 7, mono-modification of His by DEPC is reversible in the presence of other nucleophiles[538] as well as under both acidic and basic conditions (half-life for 3-carboethoxyhistidine is 55 h at pH of 7, 2 h at pH of 2, and 18 min at pH of 10[539]).

With excess DEPC, the His residue can be di-modified irreversibly. The reactivity between His and DEPC increases in acidic buffer lower than pH 6 to 7.[540] The most significant disadvantage of DEPC in His labeling is that DEPC is insoluble in water, making it essential to add water-miscible organic solvents (e.g., methanol, acetonitrile). The amount of organic solvent needs to be carefully tuned to prevent protein denaturation, which can be measured in preliminary experiments using, for example, CD. A recent study also suggests that the presence of hydrophobic residues increases the local concentration of DEPC at the protein surface, increasing the reactivity.[541]

The potential of DEPC in MS-based protein footprinting was explored through a demonstration study that used FAB-MS to characterize the reaction product between DEPC and five model peptides.[542] Taking advantage of fragmentation accompanying FAB ionization, the investigators identified major reaction products between DEPC and His residues as well as their fragmentation pathways. In one of the pioneering MS-based His footprinting studies that uses DEPC as labeling reagent, Glocker et al.[543] in 1996 mapped solvent-accessible His residues in recombinant human macrophage colony-stimulating factor

β by using MALDI-MS for analysis. Among four DECP-modified His residues, His 9 and His 15 are directly correlated with biological activity whereas the activity is not affected by labeling of His 176 and His 210. In another study, Halsall and coworkers[544] used LC ESI-MS to determine the location and modification extent of solvent-accessible His residues in α_1-acid glycoprotein. In addition to its biological significance, this work nicely illustrates a modern MS-based protein footprinting workflow, where the digested peptides are separated by HPLC, followed by MS/MS analysis to determine the modification sites, and quantification by integrating extracted ion chromatograms. Recent advances of DEPC labeling were mostly by Vachet and coworkers,[169, 535, 541, 545-548] and some of their contributions will be reviewed in Section 4.

Other than the reagents introduced above, epoxides can also label His, but these reagents, are not specific towards His. Very recently, Joshi and Rai[549] scanned a series of nucleophiles and found 2-cyclohexenone reacts with the His residue in different proteins with high specificity. Like DEPC, 2-cyclohexenone is poorly soluble in water, necessitating the undesirable addition of organic solvents during labeling. Although not without drawbacks, this study nicely demonstrates the potential of 2-cyclohexenone and its derivatives in His footprinting.

3.7. Lysine

Lysine (Lys) residue side chains and the N-terminus are the sites of primary amine groups. As these primary amines are most commonly found on protein surfaces,[169] labeling Lys residues becomes valuable for probing protein surface structure and its changes with respect to ligand binding or environmental change.[497]

Several different reagents were developed to label the primary amine group in Lys residues (summarized in Scheme 8). The most widely adopted approach is acylation by acid anhydrides, as exemplified by acetic anhydride in Scheme 8. Reaction between acetic anhydride and a Lys residue (Scheme 8, top-left) is highly pH-dependent, as the acetic anhydride readily hydrolyzes under acidic pH. Acetic anhydride can also react with hydroxyl groups found on Ser and Thr sites and aromatic Tyr sites, and with the imidazole ring (His). Formation of *O*-acetyl tyrosine can be minimized under alkaline pH or in the presence of acetate.[550-551] The other side reactions (with Ser, Thr and His) are also reversible and can be minimized by optimizing the conditions.[552] Although acetic anhydride is one of the first Lys labeling reagents,[553] it still is used today in MS-based protein HOS analysis.[497, 554-562] Lys footprinting by acetic anhydride was first demonstrated by Fenselau, Vestling and coworkers in 1991[563], where they studied the melittin binding sites in calcium-bound calmodulin. By comparing Lys modifications of calcium-bound calmodulin under both melittin bound and unbound states, they identified Lys 21, 75 and 148 as interacting Lys residues by FAB-MS analysis. In another pioneering demonstration, Przybylski and coworkers[497] analyzed the surface topology of egg white lysozyme. Footprinting Lys residues in egg white lysozyme and quantifying by ^{252}Cf plasma desorption MS, they obtained reactivities for six Lys residues and showed the reactivities correlate well with the SASA values derived from a crystal structure. The results highlight early examples of the

potential of targeted amino acid labeling in combination of MS analysis, primitive by today's opportunities, for analyzing protein HOS.

Another popular anhydride for Lys modification is succinic anhydride (Scheme 8, middle-left).[564] Under physiological pH, Lys is usually positively charged as the primary amino group is protonated. When Lys reacts with succinic anhydride, the product is a carboxylic acid that deprotonates under neutral pH (Scheme 8). In other words, Lys modification by succinic anhydride results in charge reversal, which usually leads to dissociation of multimeric protein aggregates and has been widely utilized to solubilize insoluble proteins.[565-568] Another unique feature of succinic anhydride is that it can efficiently modify Lys residues at acidic pH,[169] which is significantly different than those for acetic anhydride. Other than amino groups, succinic anhydride is also found to be reactive towards Tyr residues.[569] In the earliest example of Lys footprinting with acetic anhydride and MS-based protein HOS analysis (1996), Przybylski et al.[570] studied the *Rhodobacter capsulatus* general diffusion porins. MS together with X-ray crystallography were used to identify the N-terminus and three other modified solvent-accessible Lys residues (Lys 46, 298 and 300). Charge reversal upon succinylation induced an increase in cation selectivity and single-channel conductance of the porin.

Other than acetic and succinic anhydrides, the acylation of Lys can also be done with other anhydrides, including citraconic anhydride,[571-572] maleic anhydride,[573-574] trimellitic anhydrides,[575] phthalic anhydride,[576] 3-hydroxyl phthalic anhydride,[575] hexahydrophthalic anhydride,[577-578] methyltetrahydrophthalic anhydride,[577, 579] succinic anhydride,[580-581] *cis*-aconitic anhydride[580, 582] and fatty acid anhydrides[583].

Unlike succinic anhydride that reverses the charge of Lys upon labeling, methyl acetimidate labeling retains the positive charge on the Lys residue at physiologically relevant pH (Scheme 8, bottom-left).[584] Methyl acetimidate is a representative reagent in the imidoester family that targets α-amino groups. Other popular imidoester reagents include ethyl acetimidate,[585] methyl isonicotinimidate,[586] *S*-methylthioacetimidate,[587] isethionyl acetimidate,[588] and *S*-sulfethylthioacetimidate[589]. The latter two are sulfonic salts, are membrane-impermeable, and can be utilized to study soluble domains of cell membrane and membrane-bound proteins, providing spatial specificity (inner and outer membrane sides).[590] *S*-Methylthioacetimidate also labels Cys, resulting a methyl disulfide with the sulfhydryl group.[591] The most significant drawback for imidoesters is their limited half-life in water owing to the rapid hydrolysis of the esters.[584, 592] Therefore, imidoesters have not been often used in protein HOS analysis. The bis-imidoesters, however, are a popular cross-linking reagent, and details on this application are in section 3.9.1.

N-Hydroxysuccinimide ester (NHS-ester, Scheme 8, top-right) derivatives are another class of reagents in Lys labeling. NHS-ester was adopted in protein modification by Blumberg and Vallee[593] in 1975. Its sulfonic salt, sulfo-NHS ester, was developed by Staros[594-595] in 1982 and was widely adopted owing to its improved solubility.

Other than Lys, NHS-esters also react with Ser, Thr, and Tyr residues.[596] The NHS-ester is also frequently used for biotinylation of proteins, a process that is of great importance in

protein purification because the modified protein binds tightly with streptavidin (and also avidin).[597-598] The biotin derivative of the NHS-ester has been widely used in MS-based Lys footprinting and in locating binding sites.[599-604] In pioneering work, Knock et al.[600] in 1991 footprinted *Aplysia* egg-laying hormone with a biotin-functionalized NHS ester. Time-dependent labeling of the hormone revealed that among three amino groups (Lys 36, Lys 8 and N-terminal NH_2) that were labeled by NHS-ester, Lys 36 is the most solvent-accessible whereas the N-terminal amino group is the most protected. In combination with data from a bioactivity assay, they concluded that Lys 8 and the N-terminal amino group are critical for preserving bioactivity.

Another biologically significant reagent that is based on NHS-ester chemistry is the Bolton-Hunter reagent, succinimidyl-3-(3[^{125}I],4-hydroxyphenyl)propionate, which plays an important role in protein radiolabeling (^{125}I is radioactive).[605] The fatty acid of sulfo-NHS is also used for footprinting because it can modify membrane proteins.[606] NHS-esters are also widely used in chemical cross-linking of proteins, as discussed in section 3.9.1.

2,4,6-Trinitrobenzenesulfonic acid (TNBS) reacts with primary amines with reasonable specificity (Scheme 8, middle-right), and the incorporation can be easily measured by utilizing its optical absorbance at 420 nm, a characterization strategy that is readily adoptable.[607-609] These unique features to footprint free amino groups (N-terminus α-amine and ε-amine in Lys residues) in proteins at the time (1960s) were utilized when routine spray or desorption ionization coupled with high resolution MS analysis was not available. Moreover, protein HOS analysis and conformational changes can also be followed with TNBS coupled with absorbance spectroscopy in a protocol that is similar to protein HOS analysis with fluorescence spectroscopy (absorption versus emission).[610-612] TNBS footprinting of the N-terminal α-amino group induces a strong hydrophobic shift in the LC separation, and this feature was utilized in peptide separations of complex proteomic samples.[613] The combination between TNBS labeling and MS detection in protein HOS interrogation seems promising but is not yet well established.

Similar to TNBS, another potentially favorable yet poorly demonstrated footprinting reagent is methyl acetyl phosphate (Scheme 8, bottom-right).[614] As the phosphate group carries negative charges under physiological conditions, methyl acetyl phosphate becomes a useful probe for characterizing anion binding sites.[615-617] A similar phosphate-containing Lys labeling reagent is pyridoxal-5′-phosphate (PLP), which also preferentially binds to anion binding sites prior to Lys labeling.[618-619] Its fluorescence[620] and UV absorbance[621] properties were utilized to study protein conformational changes. The application of PLP in MS-based protein footprinting, however, is not well tested. One problem is that the phosphate group will cleave to lose phosphoric acid during the CID process, preempting useful sequence-specific fragmentation. This problem is resolvable by using ETD in the MS/MS.

Other than the reagents discussed above, dinitrofluorobenzene,[622] 4-chloro-3,5-dinitrobenzoic acid,[623] cyanate,[624] aldehydes (formaldehyde, glycolaldehyde) coupled with reducing reagents (sodium borohydride, sodium cyanoborohydride or amino boranes)[625-626] can also label Lys residues. Reducing sugars are also capable of reacting with the ε-amino

groups in Lys.[627] These reagents, however, were not designed or used for protein HOS analysis and, thus, will not be covered further.

3.8. Other residues

Methionine (Met) is an attractive footprinting target, yet its labeling by targeted reagents is challenging. Despite being easily oxidized under various conditions, Met is only reactive with targeted labeling reagents under acidic conditions, where Met functions as a nucleophile.[628] Alkylating reagents including iodoacetate,[290] methyl iodide,[629] iodoacetamide,[630] and iodoacetic acid,[631] all of which react with Met in a pH range of 2 – 4. Furthermore, there are only a few demonstrations where these reactions occur under gentle conditions (iodoacetate with Met residues in pig kidney general acyl-CoA dehydrogenase pH = 6.6).[632] Thus, the likely disruption of protein native structure by placing it in an acidic environment make this reagent too risky as a footprinter.

Site-specific backbone cleavages of Met-containing peptides by cyanogen bromide (CNBr) was extensively used in the 1980s.[271, 633-634] Upon reacting with CNBr, Met forms a five-membered ring with methyl thiocyanate as the leaving group. The five-membered ring subsequently cleaves to yield a peptide homoserine lactone and subsequently a peptide homoserine after hydrolysis. This reaction was usually coupled with top-down MS for analysis,[172, 635] but top-down analysis becomes less necessary owing to the increasing effectiveness of current methods for inducing fragmentations via MS/MS.

Another study by Reid et al.[636] utilized ω-bromoacetophenone as a Met alkylating reagent, and subsequent CID activation in MS/MS analysis caused a neutral loss that leaves a single characteristic product ion for Met. All in all, Met footprinting by targeted labeling reagents seems to be ineffective in contrast to Met oxidation[637-639] and the fast-labeling by hydroxyl radicals in the synchrotron and FPOP platforms (see section 5 and 6).

Serine (Ser) and threonine (Thr) both contain hydroxyl groups in their side chains, making these two residues as likely targets for different enzymatically introduced PTMs including *O*-linked glycosylation[640-642] and phosphorylation[643]. Introducing chemical modifications, however, is quite challenging. Both Ser and Thr can be acylated at lower reaction rates by *p*-nitrophenyl acetate,[644] a reagent that primarily reacts with the stronger nucleophilic Tyr[645] and Lys[646]. When located in N-terminus, Ser and Thr can be oxidized by periodic acid to form an aldehyde.[647] Formic acid will esterify Ser and Thr residues at high concentrations in a reaction known as *O*-formylation.[648] NHS-esters also react with Ser and Thr as side reactions.[596] These reactions, however, are not of sufficient yield to footprint Ser and Thr residues in proteins under physiological conditions.

Asparagine (Asn) and glutamine (Glu) are the amide derivatives of Asp and Glu, respectively. The primary modification they undergo is deamidation, which occurs naturally as a PTM[649] and is also observed during cyanogen bromide/formic acid cleavage.[650]

Glycine (Gly), alanine (Ala) and valine (Val), leucine (Leu), isoleucine (Ile) and proline (Pro) are generally inert to most chemical modifications that target functional groups as their residue side chains consist of unreactive H, alkyl, and cycloalkyl groups. Although the

phenyl group of phenylalanine (Phe) can undergo electrophilic substitution, its chemical activation in a protein is also challenging under psychological conditions because the phenyl group is not reactive. Although Leu, Ile, Pro, and Phe are not activated by normal chemical processes, remarkably they can be modified by free-radical reactions, as will be covered in section 5.

3.9. Chemical Cross-linkers

Chemical cross-linking occurs via the formation of covalent bonds between interacting proteins and within a protein on adjoining regions. This structural proteomics tool often uses a bifunctional chemical reagent and can be viewed as bifunctional footprinting. Many reagents have been developed, promoting more and more applications of chemical cross-linking. The character of a cross-linking reagent is determined by the nature of chemistry, spacer length, and built-in functional groups. Cross-linking can be an effective complement to monofunctional reagents that serve as footprinters, and therefore the subject is briefly covered in this review particularly to make that point. The emphasis is on the commonly used reagents, which fits the theme of footprinting. Indeed, the location of monolinks can be viewed as a footprint. Our discussion is organized around the cross-linking reagents as follows.

3.9.1. Amine-reactive Cross-linkers: NHS-Ester and Imidoester

***N*-hydroxysuccinimide Ester:** NHS-esters are the most widely used cross-linkers in field. The ester group undergoes attack by nearby nucleophilic sites (e.g., primary amines on Lys side chains or at the N-terminus of a protein/peptides, hydroxyl groups on Ser or Thr, and even sulfhydryl groups on Met) to form C-X bonds (X = N, O, S). The differing reactivities with various nucleophilic groups, however, depends on reaction conditions and can introduce bias. Primary amines possess the highest reactivity at physiological pH, and their reactivity can be further enhanced when the pH is > 7.[595, 651] The hydrolysis of NHS-esters has a half-life of 4-5 hours at pH 7 and 0 °C[652]; the hydrolysis, however, is accelerated under alkaline conditions and at higher temperature.[653-654] Other possible products (i.e., esters and thioesters formed with Ser/Thr or Met) are less stable and undergo more rapid hydrolysis.[654] Although the reaction is favored under acidic conditions (pH = 6.0), cross-linking at pH = 7 still occurs. The current consensus is to consider all possible residues as sites for reactions in simple protein systems, whereas only Lys residues and the N-terminus are recommended for cross-linking a large complex or in a whole proteome study to minimize dispersion of cross links and maximize probability for detecting the cross-links.[655]

The first NHS-ester originated in late 1970s as a homo-bifunctional cross-linker.[656] Since then, many NHS-esters possessing useful physical and chemical properties have made them suitable for answering a range of biological questions. Designs include cross-liners with high hydrophobicity and zero charge, being lipophilic and membrane-permeable and ideal for intramembrane cross-linking (e.g., disuccinimidyl suberate (DSS) and disuccinimidyl glutarate (DSG), Scheme 9). Other cross-linkers incorporate a sulfonate group, which imparts water-solubility and avoids steps of pre-dissolution in organic solvents that could perturb aqueous conditions and cause some protein denaturation.

Currently, sulfo-NHS esters have become the dominant cross-linkers in characterizing soluble proteins and their interactions. *bis*(Sulfosuccinimidyl)suberate (BS3, Scheme 9), the most extensively used sulfo-NHS cross-linker, can be encoded with deuterium to facilitate better cross-link assignment. The spacer length is 11.4 Å, allowing cross-linking for residues separated by 27 Å measured between two α carbons in an amino acid residues that are linked (termed Cα).[657]

New developments in NHS-esters resonate well with the rapid growth in proteomics research enabled by advanced MS. More complicated systems with larger-scale protein candidates require better sequencing in MS/MS for a confident cross-linking identification. The disadvantage of using conventional cross-linkers is that the user must sequence specie made up of two cross-linked peptides and the cross-linker, introducing complexity into fragmentation and challenging the acquisition of high-quality, readily interpretable MS/MS data. Cleavable cross-linkers are, therefore, designed to address that problem.[658] NHS-esters have incorporated chemical-cleavable motifs (e.g., S-S bond in 3,3'-dithiobis(sulfosuccinimidylpropionate) (DTSSP)[651]) and CID-cleavable functional groups that include C-S bonds (e.g., disuccinimidyl sulfoxide (DSSO)[659] and cyanurbiotindimercaptopropionyl succinimide (CBDPS)[660]) and C-N bonds (e.g., disuccinimidyl dibutyric urea (DSBU)[661] and *N*-hydroxyphthalamide ester of biotin aspartate proline (BDP-NHP)[662]). Chemical structures of these cross-linkers are shown in Scheme 9. In addition, some NHS-crosslinkers contain biotin tags (e.g., CBDPS and BDP-NHP), to provide a means of enriching the crosslinked species by affinity purification.

Imidoester: Imidoesters, introduced in 1966 as one of the oldest reagents for protein cross-linking, are water-soluble reagents that react specifically with primary amines (see Lys footprinting section above).[663] The functional imidate group reacts to form an amide bond via a few intermediates at an optimized pH range of 8-10.[653] One major advantages of using imidoester cross-linkers is that the reaction product, an amidine, carries one positive charge. Charge removal that occurs with most lysine-targeting cross-linkers may disrupt intramolecular and intermolecular interactions and distort protein conformation, giving a biased result. The lifetime of imidoesters, however, is limited by rapid hydrolysis, being less than 30 min.[664-665] The most commonly used cross-linkers in this class are dimethyl pimelimidate (DMP), dimethyl suberimidate (DMS) and a cleavable analog, dimethyl 3,3′-dithiobispropionimidate (DTBP), as depicted in Scheme 10.

3.9.2. Carboxylic Acid-reactive Cross-linkers: Carbodiimide and Dihydrazides—

The most widely used carbomiimide is EDC (Scheme 11), also known as a "zero-length" cross-linker.[404, 666] When this reagent facilitates cross-linking of carboxylate groups and primary amines, there is no spacer chain inserted between the targeted proteins, but rather an amide bond (~ 3 Å) between COOH and NH_2-containing sidechains.[404, 666] One critical reaction intermediate, *O*-acylisourea, is not stable in aqueous condition (see section 3.4 and Scheme 5), and it continues to degrade back to the carboxyl group. Therefore, sulfo-NHS is often incorporated in the cross-linking protocol to transform the *O*-acylisourea into a stabilized NHS-ester for more efficient conjugation. EDC cross-linking shows the highest reactivity at pH 4.5 and still a moderate reaction efficiency at neutral pH.

[667] 2-(*N*-Morpholino) ethanesulfonic acid (MES) and phosphate buffer are compatible with carbodiimide reagents; however, more concentrated reagents should be used in the latter buffer owing to the reduced reactivity.

Another commonly used cross-linker for Asp and Glu is dihydrazides. In 2008, Kruppa and Novak[668] first reported its use in combination with EDC activation. The reaction was carried out in acidic conditions (pH = 5.5), which is not physiologically friendly, to give a low cross-linking yield. Later in 2014, Aebersold and coworkers[669] reported a new coupling reagent (other than EDC), 4-(4,6-dimethoxy-1,3,5-triazin-2-yl)-4-methyl-morpholinium chloride (DMTMM) and achieved significantly increased reaction yields and better biocompatibility at neutral pH. Recently, Lei and coworkers[670] developed a coupling reagent-free crosslinker, *bis*(trimethylsilyldiazomethyl)dioxaoctane (Scheme 11), that offers selectivity and efficiency under physiological conditions. Isotopic encoded dihydrazides are now commercially available with different spacer lengths (e.g., adipic acid dihydrazide (ADH) and pimelic acid dihydrazide (PDH), Scheme 11).

3.9.3. Sulfhydryl-reactive Cross-linkers: Maleimide—Maleimide cross-linkers react specifically with sulfhydryl groups at pH 6.5-7.5 to form stable thioethers.[671-672] Under alkaline conditions (pH > 8.5), primary amines are also possible targets but not Tyr and His.[673] One major concern in maleimide cross-linking is to conjugate free sulfhydryl groups, requiring prior reduction of existing disulfide bonds; breaking the -S-S- bond has high potential to distort protein native structure. A more common way of employing maleimide chemistry is in combination with NHS-esters, where both functional groups are coupled onto a heterobifunctional cross-linker. These cross-linkers can be incubated with a protein sample in a stepwise manner, reducing disulfide bonds after reaction with primary amines.[653] In addition, to ensure the best cross-linking performance, many thiol-containing compounds (e.g., DTT and BME) should be eliminated in the reaction buffer.

3.9.4. Carbonyl-reactive Cross-linkers: Hydrazide—Hydrazides are carbonyl-reactive reagents that exhibit highest reactivity at pH 5-7. Aldehydes and ketones are major targets that can be found in glycoproteins introduced by oxidation of the polysaccharide.[653] The hydrazone bonds thus formed are moderately stable in aqueous solution and can be further secured by reducing the double bond to a secondary amine.

3.9.5. Photoreactive Cross-linkers: Aryl Azide and Diazirine—Photoreactive cross-linkers are generally nonspecific owing to the high reactivity of the intermediate species, a nitrene, carbene, or free radical. The most adopted chemistry utilizes nitrenes and carbenes, whose precursors are azides or diazirines, respectively. Among the three major categories, phenyl azides play a dominant role in current applications. Different substituents on the aromatic rings shift their UV absorption dramatically; therefore, they are selected with a biological question in mind.[653] Nitrophenyl azides, which can be activated at 300-460 nm, are compatible with most studies because this long wavelength causes minimal damage to protein molecules. Upon UV activation, the nitrene diradical can insert into most chemical bonds but with a preference for active C-H and N-H sites.[674] Diazirines are a relatively new class, first reported in the 1990s, and they have better photostability than phenyl azides.[675]

Carbene diradicals are usually generated photochemically at 355 nm, and they show reactivity with both single and double bonds. Like the nitrene diradical, heteroatom-H bonds undergo easier insertion. Some diazirine reagents are designed as analogs of amino acids (e.g., photo-Leu and photo-Met[676]) that can be incorporated into the protein sequence during translation for *in-situ* radical generation. High reactivity of carbenes and nitrenes can also cause problems in cross-link identification. The use of homobifunctional photoreactive cross-linkers tends to make product analysis complex; therefore, one radical precursor is usually combined with an amine- or sulfhydryl-reactive motif. The commonly used cross-linkers are *N*-5-azido-2-nitrobenzoyloxysuccinimide (ANB-NOS)[677] and sulfosuccinimidyl 4,4'-azipentanoate (sulfo-NHS-diazirine, sulfo-SDA), as seen in Scheme 12.

3.9.6. Summary—We have seen extensive development of chemical cross-linking during the past two decades, enabled by evolving MS instrumentations, new data processing software, and novel cross-linkers. Chemical cross-linkers are bifunctional protein footprinters, which are governed by similar principles as protein footprinting by targeted reagents. The bi-functional nature of the reagent allows generating distance restraints between two cross-linked residues, and such restraints can be further utilized to locate protein/protein binding interfaces, to assess protein topologies, to characterize the protein interactome in a large complex, and to facilitate protein docking and modeling. Some applications of chemical cross-linking are discussed in section 4.3.

3.10. Conclusion and Perspective

Protein footprinting takes advantage of early research that provided many effective chemical reactions for protein labeling. These reagents can now serve as probes to characterize protein SASA and as a basis to reason about protein HOS. The sites of modification can now be efficiently measured by MS, owing to the rapid development of LC separations and hybrid mass spectrometers with MS/MS capabilities. The chemical cross-linker, which is viewed as a bifunctional protein footprinter, when connected to two proteins offers valuable distance restraints between the proteins. These targeted footprinting reagents coupled with MS detection now are utilized to answer several biological questions and are becoming increasingly significant in structural biology, as will be discussed in Section 4.

A limitation of targeted footprinting is that reagents primarily react with one or a few residues that contain functional groups including bases, acids, nucleophiles and aromatic rings, leaving a sizable fraction of the amino acid residues to be “silent”. Moreover, the footprinting reactions are relatively slow, making most targeted footprinters unable to characterize fast protein dynamics (e.g., protein folding and protein aggregation). To overcome these drawbacks requires a new approach that has broader residue coverage and higher reaction rate. Fast footprinting reagents represented by reactive radical species meet these requirements as discussed in section 5.

4. Applications of Targeted-Labeling Reagents

Targeted-labeling has become a mature field in structural proteomics. Research in targeted-labeling has evolved from developing reagents and methods to addressing biological questions or, in many cases, developing a method and using it to solve a biological problem.

The maturation of the field runs parallel with MS instrumentation and method development. The key enabling progresses are (1) developing chemical reactions that are suitable for protein labeling and (2) utilizing high sensitivity, specificity, and speed now routinely available with modern mass spectrometer systems for analysis. Both steps are mature and permit careful application where perturbation of structure by the inserted reagent can be minimized or even eliminated.

A general workflow for bottom-up protein HOS analysis through irreversible protein labeling (through either targeted labeling reagents or reactive radical species) is shown in Figure 5 below.

In the general workflow, a protein of interest is first labeled in a native or native-like environment, during which the labeling reagent reacts with the solvent-accessible amino acid sidechains. Proteolytic digestion cleaves the protein molecules into peptide fragments that are then submitted to LC separation and MS analysis. By comparing the mass-to-charge (m/z) ratios of the precursor and its corresponding fragments, the investigator can assign chromatographic peaks to either the unmodified or the modified protein via its “proxy” peptides. Quantifying the modification extent can be achieved by integrating the corresponding chromatographic peaks (via extracted ion chromatograms) and comparing areas assigned to “modified” and “unmodified” peptides. When LC is insufficient to separate modified peptide isomers, fragmentation by ETD to allow comparison of the resulting product ion intensities may be an alternative approach for accurate quantification.[678] Assignment of the precise location of the modification can often be ascertained by MS/MS, on-line with the chromatography. The underlying assumption is that a residue side chain that is more solvent-accessible will be modified more heavily as compared with a residue that is buried inside the 3D structure of a protein. Coarse aspects of protein HOS can be elucidated by analyzing the modification fractions of the intact protein, “proxy” peptides, and even single-residue levels, taking advantage of the specificity of the labeling chemistry.

Conventionally, protein footprinting is almost exclusively executed in a differential manner, for which the labeling fractions for a specific region or residue are compared for different protein states. The difference in states can be achieved by incorporating a binding partner, changing the temperature, varying the denaturant concentrations or pH, or modifying the protein in metagenesis. The changes in protein conformations that occur with these perturbations can be elucidated with spatial resolution limited by the number and spacing of the targeted residues. Recent developments also forecast that elucidation and prediction of protein HOS protein footprinting data for a single state can be done, as will be covered in later sections.

Generally, the labeling is irreversible, allowing a wide range of post-labeling sample handing procedures (i.e., sample enrichment, deglycosylation, and longer LC gradients) as compared to that used for HDX, where labeling is reversible and precautions are necessary to minimize back exchange. The irreversibility feature also allows addressing problems that HDX cannot.

Two disadvantages can limit the approach. First, the coverage is limited to the targeted residue(s), and the number of them in the protein of interest can be low. Second, because the

labeling chemistry is generally slow (minutes), there is always a question whether the targeted protein undergoes a conformational change in the early stages of labeling and then continues to be modified to yield a composite and misleading footprint.

Given the maturity of the field and the large number of applications in the literature, we will select several applications of protein footprinting by targeted labeling reagents. The applications will be grouped by the biological questions that are addressed. We will limit our review to publications since 2009 and primarily highlight demonstrations that either embody novel developments or implement improved workflows. For work prior to 2009, we recommend a comprehensive review by Mendoza and Vachet[169] for a detailed historical perspective and early applications. For a discussion of reagent and method development, the reader is directed to section 3 where pioneering work is discussed.

4.1. Analyzing Metal-Ion Binding

Metal ion-protein interactions facilitate many cellular functions, especially signal transduction, as 25-50% of all proteins found in organisms contain metal ions.[679-682] Metal ions interact with proteins by coordination whereby electron pairs from the amino acid side chains bond with the vacant orbitals of the metal ions.[682] We will classify the protein-binding metal ions into two distinct categories based on their coordination properties. Soft metal ions represented by Zn(II), Cu(II), Cd(II) and Fe(II) bind with His and Cys whereas hard metal ions (e.g., Ca(II) and Mg(II)) usually coordinate with oxygen-containing functional groups in Asp and Glu.[683-684]

Many biophysical approaches have been applied to characterize protein-metal ion interactions, including MS,[685] NMR,[686] X-ray crystallography,[681] cryo-EM,[687] and fluorescence[688]. One approach is native MS whereby complexes are directly observed, but this begs the question of whether the gas-phase structures are secure and trustworthy reporters of those in the liquid phase. Footprinting avoids this question by using the mass spectrometer only as a measurement approach, not a reaction vessel. Footprinting can be conducted by HDX,[232, 689] fast irreversible labeling,[690-691] or slow irreversible labeling. All can reveal metal-ion binding sites and the corresponding protein conformational changes induced by the metal binding. HDX probes the binding-induced backbone conformational changes, whereas Asp and Glu, commonly present in a binding site of a hard metal ion, do not react well with most of the fast-labeling free radicals in that version of footprinting. Although capable, HDX and fast free-radical footprinting (next section) report the consequences of metal-ion binding by modifying regions of the protein (i.e., nearby peptide bonds in HDX) that may not be directly involved in binding. A direct footprinting experiment seems better suited for probing metal-ion binding because they probe directly the metal ion binding unlike indirect methods that report on conformational changes occurring nearby. All of this assumes that the structural perturbation caused by the footprinting is minimal.

As examples of a direct, targeted footprinting reagents, DEPC affords modification of His, carbodiimide-activated reagents (e.g., GEE) label Asp and Glu, and succinimide derivatives, iodoacetic acid, and *N*-alkylmaleimides, for example, label Cys.[169]

4.1.1. Protein Binding with Soft Metal Ions—Protein binding of soft metal ions, Cu(II) and Zn(II), is the most extensively studied. In a pioneering assessment of Cu(II) binding sites in a prion protein (PrP, from human), Qin and Westaway[692] in 2002 applied DEPC to footprint histidine-dependent Cu(II) binding sites and used MALDI for the analysis. No histidines are protected upon Ca(II), Mn(II), or Mg(II) binding, one or two residues are protected by binding of Zn(II) or Ni(II) ions, and five histidines are protected upon Cu(II) binding. Through a classical bottom-up approach, the investigators pinpointed the five histidine residues in mouse PrP23–231 that show reduced DEPC footprinting upon chelating with Cu(II), revealing the Cu(II) binding sites, which were further confirmed by a separate electron paramagnetic resonance (EPR) study.[693] Subsequently, the same group successfully extended the method to identify the Cu(II) binding sites in doppel (a glycosylphosphatidylinositol-anchored protein).[694]

In 2007, Sarkar and coworkers[695] applied DEPC footprinting in combination with EPR, UV and fluorescence spectroscopies to pinpoint the critical Cu(II) binding residues of human copper metabolism gene MURR1 (mouse U2af1-rs1 region1) domain (61-154) as His101, Met110 and His134. By adopting similar strategies, Zhao and Waite[696] investigated the metal-binding properties of mcfp-4 matrix protein in load-bearing junctions, Binolf et al.[697] characterized the Cu(II) anchoring sites in α and β-synuclein, Vachet and coworkers[545-546] located the Cu(II) binding sites in β-2-microglobulin and its pre-amyloid oligomers, and Karmakar and Das[698] identified the copper binding sites in αA crystallin.

Another relevant yet distinctive demonstration in 2009 is by Ginotra and Kulkarni[699], who characterized the solution structure of $Cu^{2+}(His)_2$ under physiological conditions. The coordination between Cu(II) and His in proteins occurs through a $Cu^{2+}(His)_2$ complex, whose coordination regime is either N4O4 or N3O2 donor atoms. The former was supported by various spectroscopic techniques in solution whereas the latter was favored from X-ray crystallography at a pH of 3.7. By DEPC labeling of $Cu^{2+}(His)_2$ complex under physiological conditions and MS identification, the investigators found the most abundant species was a three DEPC adduct, indicating that the $Cu^{2+}(His)_2$ complex exists in solution as a neutral five-coordinate structure with N3O2 donor atoms.

Protein binding with Zn(II) usually involves the canonical Zn(II) binding motif, termed a zinc finger, whereby a Cys thiolate is the chelating functional group.[700] Binding with Zn(II) greatly reduces the solvent accessibility of the cysteine side chains and slows the footprinting. Forest and coworkers[701] in 1999 investigated Zn(II) binding of the ferric uptake regulation protein from *E. coli* by using IAM footprinting. Among three reactive Cys residues, Cys92 and 95 are involved in the Zn(II) binding. The remaining Cys132 alkylates with the fastest reaction rate among the three, implying that it is surface-exposed and unbound.

In 2001, Apuy el al.[702] used cleverly designed NEM-based Cys labeling in a pulsed fashion. Their experiment established the relative cysteine thiolate reactivities of six zinc fingers in metal-response element-binding transcription factor-1 as F5 > F6 ≫ F1 > F2 ≈ F3 ≈ F4, indicating lower binding affinities for zinc fingers F5 and F6. This study is also an early

example of the use of isotopic encoding in protein footprinting whereby the investigators used h_5-NEM and d_5-NEM to allow a better quantification.

Atsriku et al.[703] in 2005 investigated the relative reactivities of Cys residues in the zinc finger of estrogen receptor by iodoacetic acid labeling and found that Cys 240 is more reactive than Cys 237, although both are located in the second zinc finger of the estrogen receptor. The differences in reactivities are explained by the unequal positioning towards basic amino acids that affects the thiol pK_a. Hanas and coworkers[704-705] in 2005 used a Cys_2His_2 zinc finger peptide, Sp1-3, as a model system to investigate the interaction between Zn(II), Au(I) and the zinc finger protein. In addition to identifying the binding site through Cys footprinting by IAM, the investigators determined the relative binding affinities between the zinc finger and Zn(II) and Au(I). Upon lowering the IAM concentration (100 μM), Zn(II) binding becomes distorted whereas the Au(I) binding was not affected at 100 μM IAM and was diminished at 500 μM IAM, a concentration that eliminates Zn(II) binding. These results indicate that the zinc finger in Sp1-3 binds tighter to Au(I) than to Zn(II).

Millhauser and coworkers[706] in 2007 characterized the Zn(II) binding properties of PrP (from Syrian Hamster) by DEPC footprinting. Syrian hamster PrP combines Zn(II) and Cu(II) binding in one protein; the Zn(II) binding, however, can change the overall Cu(II) redox properties by altering the distribution of copper ions among various binding modes. More importantly, DEPC footprinting coupled with a Zn(II) titration revealed the zinc binding affinity of prion protein 60-91, demonstrating new opportunities for targeted labeling reagents in the quantitative understanding of protein metal-ion interactions. Upon binding with Zn(II), the number of DEPC-reactive sites decreases, leading to a decreased DEPC footprinting as measured by MS. The system composition as a function of Zn(II) concentration (changed via a titration) can thus be monitored by quantifying the extent of DEPC footprinting and can be fitted by modeling to extract binding affinity.

Karmakar and Das[707] in 2012 footprinted α-crystallin by DEPC followed by MALDI-ToF analysis and identified His79, 107 and 115 as key Zn(II) binding residues in αA-cystallin whereas His104, 111 and 119 are critical for Zn(II) binding of αB-crystallin. Their method is limited proteolysis; regions in which Zn(II) is bound show missed cleavages in trypsin proteolysis because the Zn(II) binding stabilizes the region in which it binds and causes missed cleavages. In 2013, Russell and coworkers[708] used NEM labeling to map non-binding sites and to detect directly peptides containing the metal to locate the Zn(II) and Cd(II) binding to human metallothionein-2A. By combining bottom-up, top-down, and ion mobility approaches, the investigators not only identified the metal binding sites and binding orders but also provided insights on the structural transitions during the metal binding and demetallation in the gas phase. The idea of footprinting the metal chelating groups with targeted labeling reagents was also adopted to label specific cysteine residues by using reversible metal protection, which is important in protein engineering.[709]

In another study, Ramakrishnan et al.[710] characterized the Zn(II) binding sites of hepatitis B virus X protein (HBx) through HDX and NEM footprinting. HDX locates four peptides that exhibit decrease in deuterium uptake upon binding with Zn(II) whereas NEM footprinting

pinpoints the critical Cys residues that are responsible for the Zn(II) binding. Moreover, the NEM footprinting in this study was executed as a kinetic study, where the use of multiple NEM labeling times increased the confidence for identification of sites as is found with HDX kinetic curves and can provide some assurance that the protein structure is not perturbed (perturbation would give a change in kinetics). Time-dependent footprinting by targeted labeling reagents is discussed in section 4.3.

4.1.2. Protein Binding with Hard Metal Ions—In the case of hard ions, Ca(II) is one of the most characterized owing to its biological significance in signaling.[711-712] The canonical Ca(II) motif, an EF-hand, utilizes the negatively charged carboxyl groups in Asp and Glu inter alia to chelate Ca(II) ions.[679, 713] In a study by Zhang et al.[714] in 2012, the Asp and Glu residues in calmodulin (CaM) were footprinted by GEE in a method evaluation experiment. The Asp and Glu located on the EF-hands of CaM show reduced GEE footprinting upon binding with Ca(II), which is consistent with a SASA calculation of these residues. This study successfully demonstrates the efficacy of targeted labeling reagents in identifying hard-metal ion binding sites with high spatial resolution. By similar approach in the same year, Arata and coworkers[715] identified the Ca(II) binding sites in sarcoplasmic reticulum Ca^{2+}-pump ATPase by DEPC footprinting.

Very recently, Guo et al.[471] examined the Ca(II) and Mg(II) binding properties of CaM by BHD footprinting and MS analysis. Besides demonstrating the efficacy of BHD, a new footprinter, in identifying metal binding sites, the investigators used comparison of the modification extents between Ca(II)-bound CaM and Mg(II)-bound CaM to determine that the conformational changes of CaM induced by Mg(II) binding are less significant than those by Ca(II). Because the high resolution structure of Mg(II)-bound, full-length CaM is not currently available,[716] this study shows the opportunities for footprinting to assist in HOS studies where X-ray crystallography is difficult. Successful probing of the low affinity interactions between Mg(II) and CaM also shows the potential of using targeted labeling reagents in protein-metal ion analysis and illustrates again opportunities afforded by isotope encoding.

Although powerful, the uses of targeted labeling reagents in probing protein-metal interactions are not numerous. An important reason is that the metal-binding pocket is usually conserved, making the size of the labeling reagent critical. Another reason is that reaction rates between targeted labeling reagents and the residues are usually slow, making it challenging to characterize metal-binding systems with low binding affinities (whose metal ion off-rates are usually fast). Footprinting by using fast-labeling reagents, although an indirect method, can also overcome the above disadvantages to characterize protein-metal ion interactions, a subject to be covered in section 6.4.

4.2. Mapping Cys and Disulfide Bonds

Disulfide bonds are critical in protein folding and protein structural stabilization, making localization of disulfide bonds an important task. MS-based approaches contribute significantly to the determination of disulfide bonds.[717] Although many methods including plasma-induced oxidative cleavage,[718] ETD-based disulfide fragmentation,[719] electron-

transfer higher energy dissociation (EThcD)-based disulfide fragmentation,[720] UVPD-based disulfide fragmentation,[721-722] on-line electrolytic cleavage,[723] and ion mobility[724] were applied to characterize disulfide bonds, they either require advanced instrumentation or suffer from disulfide scrambling. Researchers also developed novel algorithms that identify disulfide bonds by examining MS/MS fragmentation patterns of disulfide-linked di-peptides.[725-726] Its application in unknown systems, however, is limited because the fragmentations are poor and the enrichment is challenging, problems that also confront cross-linking. Although classical, disulfide bond identification by targeted Cys labeling may be an effective and reliable approach, with potential for mapping disulfide bonds. Therefore, to illustrate opportunities in this area, we will review a few examples that are either pioneering studies or show novel workflows

The potential of MS in disulfide mapping was first demonstrated by Morris and Pucci[727] in 1985 remarkably with FAB-MS, where they identified disulfide-linked dipeptides by aligning the peptide masses with the protein sequence. Some of the early FAB-MS based efforts were reviewed by Smith and Zhou[728] in 1990. These methods evolved into quantitative assessments of free Cys and disulfide bonded by MALDI-MS, where a “count” of the free Cys residues in a protein can be made by analyzing the mass shift upon modifying the free Cys residues.[729-730]

To locate disulfide bonds is challenging and cannot be done universally with MS/MS because fragmentation is not always cooperative. In a pioneering study in 1996, Watson and coworkers[731] utilized 2-nitro-5-thiocyanobenzoic acid (NTCB) to footprint free Cys and cystine. NTCB is a cyanylation reagent developed by Vanaman and coworkers[732] in 1973, and it labels free Cys by replacing the hydrogen of the thiol with a cyanide. The cyanylated Cys undergoes backbone cleavage under alkaline pH (Scheme 13). The method is utilized by choosing specific peptide cleavages, guided by location of free Cys residues and determining the location of free Cys residues by analyzing the resulting peptides, here by MALDI-MS. Its application in disulfide mapping was by a differential approach, where the protein is footprinted by NTCB under both native and reduced conditions (TCEP was used for disulfide bond reduction). The Cys residues that are not cleaved under native condition but cleaved under reducing condition can be assigned to disulfide bonds.

Modern disulfide-bond footprinting makes use of the silence of Cys residues towards labeling reagents when they are covalently bound to form a disulfide bond. To distinguish disulfide-bonded and solvent-inaccessible Cys requires careful design and suitable control experiments. In one of the early applications in 2000, Glocker and coworkers[733] developed a general workflow to map disulfide bonds with targeted labeling reagents. They applied their approach to heat shock protein Hsp33, a redox-regulated molecular chaperone with six Cys residues. In its reduced state, all six Cys are in the thiol form, and the protein is not biologically active. Exposing the protein to oxidizing conditions promotes conversion of Hsp33 into its active form, during which the protein folds, assisted by formation of disulfide bonds. Upon IAM footprinting followed by MS analysis, all six Cys in reduced Hsp33 can be alkylated. In the oxidized state, however, Cys 232, 234, 265 and 268 are silent in IAM footprinting. Peptide-level MS analysis suggests that two disulfide bonds are Cys232-S-S-Cys234 and Cys265-S-S-Cys268. Cys141 was found to be highly reactive in both protein

states, indicating that it is not involved in disulfide formation. In contrast, the modification extent of Cys 239 decreased significantly but did not disappear for the oxidized state, suggesting that Cys 239 is not involved disulfide bonding but rather part of a significant conformational change, burying it upon Hsp33 activation.

In a 2009 study, Chumsae et al.[309] incorporated Cys fluorescence labeling with MS-based peptide mapping to study the unpaired Cys residues in human Immunoglobulin G subclass 1 antibody (IgG1). Although all 32 Cys in IgG1 can be involved in disulfide bonds, the presence of small amounts of free Cys is a common feature in recombinant and wildtype IgG1 antibodies. To differentiate the free and disulfide-bonded Cys residues, the IgG1 was first labeled with 5-idoacetamidofluorescein (5-IAF), a fluorescent reagent that reacts with free Cys residues. Subsequently, the 5-IAF labeled IgG1 was submitted to disulfide bond reduction and iodoacetic acid labeling. As a result, the free Cys residues are labeled with a fluorescence probe whereas the cystine residues are labeled with iodoacetic acid. Upon digestion, the peptides were submitted to LC separation, fluorescence detection, and MS analysis. As the free Cys residues are less abundant in IgG1, the fluorescence labeling improves the detection of free Cys-containing peptides. This study also is a good example of an integrated approach that addresses an important biological question (especially in pharma and biotechnology).

One year later in 2010, Weerapana and coworkers[734] developed an isotopically-encoded IAM derivative with an attached phenyl ring. The carbons of the phenyl ring can be either ^{12}C, the light form, or ^{13}C, the heavy form, to allow isotope encoding. A subject protein was first labeled to give the light form, tagging the free Cys resides. TCEP was then added to reduce the disulfide bonds, followed by a second stage of labeling where any Cys formerly in a disulfide bond is are now labeled by the heavy form. Although originally demonstrated for quantitative profiling of Cys reactivities in primary structure proteomics,[734-735] the idea of isotopic-encoded reagents is readily applicable in footprinting disulfide bonds. It avoids the problem of using two different reagents (one to label free Cys and another to label the disulfide-bonded Cys after reduction). The reactivities of two different reagents are seldom the same, leading to ambiguities in quantification. Isotopic-encoded alkylating reagents nicely overcome this drawback and add precision and efficiency.

More examples of targeted Cys footprinting in combination with MS peptide mapping with discussions of experimental protocols and issues of disulfide scrambling can be found elsewhere.[169, 736-737]

4.3. Characterizing Protein-Ligand and Protein-Protein Binding Interfaces

Among all biological questions that MS-based protein HOS elucidation can address, locating protein-protein binding interfaces is the most widely asked. Upon interacting with a binding partner, the solvent accessibility of the binding interface usually decreases, leading to a decreased footprinting. Here we present three examples of targeted protein footprinting where improved methodology was developed. Each example shows unique features from an analytical perspective.

During the past decade, carboxyl group footprinting by GEE has been adopted in characterizing the structure of antibodies as well as their interaction with antigens and drugs.[738-743] In a particular example, Li et al.[738] applied orthogonal MS-based footprinting approaches to characterize the interaction between the extracellular region of human interleukin-6 receptor α-chain (IL-6R) and two types of adnectin (adnectin 1 and 2) that bind with picomolar and nanomolar affinity, respectively. Different from labeling in many other studies, GEE footprinting was executed in a time-dependent manner (Figure 6a-c) as commonly seen in HDX studies. Region 135-138 becomes protected upon ligand binding (Figure 6a), and the differences are made more apparent by obtaining kinetic curves rather than relying on single time points. Subsequent MS/MS analysis indicates the GEE labeling is exclusively on residue Glu 140.

In comparison to region 135-148, region 274-284 becomes deprotected upon binding with adnectin 1 but does not change significantly when bound to adnectin 2 (Figure 6b). Region 27-41 was not involved in binding as the GEE labeling extents remain comparable with and without IL-6R binding. The investigators concluded that the adnectin 1 and 2 binding region is a flexible loop between two β-strands in the cytokine-binding domain of IL-6R, which was verified by other MS-based footprinting in this study. Besides demonstrating the advantages of applying orthogonal methods in characterizing a single protein system, the protocol executed the targeted labeling in a kinetic way, significantly enhancing the confidence in the data interpretation as compared with the commonly used single time point labeling.

In examples in 2008 and 2011, Kiessling and coworkers[744-745] developed isotope-coded affinity tag (ICAT) coupled targeted labeling reagent for protein footprinting. The bromoacetamide ICAT reagent, often used to alkylate free Cys residues, was repurposed for footprinting (Figure 7a). The idea of ICAT originates from proteomics,[746-747] where isotopic encoding enables absolute quantification, and the affinity tag facilitates post-labeling enrichment. Here the goal is to footprint the binding interface of adaptor protein CheW and the multidomain histidine kinase CheA (and its Cys-depleted form CheA*) in the *Escherichia coli* (E. Coli) chemotaxis signaling system. As protein-protein interactions in signaling systems are usually transient and low in affinities, it is necessary to add excess binding partners to the system to shift the binding equilibrium to the bound state. When the binding partner is a large protein, as exemplified by CheA, excess protein will create an intense protein/peptide background and potentially overwhelm the MS detection. The ICAT footprinting reagent enables post-labeling enrichment, making it possible to label the CheW under high CheA concentration without concern for the high CheA background during MS analysis.

The isotopic encoding enables accurate quantification. As depicted in Figure 7b, the complex is first footprinted by the heavy reagent, where all the solvent accessible Cys residues can be labeled. After a certain labeling time, the protein complex is denatured, and the light-reagent is added, during which those Cys residues that were originally protected can now be labeled by the light reagent. The sample is then digested and submitted to affinity enrichment. In this study, the Cys footprinting by heavy reagent was executed under multiple time points (t_{Alk}), and the relative fraction of a specific Cys residue under solvent-

accessible and protected states was quantified by comparing the signal intensities from a single injection of the heavy and light-labeled species. Alkylation rates of specific Cys residues can be obtained by plotting the fraction of labeling by the light reagent as a function of t_{Alk}, where a more abundant light-labeled fraction indicates a decrease in solvent accessibility upon binding with CheA.

In the experiment, CheA* is used instead of native CheA to minimize the effect of free Cys from CheA on the alkylation kinetics of CheW Cys residues. As there is no Cys in the CheW sequence, several mutants were expressed and purified, each with a single-site Cys mutation to facilitate the alkylation footprinting. Cys residues in CheW that show decreased alkylation rates upon mixing with CheA* are the binding sites, as exemplified in Figure 7d. Among nine mutants that were analyzed, four showed significant decreases in alkylation rates upon binding with CheA* (46, 48, 59, 60), indicating that these four positions of CheW are likely involved in CheA binding. The enrichment by ICAT not only offers a better quantification, but also enables the footprinting of transient and weak-binding partners. Taken together with the two earlier examples by Ramakrishnan et al.[710] and Li et al.[738], footprinting of targeted residues that were executed at multiple labeling times will significantly enhance the confidence of the data interpretation.

In a third study, Vachet and coworkers[546, 748] studied the pre-amyloid dimer and tetramer of β-2-microglobulin (β2m) by footprinting with different reagents. This study nicely demonstrates a canonical workflow and data presentation of protein HOS analysis by multiple targeted labeling reagents, where the focus is the differences between ligand-bound and ligand-unbound states, and the results are mapped onto existing structural models or used to construct a new model based on the footprinting results.

Like many other amyloid-forming proteins, β2m self-associates into fibrillar amyloid in the presence of Cu(II) and can be deposited in the musculoskeletal system. Because targeted labeling reagents are usually reactive with specific amino acid residues, a strategy of using several labeling reagents is effective to increase the amino acid coverage. By combining sulfo-*N*-hydroxysuccinimide acetate, DEPC, and 2,3-butanedione labeling, the investigators interrogated the N-terminus and Asn, Arg, His, Lys, Ser, Thr and Tyr residues in β2m. Comparison between the footprinting of β2m in monomeric and dimeric states suggests that the dimer interface is formed by antiparallel stacking of ABED β-sheets by two β2m monomers. Further, in-solution footprinting data rule out the interaction of D-D strands in the dimer, which is not consistent with a previously resolved X-ray crystal structure, emphasizing the need to use complementary HOS structural characterizations. In a subsequent study with similar experimental procedures, the interface of β2m tetramer was identified as D strands from one dimer unit and G strands from another dimer unit.[748]

Because β2m tends to aggregate, the same group also studied the binding sites of its amyloid inhibitors (e.g., rifamycin SV, structure depicted in Figure 8a), and the results are in Figure 8.[749] The changes in modification fractions upon binding with rifamycin SV (Figure 8a) show that four residues become protected (K6, K91, K94 and R97), whereas the N-terminus becomes more exposed. These results were mapped onto the β2m surface structure (Figure 8c) and compared with protein-ligand docking. The comparison strongly suggests a binding

pocket between Lys75 and Arg 97 (Figure 8d). Considering all the results, the authors concluded that rifamycin SV likely binds near Lys 94 and Arg 97 and perhaps near Lys 91, which is along the G-strand of β2m (Figure 8b). The mismatch between docking and footprinting is likely due to the structural perturbation of β2m induced by rifamycin SV; however, the similarity is encouraging. Two other ligands were also evaluated in a similar fashion.

Lastly, targeted labeling reagents were also adopted to footprint protein-nanomaterial interfaces to provide critical insights in the toxicity and potential biomedical applications of nanomaterials.[750-752] Determining protein-protein and related interfaces with fast labeling reagents is also attracting considerable attention, and this subject will be covered in section 5 and 6.

4.4. Assessing Topology and Stoichiometry through Chemical Cross-linking

Chemical cross-linking has developed as a complementary area of research owing to its capability to probe HOS and to locate and define protein/protein interfaces. Our intention, however, is not to review this topic comprehensively, but to describe the workflow, show how XL can be viewed as a means of footprinting (i.e., “double footprinting”), discuss its role in integrated approaches, and highlight some recent developments to unify the methodology described in this work.

Cross-linking mass spectrometry (XL-MS) is effective at assessing protein complex topologies and elucidating protein structures besides capturing protein-protein interactions. Conceptually, XL utilizes bifunctional labeling reagents to cross-link (footprint) the constituent proteins forming an interface, thus providing information on the interacting species and their interfaces. When dealing with large proteins, XL can also report on the overall protein conformation.

To date, most of the MS-based XL studies have been by a bottom-up approach, whose workflow is presented in Figure 9. Briefly, proteins are first incubated with chosen cross-linkers under the optimized conditions that are established usually by monitoring with techniques simpler than MS (e.g., gel electrophoresis). The tethered proteins are then submitted to enzymatic digestion, enrichment of informative peptides, and LC-MS/MS for separation and detection. The MS data are further analyzed by using search engines to identify cross-linked peptides with an uncertainty specified by mass tolerance and false discovery rate (FDR). Significant advances since 2008 in data analysis have facilitated this approach; new software includes but is not limited to pLink,[753] xQuest,[754] XlinkX[755] and StavroX[756]. Generated cross-link maps not only identify the connectivity of the adjacent protein subunits but also provide distance restraints as given roughly by the molecular separation between the two reactive functional groups of the cross-linker.

XL-MS alone is a middle-to-low spatial resolution approach because usually there are limited number of reactive residues at or near an interface of two proteins, and few crosslinks form. Young et al.[757] in 2000 showed that by combining XL distance restraints and computational modeling is a compelling way to improve the resolution for elucidating protein structures. The workflows can be adapted for integrative modeling[758-759] and *de*

novo structure prediction[760-761]. The major challenges of computational studies are the sampling and scoring of the generated models[762]. Larger data sets derived from XL-MS effectively decrease the size of the sampling space and benefit the scoring function, thus promoting efforts to find high-confidence models. Given there can be various reactive groups and spacer lengths on cross-linkers, a strategy involving multiple reagents should be taken to insure comprehensive information.

In 2014, Chait and coworkers[759] demonstrated the use of DSS and a zero-length EDC in characterization of the nuclear pore sub complex of Nup84. Two data sets generated from use of two reagents delivered different but complementary structural information that significantly benefited the subsequent model construction. Many other studies adopted similar ideas by combining amine-targeting reagents and carboxyl-targeting reagents (e.g., dihydrazides[669, 763]) or nonselective cross-linkers[764-765]. In addition, the use of reagent combinations with different spacer lengths is recommended because short cross-linkers yield fewer cross-links but with narrower distance restraints, whereas long cross-linkers afford more cross-links but less structural definition because the distance assignments are over a broader range.[762]

New sample preparation methods also have developed rapidly (e.g., on-bead cross-linking[761]), improving the cross-linking chemistry and providing better analysis sensitivity. Many examples are discussed in recent reviews.[658, 766-767]

By way of contrast, footprinting by targeted and free-radical reagents and/or by HDX maps solvent accessible regions and reflects differences in protein dynamics or binding events. This information provides deeper understanding of the entire protein structure, not just interfaces, and can adjudicate constructed 3D models from XL for in-solution proten.[768-770]

XL is not limited to structural characterization of single protein complex, but rather it can promote protein-protein interactions (PPIs) studies in proteome-wide investigations.[771-774] To meet the need for understanding the roles, functionalities and mechanistic behavior of many protein complexes through their PPIs maps, cleavable XL reagents have been developed,[775] simplifying and increasing the accuracy for identification of cross-linked peptides. Incorporation of affinity groups and sophisticated enrichment procedure have led to success; examples are studies performed on E. coli[773] and Caenorhabditis elegans (*C. elegans*)[774]. For example, the Heck group[776] reported a XL-MS study of whole human cell lysates in which they identified 2179 unique cross-links. These protein complexes (e.g., 80S ribosomal core complex) reveal novel interactions and provide new structural insights.

To summarize, the increasing number of publications based on XL-MS continue to demonstrate its utility in MS-based biophysics, particularly in combination of other techniques. Integrating XL with other methods enables characterization of dynamic biological systems even of heterogeneous systems. The continuing development of cross-linkers will increase applications. Reagents that react more rapidly and target more and more amino acids, and instrumentation advances that provide new fragmentation methods in MS/MS (e.g., CID, ETD, EThCD and UVPD), are expected for the future. Furthermore, improved separation and enrichment procedures will accommodate the increasing mixture

complexity following XL and digestion and allow detection of low abundant yet informative cross-linked species.

4.5. Footprinting Fast Kinetic Processes

Given the high reactivity of the Cys thiol group, specific labeling reagents were also developed to follow protein folding in addition to footprinting a static state.[777] An early application addressed slow events in the folding of recombinant human macrophage-colony stimulating-factor β, which takes tens of hours to complete.[778] Melarsen oxide (*p*-(4,6-diamino-1,3,5-triazin-2-yl)aminophenylarsonous acid) used in this study footprints Cys in 10 min, which is sufficiently fast for this slow folding system but far too slow to footprint most protein folding.

To shorten the footprinting time scale and make Cys footprinting capable of monitoring protein folding pathways in general, other reagents, methyl methanethiosulfonate (MMTS)[779] and DTNB,[316] were applied because they react with Cys on the time scale of millisecs. Furthermore, the steric sizes of these reagents can provide insight on the structural changes during conformational opening/closing.[780] These reagents were successfully applied in a pulse-labeling approach to follow unfolding of apo-myoglobin.[781-782]

In an elegant demonstration of specific amino acid footprinting, Jha and Udgaonkar[783] in 2007 applied pulse Cys labeling by MMTS to study the fast folding reaction of barstar. Tracking the labeling of ten Cys residues as a function of refolding times showed that four remain solvent-accessible throughout the folding. The other six Cys residues become protected upon folding, and their rates of reaction vary by 3-fold and are dependent on their locations in the protein. The investigators showed the general workflow of MS-based protein folding analysis and demonstrated footprinting with a single residue can provide sound information. Unfortunately, Cys is the only residue that can be labeled on the millisecond time scale, probably because both the -SH group and the reagent are reactive. A workaround may be to express the protein with more Cys residues located strategically to inform on the roles of various regions. The downside is that the proteins may respond to these substitutions to adopt a non-native state. Thus, a general approach to study folding by specific amino acid labeling will be difficult to achieve. Moreover, labeling times are still too long for probing short lived intermediates and fast folding. Fast free radical labeling reagents can overcome these drawbacks, as will be discussed in section 6.2.

In an unusual approach to fast reactions, McLuckey and workers[784-787] starting in 2009 demonstrated the covalent labeling of peptides in the gas phase. They illustrated the reactions between peptides and 4-formyl-1,3-benzenedisulfonic acid (reacts with primary amines),[784] NHS-ester (reacts with primary amine and carboxylates),[785-786] Woodward's Reagent K (reacts with carboxylic acids)[787]. Although not yet applied in gas-phase protein footprinting or folding, this approach is potentially advantageous because gas-phase ion reactions are rapid, sometimes even collision controlled. A disadvantage is that reactions in the gas phase may not be relevant to in intro and in vivo biochemistry.

4.6. Footprinting in vivo

It can be questioned whether protein biophysical properties and their HOS obtained in vitro are truly reflective of those in vivo as the native environment in which a protein functions are challenging to reproduce outside a living cell. Thus, protein HOS analysis in vivo is a long-sought goal of protein biophysics. Macromolecular crowding within the cell limits the diffusion of the protein molecules, and that further affects the biophysical properties of proteins including their interactions with nucleic acids and their reaction kinetics and association rates with their binding partners.[788-789] Protein footprinting in vivo may be the solution. When one recognizes that the expanding capabilities of MS-based proteomics analysis permit deeper and deeper analysis of an entire proteome, the goal of in vivo footprinting comes closer to realization.

Early developments of protein in vivo labeling primarily focus on the localization and quantification of proteins in the cellular environment. For localization purposes, a common practice is to attach fluorophores covalently to the target proteins.[790-791] The fluorophores can be either small organic molecules[792] or proteins[793], which then illuminate under a fluorescence probe. The labeling can be non-covalent and mediated by an engineered ligand that has a fluorophore attached.[794-795] Here the labeling efficiencies are generally low but relatively specific. Recent demonstrations couple FRET with protein in vivo labeling (semisynthetic protein switches) to allow characterization of PPIs and protein conformational changes.[796] Despite success in protein engineering and controlling the functions of proteins, these approaches have low structural resolution and sometimes low sensitivity that limit applications in protein HOS analysis.[790]

Protein labeling in vivo coupled with MS are used for quantification in proteomics and metabolomics. These approaches almost always involve isotope encoding for increasing accuracy and speed. Although these methods are used more and more, their goal is not structural information. For this reason, and because these approaches were reviewed elsewhere,[797-799] they will not be discussed further.

High resolution protein HOS analysis in vivo is challenging. Among all three high-resolution approaches, NMR has the richest history of characterizing proteins in vivo.[800] Because a protein's X-ray structure cannot be acquired under native conditions, that approach holds little promise. Macromolecular crowding makes it almost impossible to obtain cryo-EM images for a specific protein of interest under in-cell conditions.[801] Protein footprinting in vivo was first done by cross-linking, which can elucidate topological features of protein and protein complexes and capture PPIs to reveal their biological functions. Implementation of cross-linking chemistry in the native environments are challenged by the heterogeneity and complexity of the cross-linked products.[802-803] The Bruce lab[804] in pioneering efforts starting in 2009 developed a series of MS-cleavable cross-linkers (i.e., protein interaction reporter (PIR)) that undergo characteristic fragmentation during CID, thus providing more precise cross-links identification. To optimize the acquisition of fragments for MS3 sequencing, the investigators developed a real-time analysis for cross-linked peptides technology (ReACT).[662, 805] In addition to biotin-based enrichment, ReACT has been successfully applied to XL in many organisms (e.g., *Shewanella oneidensis*,[804] *E. coli*,[806] *Pseudomonas aeruginosa*,[807] *Acinetobacter baumannii*,[808] and *human cells*[809]).

Other cleavable cross-linkers are also available (e.g., *bis*(succinimidyl)-3-azidomethylglutarate (BAMG)[810] and azide-A-DSBSO[811]).

Recently, Liu et al.[812] characterized the interactome of native mouse-heart mitochondria with DSSO and identified 3322 unique physical contacts, the largest survey to date of mitochondrial proteins interactions. In vivo cross-linking experiments reveal localization of many subunits and provide evidence for coexisting respiratory super-complex assembly.

In other demonstrations, Blankenship and coworkers[813-814] combined in vivo XL-MS with time-resolved spectroscopy and characterized a fully functional megacomplex composed of a phycobilisome antenna complex and photosystems I and II from the cyanobacterium *Synechocystis PCC 6803*. More applications and progress have been reviewed lately.[803, 815] Although XL-MS has shown its effectiveness, there are still many challenges raised by the complexity of biological systems. More and better methodologies in the sample preparation, enrichment and MS detection will allow more comprehensive characterization of interactomes, providing another dimension of information to understand the molecular machinery that impacts living systems.

Another approach to in cell footprinting is illustrated by the investigation of the membrane protein human vitamin K epoxide reductase (hVKOR) by Li, Gross, and coworkers.[816] Membrane proteins are appropriate targets for in vivo footprinting, because retaining their native structures in vitro can be challenging, especially for complexes with multiple subunits.[817] Although native MS allows probing non-covalent interactions associated with membrane proteins, structural information is hard to obtain with this approach.[151, 818-819] In the study of hVKOR, Li and coworkers[816] targeted an intramolecular disulfide bond (Cys51-Cys132) that stabilizes a key intermediate redox state, a state that can perturbed by binding with warfarin, a highly prescribed drug to prevent blood clotting. In brief, h_5-NEM was added to penetrate live cells and footprint free Cys in the native environment. After lysing the cells, the remaining disulfide bonds were reduced and labeled with d_5-NEM to footprint the newly reduced Cys (Figure 10a) in a methodology discussed in Section 4.2. The sample was submitted to LC-MS and MS/MS for identification (Figure 10c-d). The partition of a specific Cys residue in its free and disulfide-bounded states can be obtained by quantifying the ratio of its h_5-NEM and d_5-NEM labeled species (peak intensities in the MS spectra), defined as “apparent oxidized fraction” (Figure 10b).

To facilitate a differential footprinting to illustrate whether a specific Cys residue prefers the free or disulfide-bounded state in the native cellular environment, the experiments were executed in two different conditions, illustrated in Figure 10b as “native” and “DTT”. The “native” state denotes the footprinting under native cellular environment as mentioned above. The “DTT” state, however, was executed under reducing conditions. Upon admitting DTT to the cell, the disulfide-bound Cys residues under native state were reduced and footprinted by h_5-NEM. As a result, apparent oxidized fractions for the disulfide-bounded Cys residues decreases under “DTT” state as compared with “native” state, as seen for Cys43, 51, 132 and 135. The remaining three Cys residues (Cys16, 85 and 96) do not show decreased apparent oxidized fractions, indicating that these three Cys residues are in reduced state (free Cys) under native cellular environment. By such approach, the investigators were

able to elucidate the native architecture of hVKOR, reveal the electron-transfer pathway, and propose an hVKOR catalysis inhibition mechanism by the ligand warfarin. A subsequent paper summarizes the precautions, technical difficulties, and advantages of *in vivo* membrane protein footprinting.[820]

In another demonstration, Li, Gross, and coworkers[821] applied *in vivo* carboxyl group footprinting to probe formation and breakage of the salt bridges that are hypothesized to transport carbohydrates of human glucose transporters (GLUTs). By footprinting with isotope-encoded reagent GEE, they identified key salt bridges in GLUT1 on both its intracellular and extracellular sides. Subsequent mutation of the residues involved in salt bridges lead to a significant substrate uptake deficiency of the cell, providing confirmation that salt bridges serve as molecular switches. The investigators conducted footprinting under different substrate conditions to reveal the gating mechanism of the transporter as well.

MS-based *in vivo* footprinting, as a probe of protein solvent accessibility, offers structural evidence that can be directly related to functional states. A challenge is the complexity introduced by the high crowding of intracellular components, requiring use of large quantities of reagent that must be admitted to the cell. The dynamic range of cell proteins is high, and following low-abundance proteins also offers challenges. Nevertheless, the success in answering focused questions in a few examples demonstrate that protein footprinting in vivo by targeted labeling reagents has significant promise. Like in vivo cross-linking, better strategies in post-labeling sample enrichment will enable broader adoption of this method.

4.7. Integrating Footprinting with other Approaches

Each of the methods reviewed here has limitations that may be overcome by combining with other methods. Integrating footprinting with other approaches is most seen with XL, owing to the limited structural resolution of XL but also its distance restraints that can be readily used as inputs in modeling.

To construct better a 3D model to near-atomic resolution, the XL platform can be coupled with electron microscopy[822-823] and X-ray crystallography.[759-760, 824] Electron density maps often show areas that diffract poorly because they are flexible or heterogeneous. To localize each subunit accurately, restrained distances can be contributed by XL-MS. One compelling example is reported by Greber et al.[825], who determined the architecture of the porcine 39S large proteome in the mammalian mitochondrial ribosome. A previous cryo-EM structure was resolved at 4.9 Å. Many of the protein extensions (a sequence change extending the amino acid sequence at the N- or C-terminal end with one or more amino acids) that do not have homology models cannot be refined at this resolution. In a combined approach, distance restraints from XL can be used in refining structure considerations, leading to a higher spatially resolved model (at 3.4 Å). The better-described protein assembly now reveals many interaction “hotspots” (e.g., the active site of peptidyl transferase and the path of its idiosyncratic exit tunnel). Integration of native MS and XL-MS can lead to remarkable structure elucidations[826-829] of macromolecular assemblies that are usually difficult to purify and crystalize by traditional methods. Native MS can determine topology and stoichiometry of protein complexes. The approach is even more effective when combined with ion mobility MS, although direct determination of the critical binding residues is nearly impossible. On

the other hand, XL-MS reveals the topology and connectivity of interacting regions by using solution chemistry and gas-phase analysis (via MS). The two strategies complement each other by providing architectural information of multiprotein assemblies.

Because cross-linking occurs via strong, covalent bonding, integrating it with other approaches may allow detection of transient protein-protein interactions that are hard to investigate otherwise. For example, the yeast initiation factor 3 (eIF3) protein, consisting of six subunits, regulates translational processes as a scaffold for many initiation factors. The molecular architecture, however, is elusive owing to its dynamic nature. Politis et al.[830] in 2015 determined the composition of the complex by sequentially dissociating subcomplexes, monitoring them by native MS, and coupling that information with physical contacts and approximate distances taken from cross-linking. The integrated information was encoded as connectivity restraints for scoring purposes in the model generation. The outcome is a high-resolution, 3D topological model of eIF3 assembly in complex with eIF5. To preserve the transient and dynamic interactions, a two-step cross-linking protocol was utilized, in which formaldehyde fixation is implemented at sub-stoichiometry levels prior to initiating the cross-linking chemistry.[831] Structural stabilization of this type greatly facilitates cross-link formation and can be reversed at high temperature before MS identification.

Other MS-based footprinting methods have also been used in conjunction with XL-MS (e.g., footprinting by targeted labeling reagents[832] and HDX[768, 833-835]). In one example, Zhang et al.[768] evaluated the combination of HDX, XL-MS, and molecular docking for characterization of the binding interface of interleukin 7 and its α-receptor. HDX reports widespread protection in the receptor. There is, however, no differential evidence of binding-induced protection or remote conformational change. By employing different reagents in XL, the investigators significantly increased the spatial resolution of binding site assignment. To generalize the integrated approach, protein-protein docking was executed with different number of crosslinks as distance restraints. With model clustering and HDX adjudication, a high confidence model was obtained with root mean square deviation (RMSD) below 2.0 Å (with respect to the known crystal structure) with only two crosslinks.

Integrated methods can now play a role in protein structural modeling. By utilizing the structural restraints from DEPC labeling, cross-linking, and native MS for protein structural modeling, Politis and coworkers[832] in 2017 successfully constructed structural models of several protein complexes, tryptophan synthase, carbamoyl phosphate synthetase, and the double heterohexameric ring RvB1/2 with high-resolution subunit structures. A comparison of a representative model for tetrameric tryptophan synthase derived from all available structural restraints and its corresponding crystal structure (Figure 11) show agreement with a RMSD of 9.6 Å. Systematic evaluation of the modeling show that restraints from DEPC labeling and chemical cross-linking markedly increase the predictive power.

The workflow was tested by employing three model systems and then applied to a study of the F-type ATP synthase from spinach chloroplasts, a protein complex without a high-resolution structure. By integrating these experimental measurements with molecular dynamic simulations, the conformational states of the peripheral stalk as well as the flexible

regions within the complex were revealed. This work demonstrates the potential of MS-based footprinting data to aid computer modeling.

In other work in 2019, Aprahamian and Lindert[836] describe in detail a Rosetta script that utilizes DEPC footprinting data to provide better restraints in protein structure predictions. Restraints from cross-linking can direct the modeling of protein complexes with multiple subunits; however, the short supply of modifiable residues for DEPC labeling constrained the SASA information. Fast labeling reagents (radicals) generally modify multiple residues in a single footprinting experiment that overcomes this drawback. More details about computer-aided protein structural modeling and radical footprinting-aided protein structural predictions can be found in section 6.6.

4.8. Conclusion

To conclude, protein footprinting by targeted labeling reagents has been utilized to address a number of biological questions and is considered as a powerful tool for MS-based protein HOS analysis. As mentioned at the beginning of the section, two major disadvantages limit its broad application. The limited targeting residues can be overcome by developing and adopting novel labeling reagents. Fast radical species can also complement such limitation, as discussed in section 5 and 6.

Another question is whether the targeted protein undergoes a conformational change in the early stages of labeling and then continues to be modified to yield a composite and misleading footprint. In a study of interferon-β1a, Kaltashov and coworkers[837] demonstrated that alkylation of Cys17 induces steric clashes within the native structure, as seen by the unfolding of helix D containing a 88-102 segment. On the contrary, there are also numerous studies to support the validity of targeted protein footprinting, either by a combination of multiple footprinting approaches[738, 838-839] or by comparing the targeted footprinting results with crystal structures[169, 540, 840]. In a particular example, Li et al.[738] used HDX, GEE footprinting and hydroxyl radical footprinting to study the binding region of IL-6R to adnectin 1 and 2. All three footprinting approaches suggest the same binding region of 135-141. In other words, the validity of the slow but targeted GEE labeling is supported by two other protein footprinting approaches that functions at different time scales (20 s to 10 min for HDX, sub-millisecond for hydroxyl radical footprinting).

The contradicting judgements on the effectiveness and validity of protein footprinting by targeted reagents are system dependent. In selected systems, modification of critical residues will induce catastrophic protein conformational changes. It is thus important to characterize a protein system with multiple footprinting approaches. Different labeling time scales of these approaches can also be utilized to provide complementary and synergistic understanding of a protein's HOS.[839]

5. Fast Labeling Reagents – Reactive Radical Species

Thus far, we reviewed two means of footprinting: HDX and specific amino acid labeling. Both involve covalent labeling, but HDX footprinting is reversible, imposing constraints on protein and peptide analysis to minimize back exchange. HDX is less disruptive of protein

structure than specific amino acid labeling because it occurs in medium in which H_2O has been replaced by D_2O. The concentration of the "reagent" D_2O is 50 M, a concentration that changes negligibly over the time of footprinting. Exchange occurs by pseudo first order kinetics on the microsecond to many hours time scale. The coverage is nearly complete, including all the common amino acids except Pro, and the modifications that are counted occur on the peptide backbone.

In contrast, specific amino acid labeling has low coverage, modifying one or a few amino acid side chains. Some reagents that modify $-COO^-$ or $-NH_3^+$ groups change the local charging of the protein; other reagents add bulky steric hinderance to the protein (even as large as another protein), both modifications posing a danger of structure disruption. Although a few footprinting reactions occur on the millisecond time scale, most require minutes or more during which the modified protein can change conformation and continue to react and produce a footprint that is composite. The concentrations of reagents are 10^2 to 10^4 times greater than that of the protein, unlike HDX where the concentration of D_2O is approximately 10^7 times greater than that of the protein. Considering that a large protein could have 10^3 potentially reactive amino acid residues, the reagent concentration may change, causing the reactions to have mixed kinetics.

The third class of footprinting reagents, fast labeling regents, enjoys features of HDX and specific amino acid labeling but has some important advantage over both. The modifying reagents are usually radical species that react with solvent-accessible amino acid residues to report on protein SASA. This form of footprinting shares characteristics with both HDX and specific amino acid labeling. Given the high reactivity of radical species, the labeling time can be as short as μs,[841] which makes possible the fastest footprinting available to follow protein dynamics, providing a "snapshot" of the protein SASA with residue-level resolution for those residues that react. Fast footprinting can also probe protein folding/unfolding. The theoretical coverage is broader than that of specific amino acid labeling, but it is nearly impossible to realize the coverage of HDX because the reactivity between radicals and the side chains can vary by ~ 10^3, and the reactions will emphasize the more reactive side chains. The reagent concentrations are 10^2 to 10^3 times to that of a protein; for large proteins and reactive reagents, the free radicals will become limiting reagents. Both specific amino acid labeling and free radical labeling usually produce irreversible modifications, thereby facilitating effective protein isolation and digestion prior to the MS analysis.

In this section and the next, we will review all available fast labeling reagents and describe their generation, development, biological relevance, and application in protein footprinting. We will also discuss their advantages and limitations.

5.1. Hydroxyl Radical

Hydroxyl radical ($^{\bullet}OH$) was initially used for nucleic acid footprinting, where it reacts with solvent accessible hydrogens in deoxyribose (DNA) and ribose (RNA), cleaving their nucleic acid chains.[164] The motivation is to footprint nucleic acids, to reveal their SASA and determine their HOS, and to map protein DNA/RNA interactions. Later, the idea was extended to protein footprinting. For DNA/RNA footprinting, the approach is based on

selective cleavages, whereas with protein footprinting, the approach is based on chemical modifications. Today, ●OH has become the most used fast labeling reagent.

5.1.1. Biological Relevance—The hydroxyl radical is a naturally occurring reactive oxygen species (ROS) that participates in several cycles that regulate several physiological functions of living organisms.[842-844] Early studies identified the important signaling role of ●OH in regulating several physiological functions of living organisms, especially its contribution to retrograde redox signaling from organelles to the cytosol and nucleus.[842, 844] The size and hydrophilicity of ●OH are similar to those of the water molecule,[845] allowing it to probe the SASA of biomacromolecules (to travel where water can travel). The oxidative damage in many pathologies caused by ●OH naturally and in radiation damage attracted early attention, motivating determination of its rate constants[170, 846] and mechanisms[847] in reactions with amino acids. The reaction rate constants between ●OH and amino acids range from 1.7×10^7 to 3.5×10^{10} $M^{-1}s^{-1}$ with preference toward aromatic, heterocyclic and sulfur-containing sidechains (Table 1). The broad residue coverage in ●OH reactions contrast significantly with the targeted or specific labeling reagents covered above. The early fundamental studies, likely driven by radiation concerns, form a solid foundation for the use of ●OH in protein footprinting, contributing to its growing applications.

5.1.2. Generating ●OH in Solution—The generation of ●OH has a long history, during which many different methods were developed. In this section, only methods that are useful for footprinting biomacromolecules will be reviewed. Early approaches made use of ●OH-induced protein backbone cleavages,[164] similar to those in nucleic acid footprinting. Upon cleavage, gel electrophoresis was used to determine the cleavage sites. Low cleavage efficiency, lack of accurate mass determination, and low precision greatly limits the further development of such an approach; thus, it will not be covered in detail.

5.1.2.1. Fenton and Fenton-like Chemistry: The catalytic property of Fe(II) in promoting the oxidation of tartaric acid by hydrogen peroxide (H_2O_2) was first reported by Fenton in 1894.[848] Later on, Cu(I), Ti(III), Co(II) and Cr(III) were found to behave similarly.[849-852] Such processes were later called Fenton reactions. Although it was supposed that ●OH is the key reactive species in Fenton chemistry, it was not well established until Haber and Weiss[853-854] first proposed a chain reaction mechanism in 1932. The understanding of the mechanism was later expanded by Barb and coworkers[855-856], and it is now referred to as “classical Fenton pathway”, as summarized in Eq. 2-8 below.

$$Fe^{2+} + H_2O_2 \rightarrow Fe^{3+} + \bullet OH + OH^- \quad (2)$$

$$Fe^{3+} + H_2O_2 \rightarrow Fe^{2+} + HO_2^{\bullet} + H^+ \quad (3)$$

$$H_2O_2 + \bullet OH \rightarrow HO_2^{\bullet} + H_2O \quad (4)$$

$$HO_2^{\bullet} \leftrightarrow O_2^{-\bullet} + H^+ \quad (5)$$

$$Fe^{3+} + HO_2^{\bullet} \rightarrow Fe^{2+} + O_2 + H^+ \quad (6)$$

$$Fe^{3+} + O_2^{-\bullet} \rightarrow Fe^{2+} + O_2 \quad (7)$$

$$Fe^{2+} + {\bullet}OH + H^+ \rightarrow Fe^{3+} + H_2O \quad (8)$$

In Fenton chemistry, ●OH is generated by oxidation of Fe(II) and Fe(III) with H_2O_2 (Eq. 2 and 3). This chemistry is not optimum for footprinting biomacromolecules. For example, the reaction has an optimal rate at pH of 3 – 4,[855-856] which is clearly denaturing for many biomolecules. Under physiological conditions, however, Fe(III) readily precipitates.

In 1985, Tullius and Dombroski[857-859] proposed an elegant system that utilizes Fenton chemistry to map DNA-protein binding sites. By incubating Fe(II)-ethylenediaminetetraacetic acid (Fe(II)-EDTA), H_2O_2, and ascorbate with DNA, they achieved an effective footprint after a few minutes. The approach exploits Fenton chemistry in two ways. First, with EDTA as chelators for Fe(II) and Fe(III), the solubility of these ions under physiological pH increases significantly. EDTA also minimizes the binding of these ions to biomacromolecules and increases their catalytic efficiency.[860] Second, ascorbate can reduce Fe(III)-EDTA back to Fe(II)-EDTA, fulfilling a cycle. Thus, the Fe(II-EDTA)/H_2O_2/ascorbate Fenton system had become the usual approach for footprinting, and it was applied in many subsequent DNA footprinting studies.[861]

For protein footprinting, the system was first applied to footprint cAMP receptor protein under backbone-cleavage conditions by Heyduk and coworkers[862] in 1994, and then by Sharp and Hettich[863] in 2003, who extended oxidative labeling to apo-myoglobin by using ●OH to map amino acid side chains as a measure of their SASA. A more recent variation on this theme by Monroe and Heien[864] combines electrochemistry with this classical reaction in which an electrical flow cell was used to reduce Fe(III) to Fe(II), thus completing a cycle. Footprinting of ubiquitin demonstrated the efficacy of such method in probing protein SASA.

Another powerful approach using Fenton chemistry was first demonstrated by Rana and Meares[865-867] in 1990. As a replacement of Fe(II)-EDTA in a classical Fenton system, they synthesized a novel class of reagents represented by Fe-(*S*)-1-(*p*-bromoacetimidobenzyl)-EDTA (Fe-BABE). Fe-BABE is composed by three structural units (Scheme 14), a metal-chelating unit that binds with reactive metal centers to facilitate ●OH generation, a sulfhydryl reactive unit that reacts with cysteine residues on proteins, and a linker separating them. The design localizes the Fe-BABE in a specific position of a protein. Upon incubating with H_2O_2, ●OH is only generated in close proximation with the localized metal center. Fe-BABE has the advantage of high conjugation rate with proteins, high anchoring yield, and compatibility with neutral pH, making such site-directed ●OH footprinting effective in

probing spatial relationship in protein-nucleic acid[868-870] and protein-protein[871] complexes. Very recently, this approach was adopted for characterizing protein-carbohydrate interactions,[872] whose details will be discussed in Section 6.7.

Fenton chemistry is probably the most easily accessible method for ●OH protein footprinting, as it can be achieved without the help of sophisticated instruments. The biological relevance of iron makes it "friendly" with most biological systems, as demonstrated by in vivo footprinting of the membrane protein porin OmpF.[873] Moreover, given that multiple reactive metal centers can initiate Fenton-like reactions, successful ●OH protein footprinting can be achieved by using Co(II),[874] Cr(III),[874] Ni(II),[875] Cu(II)[876-877], and Mn(II)/Mn(III) for generating ●OH upon reaction with H_2O_2.[851] This general property makes Fenton-like chemistry worth considering to footprint proteins that bind to these active metal centers.

On the other hand, ●OH generation by Fenton chemistry usually takes minutes, during which the protein may get over labeled and alter its conformation during the footprinting owing to the changes in hydrophilicity or perhaps to some modification of amino acid residues with low SASA.[878] Once the protected region becomes exposed, additional ●OH can further label the newly-exposed sites, generating a misleading readout. Newer ●OH generation approaches usually label proteins on the time scale of milliseconds or less to minimize over labeling. Although a subsequent study employing Fenton chemistry achieves a steady ●OH concentration at 2 ms, the amount of H_2O_2 (30%) required is certainly stressful to most biomacromolecules.[879]

5.1.2.2. Synchrotron Water Radiolysis: A synchrotron X-ray source is capable of delivering a continuous spectrum of $10^{14} – 10^{15}$ photons per second with energies ranging from 5 to 30 kV.[880] Implemented by Chance and coworkers[881-883], synchrotron-based ●OH footprinting was first demonstrated for nucleic acids and later for proteins[884]. The latter initiates the modern era for protein footprinting by fast-labeling reagents because, for the first time, the labeling timescale was reduced to milliseconds.[845] Mechanistically, synchrotron X-rays utilize water as the ●OH precursor. High energy photons ionize water to produce hydrated electrons (e_{aq}^-) and activated water (H_2O^*), and these initiate the subsequent reactions as summarized in Eq. 9-11 below.[170]

$$2H_2O + e^- \text{ (ionizing irradiation)} \rightarrow H_2O^{+\bullet} + H_2O^* + e_{aq}^- \quad (9)$$

$$H_2O^{+\bullet} + H_2O \rightarrow \bullet OH + H_3O^+ \quad (10)$$

$$H_2O^* \rightarrow \bullet OH + H^\bullet \quad (11)$$

Besides labeling solvent-accessible amino acid side chains in the protein, ●OH undergoes quenching reactions due to its high reactivity. Under anaerobic conditions, primary quenching is a self-recombination at a diffusion rate limit (Eq. 12 - 13).[885]

$$\bullet OH + e_{aq}^{-} \rightarrow OH^{-} \quad (12)$$

$$2^{\bullet}OH \rightarrow H_2O_2 \quad (13)$$

Under aerobic conditions, oxygen is involved in the quenching process, leading to other ROS (Eq. 14-15).

$$e_{aq}^{-} + O_2 \rightarrow O_2^{-\bullet} \quad (14)$$

$$H^{\bullet} + O_2 \rightarrow HO_2^{\bullet} \quad (15)$$

In subsequent studies, $^{\bullet}$OH dosimetry, the effects of different buffers, different beam currents and other additives in the system were thoroughly investigated.[886] These efforts were comprehensively reviewed elsewhere.[170]

Synchrotron-based water radiolysis has significant advantages in protein footprinting, as it utilizes water as $^{\bullet}$OH precursor. Water concentration is ~55 M, and it is not limiting. Although water interacts with proteins, there are many more molecules that constitute bulk, and this may not be the case for other radical sources. More importantly, water is the medium for biological systems, and its use simplifies the experimental procedure. The fast labeling speed, easy dose control (by controlling exposure time with a shutter[886]) and high reproducibility all contribute to its utility. An obvious downside is there are limited synchrotron sources. A recent development of a new beamline should make the method more powerful and more accessible than in the past to the general research community.[887]

5.1.2.3. Laser Photolysis of Hydrogen Peroxide: Upon exposure to UV around 250 nm, H_2O_2 homolytically cleaves into two $^{\bullet}$OH with a primary quantum yield of 0.4 – 0.5.[888-889] In the absence of reactive substances, the resulting $^{\bullet}$OH reacts with the H_2O_2 that did not undergo photolysis as shown in Eq. 16-18.

$$H_2O_2 \rightarrow 2\bullet OH \quad (16)$$

$$\bullet OH + H_2O_2 \rightarrow H_2O + HO_2^{\bullet} \quad (17)$$

$$HO_2^{\bullet} + H_2O_2 \rightarrow H_2O + O_2 + \bullet OH \quad (18)$$

The rate constants for the latter two reactions are 2.7×10^7 and 7×10^9 $M^{-1}s^{-1}$, respectively.[889] Large reaction rate constants guarantee fast labeling.

In 2004, Sharp et al.[890] first footprinted lysozyme and β-lactoglobulin by ●OH generated from H_2O_2 photodissociation. For this protocol, the protein sample contains 15% H_2O_2, and the Irradiation (by a UV lamp) takes up to 5 min. This high H_2O_2 concentration is stressful to many proteins. Moreover, the long labeling time is a risk that the system will be over labeled, as discussed above.

To reduce the labeling time and lower the H_2O_2 concentration, Aye and Sze[891] replaced the UV lamp with a pulsed Nd:YAG laser that operates at 266 nm (frequency quadrupled). They used a light pulse energy of 2 mJ/pulse and a pulse width is 3-5 ns in a static system. H_2O_2 was added to 0.3% just prior laser irradiation to minimize exposure of the protein to a mild oxidizing agent. The residue H_2O_2 after irradiation was removed by snap-freezing and lyophilizing the aliquot (possibly a source of error as protein oxidation by H_2O_2 can occur in the solid state at low T as reported later[892]). These improvements over Fenton chemistry combine to achieve a moderate oxidation of ubiquitin with a single laser shot. As compared with Fenton chemistry, the H_2O_2 concentration and labeling time were both reduced significantly, allowing a higher confidence of the result.

At the same time, Hambly and Gross[841] reported a method that couples H_2O_2 laser photolysis and a flow system to footprint proteins oxidatively, which was later named fast photochemical oxidation of proteins (FPOP). As compared with using a Nd:YAG laser, the KrF excimer laser they used has an output of 248 nm, which is closer the λ_{max} of H_2O_2. The laser pulse width was 17 ns, and the power was 50 mJ/pulse, both readily achieved with such a laser. These efforts combine to afford measurable oxidation levels of proteins with 0.04% H_2O_2. The flow system, as illustrated in Figure 12, ensures that the proteins in the aliquot are only irradiated once. Flow rate was calculated in correspondence with laser pulse width and frequency to allow a 20 – 25% exclusion volume, which minimizes any “double shots” of the protein solution. Left-over H_2O_2 was decomposed by catalase in the collection tube. Moreover, the reaction duration was controlled and became tunable by adding a radical scavenger (Glu[841] and later His[181]), which not only limits the labeling time to 0.5 μs for minimizing over-labeling but also allows better control of the labeling process[878] and makes possible probes of fast kinetic processes including protein folding/unfolding[893-894]. These advantages make FPOP the most adopted platform for protein footprinting by fast labeling reagents.

As compared to synchrotron water radiolysis, H_2O_2 photolysis retains most of its advantages in generating ●OH. Although H_2O_2 is a necessary precursor, low concentrations minimize any oxidation interference to protein native states. Most importantly, H_2O_2 photolysis makes the ultra-fast ●OH protein footprinting more accessible to the general research community although efforts are underway, principally by a commercial developer, to incorporate a discharge lamp to replace the laser, which imposes safety requirements and some expertise for handling. Nevertheless, subsequent developments take advantage of the strengths of FPOP, and a description of several applications will be given in Section 6.

On the other hand, H_2O_2 is a relatively strong oxidant, which may make this approach troublesome for proteins that are prone to oxidation. A modified FPOP apparatus with a mixer located just before laser window largely minimizes the H_2O_2-induced protein

oxidation.[895] A recent report suggests that H_2O_2 can interact with the protein, giving local high concentrations of the H_2O_2 and the radicals on regions of the protein surface.[896]

In response to the original claim that the radicals have been scavenged in ~ 1 μs, Konermann and coworkers[897] employed a reporter dye to follow the FPOP kinetics and showed that the free radical oxidation of the dye extends over tens of ms, indicating a longer radical lifetimes than the original prediction. This phenomenon likely applies to the secondary radicals formed as $^{\bullet}$OH reacts. It remains to be seen if these less reactive radicals react with the protein. The assertion about μs lifetime is probably correct for the primary radicals (i.e., $^{\bullet}$OH).

Another consideration for this platform is the potential migration of initially formed protein radicals to other reactive residues that are buried below the surface. The investigators found that two solvent-inaccessible residues were modified by FPOP, possibly in accord with a potential long-distance radical transfer (radical jumping) to buried residues.[898] This and other considerations need further attention to make FPOP more robust and applicable to more biological systems.

5.1.2.4. High Voltage Electrical Discharge: High voltage electrical discharge takes advantage of the requirement to use mass spectrometry in the analysis by a simple adaption of a typical ESI source to increase the spray voltage to 6-8 kV.[899] To make the radical, Downard and coworkers[899-900] increased the potential difference between the emitter tip and the grounded collection plate (either the MS inlet or a collection vessel) to induce a corona discharge, during which oxygen in the nebulizer gas will be activated to give a plasma at the tip of the emitter (Eq. 19-20).

$$O_2 \rightarrow O_2^{+\bullet} + e^- \quad (19)$$

$$O_2^{+\bullet} + H_2O \rightarrow H_3O^+ + \bullet OH \quad (20)$$

Meanwhile, water from the ESI spray can be activated as well (Eq. 21).

$$2\ H_2O \rightarrow H_2O^{+\bullet} + e_{aq}^- \rightarrow H_3O^+ + \bullet OH + e^- \quad (21)$$

By switching the nebulizer gas from air to pure O_2, the oxidation efficiency can be doubled.[901] The approach is also compatible with both positive and negative polarities.[902] The oxidatively labeled protein is then submitted directly to the mass spectrometer for top-down analysis (proteins are dissolved in ammonium acetate to facilitate sufficient ionization), or it can be accumulated in a collection vessel for further treatment and proteolysis. In subsequent studies, an O_2-assisted electrical discharge has been successfully utilized to study protein complexes between ribonuclease S-protein—S-peptide[903] and calmodulin—melittin[904]. In a more recent twist, Maleknia and Downard[905] joined MALDI and electrical discharge protein footprinting to afford an even higher throughput.

Given the popularity of ESI in protein analysis, high voltage electrical discharge makes ●OH protein footprinting readily available to almost every MS lab. The fast-labeling timeframe and high labeling efficiency seem to be promising. Given that charge-induced protein unfolding occurs in an ESI source,[906] a question arises whether the protein of interest can maintain its high-order structural integrity during the oxidative footprinting. It is always preferred to perform protein footprinting under native or near-native states to minimize these ambiguities, where a high-voltage ESI spray is not optimal. Moreover, it is challenging to footprint binding systems with weak interactions through this method, as weak interactions are less likely to be preserved in an ESI droplet than in neutral solution. The labeling time frames and the radical lifetimes also remain to be determined.

The concern of charge-induced unfolding by electrical discharge-based ●OH labeling was recently addressed in 2017 by Minkoff and Sussman, who developed a novel experimental approach named plasma induced modification of biomolecules (PLIMB, Figure 13).[907] Instead of delivering the protein through an ESI source, the protein aliquot was placed in a grounded Eppendorf tube with a charged needle on top of the liquid. A plasma discharge is induced when supplying 1 – 31 kV of potential to the needle with frequencies of 0 to 15 kHz. Over a period of 60 s, denatured and native bovine serum albumin were oxidatively labeled to achieve modification fractions up to 15 % at peptide level. As part of the initial demonstration, PLIMB was adopted to characterize the epidermal growth factor-induced structural changes in the extracellular domain of its receptor. These examples demonstrate efficacy in facilitating ●OH-based protein footprinting.

PLIMB offers a benchtop solution for radical protein footprinting by overcoming the major drawback for conventional electrical discharge methods, as the protein of interest is now footprinted in solution under near-native conditions. On the other hand, the plasma discharge in PLIMB only happens at the surface of the aliquot. Given the short lifetime of ●OH,[170] most of the ●OH labeling occurs in limited regions of the solution. Means to uniformly label the sample aliquot and to minimize the over labeling are likely to be future developments of PLIMB.

5.1.2.5. Gamma Ray Water Radiolysis: Gamma ray (γ-ray) is an electromagnetic radiation that composed of high energy photons. Similar to synchrotron X-ray water radiolysis, γ-rays excite water molecules and trigger reactions that produce ●OH (Eq. 2-8).[908] γ-ray-based ●OH footprinting, first applied to study nucleic acids,[909] was implemented by Nukuna et al.[910] to footprint cytochrome C in 2004. This approach was adopted by a few research groups in subsequent years,[911-916] but more recently, the approach is seldom used due to safety concerns of the highly-penetrable nature of γ-rays and the emergence of other approaches.

5.1.2.6. Other Hydroxyl Radical Generation Methods: Besides the methods introduced above, there are other methods that for ●OH footprinting, including ultrasound sonolysis,[917-918] fast neutrons,[919-921] peroxynitrous acid decomposition,[922-923] pulsed electron beam,[924] photolysis of *N*-hydroxypyridine-2(1H)-thione,[925-926] boron-doped diamond electrochemical surface mapping,[927] and ozonolysis[901]. Because these methods were only

used in nucleic acid footprinting or not developed for protein footprinting, they will not be covered further in this review.

5.1.3. Residue Specificity and Proposed Reaction Pathways—One of the unique advantages of $^{\bullet}$OH in protein footprinting is its broad reactivity. Xu and Chance[170, 912, 928-930] conducted systematic studies and found that the reactivity between $^{\bullet}$OH and amino acid residues rank as Cys > Met > Trp > Tyr > Phe > cystine > His > Leu, Ile > Arg, Lys, Val > Ser, Thr, Pro > Gln, Glu > Asp, Asn > Ala > Gly. Among all these residues, Gly, Ala, Asp and Asn are unlikely to serve as useful probes owing to their low reactivity (also see Table 1). Although the reactivities for Ser and Thr are higher than that of Pro, which has been found to be a reactive and useful substrate, their oxidation products are not easily detectable and may be dispersed among several pathways (e.g., oxidation of -OH to =O). From rate constant determinations and reports of experience with $^{\bullet}$OH and protein modification, the general conclusion is that 14 out of 20 amino acid residue sidechains are active in $^{\bullet}$OH-based protein footprinting experiments. In our experience, the presence of highly reactive residues (Cys, Met, Trp, Tyr, Phe, His) may siphon most of the reagent radicals to their modification, reducing the coverage. The products resulting from oxidative modifications are residue-dependent, and they have been covered in detail in the Xu and Chance review[170]; most are +16 Da oxidations as summarized in Table 2 Below.

Mechanistically, $^{\bullet}$OH activates the solvent accessible sidechains by removing H$^{\bullet}$ from an activated site, adding a $^{\bullet}$OH to a double bond, resulting in a protein radical that is subsequently quenched differently depending on the origin of the radical (H_2O or H_2O_2).

For synchrotron radiolysis, Xu and Chance,[170, 928-930] in a comprehensive review, summarized the modification pathways of $^{\bullet}$OH-active amino acid residue sidechains.[170] Leu, Ile, Val, Pro, Arg, Lys, Glu and Gln sidechains are activated through H$^{\bullet}$ abstraction whereas His, Phe, Tyr, Trp and Met are primarily by $^{\bullet}$OH addition. The resulting protein radicals are subsequently quenched by dissolved O_2 in aerobic conditions. Reaction pathways between $^{\bullet}$OH and the extremely reactive Cys and cystine residues are complicated and not well understood. Alternatively, a likely reaction pathway that covers major oxidative products was proposed for Cys.[930] Similar pathways should apply to the electrical discharge-based $^{\bullet}$OH labeling, as the precursor for $^{\bullet}$OH is also water.

In contrast to the two systems mentioned above, where uniformly distributed water is the $^{\bullet}$OH precursor, any H_2O_2 photolysis approach, as represented by FPOP, follows slightly different reaction pathways. A recent quantum calculation study revealed the hydrogen bonding between H_2O_2 and amino acids including His, Arg, Tyr, Cys, Thr, Gln, Asp, Lys, Met and Trp.[931] Such hydrogen bonding will induce a pre-formed H_2O_2 – amino acid residue complex, which will result in a local fluctuation in $^{\bullet}$OH concentrations upon laser photolysis. Liu, Gross, and coworkers[896] studied the reaction pathways between $^{\bullet}$OH and 13 different amino acid residues on a FPOP platform. By using ^{18}O-enrichment of all three available oxygen sources (H_2O, H_2O_2 and dissolved O_2) on an FPOP platform, one at a time, they differentiated three classes of residues based on their oxygen uptake preferences. His, Arg, Tyr, and Phe preferentially take oxygen from H_2O_2. Met competitively take oxygen from H_2O_2 and dissolved O_2, whereas Leu, Ile, Val, Pro, Lys, Asp, Glu and Gln take

oxygen exclusively from O_2. Given that the $^{\bullet}$OH activation pathway is very similar to that in water radiolysis, such differences in oxygen uptake preferences reveal a different pathway for some activated residues than described in the Xu and Chance[170] review. Besides quenching by dissolved O_2, selected activated residues can also be favorably modified by reaction with another $^{\bullet}$OH in the FPOP setup, owing to hydrogen bonding with H_2O_2 and preferential localization of the reagent and, of course, the radicals.

As mentioned earlier, $^{\bullet}$OH is also capable of cleaving protein backbones, whose pathways is reviewed elsewhere.[170, 847]

Summarizing the role of $^{\bullet}$OH in footprinting, we recognize unprecedented advantages as a fast protein footprinter. Biological relevance, similar size and hydrophilicity as water, fast labeling time, high labeling efficiency, multiple generation methods, broad residue coverage, well established platforms, and mature understanding of the labeling pathways make it the most utilized fast-labeling reagent. Its demonstrated utility forecast many more promising applications (see section 6). On the other hand, the +16 Da from oxidative labeling can be problematic, as oxidation is common in native biological systems, and it is challenging to distinguish the oxidations that exist prior to labeling and those that are from $^{\bullet}$OH reactions. Other oxidations besides those producing +16, can add background of many low abundance products to complicate the analysis. Furthermore, even though 14 amino acid residues are reactive with $^{\bullet}$OH, those that are most reactive (S-containing, aromatics) can be too competitive, reducing the overall coverage and spatial resolution achieved for the protein. These drawbacks motivate the development of other fast labeling reagents that provide complementary coverage to $^{\bullet}$OH labeling and employ an MS tag other than +16 Da.

5.2. Sulfate Radical Anion and other Sulfur Containing Radicals

5.2.1. Biological Relevance—Sulfate radical anion, $SO_4^{-\bullet}$, is a potent oxidant with a reduction potential of 2.43 V at neutral pH.[932] Its strong oxidation capability can cause considerable damage to different cellular components including lipids, carbohydrates, proteins and DNA/RNA.[933] It is an exogenous factor that promotes other oxidant formation in biological systems,[934] and it has been applied to inactive pathogenic microorganisms in disinfection[933]. Many investigators hold that the oxidation pathways of biomolecules by $SO_4^{-\bullet}$ are like those of the $^{\bullet}$OH; however, detailed mechanistic studies are still needed.

5.2.2. Radical Generation in Solution and Applications in Biology—The production of the sulfate radical anion in vitro primarily utilizes two precursors, persulfate ($S_2O_8^{2-}$) and peroxymonosulfate (HSO_5^-). Activation methods are needed to cleave the O-O peroxide bond and give $SO_4^{-\bullet}$ generation. UV irradiation[6], thermolysis, radiation[2] and transition-metal catalysis[935-936] are possibilities. As a promising oxidant, $SO_4^{-\bullet}$ may be useful for answering biological questions. In 1983, the Werbin group[937] cross-linked DNA with lysosome to study reactive mechanism of a carcinogen, *N*-acetoxy-*N*-acetyl-2-aminofluorene (N-AcO-AAF). The Kodadek[935] and Jovin groups[936] both demonstrated efficient $SO_4^{-\bullet}$-generation from a ruthenium complex, Ru(bipyridine)$_3$, for crosslinking initiation. The latter study further shows that $SO_4^{-\bullet}$ induces tyrosyl radical formation,

allowing inter cross-links between alpha-synuclein (αSyn) aggregates. The covalently bound large oligomers exhibit distinct biophysical properties and increased toxicity.

5.2.3. $SO_4^{-\bullet}$-based Protein Footprinting: Residue Specificity and Proposed Reaction Pathways—Bridgewater and Vachet [938-940] in 2005-2006 first used sulfate radical anion to determine binding and map the SASA of proteins. Their generation of $SO_4^{-\bullet}$ utilizes a metal-catalyzed oxidation (MCO), a process that enables radical formation at the site of a redox-active metal when bonded to a peptide/protein (Scheme 15). Cu/Zn superoxide dismutase was chosen as a model system in the presence of ascorbate and persulfate. High concentrations of ascorbate (i.e., 100 mM) rapidly initiate the redox cycle through Cu(II) reduction to provide scavenger-generated $SO_4^{-\bullet}$, which reacts by pseudo-first order kinetics. The study showed that at an optimized $SO_4^{-\bullet}$ concentration (i.e., one generated from 1 mM persulfate) allows the oxidation to occur only on the nearby Cu-bound amino acids. Increasing the persulfate concentration allows modification of non-Cu-bound residues within 10 Å radius of the Cu center. UV-Vis absorption spectroscopy and oxidation kinetics further confirmed the survival of the intact protein structure throughout the analysis, showing promise for future applications under their conditions. Although the steric effects of a specific residue may alter its oxidation extent, this tunable $SO_4^{-\bullet}$-based approach provides another approach for three-dimensional mapping of the protein environment around a reactive site. This approach may be particularly important to map metal-binding residues that have low solvent accessibility, and it may be incorporated into an FPOP platform.

In 2010, the Gross group[941] generated sulfate radical anion on the FPOP platform by photolysis of $^{-}OSO_2$-O-O-O_2SO^{-} at a quantum yield of 0.55. As a stronger oxidant than hydroxyl radical, the sulfate radical anion gives comparable extents of modification on the protein-level with 3-5 times lower amounts of precursor (Figure 14a). Incubation with persulfate anion without laser irradiation doesn't introduce observable oxidation on the protein, showing negligible background from the precursor reagent. In addition, the investigators showed that the reactivity and specificity of $SO_4^{-\bullet}$ is similar to those of $^{\bullet}OH$ for residues Met, Trp Glu and Ser; the reactant radical favors His and Tyr (Figure 14b and 14c). The overall reactivity ranking of $SO_4^{-\bullet}$ is:

$$\text{Met} > \text{Tyr} = \text{Trp} > \text{Phe} = \text{Glu} = \text{His} > \text{Ser} > \text{Pro} > \text{Asp} = \text{Thr} > \text{Lys} = \text{Gln} > \text{Leu} = \text{Val} = \text{le}$$

Oxidation sulfate-radical oxidation can happen through multiple pathways. Aromatic and Met side chains are the main targets for the strong electrophile $SO_4^{-\bullet}$ and form a radical cation intermediate, which subsequently undergoes either fragmentation or hydration.[942-943] $SO_4^{-\bullet}$ can also oxidize a carboxyl anion ($R\text{-}COO^{-}$) to give acyloxyl radicals ($R\text{-}COO^{\bullet}$) followed by decarboxylation to generate carbon-centered radicals.[943] Moreover, hydrogen abstraction by $SO_4^{-\bullet}$ is another pathway to oxidative modification, likely occurring on Leu, Ser and Phe.[944]

Surprisingly, although sharing some similarities, persulfate FPOP and hydroxyl FPOP also have different chemical outcomes. For systems where there is need to maintain more "physiologic-like" conditions, the lower amount of reagent for persulfate anion makes it a more desirable choice. Different physical properties of the two radicals also determine their

preferred circumstances for surface mapping. Negatively charged $SO_4^{-\bullet}$ is prone to form electrostatic interactions with other positively charged groups, introducing a possible bias. One example is shown by Gau et al.[941], who compared per-residue fractional modification for six histidines in apomyoglobin to their SASA values calculated from an X-ray and NMR study. A good correlation ($R^2 = 0.83$ in Figure 15b) shows the potential of $SO_4^{-\bullet}$ footprinting to be an effective experimental measure of SASA. The interaction of $SO_4^{-\bullet}$ and H64, an axial ligand of the heme iron, however, contributes to the enhanced reactivity of H64 (Figure 15a). On this matter, the hydroxyl radical, which bears no charge and has a comparable size to water, may be a better choice as footprinter that responds to SASA. In addition, the hydroxyl radical is more membrane-permeable, suitable for studies on micelles, liposomes and nanodics.[945] The sulfate radical anion, on the other hand, reacts more efficiently on extracellular-accessible residues. The combination of the two in a tandem format may be effective in addressing complicated protein systems consisting of phospholipid bilayers imbedded with protein analyte.

5.3. Carbonate Radical Anion

5.3.1. Biological Relevance—The carbonate radical anion, $CO_3^{-\bullet}$, is formed primarily from the bicarbonate-carbon dioxide pair that exists in cells to maintain physiological pH.[946] Superoxide dimustase (SOD),[947] xanthine oxidase (XO)[948] and hemoprotein in an iron (III) state can adopt conditions whereby the buffer components are sources of $CO_3^{-\bullet}$, causing oxidative damage on biomolecules.[949] Owing to its longer half-life compared to those of other radicals (e.g., $^{\bullet}OH$), $CO_3^{-\bullet}$ can diffuse farther and cause oxidation distant from its site of formation. One of the well-recognized roles of $CO_3^{-\bullet}$ is to modulate peroxynitrite activity by abstracting hydrogen from amino acids, primarily tyrosine. The sequential NO_2 addition will lead to nitro-substituted residues, which may be involved in many chronic diseases.[950]

5.3.2. Radical Generation in Solution and Applications in Biology—Carbonate radical anion can be produced in vitro in many ways including UV photolysis[951] of a cobalt complex, $[Co(NH_3)_4CO_3]ClO_4$, in phosphate buffer, enzymatic production from SOD1 in a bicarbonate buffer[951], pulse radiolysis[952] of an N_2O saturated $NaHCO_3$ solution, and laser flash photolysis of persulfate anion in bicarbonate buffer.[953] To monitor the production of $CO_3^{-\bullet}$, EPR spin trapping is often engaged.[946] In 2001, Geacintov and coworkers[953] generated $CO_3^{-\bullet}$ as a secondary radical from the sulfate radical anion and, for the first time, characterized its site-selective oxidation of guanine in double-stranded oligonucleotides. Subsequently, many groups focused on the consequences of protein oxidation in biology. One of the foundation studies was done in 1973,[954] where the rate constants of the carbonate-radical reactions towards some biochemical compounds, including many free amino acids, were measured. Tyrosine, tryptophan and methionine are the most reactive with rate constants on the order of 10^8 $M^{-1}s^{-1}$. Gebicki and coworkers[952] showed that horseradish peroxidase (HRP) and other proteins that are rich in Tyr, Trp, and Met residues experience a 20-30% loss in their activity after exposed to 100 μM $CO_3^{-\bullet}$. Paviani et al.[951] characterized a ditryptophan cross-linked product of lysozyme under carbonate radical anion mediated reactions; the study delineated the origin of a previously detected ditryptophan in the non-amyloid aggregation of human SOD,[955] a process that may be pathogenic for amyotrophic lateral sclerosis[956].

5.3.3. $CO_3^{-\bullet}$-based Protein Footprinting: Residue Specificity and Proposed Reaction Pathways—The carbonate radical anion as a protein footprinter was first evaluated by Zhang et al.[957] and demonstrated on a FPOP platform. The hydroxyl radical generated from hydrogen peroxide photodissociation reacts with carbonate/bicarbonate (CO_3^{2-}/HCO_3^-) buffer to form $CO_3^{-\bullet}$. To ensure its dominant presence in solution, highly concentrated CO_3^{2-}/HCO_3^- (e.g., 700 mM) is necessary, supported by a numerical simulation based on second-order kinetics. Experimentally, Zhang et al.[957] showed no modification in a no-laser control and a similar oxidation pattern as that produced by $^{\bullet}$OH FPOP upon laser irradiation (Figure 16a). The last thorough study of $CO_3^{-\bullet}$ prior to this work took free amino acids as substrates,[954] and that may not be relevant for proteins in solution particularly because the N-terminal amines of the free amino acids may complicate the measurements of side-chain reactivity. Therefore, a systematic study of model peptides and proteins was conducted, taking into consideration the residue context, solvent accessibility, and local environment. From the results, the reactivity of the carbonate radical anion can be assigned as follows:

$$\text{Met} \approx \text{Trp} > \text{Tyr} > \text{His} \approx \text{Phe}$$

The outcome is similar to that reported previously.[958]

Given that $CO_3^{-\bullet}$ ($E^\circ = 1.58$ V at pH = 7) [959] is a weaker oxidant than $^{\bullet}$OH, the former showed more specificity towards residues with electron-rich side chains (i.e., Met, Trp and Tyr), which underwent even more oxidation than with $^{\bullet}$OH (Figure 16b). Phe and His are also reactive but only modestly. Other aliphatic amino acids are basically inert. The pH also has considerable effect on the reactivity of a specific residue (e.g., His where the imidazole ring carries more charges at pH ~ 6 than under neutral or basic conditions). The electrostatic interaction between the positive side chain and the negative charged $CO_3^{-\bullet}$ may contribute to a higher local radical concentration that promotes the oxidative chemistry. The oxidation pathway is proposed in the *Summary and Perspective* (Figure 22), where the $CO_3^{-\bullet}$ forms a protein-centered radical that undergoes addition of hydroperoxyl radical. Water hydrolysis finally leads to an oxidized product.

The carbonate radical anion can be a good candidate to characterize structural dynamics and binding interfaces of protein complexes, especially when the involved residues are reactive with it. The more specific modifications not only enable higher oxidation levels to reveal subtle differences but also allow faster data analysis and higher throughput. A limitation of its use is also obvious; compared to $^{\bullet}$OH, $CO_3^{-\bullet}$ has a narrower range of reactivity, and the larger size of $CO_3^{-\bullet}$ compared to $^{\bullet}$OH would likely afford lower spatial resolution footprints. In addition, the pH of the relatively high concentration of the CO_3^{2-}/HCO_3^- buffer used in the FPOP experiments is basic, possibly not friendly for maintaining a protein's native state. Furthermore, its generation is not straightforward, diminishing its convenience as a footprinter. It may be that the other production methods can relieve the concerns. Nevertheless, the outcomes show the value of the FPOP platform in fundamental studies of radicals and radical ions that are relevant in biology.

5.4. Carbenes

5.4.1. Biological Relevance and Radical Generation in Solution—Diazirines, common precursor of carbene diradicals, were synthesized in 1960 [960] and emerged as a versatile photoaffinity labeling (PAL) agents in the late 1970s.[961] Investigators typically activate diazirines with a UV laser at approximately 350 nm to cause release of N_2 molecules and give an equimolar amount of carbene diradicals. Highly reactive carbenes form irreversible covalent bonds with proteins, allowing stringent downstream affinity purification and target identification. The use of diazirine-based PAL is an effective strategy to understand protein-drug or other small molecule interactions and identify new drug binding sites. To address specific questions, investigators have designed and synthesized several diazirine analogs to adapt the affinity agent to the protein sample environment. For example, adamantylidene, a lipophilic reagent and an analog of adamantane, was used to obtain topological information of Na/K ATPase[962] and Ca-ATPase[963] in membranes as early as 1983. In addition, H-diaziflurane, an analog of halothane, allowed the examination of binding sites of inhaled anesthetics and their action mechanism.[964]

More recently, reagents containing diazirines were adopted as a new class in photo-activatable cross-linkers, and several were described.[667, 965] The ability to react with many bond types or amino acid residues makes carbenes powerful reagents to capture protein dynamics and intermolecular interactions. Obtaining multiple cross-links magnifies the information by providing more distance restraints on an interacting protein system, and thereby furnishing vital data for molecular simulation or docking to give a more complete description of the system.

5.4.2. Residue Specificity and Proposed Reaction Pathway—Richards et al.[966] first described the carbene diradical as a footprinting reagent in 2000. Methylene was generated from diazirine gas (CH_2N_2) upon UV irradiation and allowed to footprint α-lactalbumin. The labeling yield, however, was low, owing to the limited solubility of gaseous CH_2N_2 in aqueous media. Furthermore, the explosive gas requires conscientious preparation, storage, and safe handling, limiting wide application.

Later in 2011, Schriemer and coworkers[967] reported a new diazirine-based reagent, photoleucine (Reagent **1** in Scheme 16) that has higher water solubility and stability than CH_2N_2. The reaction platform incorporates a Nd:YAG pulsed laser (355 nm, 1000 Hz) for radical initiation and a 96-well plate cover with lids with slits, allowing the laser beam to enter the protein solution. With this experimental setup, the investigators obtained a maximum conversion of the diazirine to the carbene diradical by using an irradiation time of 2 min in the absence of other competitive chromophores. Furthermore, they found that photoleucine does not react with targeted proteins without laser activation. Upon photolysis, irreversibly labeled products exhibit a characteristic +115.03 Da mass shift (Figure 17a and 17b).

$$\Delta mass_{\mathrm{av}} = \left[\frac{\sum m_i I_i}{\sum I_i}\right]_{\mathrm{labeled}} - M_{\mathrm{unlabeled}} \quad (22)$$

To examine the labeling sensitivity of carbene diradicals for different accessible surfaces of proteins, two calmodulin systems (i.e., with/without Ca^+ and bound/unbound to the peptide M13) were investigated. The average number of labels on each protein molecule can be estimated by determining the difference in the centroid masses between the labeled and unlabeled proteins as seen in a deconvolved mass spectrum of the intact protein (Eq. 22 and Figure 17c, d), where m_i and I_i represent mass and signal intensity, respectively. A reduction in protein surface area resulting from Ca^+ binding or M13 binding is reflected clearly as the measured labeling extent over 2-10 min of irradiation; namely holo-CaM is 45 ± 7% less labeled and M13-CaM is 39 ± 5% less than apo-CaM.

Residue-level quantification of carbene-induced modification needed attention, and that was discussed in a sequel study.[968] Theoretically, carbene diradicals can insert into X-H bonds and C=C bonds.[970] Insertion into carboxylic acid functional groups will form labile esters that can be lost in CID fragmentation, thus complicating data interpretation and even losing information. The Shriemer group[968] chose ETD fragmentation as an alternative to CID and compared the two fragmentation methods by reporting the fraction modified for each y/z ion. Although most fragments shared the same trend, the y_{10} ion gave poor precision because it undergoes a neutral loss (Figure 18a). Notably, reducing the collision energy reduces the loss, but the abundance of the peptide fragments (product ion in MS/MS) is also reduced. ETD is a superior fragmentation method for retaining labile modifications to afford more comprehensive information than CID. ETD, however, performs poorly when peptides are low in charge and small in size. The best approach might be to use a combination of the two modes of MS/MS.

Another issue is the electrostatic interaction between the carbene precursor and various amino acid side chains; the interaction concentrates the precursor molecule around the site, promoting more modification and a biased residue preference. Switching to another carbene precursor reagent, 4,4-azipentanoic acid (**2** in Scheme 16), that contains no positively charged amine group, shows the effect. Although both reagents give similar results for Tyr, Lys, Glu, and Asp, positive-charged photoleucine shows higher reactivity with the negatively charged aspartic acid (Figure 18b). In addition, the ionic strength of the buffer and solution temperature also affect the electrostatic interaction, where increasing ionic strength decreases electrostatic interactions[971] and higher temperatures will lower the dielectric constant[972].

A related approach was also reported by the Gross group[973] in 2015, when they adapted carbene generation in solution on the FPOP flow system. Careful control over the exclusion volume guarantees that photoleucine and the protein CaM are mainly irradiated once, thus diminishing concerns of perturbing the solution equilibrium by the generated nitrogen gas and causing conformational change with excess labeling. The outcome is less modification for holo-CaM, consistent with its more compact conformation and significant labeling on Try, Asp and Glu, possibly owing to interactions of the protein with photoleucine, concentrating the reagent on the protein surface.

In 2017, Schriemer and coworkers[969] refined the carbene platform to employ a single-shot laser with higher energy (i.e., 150 mJ) to avoid nitrogen perturbation and protein

conformational change at the induced air-water interface. Prior to irradiation, the sample solution was snap-frozen by liquid nitrogen before laser irradiation to restrict radical diffusion, to maintain protein HOS, and to minimize quenching of carbene radical and increase modification. To establish residue specificity with carbene chemistry, the investigators, in a Herculean study, footprinted 777 peptides by using three different precursors, a negatively charged precursor **2** (Scheme 16), a neutral reagent **3** (3,3'-azibutan-1-ol, Scheme 16), and a positively charged reagent **4** (3,3'-azibutyl-1-ammonium, Scheme 16). The labeling trends are similar for the three reagents, and the bond insertion propensities generally are a function of side-chain polarity and size. Reagents **2** and **3** both favor Arg, Glu and Asp, whereas, the neutral reagent **4** shows higher reactivity with His (aromatic and neutral) in addition to the three residues, Arg, Glu, and Asp. Remarkably, many hydrophobic amino acids show noticeable modification (Figure 18c), supporting the high reactivity of carbenes, even with aliphatic groups. The nature of the carbene precursor also has an impact on the residue selectivity from participating in complex molecular interactions to increasing the local concentration of the precursor ion at the protein surface.

Manzi et al.[974] tested a carbene precursor, 4-(3-(trifluoromethyl)-3H-diazirin-3-yl)benzoate (reagent **5**, Scheme 16) that is more reactive than those from reagents **1** – **4.** The investigators' design involved installing an adjoining trifluoromethyl group (Figure 19a), leading to the use of less reagent and less irradiation time (i.e., 10 mM for 4 s irradiation). Further, the labeling efficiency improved in comparison to the use of photoleucine at 100 mM and 16 s irradiation. The improved reactivity is due to increased stabilization of the carbene radical by the added trifluoromethyl group and increased hydrophobicity but little change in zwitterionic character. They tested the new reagent on an unknown protein complex (i.e., the deubiquitinating enzyme ubiquitin specific protease 5 (USP5) upon binding with di-ubiquitin (di-Ub)). USP5 is a multi-domain cysteine protease including two ubiquitin associated domains (UBA) and a Zn-finger ubiquitin-binding domain (ZnF-UBP). Previous studies showed the binding stoichiometry between USP5 and di-Ub to be 1:1, suggesting additional binding sites than those in Znf-UBP. These sites were not identified. The investigators footprinted the C335A mutant of USP5 with carbenes in the presence and absence of one equivalent di-Ub and observed distinct binding regions (Figure 19b), which were mapped onto the X-ray structure of USP5 (Figure 19c). The catalytic domain was shown to be the other binding site and, additionally, a remote conformational change for the region represented by peptide G606-K630 was found. The design of new, successful radical precursors indicates that there are more opportunities for improvement and application, emphasizing the potential of carbene footprinting as an effective and accurate structural probe for HOS of proteins.

The pathways for carbene chemistry may involve several radical intermediates whose structures and reactivities can be tailored by using different precursors. For example, it is possible to generate by photolysis not only singlet[975] and triplet carbenes[976] but also diazo isomers that further decompose into carbocations.[977,978] Although a singlet carbene preferentially inserts into O-H, N-H and S-H bonds,[977] it is challenging to pinpoint the dominant pathway just from the nature of the modified products. Insertion into Thr can be done by singlet carbene through O-H bond insertion or by triplet insertion into the

methylene group located on the amino acid side chain. In addition, the small energy difference (i.e., ~ 2 kcal/mol[979]) between the two states add complications because mixtures of products can form. Because heteroatom-containing residues are usually the favored sites of reaction (e.g., Glu, Asp, Tyr and Arg), the singlet state may be favored; however, blended pathways are more likely. A general route is shown in Scheme 17.

Carbene footprinting has high potential in structural biology. The labeling time is shorter than 10 ns,[980] faster than most protein folding. Irradiation on a flow-system or excitation after snap freezing eliminates deceptive modifications originating from carbene insertions in a protein that has undergone a protein conformational change. Compared to the hydroxyl radical, the short survival time of carbenes owing to reaction with solvent water obviates the need for a scavenger. Carbene generation by diazirines is at a less damaging wavelength to proteins (i.e., ~ 350 nm). In addition, most carbene precursors do not react with proteins prior to laser irradiation (unlike H_2O_2 for $^{\bullet}OH$), and this lack of reactivity minimizes background interference. Furthermore, the resultant mass shift for carbene modification can be adjusted to be bio-orthogonal by tailoring the precursor design. The physical properties of reagents, however, can favor preconcentration on the surface of the protein, possibly delivering biased residue preference or even information loss. Those properties can also be chosen advantageously to promote binding in lipid membranes, permitting footprinting of transmembrane proteins. As this field develops and more diverse carbene reagents are implemented, a better understanding of interactions will emerge to permit rational design of new carbenes. New footprinting reagents that can target specific residues or provide comprehensive coverage are expected in the future.

5.5. Trifluoromethyl Radical

5.5.1. Biological Relevance and Applications—Fluorine-containing compounds are extremely rare in biology; only five entities containing F have ever been identified.[981] The most common molecule is fluoroacetate, which is found in many tropical plants as a toxin. Footprinting reactions that insert either fluorine or fluorine-containing substrates may be advantageous because fluorine is the most electronegative[982] (Pauling Electronegativity = 4.0) common substance and has a small radius (1.33 Å), not so dissimilar to that of H,[983] allowing F to be a surrogate for H.

Introduction of fluorine alters existing compounds to be more metabolically and thermally stable, more lipophilic, and possibly more interactive with a targeted protein[984] through contact with hydrophobic patches. Therefore, anthropomorphic fluorinated compounds already play a role in pharmaceuticals, up to 20-25%[981]. One indispensable integrant is the trifluoromethyl group (CF_3) found in several drugs (e.g., Celebrex (Pfizer) and Sarafem (Eli Lilly)).

The CF_3 group was utilized early in several applications in structural proteomics. In 1962, Singer[985] developed affinity labeling, in which a targeted protein non-covalently interacts with a probe molecule (e.g., a drug). The probe is comprised of the drug plus a reactive motif installed by chemical synthesis. The probe is activated so that it covalently binds with the protein in a similar way as the drug to “mark” the binding site.

The Brunner group[986] advanced the approach by introducing a CF_3 group in a diazirine-containing reagent, 3-trifluoromethyl-3-phenyldiazirines (TPDs). TPDs are chemically stable and exhibit high quantum yields for carbene formation upon UV irradiation. Even though the linear diazo rearrangement is inevitably formed upon UV irradiation, CF_3 and phenyl stabilize the linear diazo and prevent it from undergoing intramolecular rearrangements (e.g., to an arylalkyl diazo derivative that competitively diffuses away from the active site before decomposing to the carbene, leading to a complex labeling patterns) and diminished side-chain reactions.[970]

5.5.2. Radical Generation in Solution—Trifluoromethyl radicals were generated in late 1940s from the reaction of homogenized CF_3I[987] in the presence of ethene. Because gaseous CF_3I is not easy to control and store, other radical precursors including $Te(CF_3)_2$[988] and trifluoroacetic anhydride[989] were later developed. High temperature and low radical yield limit their application, however. Alternatively, Togni's[990] and Umemoto's[991] reagent are better choices, and they require activation by various transition metals (e.g., $Ru(bipyridine)_3Cl_2$[992-993] and CuI[994]). The increased efficiency of generation and the reactivity of the radical depend largely on the metal-containing compounds that are used.

Whereas, organic solvents are usually necessary to retain the activity of the catalysts. A more biological compatible $^{\bullet}CF_3$ precursor is the Langlois reagent, first reported in 1991[995] and promoted by Baran and coworkers[996-997]. The system consists of sodium trifluoromethanesulfinate (CF_3SO_2Na) and *t*-butylhydroperoxide (TBHP) as an oxidant. In the absence of transition metals, $^{\bullet}CF_3$ can be initiated from the oxidant and generated in an aqueous buffer. Trifluoromethylation on various heteroarenes including pyridines, uracils and xanthines occurs with moderate to good yields (33%-96%). In addition, a protein system, β-lactamase, could be successfully labeled in Tris buffer while maintaining the protein's functionality. More recently, Fennewald et al.[998] incorporated an addition catalyst, TPGS-750-M, to achieve a better yield under milder reaction conditions.

5.5.3. $^{\bullet}CF_3$-based Protein Footprinting: Residue Specificity and Proposed Reaction Pathway—Trifluoromethyl radical as a footprinting reagent, was implemented by Cheng et al.[999] in 2017 to be used on the FPOP platform. The radical precursor is the water-soluble salt, $NaSO_2CF_3$ (Langlois reagent). The $^{\bullet}CF_3$ formation is initiated by the $^{\bullet}OH$, from photolysis of hydrogen peroxide. A likely mechanism is the $^{\bullet}OH$ displaces $^{\bullet}CF_3$ by attack on the S=O bond to form $HOSO_2^-$, the conjugate base of sulfurous acid, a mechanism different than that suggested in the original paper. The subsequent trifluoromethylation of proteins likely occurs by capping a protein radical (generated through $H^{\bullet}$ abstraction by either $^{\bullet}OH$ or $^{\bullet}CF_3$ (Figure 22).

The investigators tested the ability of the $^{\bullet}CF_3$ to footprint neuropeptide Y (18-36), apo-/holo-myoglobin (aMb/hMb), and VKOR, a transmembrane protein, on the FPOP platform. After laser irradiation, multiple CF_3-adducts were formed for the intact protein as evidenced by mass shifts of +67.987 Da for each CF_3 addition (Figure 20a). Notably, the trifluoromethylation of VKOR occurs selectively on the solvent-exposed region rather than in the transmembrane regions. Though $^{\bullet}CF_3$ is hydrophobic, it is generated from a water-soluble precursor that is not membrane permeable. Given the hydrophobicity of $^{\bullet}CF_3$, its

generation in the “unfriendly” aqueous environment explains, in part, its high reactivity. The addition of a CF_3 group to the protein increases the hydrophobicity of the peptides formed by digestion, shifting their reversed-phase retention times to longer values, a phenomenon that is different for $^{\bullet}OH$ footprinting, where the peptides have higher hydrophilicity and usually elute earlier than their corresponding unmodified peptides (Figure 20b).

The $^{\bullet}CF_3$ can react with 18 out of 20 different amino-acids residues, except Met and Cys, showing its complementary nature with $^{\bullet}OH$, which reacts rapidly with Met and Cys. There is some evidence that residues containing aliphatic side chains, which are inert with $^{\bullet}OH$ (e.g., Gly and Ala), are reactive with $^{\bullet}CF_3$ (Figure 20d). The reactivities with various residues, however, are not identical. $^{\bullet}CF_3$ is highly electron deficient and, thus, preferentially reacts with aromatic side chains (e.g., Trp, Tyr, His and Phe). Furthermore, $^{\bullet}CF_3$ successfully reports the structural difference in aMb/hMb, as expected for a good footprinter. As found in previous studies, region 80-96 undergoes significant conformational changes in the conversion between the two states, and that change is confirmed by $^{\bullet}CF_3$ footprinting on His 81/82/93 (Figure 20c). Similarly, His 119 also undergoes more modification in the apo-state whereas other residues react to comparable extents in both the apo and holo states.

Trifluoromethyl radical footprinting appears to have interesting advantages. The broader and complementary residue coverage compared to $^{\bullet}OH$ makes it a useful candidate in the structural biology “tool-box”. Combination of $^{\bullet}CF_3$ and $^{\bullet}OH$ in tandem allows more comprehensive characterization of the residues on a targeted protein than either radical alone, therefore providing a better opportunity to capture subtle structural changes. In addition, $^{\bullet}CF_3$ can survive in the presence of typical radical quenching reagents[996, 999] like dimethyl sulfoxide and retain its reactivity. In many membrane protein systems where a detergent is necessary for solubilization, $^{\bullet}CF_3$ footprinting has potential provided a precursor can be redesigned that will partition from water to the membrane (detergent). One limitation of using the Langlois reagent as precursor is the need for initiation by $^{\bullet}OH$. Reagents that quench $^{\bullet}OH$ will also lower the trifluoromethylation yield. Alternative fluorination reagents are expected in the future.

5.6. Iodine Radical

5.6.1. Biological Relevance—In physiology, iodine plays essential roles in metabolic regulation of thyroid function, especially hormone production.[10001001] Nearly all ingested iodine is carried and circulated as iodide,[1002] which in the presence of ROS or thyroid peroxidase (TPO)[1003], can be oxidized into molecular iodine, which oxidizes tyrosine residues on thyroglobulin to form thyroxine and tri-iodothyronine hormones.[1004] The reactive specie causing iodination, however, are not settled, although a likely one is the iodine radical.[1005]

Iodination strategies have been widely adopted in radioimmunology.[1006] Iodide radical appears to react also with histidine residues[1007] under more alkaline conditions but giving a lower yield than with Tyr.

5.6.2. Radical Generation and Applications in Biology—Generation of iodine radical in a bio-relevant condition is usually achieved by TPO[1008,1009] or UV photolysis[1010] of iodine-containing compounds. When iodine is directly incorporated into DNA and proteins, the photo-labile C-I bond can produce useful radicals to address mechanistic and structural questions concerning the region surrounding the C-I bond. The generated iodine radical, on the other hand, seems to serve as only as a leaving group.

In 2005, Hiroshi and co-workers[1011] utilized 5-iodouracil as a substitute reagent for DNA synthesis. UV photolysis of the modified DNA causes a strand break to give products that serve to probe local structure.[1012] A subsequent study further elaborated the method to include interactions of DNA and proteins.[1013] A photochemical reaction forms cross-links that report on interactions between proteins and the targeted DNA both in vivo and in vitro.

Ly and Julian[1014-1015] implemented starting in 2008 a similar strategy for footprinting proteins. Starting with electrophilic iodination of a protein, the investigators isolated and photolyzed the intact protein at 266 nm in a linear ion trap mass spectrometer to generate odd-electron species that modify nearby Tyr and His resides and direct subsequent CID fragmentation. Radical-directed dissociation dominates the cleavages via characteristic pathways, primarily backbone fragmentations at modified Tyr residues. Secondary backbone cleavages were also observed in proximity of modified Tyr, especially if Pro is present. Similar chemistry occurs via His iodination in the absence of Tyr. The informative fragments can report on the presence of *D*-amino acids,[1016] elucidate protein tertiary structure, and assist with identification of proteins in proteomics experiments. Later on, Ranka et al.[1017] characterized the free iodo-tyrosine rearrangement pathways under UVPD to show that loss of iodide radical leads to a high-energy radical in the aromatic ring that engages in hydrogen/proton rearrangements. This study provides fundamental understanding of UVPD-based top-down analysis of iodinated proteins. More applications and detailed analysis are expected for these novel approaches.

5.6.3. $I^{\bullet}$-based Protein Footprinting: Residue Specificity and Proposed Reaction Pathways—The iodine radical has potential to be an effective fooprinting reagent given its specific reactivity towards tyrosine and histidine. In footprinting, one precursor for the free radicals is 4-iodobenzoic acid, an organic iodide with some water solubility. The $I^{\bullet}$ is formed presumably in concert with a $^{\bullet}C_6H_4COOH$ (represented by $R^{\bullet}$ in Figure 22) by photolysis of I-C_6H_4-COOH at 248 nm. The carboxylphenyl radical likely abstracts an $H^{\bullet}$ from the OH of Tyr or from the NH of the imidazole ring to give a stabilized radical that is subsequently “capped” by reaction with $I^{\bullet}$ to give an iodinated protein (Figure 22), although there may be other mechanisms. This chemistry can be initiated on an FPOP platform, as shown by Chen et al.[181] in the presence of a histidine scavenger to control the $I^{\bullet}$ lifetime and thereby reduce labeling-induced conformational changes.

After laser irradiation, the hMb and aMb were analyzed as intact proteins (Figure 21), where a single addition of $I^{\bullet}$ leads to 125.90 Da mass shift. Modifications occur to give more mono-, bi- and tri-iodinated aMb than for hMb, consistent with a more exposed conformation for aMb resulting from heme removal. In contrast to $^{\bullet}OH$ oxidation, the nearly exclusive iodination on Tyr and His simplifies the interpretation and data analysis,

making possible a coupling with top-down MS for residue-level information. Top down ECD fragmentation on a 12 T FT-ICR gave a $*z_8^+$ ion that showed that iodination of Tyr146 was 26% for aMb but not detectable for hMb. On the contrary, iodination of Tyr103 (difference between $*z_{55}^+$ and $*z_{44}^+$) was similar for both proteins. The results can show that Tyr146 must be involved in heme-binding.

Owing to the limited sequencing efficiency of ECD technology at the time of the research, modified residues located in the middle region of a protein would be better analyzed with traditional bottom-up methods. His residues, although 30-100 times less reactive than Tyr, [1018] can also be addressed via a bottom-up strategy. Iodine radical footprinting may become a sensitive structural probe as is seen in an application to two other protein systems (i.e., apo-/holo-carbonic anhydrase II and EDTA-/zinc-insulin). The capability of this approach to yield structural information is seen by the abundant labeling of the region that carries the incipient f helix in apo state and the remarkably low to non-detected footprinting of that region of the holo state.

Although the coverage afforded by the iodide radical is limited, footprinting two targeted residues can answer specific questions with easier data analysis. Compared to $^{\bullet}$OH footprinting, the unique and larger mass shift increases the confidence of assigning the modification sites. Moreover, the precursor of the iodine radical doesn't react with proteins, which minimizes the background modification and allows simplified post-label sample handling. Unlike specific amino acid labeling, the modifications on the FPOP platform are fast, alleviating concerns about labeling-induced conformational changes.

5.7. Summary and Perspective

Radical footprinting is an effective means to acquire HOS information for proteins. Radical reactions are much faster (nano to milliseconds) than reactions of a conventional chemical reagent that modifies one or a few amino acid residues. Therefore, free radical footprinting will deliver fast, broad, and less biased information by largely avoiding questions of labeling-induced perturbation of protein structure. In addition, the short timescale can allow a sensitive report of subtle structural and even dynamical changes. An advantage of the labeling speed is the successful temperature jump, two-laser experiment on the FPOP platform where $^{\bullet}$OH footprinting can successfully track the folding of barstar at times as short as a few tenths of millisecond.[1019] An example of versatility is the tracking of multiple intermediate oligomeric states during amyloid beta aggregation.[1020]

Although different radicals react via distinct pathways, they share similar features (Figure 22a). Many radicals (e.g., $^{\bullet}CF_3$, $I^{\bullet}$, $SO_4^{-\bullet}$, $CO_3^{-\bullet}$, $^{\bullet}$OH) permit modification by forming a protein-centered radical that is subsequently quenched, whereas others (e.g, $^{\bullet}$OH and carbene diradicals) can directly add to a protein molecule. Whatever the process, the informative modifications are usually by an irreversible covalent bond to an amino acid side chain, facilitating downstream sample handling and analysis comparing to that of reversible labeling. A protein footprinting-based "toolbox", that is being built for the future, will contain radicals that show different residue specificity to address specific biological questions (Figure 22b). For example, when protein systems are rich in Glu and Asp (e.g., as for calcium-binding proteins), GEE or carbene footprinting may be a good choice with quick

and simple data analysis and high throughput. More importantly, investigators can customize reagent combinations for targeting specific residues or for obtaining high coverage. Other radical species (e.g., nitric oxide radical) will be tested, and new radical precursors will emerge soon to footprint both soluble and transmembrane proteins. A “toolbox” with diverse reagents and associated modeling software will aid investigations of complex biological questions with effectiveness, sensitivity, and accuracy.

6. Applications that Utilize Fast Labeling Approaches

Since the initial introduction of protein footprinting by free radicals in 1999,[884] combinations of different reactive species and several experimental designs have successfully demonstrated the reliability of fast-labeling approaches and its ability to address various biological questions. In this section, we will discuss recent advances since the Chance review in 2007[170] and highlight key developments.

6.1. Mapping Epitopes

Monoclonal antibodies (mAb)[1021] are important biomacromolecules owing to their broad applications in analytical assays[1022-1024] and their profound potential in therapeutics.[1025-1026] Antibodies bind to antigens with high specificity and strong affinity, and this property has been utilized for some time in immuno-histochemistry[1022] and in the enzyme linked immunosorbent assay (ELISA),[1023] assays that are now standard practice around the world. The highly specific recognition also makes it possible to develop targeted therapeutics.[1025-1026] These advances rely on a deep understanding of antibodies from both a structure and functionality perspective.

Interacting surfaces in antibodies and antigens are termed as paratopes and epitopes, respectively. Paratopes mainly consist of loop regions of 10–15 amino acid residues and are termed “complementarity determining regions” (CDRs). Paratopes of a typical mammalian antibody are found in six CDRs, three from the heavy chain and the remainder from the light chain.[1027] Although the combinations of amino acid residues that comprise the six CRDs are nearly unlimited,[1028] the structure and position of the paratopes are usually well-defined in accord with the rigid scaffold of the antibodies.

Antigens, however, differ dramatically from antibodies and from each other. Epitopes in antigens do not exist in a specific structure. The binding site for the antigen (epitope) depends on the location of the actual binding interface that interacts with antibodies. In other words, epitopes can be located anywhere on the antigen surfaces.[1029] Moreover, an epitope can be either linear (consecutive) or conformational (assembled).[1030] A consecutive epitope is composed of a single continuous structural motif, whereas an assembled epitope consists of multiple and non-adjoining binding motifs. As the majority of reported epitopes are assembled,[1029-1030] a complex binding scheme usually pertains and requires responsive methods for mapping epitopes.

X-ray crystallography,[1031] NMR[1032] and alanine-scanning mutagenesis[1033] are the most commonly used high-resolution biophysical approaches in mapping epitopes. X-ray crystallography and NMR reveal the binding regions, allowing assignment of epitopes as

surfaces on the basis of proximity of the antibody and antigen. Such contact, however, may not always lead to structural recognition. Mutagenesis maps the epitope from a functional aspect, but that approach may not be informative for high order structure and the amino acid substitutions may affect the protein HOS. Alanine scanning, whereby amino acid residues are replaced one at a time or in a group (called “shave” analysis) coupled with binding assays to judge the effect of the mutation, locating functional epitopes with high confidence. Other functional assays including but not limited to studies of synthetic peptides representing the antigen[1034] or represented by antigen truncation[1035] were also developed as high throughput but low spatial resolution approaches as compared to the alanine scanning.

To complement these approaches, MS-based epitope mapping methods were developed substantially and now are regarded as reliable approaches.[1036-1038] Two different schemes were originally used; that is, epitope excision[1036] and epitope extraction.[1039] Both approaches utilize the specific binding between antigen and immobilized antibodies. In an epitope excision workflow, an immunocomplex is formed in solution, after which a protease is added to digest the antigens. The peptides from the antigen that contain the epitope remain bound with an immobilized antibody, and they are then extracted and characterized by MS. Epitope extraction, however, starts by digesting antigens and utilizes the resulting peptides in a peptide-immobilized antibody complex. In this case, those peptides that bind the antibody represent epitopes.

In both schemes, the investigator identifies epitope peptides by using MS and then sequences them by MS/MS. The amount of antigens required can be as low as sub-pmol[1040]. MS-based approaches significantly lower the sample amount and reduce the need for sophisticated sample preparation and data analysis as compared with X-ray crystallography and NMR, while preserving mid-to-high spatial resolution from a structural view. MS-based approaches locate potential epitopes with significant less effort, providing valuable guidance for designing proceeding mutagenesis and other biological functional assays to locate functional epitopes confidently.

More recently, MS-based epitope mapping approaches utilize HDX to label the protein chemically and monitor changes in SASA that result when antigens bind with antibodies.[1041] Thanks to the high binding affinities for many immunocomplexes, off-rates do not heavily distort the HDX kinetics. Both the antigen and the immunocomplex can be footprinted under native-like conditions, minimizing potential perturbations of structure. Although the HDX rates are significantly slowed (quenched) at a pH of 2.5 and 0 °C,[184-185]back-exchange cannot be avoided. Proteases that function under acidic environments are generally limited to pepsin and Fungal protease XIII,[1042] both of which are non-specific, and the resulting peptide mixture is complicated and challenges the data analysis. Moreover, H/D scrambling during MS/MS analysis limits the spatial resolution to the peptide level; that resolution can be increased possibly to the residue level by using ECD[135] and ETD[217], which presumably do not scramble the D labels.[216-217]

Epitope mapping by fast labeling methods was first demonstrated by Jones and Gross[1044] in 2011, where the epitope of serine protease thrombin was footprinted with hydroxyl radicals on the FPOP platform. Two regions show binding-induced protection as evidenced by the

decrease in extent of modifications (representative results are in Figure 23a), where five distinct peptides exhibit increased protection upon binding (darker bar represents unbound and lighter bar represents bound). The protection spans 42 amino acid residues, but such protection seems too extensive considering the size of thrombin. Taking advantage of the irreversible labeling of FPOP chemistry, the investigators could further assign protection at the residue level (results in Figure 23b). Among 14 resolvable residues, protection in the antibody-bound form occurs between residue D133 and Y150; those results are mapped in Figure 23c. Proposed epitopes agree well with those from an earlier HDX study.[1041]

Moreover, four residues (Figure 23b) and three peptides (Figure 23d) show deprotection upon forming the immunocomplex. This deprotection, not observed with HDX, is assigned as a remote conformational change. HDX monitors both backbone amide hydrogen bonding and solvent accessibility whereas FPOP emphasizes the latter. If allosteric or remote conformational changes do not involve changes in hydrogen bonding but occur as reorientation of amino acid residue side chains, they will not be seen by HDX.

Subsequent studies of similar design reveal the epitope of human epidermal growth factor receptor (EGFR)-Andectin 1,[1045-1046] IL-6R-Adnectin 1&2,[738] and human immunodeficiency virus 1 gp120 envelope glycoprotein,[1047] demonstrating even more the efficacy of fast labeling approaches and making a case for generality.

As mentioned earlier, changes in SASA/hydrogen bonding may not directly associated with biological recognition. Binding-induced protection can occur either from binding at the epitope region or from remote conformational change sites, which can be differentiated by site-specific mutagenesis and functional assays or possibly by crosslinking.

A 2017 study by Li et al.[1048] applied orthogonal methods including FPOP, HDX, and alanine shave mutagenesis and determined energetic epitopes of an antibody/Interleukin-23 interaction. By examining the system with FPOP footprinting, they found that five regions of IL-23 p19 domain show protection (results mapped onto the crystal structure in Figure 24a). Similarly, HDX reveals four slightly different protected regions, three of which overlap with those reported by FPOP (Figure 24b). Imperfect overlap motivates subsequent alanine shave analysis, where a series of mutants can be designed based on MS-analysis, enabling confirmation of the residues/peptides identified by the two MS methods. Four distinct mutants show significant lower binding affinities as compared with the wildtype protein. Note that all four mutants retain near wildtype-like conformations as confirmed by optical and NMR approaches. Thus, this comprehensive approach points to the first two regions of IL-23 p19 domain as epitopes, whereas protection for regions 124-139 (by FPOP) and 145-153 (by HDX) are from remote binding-induced conformational change. This study is a good example of the workflow of fast radical labeling and HDX MS to guide mutagenesis and functional assay for epitope mapping.

In addition to the advantages of low sample amount, mid-to-high resolution spatial information and high-throughput, fast labeling approaches can bring amino-acid-residue level spatial resolution to epitope mapping without the need of specialized MS instrumentation of ECD or ETD fragmentations in HDX or the effort needed for alanine-

scanning mutagenesis. Irreversible labeling is not subject to the back-exchange of the label as applies to HDX, and the sample can be examined with any fragmentation method without concern for scrambling of the label. Moreover, the labeled protein can be digested with a variety of enzymes at their preferred pH's, whose cleavages can be highly specific (e.g., trypsin), simplifying the data analysis. Fast labeling approaches are sensitive to subtle changes in the SASA of amino acid side chains, which may not be accessible to HDX.

FPOP, which generates $^{\bullet}$OH through laser photolysis of H_2O_2, controls the lifetime of the radicals to avoid perturbation of native protein conformation. The concentration of $^{\bullet}$OH needed for comprehensive footprinting is not large and is readily generated by the photolysis (~ 1 mM of radicals can be formed). In a FPOP-based epitope mapping approach, protection is evaluated through changes in the extent of modification, requiring that addition of the antibody to the antigen solution does not increase reactive sites so extensively as to quench the radicals and lower the modification extent of the antigen. This is particularly a problem when the antigen is small compared to the large antibody. This potential bias can be overcome by either introducing small molecule radical dosimeter[1049]/reporter peptide[1050] to calibrate the effective $^{\bullet}$OH concentration or by keeping the mass of total protein nearly the same in the control and the test experiments. An excellent way of doing this would be to include a nonbinding antibody when footprinting the antigen as control. To generate $^{\bullet}$OH through other approaches like synchrotron water radiolysis may also be a good alternative.[884]

6.2. Tracking Protein Folding/Unfolding

Dating back to 1961, the ribonuclease refolding experiment by Christian B. Anfinsen[2] showed that small globular proteins can fold, without assistance from other biomolecules, to their free energy minimum state. Soon after, Cyrus Levinthal[1051] argued that such protein folding would be too slow because the protein has too many possible conformations to search before finding its energy minimum, known today as Levinthal Paradox. Following the ribonuclease refolding experiment, Anfinsen later proposed a thermodynamic hypothesis wherein the protein native structure is only determined by the protein's amino acid sequence.[1052] Decades of structure determination resulted in the accumulation of over 140,000 high resolution structures in the Protein Data Bank (PDB). It is now accepted that protein folding is driven primarily by interactions including hydrogen bonding, van der Waals interactions, backbone dihedral angle preferences, hydrophobic interactions, and electrostatic interactions.[1053] Understanding protein folding pathways and their corresponding intermediates, however, remains a huge problem that now has become a field of research onto itself.

Modern views of protein folding take an energy landscape as a foundation for the folding problem. Rather than a defined folding pathway, multiple routes facilitate protein folding from an unstructured chain of amino acids to a native conformation; that is, a protein negotiates a folding funnel.[1054-1055] Modern structural prediction algorithms pioneered by Critical Assessment of protein Structure Prediction (CASP) also contribute greatly to addressing this problem.[1056] All these developments were reviewed previously.[1057-1059]

Experimentally, folding or unfolding is followed, after introducing a perturbation as a function of time, through characterization by several methods;[1060] perturbations that can be used are a sudden change typically in temperature,[893-894, 1061-1062] denaturant concentration,[1063-1064] pH,[1065] or pressure[1066]. As secondary structural motifs including α-helices and β-sheets usually form in 0.1 – 10 μs,[1067] and some small proteins can fold as fast as tens of microseconds[1068], it is important that the characterization/labeling method is fast enough to follow the process and capture any intermediates. For decades, several approaches including circular dichroism,[1069] fluorescence,[66] FI-IR,[1070] and NMR[1071-1072] have been most extensively used. Although lower in spatial resolution, the detection time limit for optical approaches can be as low as 10 fs,[1073] a time that is ideal for tracking rapid structural transitions. On the other hand, using rapid mixing and multidimensional NMR coupled with HDX has been successful in characterizing folding processes on the time scale of milliseconds with high spatial resolution.[1072] Recent developments of NMR instrumentation allow observation of folding intermediates on the timescale of 100 μs,[1066] greatly elevating the spatial resolution over that achieved by optical approaches. Modern single molecule measurements[1074] and mutational approaches[1075] also shed light on folding.

Following protein folding/unfolding by MS was first demonstrated by Chait and coworkers[1076] in 1990, who electrosprayed cytochrome C at different pHs. They observed different charge-state distributions when the protein was introduced in different conformations; an unfolded form favors higher charge states. This observation enables MS to follow, in a simple and global way, the protein conformational changes upon perturbation, a representative one being myoglobin reconstitution coupled with online continuous-flow labeling.[1077] In the same decade, HDX was married to MS,[203, 1078] and the combination was used soon after to address lysozyme folding. [1079] Further development of a “rapid mixing” apparatus made possible the measurement of folding kinetics by HDX-MS,[1071-1072, 1080] and, in combination with protease digestion, allowed peptide-level spatial resolution.[70] All these efforts empower MS in protein-folding analysis and were reviewed elsewhere.[260, 777, 1059]

The application of free-radical footprinting in folding studies was first demonstrated by Chance, Woodson and coworkers[880-881] for RNA, where a “stopped-flow” apparatus combined with synchrotron-generated ●OH radicals probed ribozyme folding dynamics. Proteolysis to form peptides and MS to locate the footprinting provided some regional specificity.

This approach was later applied to protein unfolding. By varying urea concentration, Maleknia and Downard[1081] followed apomyoglobin denaturation through a series of ●OH footprinting experiments. Upon protease digestion, they showed that helices A and B/C unfold in a cooperative fashion whereas helix G unfolds locally at lower denaturant concentration. Thermodynamic parameters were obtained, and they agree with those from fluorescence-based measurements. Although measured under equilibrium conditions, this study for the first time demonstrated the possibility for radical labeling in addressing protein folding/unfolding. Later studies by Poor et al.[1082] utilized this idea and demonstrated successfully the refolding the paramyxovirus fusion (f) protein by changing equilibrium

temperatures and determining the free energy landscape of bacterial immunity protein (Im7) folding by combining mutational analysis with free radical labeling[1083].

Although the approaches in equilibrium measurements are useful, it is challenging and likely more informative, to examine protein folding kinetically. Taking advantage of the Hambly and Gross[841] demonstration of ●OH protein footprinting through laser photolysis of H_2O_2 in a flow system, Konermann and coworkers[1084] integrated rapid mixing with ●OH labeling to study the protein folding/unfolding in a kinetics experiment. In 2009, Stocks and Konermann[1084] first built a continuous-flow rapid mixing device for probing protein conformational changes during unfolding, shown in Figure 25a. The rapid mixing apparatus has two mixing “tees”. Using three syringes, the investigators mixed native protein (hMb), H_2O_2, and denaturant HCl in a continuous fashion. By tuning the flow rate, pulsed laser frequency, the distance between the second mixing tee M2 and the window for laser irradiation, the delay time between protein denaturation and ●OH labeling can be manipulated. In this study, four different time points, 50 ms, 500 ms, 10 s and 5 min, were investigated. Using tryptic digestion, the investigators followed oxidative modifications as a function of denaturing/unfolding time of hMb regional specificity. Peptide T7 represents the region that unfolds initially upon adding denaturant (Figure 25b). Peptides T2, T10 and T13, on the other hand, stay relatively protected up to 500 ms after mixing with HCl. Peptide T16 represents the region that unfolds between 50 to 500 ms. The hMb becomes completely unfolded after mixing with HCl for 5 min. On the other hand, by starting with denatured protein and replacing HCl with renaturing buffer, the investigators could study the folding of cytochrome *c*,[1085] the folding and dimerization of S100A11,[1086] the folding of an integral membrane protein bacteriorhodopsin,[1087] and even sub-millisecond folding of apomyoglobin.[1088]

Recently, the delay time was further shortened to the microsecond timescale by a newly designed microfluidic mixer, and the unfolding was followed by FPOP. The data reveal two kinetic phases of egg lysozyme that occur before 1 ms.[1089] The requirement for low sample amounts and the achievement of regional specificity, coupled with kinetic capability open new possibilities for protein folding studies even on the sub millisec time frame.

In 2010, Chen, Rempel and Gross[893] reported a design that combined FPOP with a laser-induced temperature-jump to probe sub millisecond folding. As demonstrated in Figure 26a[893], two lasers were controlled by a signal generator and a delay circuit, and their beams were aligned to intersect sequentially at the same transparent window on the flow capillary. A Nd:YAG laser with a Raman shifter produced a “heating pulse” at 1900 nm, a wavelength that is absorbed by water to induce a temperature jump of ~ 20 °C. A fraction of second later, an excimer laser at 248 nm generated ●OH that footprints the protein as a function of time. By controlling the delay time between firing the two lasers, it is possible to track the protein folding/unfolding kinetics with high spatial and time resolution. The delay time of this two-laser approach is no longer limited by fluid dynamics, as in rapid mixing, but by the time separation between the T jump laser and the ●OH labeling laser. By tuning the reaction conditions, ●OH should be able to footprint the protein irreversibly in times as short as 1 μs[878, 893] or less, making it possible to follow folding dynamics of fast folding proteins.

The investigators successfully footprinted the first intermediate state of barstar folding, which happens within 2 ms of the temperature jump.[894] Changes of the modification fractions at the amino acid residue level revealed the key residues that serve as a nucleus for barstar early folding as seen in Figure 26b,[894] where residues H17, L20 and L24 can be assigned as closely associated with the hydrophobic core around which barstar folds; residues I5 and F74 are weakly associated with the hydrophobic core. Residues W53, L88 and many others, however, are not involved in early folding, because their fractional modification does not change with delay time, indicating their solvent exposure does not change up to 2 ms after the temperature jump.

Radical species have the advantage of short reaction time, which is ideal for following fast processes. The ●OH FPOP-based two laser approach brings high resolution to submillisecond protein folding studies,[893-894] which was not easily accessible prior to this work. Secondary structural motifs for some fast-folding proteins, however, can form as fast as 0.1 μs[1067] thus requiring an even faster probe. Carbene diradicals label protein at the nanosecond timescale,[973] suggesting that those footprinters may be appropriate to address such problems.

Despite these advantages, the two-laser apparatus is only applicable if the temperature jump is sufficient to cause the protein to fold or unfold. Folding is more restrictive as few proteins are denatured at low temperature and become renatured upon heating. The change in temperature that the laser can deliver is also limited. From this perspective, although relatively slow,[1089] with certain exceptions, rapid mixing is more universal as it can introduce various perturbations. Recent development of theta-capillary emitter for the ESI source greatly shortens the mixing time and pushes the limit down to 270 ns – 27 μs.[1090] It was demonstrated that this novel development can be used in both protein folding studies[1091] and HDX[227] of proteins at μs timescale. These exciting developments open new possibilities for protein folding studies. By spraying denatured protein and deuterated renaturing buffer through a theta-capillary emitter and analyzing the resulting protein in an ETD-based top-down fashion, it may be possible to analyze protein folding with high spatial resolution. A disadvantage may be that the protein conformational change occurring upon ESI is not physiologically relevant.

6.3. Assaying Protein Aggregation

Studies of protein aggregation and its relationship to neurodegenerative diseases date back to 1910, when Fritz Heinrich Lewy first observed unusual protein aggregates in the brains of patients with Parkinson's disease.[1092-1093] These aggregates were later termed as Lewy bodies[1094] and became the diagnostic for Parkinson's disease. Nowadays, it is well understood that a Lewy body is composed of misfolded α-Syn. Alzheimer's disease, as first described by Alois Alzheimer,[1095] is another major neurodegenerative disease induced by protein misfolding and aggregation of amyloid beta (Aβ)[1096]. A 2016 report indicates there are approximately 6.2 million people globally who were affected by Parkinson's disease.[1097] The number is 29.8 million for Alzheimer's disease.[1097] Unfortunately, neither of these diseases have cures, and their pathologies are not well understood.[1093, 1096, 1098-1099] Thus,

it is important to develop novel approaches to locate and quantify protein aggregates, to study the aggregation mechanism, and to develop therapies.

Characterization of protein aggregates is challenging, especially at high spatial resolution. The final state of these aggregates, solid Aβ fibrils, for example, can be characterized with high resolution approaches including solution (labeled by D_2O and solubilized in dimethyl sulfoxide)[1100] and solid-state NMR[1101], x-ray crystallography[1102] and modern cryo-EM[1103-1104]. The low molecular weight soluble oligomeric intermediates that "come and go" during aggregation, although physiologically important, are not amenable to those techniques owing to low solubility, high heterogeneity, intrinsic disorder, instability, and high aggregation propensity. Some of these aggregates can be investigated by atomic force microscopy (AFM) to give a high-resolution morphological picture of early aggregation intermediates.[1105] On the contrary, no site-specificity or spatial resolution are available when using such approaches.

Among all characterization approaches, fluorescence is the most widely adopted to follow protein aggregation. With the discovery of thioflavin T (ThT),[1106] a dye that when it binds β sheet-rich structures exhibits an enhancement in fluorescence, has become the classic way of following aggregation.[1107] The Aβ aggregation process can then be tracked and quantified both *in vivo* and *in vitro*. Given its broad applicability for characterizing different aggregation stages, ThT fluorescence is regarded as a characteristic of amyloid fibril formation.[1108] Nevertheless, limited spatial resolution and possible distortion of the aggregation process by adding the dye have always been major concerns.[1109]

MS-based approaches can contribute to this field from two distinct points of view. MALDI-imaging enables label-free quantification of Aβ aggregates.[1110] Ion mobility MS is capable of separating different Aβ oligomers based on their collision cross sections in the gas phase.[1111] HDX coupled with MS also reveals structural information of Aβ fibrils,[1112] protofibrils,[1113] and even Aβ aggregation kinetics[1114]. With top-down sequencing and ECD fragmentation, H/D scrambling is minimized, allowing residue-level information of Aβ oligomers.[1115-1116] These efforts were recently reviewed.[1117-1119]

The ability to study Aβ aggregates by radical footprinting was first demonstrated in 2014 when Klinger, Chance, Axelsen and coworkers[1120] utilized synchrotron-based HRF to examine the fibrils and prefibrillar forms of the 40-residue Aβ ($Aβ_{1-40}$). By comparing the protection factors for selected residues in prefibrillar and fibril $Aβ_{1-40}$, they mapped the footprinting data onto high-resolution solid-state NMR models and showed that the solution information obtained from HRF-MS is consistent with several core filament structural models elucidated in solid state, but not with other models that they rejected. Moreover, protection factor analysis supported the linear heterogeneity of the $Aβ_{1-40}$ fibrils; that is, two- and three-filament assemblies alternating along the length of the fibril.[1120] Measured protection factors of the residues on the flexible loop regions of $Aβ_{1-40}$ are also consistent with the structural constraints from solid-state NMR studies.

Later on, Li et al.[1020] applied FPOP to study the aggregation process of 42-residue Aβ ($Aβ_{1-42}$). By following the $Aβ_{1-42}$ as a function of incubation time with FPOP, the

investigators found a clear decrease in modification fraction shown in Figure 27a, consistent with a decrease in SASA owing to aggregation. By modeling the results with a two-nucleation/two-autocatalytic mechanism, they successfully fit the data (solid line in Figure 27a) and constructed a system composition plot as a function of incubation time, shown in Figure 27b. Plotting relative fractions for four components, the investigators proposed an $A\beta_{1\text{-}42}$ early aggregation mechanism, where $A\beta_{1\text{-}42}$ monomer rapidly assembles into paranuclei and further accumulates until a certain threshold. Upon passing that limit, the paranuclei self-catalyze a structural reorganization to deplete the monomers and form readily the mature fibrillar aggregates.[1020]

Upon digesting the $A\beta_{1\text{-}42}$, spatial resolution is elevated to regional and some residue levels. The N-terminal region remains solvent accessible throughout aggregation (Figure 27c) as seen by the minimal change in modification in that region during aggregation. The central (Figure 27d) and C-terminal regions (Figure 27e), however, actively participate in aggregation, as evidenced by significant decreases in modification fraction. Similar logic applies to residue-level interpretation, where SASA of H6 (Figure 27f) changes little during aggregation. Residue F19/F20 (Figure 27g) and M35 (Figure 27h) are actively involved in aggregation, and the investigators proposed that F19/F20 contributes a driving force for $A\beta_{1\text{-}42}$ aggregation by serving as a hydrophobic nucleation interface.[1020] Although some residue-level resolution was obtained, not all residues could be studied, confirming the need for alternative free-radical footprinters that prefer to react with other residues than those reactive with $^{\bullet}OH$ and give complementary information.

MS-based approaches make possible the characterization of early aggregation states, especially transiently existed intermediates, which was not possible by the earlier low-resolution optical approaches. MS coupled with radical footprinting deepens the understanding of Aβ folding mechanisms with some residue-level resolution, and this approach can be further extended to other aggregating systems. Although the footprint cannot be assigned to a specific oligomer, the approach is sensitive to the broad range of states and their changes during aggregation. Nevertheless, the approach can further evolve for aggregation studies of proteins alone or with small organic molecules or metal ions that either inhibit or promote aggregation.

From a broader perspective, the two MS-based footprinting approaches, pulsed-HDX and radical labeling, complement each other. Both methods report changes in SASA; HDX is sensitive to backbone hydrogen bonding and solvent accessibility whereas radical footprinting monitors changes in sidechain orientations. Moreover, radical footprinting can shorten the detection timescale to milliseconds. By combining pulsed HDX and fast radical labeling, one can obtain an understanding of protein aggregation intermediates and mechanisms, and these insights should prove invaluable in developing novel therapeutics.

6.4. Probing Ligand Binding, Affinity and Dynamics

$$Protein\,(P) + Ligand\,(L) \underset{k_{off}}{\overset{k_{on}}{\rightleftarrows}} Prrotein - Ligand\,Complex\,(PL) \tag{23}$$

$$K_a = \frac{k_{on}}{k_{off}} = \frac{[PL]}{[P][L]} \quad (24)$$

$$K_d = \frac{k_{off}}{k_{on}} = \frac{[P][L]}{[PL]} \quad (25)$$

Numerous proteins interact with ligands to facilitate biological processes for which quantitative understanding is vital.[1121] Protein-ligand binding affinity measurements are a quantitative measure of these processes; by definition, affinity is the equilibrium constant for the reaction of ligand binding to a protein. It can be expressed as a K_a or K_d (see equations 23 - 25). To date, three general approaches have been used to characterize such interactions. Measurements include circular dichroism,[1121] fluorescence and fluorescence polarization, [1122-1123] FT-IR,[1124] and NMR,[1032, 1125] that provide read-out of the system composition at given ligand concentrations. These readouts are further utilized, via equations 24 and 25, to derive macroscopic binding affinities. Surface plasmon resonance (SPR) measures the ligand on and off-rates, thus providing binding affinity through a kinetic approach.[76, 1126] Isothermal titration calorimetry (ITC) measures heat flow during a ligand titration, and binding affinities are obtained employing the van't Hoff equation.[74] All these methods are considered to be standard in binding affinity determination, and ITC and SPR are commonly used for their speed and ease of operation.[1127] On the other hand, these methods are limited by spatial resolution, often giving none, large sample amount requirement, and sometimes by special sample preparation.

MS-based approaches can advance this field by providing another direct approach that significantly lowers the sample amount. A caveat is whether direct MS can preserve the biological-relevant environment.[1127] Under optimal conditions, a MS-based binding assay only requires high-picomole amounts of samples.[1128-1129] Similar with concentration-measurement approaches, MS examines the binding system by measuring its composition (i.e., the concentrations at equilibrium) either directly or indirectly. The direct approach takes advantage of native spray, a gentle form of ESI whereby the protein can be sprayed in a native or near-native state, retaining non-covalent interactions[151, 1130-1131] and allowing direct measurements of the various equilibrium concentrations;[1127, 1132] this was first demonstrated by Loo *et al.*[1133], where they determined the affinities for binding between ribonuclease S-protein and S-peptide. Early applications were in several disciplines including protein-protein,[1134-1135] protein-peptide,[1136] protein-oligonucleotide,[1137] protein-small molecule,[1138] peptide-antibiotic[1139] and small molecule-RNA[1140] complexes.

This direct method has been carefully developed for quantifying protein-glycan interactions, as pioneered by Klassen and coworkers.[1127, 1141-1143] In 2019, Nguyen and Donald[1144] measured small molecule-protein interactions through nanoscale ion emitters coupled with native spray, which was not possible previously owing to the high salt concentration needed to stabilize such weak interactions. Although the method is convenient, there is always a question of whether the measured gas-phase concentrations truly represent those in solution; further, the ionization mechanism is complex and not yet well understood.[1127] The glycan/

protein interactions agree well with those determined by other solution approaches, possibly because the ligands are similar.

Indirect approaches, on the other hand, requires pre-detection labeling. Using this form of labeling in MS was first done by using HDX, where two separate titration methods were demonstrated in the early 2000s, namely, SUPREX[231, 1145] and PLIMSTEX[232]. Both utilize the differences in deuterium uptake between ligand-free and ligand-bound states at a selected exchange time. SUPREX uses denaturant as titrant, and the titration mid-point is extracted by modeling the data; those data are further extrapolated to give folding free energies and binding affinities.[231, 1146] PLIMSTEX, on the other hand, uses the ligand as titrant, and binding constants are derived by fitting the titration curve.[232] Both approaches have been extended to the peptide level, providing regional specificity and improving spatial resolution.[233]

Owing to the relatively long times used for HDX, neither of these approaches are compatible with systems with high ligand-off rates. They also suffer from post-labeling back exchange. Footprinting by radical species overcomes these drawbacks owing to the irreversible and fast labeling that pertain. In 2019, Liu et al.[1129] proposed a method named LITPOMS (ligand titration, fast photochemical oxidation of proteins and mass spectrometry) that for the first time marries fast labeling species to binding affinity determination. As shown in Figure 28, a series of aliquots with different ligand concentrations comprise the titration process. Each aliquot is FPOP footprinted with ●OH, and further analyzed by MS. LITPOMS can be executed under two different concentrations, where the high-concentration experiment reveals binding stoichiometry and the low-concentration experiment can be modeled to extract binding affinity, just as with PLIMSTEX.

A proof-of-concept study demonstrated that LITPOMS successfully yields binding stoichiometry, binding sites, and binding affinity of a tight-binding system, namely calcium-bound calmodulin (holo-CaM) and melittin. Trypsin digestion in combination with LC-MS/MS extends the spatial resolution to peptide and even amino acid residue level. Using this platform, the investigators found three peptide-level binding sites and six critical binding residues, two of which are in loop regions that do not show binding at the peptide level.[1129]

LITPOMS was quickly adopted, also in 2019, to study a more complex binding system, Ca^{2+}-CaM, in which CaM binds to four Ca^{2+} ions in a cooperative fashion.[1147] As demonstrated in Figure 29, LITPOMS successfully identifies four classes of behavior, all of which are reasonably explained. Other than the simple binding behavior shown in Figure 29b, composite binding curves in Figure 29d, f and h show a combination of binding and conformational changes induced remotely. For example, Ca^{2+} binding at the region represented by peptide 127-148 (Figure 29h) triggers a structural opening at another region represented by peptide 38-74 (Figure 29d), preparing this site to take its own Ca^{2+} and revealing allosteric behavior that was not well understood before. Such composite LITPOMS curves can be further dissected by using residue-level analysis together with several different protease digestions to increase spatial resolution. The investigators could distinguish clearly the binding and conformational changes, thus demonstrating that a

detailed picture can be obtained of calmodulin during binding with calcium by using a single approach. Moreover, binding order can be assigned through ranking the onset point of LITPOMS decrease as EF4 > EF-3 > EF-2 > EF-1,[1147] and was confirmed by a subsequent simulation study.[1148] Site-specific binding affinities can also be obtained by modeling of eight LITPOMS curves together. This measurement strategy may be particularly effective for signaling proteins that undergo numerous complex conformational changes in executing their functions.

Binding affinity measurements through radical labeling and MS is promising, as it provides most of the key information about the protein-ligand interactions via a single approach that reveals not only the binding sites and binding affinities but also the binding orders, allosteric behavior, and protein binding dynamics at high spatial resolution.[1147] To obtain all this information previously required a combination of several sophisticated methods. LITPOMS should have utility in studying complex binding systems, signaling proteins as mentioned above, as it fills the gap that exists between methods offering no spatial resolution to high-resolution x-ray or NMR structures with an approach that offers mid spatial resolution for ligand-free and ligand-bound states.

Challenges remain, however, as there is not yet a radical species that can react with all 20 amino acid residues in a single experiment. For example, $^{\bullet}$OH reacts with all 20 amino acids, but the range of reactivity is too large to allow the least reactive residue to compete with the most reactive in a single experiment, as was discussed earlier in this review. Thus, development of novel and complementary labeling reagents is vital, whereby one footprinter can react with the residues with competitive reactivity and several footprinters can cover all the amino acids in multiple experiments, or even in a single experiment utilizing multiple reagents. In that way, all residues involved in binding can report binding-induced SASA changes. Moreover, modeling of titration data can be challenging, especially for proteins that bind multiple ligands and yield titration curves whose fitting requires construction of complex mathematical models.

6.5. Labeling *in vivo* and in Animals

As discussed in section 4.5, labeling *in vivo* has unique advantages, which forecasts a bright future. In vivo labeling by radical species was first demonstrated with nucleotides, where Ottinger and Tullius[1149] used hydroxyl radicals to footprint the lambda repressor-DNA complex in live *E Coli* cells. Hydroxyl radicals in this study were generated by ionizing water molecules with a ^{137}Cs gamma ray source, which required up to 15 min to produce a sufficient concentration of radicals. To minimize heat damage to the cells during the long irradiation, Woodson and coworkers[1150-1151] utilized synchrotron X-rays to reduce the exposure time to as short as 100 ms and froze their samples (-34 °C to −38 °C) to minimize damage[1152]. Recently, similar experiments were done with a flow system to minimize double labeling and further reduce the exposure time to 10 – 20 ms.[1153] Better X-ray dose control also improves the accuracy and reproducibility.

In vivo protein footprinting by radical species, however, was not demonstrated until 2009 when Zhu and Sze[873] first performed in vivo protein footprinting with hydroxyl radicals generated by Fenton chemistry. The protein of interest was OmpF porin from *E. Coli*, an

outer membrane channeling protein that facilitates aqueous passive transport in gram negative bacteria. Their approach began with incubating live *E. coli* with Fe(II)-EDTA and H_2O_2 and then allowing reactions of $^{\bullet}$OH from Fenton chemistry to label the solvent-accessible residues *in vivo*. As demonstrated in Figure 30c, solvent accessibilities of two loop regions, L1 and L3, do not change significantly upon opening and closing the channel, suggesting that the loops are not responsible for manipulating the channel.[873] In other words, entrance of the channel is not blocked by the extracellular loops. Peptides from regions inside the channel (Figure 30d), however, are heavily oxidized when the channel is opened and barely oxidized when the channel is closed. Data support the hypothesis that the three resolved β-sheets are in the channel pore, as demonstrated by Figure 30a and b. Although voltage gating of OmpF was shown previously *in vitro*, this study for the first time reports the observation of gating phenomena in a native cellular environment.[873] Moreover, the novel footprinting also shows the capability of *in vivo* protein footprinting by radical species in addressing real biological questions.

In subsequent work, Shcherbakova *et al.*[879] shortened the timescale of $^{\bullet}$OH generation. By increasing the concentration of Fe(II)-EDTA to 2 mM, a 40% loss of fluorescence intensity was observed after 2 ms, suggesting that $^{\bullet}$OH can be rapidly generated and that this approach can label other short-lived intermediates.

Another widely used $^{\bullet}$OH generation method, FPOP, was also adopted for in vivo protein labeling. As first demonstrated by Jones and coworkers[1154], African green monkey kidney cells were mixed with H_2O_2 and submitted to KrF laser irradiation for $^{\bullet}$OH generation and protein labeling. H_2O_2 crosses the membrane through both passive diffusion and via channeling proteins such as aquaporin, allowing sufficient H_2O_2 inside the cell to give a good yield of $^{\bullet}$OH upon laser irradiation. Although H_2O_2 is toxic to live cells, the time required to execute the experiment may be short enough to avoid serious toxicity. Indeed, viability tests prior to labeling suggest that over 70% of cells remain alive under the experimental conditions used for the footprinting. The investigators observed 105 proteins that are oxidized by $^{\bullet}$OH. These different proteins were from different subcellular compartments as shown in Figure 31a, indicating an outstanding dynamic range for protein detection.[1154]

When zooming into a specific protein (e.g., actin), FPOP modification fractions can be correlated with SASA of the two different states of actin; namely, open and tight. Results in Figure 31b show a better correlation with the open state ($R^2 = 0.89$), suggesting that majority of actin molecules in the native Vero cells are in their open state.[1154] Later the same group improved the experimental apparatus by introducing a sheath buffer (Figure 31c) to reduce cell aggregation greatly and tube clogging.[1155] Their design also ensures that radiation exposure of each cell in the flow system remains comparable. As a result, the number of identified oxidized proteins increased by 13-fold.[1155]

In 2019, Jones and coworkers[1156] introduced small, live worms, *C. elegans* into the flow system, and they were able to identify oxidatively labeled proteins from different body systems as shown in Figure 31d. A closer look at the myosin chaperone protein UNC-45

suggests that the modification fractions obtained in this *in vivo* study correlate well with the SASA calculated from the crystal structure.

Owing to incomplete understanding of the absolute extent of modification, most MS-based protein footprinting approaches have been executed in a differential way, where the extent of labeling for a peptide/residue in different states (e.g., ligand-bound versus ligand-unbound) can be compared in valid way. Although promising, work by Jones et al. fails to reveal such differences up until now.

In one of the pioneering demonstration of in vivo radical footprinting through a differential approach, Zhu and Sze[1157] footprinted the structural changes of epidermal growth factor receptor upon binding with epidermal growth factor (EGF) in live *E. Coli* cells. Hydroxyl radicals were generated by an FPOP approach and the oxidation extents of EGF-free and EGF-bound states were compared. The results are consistent with crystal structures of these two states. Their study marries conventional bottom-up structural proteomics with in vivo free radical labeling, probing differential structural changes in a real cellular environment. Moreover, their workflow including enrichment by immunoprecipitation and in-gel digestion is applicable to other studies.

Another important class of in vivo protein footprinting by radical species is proximity labeling, pioneered by Ting and coworkers starting in 2013.[1158-1159] Unlike all other labeling approaches introduced prior to this study, proximity labeling is usually facilitated by enzymes. The first enzyme used to facilitate the labeling is ascorbate peroxidase (APEX), and the method was appropriately termed APEX labeling. In brief, APEX is genetically tagged onto the protein of interest, whose location in the cell is generally known. Upon adding H_2O_2 and biotin-phenol into the cell, APEX catalyzes the transformation of biotin-phenol into biotin-phenoxyl radicals, which then footprint nearby proteins (Figure 32). The biotin tag facilitates the post-labeling protein enrichment. As a result, the investigators were able to identify 495 proteins within the human mitochondrial matrix, 31 of which were not previously linked to mitochondria. APEX labeling is highly specific, as the radicals are short-lived (< 1 ms)[1160] and the labeling radius is within 20 nm.[1161] APEX labeling was optimized in 2015 by introducing different enzymes[1162] and labeling reagents,[1163-1164] making APEX labeling widely applicable to various cellular systems. On the other hand, APEX labeling is mainly used for proteomics purposes (i.e., determining primary structure). Its potential in protein footprinting for HOS elucidation remains to be explored. The idea of proximity labeling inspired another investigation of protein-carbohydrate interactions,[872] which is covered in section 6.8.

All in all, in cell and in vivo labeling appears to have unprecedented advantages in structural proteomics to complement in vitro approaches that usually do not accurately reproduce the cellular environment. Another advantage for these approaches is their application in studying membrane proteins and their complexes, which have poor solubility and instability in vitro. The short timescale of $^{\bullet}$OH labeling enables the detection of many transient structural intermediates, especially with the FPOP approach. Modern MS instruments also allow the detection of thousands of unique proteins in a single run. All these advantages forecast a strong future for *in vivo* labeling.

On the other hand, current demonstrations of in vivo labeling fail to reveal as much structural information as conventional in vitro bottom-up approaches. As there are thousands of proteins in a single cell, most current studies must still emphasize protein identification. It is still challenging to track structural changes of a single protein during a biological event. This requires better protein separation and enrichment, further development of MS instrumentation, and improved data processing software. Previous efforts have demonstrated the correlation between absolute modification fractions and SASA. By using computer-based protein structure modeling, footprinting can produce constraints that can be used to predict protein structure. In this way, we may be able to bypass the differential approach without sacrificing structural resolution. Several studies show promising results on this topic, and they will be covered in the next section.

6.6. Footprinting in Supporting Computer-based Structural Predictions

So far, all applications described in this section have been based on differential experiments, where the modification fractions for specific peptides and residues were tracked as a function of protein states. Different protein states are achieved, for example, as ligand-bound vs. unbound in epitope mapping, as native vs. mutant, after different folding times, at different aggregation states, at various ligand concentrations in affinity determination, and after conformational changes (e.g., opening and closing a channel). Although straightforward, the differential approach has some limitations. Although various systems can be characterized, comparisons require relatively pure systems where different protein states can be clearly differentiated.

Ideally, HOS would be determined directly by footprinting a single protein state. Radical labeling and even other MS-based approaches, however, are not capable of providing enough restraints to construct a high-resolution protein structure as can NMR and X-ray crystallography. Computer-based protein HOS prediction is powerful and has great potential, yet the incomplete understanding of protein folding does not allow accurate prediction of protein HOS.[79, 1058] Data from NMR,[1165] small angle X-ray scattering,[1166] cryo-EM[1167-1168] and site-directed spin labeling EPR[1169] overcome such limitations because they are based on structural restrictions or restraints.

An MS-based approach that is particularly amenable to modeling is chemical crosslinking.[761, 1170] Most of HOS elucidated from this workflow, however, is of protein complexes, because only with large and complex systems is it possible so far to obtain sufficient crosslinks for modeling. Further, the principal HOS outcome is a protein-protein interface and not the full structure although more detailed structure determinations are becoming possible. It may be that footprinting combined with crosslinking will lead to more reliable models than from either method itself.[768]

Structural prediction based on radical footprinting data was not possible until it can be properly quantized and reasonably correlated to the absolute SASA. Gerega and Downard[1171] in 2006 developed a docking algorithm named PROXIMO that adopts directly modification fractions for each resolvable residue as restraints. They were able to dock properly the calmodulin-melittin and Ribonuclease S-protein-peptide complexes. Although straightforward, their approach failed to consider the different reactivities between ●OH and

different amino acid residues, and that failure may produce bias in the footprinting data. This pioneering work expands the possibilities of radical footprinting and motivates more precise data quantification.

To date, three groups have demonstrated the efficacy of modeling footprinting results. In 2015, Huang and Chance[1172] first proposed a protection factor (PF) that successfully correlates single-state footprinting data with absolute SASA. The observed reaction rate from a dose-response curve from synchrotron-based ●OH footprinting (modification fraction versus X-ray irradiation time) is a function of both intrinsic reactivity of ●OH and the nature of the amino acid residue and its solvent accessibility.[160] Teasing out a structural contribution can be done by normalizing the observed reaction rate constant with respect to the residue-specific intrinsic reactivity. As a result, solvent accessibilities (calculated from X-ray structures) for three model systems and local structural contacts exhibit a quantitative agreement with calculated PFs, motivating future developments.

Recently, the investigators adopted this idea for characterizing the human estrogen receptor alpha (hERα), which contains a DNA-binding domain and a ligand-binding domain.[1173] Structures of these two domains are known individually but not in the complex. Using results from ●OH radical footprinting, PF calculations of resolved residues, and data from SAXS, the investigators generated sufficient structural restraints to guide successfully molecular docking. The outcome is a successful structure determination of an asymmetric L-shaped structure of the multidomain hERα, revealing key mechanisms that facilitate allosteric function.

In another elegant experiment, Xie and Sharp[1174] introduced a method for assessment of sidechain absolute SASA values by using an FPOP-based ●OH footprinting platform. By incorporating adenine as ●OH dosimeter, they obtained reaction rates for each residue through multi-point FPOP experiments (different ●OH doses). These data were further normalized with respect to intrinsic reaction rates of ●OH and free amino acids. Normalized protection factors obtained through these efforts were compared with fractional SASA, and a good linear regression was obtained.[1174] Further, two SASA prediction models were constructed for the soluble proteins myoglobin and lysozyme, and the predicted SASA's were compared with a calculated SASA from crystal structures by using a protein-unfolding MD simulation.[1174] Although the incorporation of radical protein footprinting data in some structural modeling is successful, use of the footprinting data directly in protein structure prediction is yet to be established.

In 2018, Lindert and coworkers[1175] developed a new Rosetta score term named *hrf_ms_labeling* that utilizes residue-level PFs from ●OH footprinting data as constrains to predict protein structures. PFs were calculated based on the formula proposed by Huang and Chance[1172]. With Rosetta, they generated 20,000 structural models with an *ab initio* method for four different proteins (i.e., calmodulin, cytochrome C, myoglobin and lysozyme). The Rosetta score for each model was plotted against their RMSD with respect to their native crystal structures as shown in Figure 33a. The 20,000 models for each of the proteins covers a broad range of RMSDs. Aligning the top-scoring model with the native structure allows better visualization of the differences, as there are even topology mismatches for calmodulin

and lysozyme (Figure 33b). Although there are models that have near-atomic resolution (RMSD ≤ 2Å), they were not recognized as the top scoring models by Rosetta. When rescoring the same 20,000 models with restraints from experimentally determined PFs, similar distributions were identified (Figure 33c). With the help of new scoring function *hrf_ms_labeling*, the RMSDs for the top-scoring models improve significantly for all four proteins. A visualization of the outcome (Figure 33d) shows that all models identify the correct protein topology.[1175] Structure models for cytochrome C and myoglobin come with near-atomic resolution, indicating the efficacy and applicability of the newly developed scoring function. This work demonstrates for the first time that incorporation of $^{\bullet}OH$ protein footprinting data can greatly enhance model quality in protein structural prediction, elevating the use of MS-based footprinting from a qualitative description to a quantitative evaluation. If these efforts continue to be successful, protein footprinting may no longer limited to differential experiments, and the results for a single protein state may be transformed into a high-resolution structure. The script of this newly developed scoring function and the corresponding instructions are freely available with Rosetta.

In another example, the same group[1176] developed novel Rosetta scoring function that utilizes SID MS data and demonstrated that SID data significantly enhance the confidence of structural predictions of protein complexes.

Although still in its early stages and requiring further work, structural prediction utilizing footprinting data shows significant promise. It will be necessary to generalize these workflows and make them compatible with other footprinting approaches. Further, it will be even more significant to develop a new structural prediction algorithm that is guided by footprinting data rather than by rescoring the existing models, as hinted in a subsequent study by Lindert and coworkers[836] in 2019.

6.7. Revealing Pathways in Biological Systems

ROS are those that form upon incomplete reduction of oxygen; they include superoxide anion ($O_2^{-\bullet}$), H_2O_2, singlet oxygen ($^1O_2$) and $^{\bullet}OH$.[844, 1177] These species play essential roles in regulating various functions in biological systems.[844] On the other hand, ROS are highly reactive, and are likely to induce oxidative damage at unfavorable locations. An interesting 2017 study takes a lead from free-radical damage and goes on to reveal successfully the water channels in photosystem II (PSII).[1178]

PSII is a membrane-bound oxidoreductase that catalyzes the conversion of water oxidation to molecular oxygen and simultaneously the reduction of plastoquinone. Sunlight is converted into chemical energy, and electron transfer in photosynthesis is thus initiated. A high resolution structure of PSII identified the catalytic center as Mn_4CaO_5, where substrate water is oxidized to O_2.[1179] The pathway for the substrate water molecule into the catalytic center, however, is poorly understood. As $^{\bullet}OH$ is the side-product of such conversion, and the size and hydrophilicity of $^{\bullet}OH$ are similar to those of H_2O[845], as discussed earlier, it is possible to map the H_2O channel by tracking the movement of $^{\bullet}OH$ and its oxidative damage. In other words, the $^{\bullet}OH$ modified residues leave a trail or “footprint” of natural oxidative damage that line the wall of H_2O channel, revealing the structural aspect of the PSII. Using an approach that includes analysis used for protein footprinting, the

investigators identified three distinct water channels, two of which aligned well those identified in previous studies. This work resembles that of Ting,[1158-1159] described in Section 6.5, except the oxidation occurs naturally.

This simple experimental design utilizes the naturally occurring ●OH and related species as labeling reagents to footprint PSII in vivo. The structural information obtained in this work increases the mechanistic understanding of the PSII system. Moreover, the outcome motivates further development of radical protein footprinting and ROS localization to understand the chemistry of ●OH and to augment, even supplant, other low-resolution approaches for detection of ●OH.[1177] MS-based in situ radical footprinting offers an elegant way to localize the ●OH by tracking its damage trails on the surrounding amino acid side chains. The utilization of naturally occurring radical species in protein footprinting may also provide insights into “natural” oxidative modifications and whether they introduce perturbations to native biological systems.

Inspired by this idea, a recent study focused on $CO_3^{-\bullet}$, a naturally occurring radical, and used the FPOP platform to characterize the reactions of $CO_3^{-\bullet}$ that may occur in vivo.[957] Although a reactive species, the $CO_3^{-\bullet}$ radical anion does not qualify as a good footprinter owing to ambiguity in its generation from ●OH or other strong oxidizing radicals, underscoring that novel mythologies and other radical species are necessary in the footprinting field.

6.8. Other Applications

In addition to the applications covered above, there are other promising studies showing the capability of free radical protein footprinting to address other structural concerns.

The first is the identification of bound waters in the proteins. Water plays an essential role in protein folding, structure and stability.[1180-1181] X-ray diffraction[1182] and NMR[1183] can detect highly conserved water molecules that are located bound with polar or charged residues of proteins. Few experimental approaches, however, are able to differentiate waters that are bound to the surface and the interior of proteins. Synchrotron-based ●OH protein footprinting ionizes water to give ●OH.[170, 1184] Using a careful experimental design, Gupta and Chance[1184] footprinted cytochrome C under two different temperatures of 25 °C and −35 °C.

Freezing the sample during synchrotron irradiation limits the diffusion of ●OH. A comparison of modification fractions of a certain peptide or residue under two different temperatures enables the differentiation of types of water that locate in these regions. A significant decrease (13 to 200-fold) suggest that the modification is from bulk water that gives ●OH and labels the protein through diffusion. Sites that suffer a moderate decrease (3 to 10-fold) are located on the protein surface, and these sites have bound water molecules. Residues that have minimum changes (decreases less than 2-fold) upon footprinting at two different temperatures must have internal, closely located water to give ●OH radicals that react with adjoining residues without significant diffusional motion. Results from ●OH footprinting are consistent with those seen in an X-ray structure.[1184] Further experiments utilized a time-resolved $^{18}O/^{16}O$ exchange apparatus and probed the water dynamics on the

submillisecond timescale,[1184] offering a unique view of protein-water interacting dynamics that was only possible with NMR before.[1183] Synchrotron-based ●OH footprinting has unique advantages in studying protein-water interactions, as water serves as the precursor of ●OH, and it is capable of reacting with proteins that are in different sites, even within the lipid bilayer of membrane proteins.[1185-1186]

The second application focuses on protein-carbohydrate interactions. Cell membranes are covered with heterogenous glycans that create an interactive environment and govern many cellular functions.[1187] Many cellular functions are based on protein-glycan interactions and glycan-mediated protein-protein binding, yet characterization of the protein-glycan interactions is mainly limited to glycan arrays.[1188] Very recently, Li and Lebrilla[872] reported a novel workflow termed protein oxidation of sialic acid environment (POSE) that footprints those proteins in close proximity to sialic acids, an idea that shares features with APEX labeling introduced earlier. As sialic acid usually terminates the glycan chains in the glycoproteins, the first step is to functionalize the sialic acid with an azido group (Figure 34a) and to introduce the active iron species through click chemistry, the glycan chain now serving as a probe (Figure 34b). Upon adding H_2O_2, ●OH is generated by Fenton chemistry, thus oxidatively labeling the surrounding proteins (Figure 34c). POSE allows *in situ* labeling of proteins that are closely located to glycans, providing an effective and efficient way to screen possible glycan-binding targets.

Finally, there are other promising applications of fast labeling approaches including footprinting membrane proteins,[945, 1189-1191] following the early onset of ROS oxidative damage,[1192] probing protein hidden conformations,[1193] mapping protein-DNA interactions[1194] and many more. These efforts all provide valuable information in their respective fields, but they will not be covered in detail in this review.

7. Conclusions and Perspective

MS-based protein HOS analysis has increased the throughput and decreased the sample amount requirements of protein HOS determination while becoming an effective complement to traditional biophysical characterization methods. More importantly, different protein footprinting approaches allow MS-based approaches to view protein HOS from different perspectives. For example, HDX usually measures the kinetics of exchange and infers HOS from the “labeling” of protein backbone amide bonds. Targeted or specific labeling reagents exploit various organic reactions to report on side-chain solvent accessibilities. Fast labeling reagents react with the residue side chains on the time scale of ns to ms, affording a “snapshot” of protein structure and dynamics. Taken together, MS-based protein labeling approaches “paint” the protein solvent accessible surfaces over a time frame from ns to days to afford a comprehensive understanding of the protein of interest. Moreover, modern proteomics digestion (bottom-up) workflows, top-down fragmentation techniques together with ultra-sensitive MS instruments yield not only HOS information at mid-to-high (single amino acid residue level) spatial resolution, but also dynamics of the protein under various conditions that are hardly accessible by a single technique. This is important because a footprint should be done with high coverage, unlike primary structure identification in traditional proteomics. Over the past decades, MS-based structural

proteomics approaches have grown extensively and now can answer important and challenging biological questions. None of these developments were possible without technical innovations in the field of MS.

7.1 Hydrogen Deuterium Exchange

During the past decade, HDX has grown to be a mature tool for MS-based protein HOS characterization in both academia and in the biopharmaceutical/biotechnology industry. Despite its growth and success, HDX methods still face multiple challenges. One challenge is the tedious, complex measurement, which is being met with robotic automation of the HDX measurement, making bottom-up HDX more readily applicable to most simple protein systems.[1195] Titration-based HDX workflows including SUPREX and PLIMSTEX provide site-specific binding affinities in addition to locating the binding sites.[231-232] Incorporation of ion-mobility offers an orthogonal dimension in the separation of constituent peptides prior to MS measurements, facilitating the deconvolution of overlapping isotopic patterns for co-eluting peptides.[1196] Novel fragmentation methods including ETD and ECD together with multi-enzyme digestions allow investigators to reach out for residue-level HDX information.[221] Exchange in theta capillaries[227] and in the gas phase[228-230] may allow HDX to be measured on the μs time scale. Innovations in MS instruments permit HDX to be conducted in a top-down fashion. Although promising, these novel advances still require additional demonstration to spur even broader adoption.

Most current applications of HDX focus on soluble protein systems. As HDX is reversible, its measurement by MS is ex situ, setting experimental constraints that minimize back exchange. These restraints limit application of HDX in complex protein systems; for example, glycoproteins that require post-labeling deglycosylation,[237] membrane proteins need post-labeling lipid or detergent removal,[236] and structurally rigid proteins that are challenging to denature and digest. Although pioneering studies demonstrate feasibility, routine and robust workflows still need to be developed and demonstrated before generalization and widespread acceptance will occur.

Another important aspect of HDX-based protein HOS analysis is the proper utilization of absolute deuterium uptake for structural modeling. Although most current HDX measurements are conducted in a differential manner to locate binding sites or determine the effects of mutation, absolute uptake reports on backbone dynamics and structural features of the protein. Fast exchange is typical of protein loops or intrinsically disordered regions whereas very slow exchange is characteristic of either structurally rigid or deeply buried regions. Although the concept of absolute protection estimation via HDX measurement is well appreciated, it is poorly demonstrated when combined with computer modeling to predict protein HOS.[1197-1199] The quantitative assignment of protection not only requires high-quality data acquisitions but also reliable data processing. As it is challenging, the outcoming is also rewarding. Incorporating protection extent from HDX measurements into protein structure prediction will greatly elevate the contributions of HDX to structure determination, as is seen in recent radical labeling demonstrations.[1175]

7.2 Irreversible Labeling

As compared with HDX, protein HOS analysis by irreversible labeling and MS has a shorter history even though other opportunities of specific amino acid labeling originated 60 y ago. Many applications both for specific amino acid labeling and free radical footprinting, however, have been developing during the past decade. One advantage is the irreversibility of the labeling, making it compatible with sophisticated post-labeling sample treatment such as long gradients in HPLC or extensive signal averaging as in top-down studies. These features enable approaches that answer broad biological questions about many types of proteins.

Despite its broad compatibility, a missing piece of the picture is membrane protein footprinting. Early studies incorporating nanodiscs[1200] and other membrane mimetic systems[1201] show the feasibility of footprinting membrane proteins. Although these demonstration studies used both targeted labeling reagents[816, 820-821] and fast radical species[873, 945, 1190], the primary focus was the soluble domain. An effective footprinting approach for the transmembrane domains of membrane protein remains to be established although there are hints that productive footprinters exist. Unlike HDX, whose labeling reagent, D_2O, cannot be extensively partitioned into bio-membranes, the targeted labeling reagents and the radical precursors can be chemically tailored to favor the membrane where they can footprint the transmembrane regions and yield information on those regions that are buried and those that adjoin the membrane.[1202]

Another fundamental aspect of targeted and radical protein labeling that remains to be addressed is the effect of microenvironment; that is, the effect of adjacent residues on the reactivities between targeted residue and the labeling reagents. Such effects are mainly explained as fluctuations of local reagent concentrations, local hydrogen-bonding schemes, or the electronic or steric environments determined by the nearby functional groups. The effect of adjacent residues on the exchange rates in HDX was thoroughly studied and is now well established.[206] For footprinting by targeted labeling reagents, a few studies hint that adjacent residues play a role.[497, 541, 1203-1207] In the case of radical footprinting reagents, there are two recent reports that discuss local concentration fluctuations of labeling reagents.[896, 1208]

Understanding the effect of the microenvironment on labeling efficiencies is crucial in determining the intrinsic structural factors that are involved in interpreting footprinting data, and these effects should not be overlooked. Only from a deep understanding can we take full advantage of footprinting results and their incorporation into protein structural modeling. The needed studies for irreversible labeling, however, are more challenging than those for HDX, whose labeling reagent is high-concentration solvent, D_2O, itself. One can reasonably assume that the effect of microenvironment will be reagent-dependent, further complicating efforts to unravel the effects but also offering an opportunity to tailor reagents.

From a practical perspective, several issues need to be addressed in upcoming research in this field. First is the implementation of novel labeling reagents. As mentioned earlier, a good footprinter needs to provide a distinct mass tag that can be properly differentiated from naturally occurring PTMs. Because targeted labeling reagents generally introduce mass tags

that do not occur naturally, protein footprinting by radical species is mostly carried out with hydroxyl radicals, which label protein by oxidation, producing a +16 Da mass shift inter alia. As oxidation often occurs not only naturally but also during post labeling sample handling and even during LC separations, it is sometimes ambiguous to distinguish the oxidations from footprinting and those from other processes. This small limitation can be overcome by development of novel labeling reagents that not only retain the advantages of widely adopted hydroxyl radicals but also "paint" the protein surfaces, affording another distinctive mass tag.

Another possible way to address this issue is to develop cleavable or isotopically encoded radical precursors as labeling reagents, an idea that has been extensively utilized in protein chemical cross-linking and in protein footprinting. Using this approach, investigators employ targeted labeling reagents that can readily accommodate isotopic encoding to shift the mass of the mass tag. These efforts will surely shorten the analysis time and increase the confidence of identification and quantification in radical-based protein footprinting. This is difficult with hydroxyl radical footprinting because at best the reagent mass can only be shifted by 2 Da, which is insufficient to resolve for large peptides and proteins.

The second is the development of novel labeling reagents (examples were discussed in section 5) especially for residues that are activated with difficulty and, therefore, react sparingly. Although it is feasible to activate selective C-H bonds from an organic chemistry perspective, to achieve it under physiological conditions is considerably more challenging because the modification must be done rapidly. Labeling of Ala, Gly and Pro whose side chains are functionalized with difficulty is likely only with free radicals, but even then, the reactivity will be low considering that proteins contain many other reactive residues. Although specific labeling of Gly residues at the protein N-terminus by targeted labeling reagents was demonstrated recently,[1209] general modification of these residues is difficult and been realized only in one study to our knowledge.[1210] Moreover, bridging the fields of protein chemical modification and protein footprinting offers the opportunity to "reinvent the old". Protein chemical modifications have been extensively developed for many years to satisfy several biological and analytical needs. Some of the reactions and reagents that are adopted in those studies can be used to footprint proteins as well, as has been done in the past and continues today (consider DEPC, GEE, IAM, NHB, TNM footprinting, for example).

Last is a technical comment to emphasize the need to conduct thorough evaluations when applying a labeling reagent to study a specific protein system. Technical issues including the compatibility of the labeling reagent and the protein, the optimum reagent dose and labeling time to minimize double-labeling, to achieve the proper normalization of labeling extents in differential experiments, and to invoke the statistical justifications of differences in labeling extents, and many more. These points should be considered as standard operating procedures, yet few studies to date report evaluations prior to presenting the results, perhaps not surprising given that the field is young. Many of these issues can be addressed by, for example, optical evaluation of protein integrity (by ion mobility MS, CD, infrared spectroscopy or other low-resolution biophysical approaches) and the use of a reporter small molecule or peptide dosimeters to enable normalization between different states of the

protein. These efforts and results should be reported in future studies to convince the user community that the methods are robust.

7.3 Broad Perspective

From a broad view, each MS-based labeling approach will contribute to the understanding of protein HOS from a different perspective, motivating the thoughtful and creative choice of different reagents. As mentioned above, the methods of HDX, targeted labeling reagents, and radical species inform on protein HOS and their changes on different time scales. Their targeted amino acid residues on the protein are also different. Applying combinations of different approaches can provide a deeper understanding of the protein and a higher resolution structure. Recent demonstrations have shown the power of such integrated strategies.[738, 768, 838-839, 1048, 1211-1215] Its broad application, however, remains to be explored.

Platform integration not only expands the protein footprinting approaches but also requires clever application of the various sample handling and MS techniques. For example, one can couple native MS and protein footprinting in a preliminary analysis to assist in the design of a study of protein ligand interactions, to determine mixing ratios that push the binding equilibriums to the product complex, and to explore the binding regions. Ion mobility MS coupled with protein footprinting will illuminate protein conformational changes during and after labeling, providing a view of protein conformational changes induced by chemical labeling. Multiple ion dissociation techniques coupled with different enzymatic digestions will deliver better sequence coverage, even to the residue level, which is one goal in MS-based protein HOS analysis.

Improved reversed-phase chromatography and adoption of other separation strategies (e.g., normal phase, capillary electrophoresis) will allow separation of isomeric peptides formed in labeling (e.g., chemically modified peptides that bear the same modification on multiple residues) and their quantification from extracted ion chromatograms and other approaches. Improved digestion strategies (e.g., mixed and immobilized enzymes) will also improve spatial resolution. Better separation will also minimize ion suppression during ionization, separate structural isomers that have the same *m/z*, and ultimately improve the precision of quantification and the spatial resolution of the protein HOS analysis. Enhanced separation capability, possibly even with 2D approaches, is particularly important for footprinting complex mixtures of proteins or large proteins that digest to provide a large number of peptides. Modern protein and peptide separation approaches, including multi-dimensional LC,[1216-1217] size exclusion chromatography,[1218-1219] ion-exchange chromatography,[1220] have all been coupled with MS analysis. Although most of the current demonstrations are for primary-structure proteomics and native MS, they can surly be adopted for protein HOS analysis soon.

Upon obtaining the MS data, database searching and spectra identifications by software is also critical. Over the past decade, we witnessed a burst of MS software for MS/MS identification, de novo sequencing, HDX, irreversible labeling, chemical cross-linking, native MS, ion mobility MS, for proteomics, glycomics, lipidomics, and metabolomics. Although these developments largely contribute to data processing and visualization, they

will continue to be important components in the “engine” of MS-based structural proteomics and ultimately lead to more automated data processing.

Lastly, to increase the spatial resolution of MS-based protein HOS studies, computer modeling is also critical. As discussed in section 6.6, pioneering efforts demonstrate early efforts pointing to a promising future of this area. Incorporating footprinting data into structural predictions in a straightforward way breaks the resolution limit of MS approaches, making MS-based protein HOS analysis a biophysical method that delivers high resolution results as does X-ray crystallography, cryo EM, and NMR or that, at least, complements them, even for protein complexes[1176]. A simple example is the use of footprinting to recover the information loss for flexible protein regions in an X-ray crystal structure. Thus, footprinting data can increase the confidence of protein structural predictions both on its own and in combination with other approaches.

To achieve these goals, deeper understanding of footprinting fundamentals is crucial, because only from a solid understanding of fundamentals can we to evaluate the footprinting data properly, especially for footprinting a single protein state rather than employing a differential experiment. Development of user-friendly software that can take footprinting data as input for structural modeling is also needed.

7.4 Concluding Remarks

The combination of advanced MS instrumentation, novel protein labeling workflows, wide ranging labeling reagents, careful experimental design, and precise data processing will continue to advance MS footprinting as a tool well beyond protein molecular weight and primary structure determination. MS as a robust and informative protein structural characterization tool has been established during the past 30 years, and we predict that MS-based approaches will continue to contribute significantly to the field of structural proteomics and the broader field of structural biology.

Acknowledgments

This work was supported by the National Institute of Health NIGMS Grants 5P41GM103422 and 1R01GM13100801 (to MLG).

Biography

Xiaoran Roger Liu received his B.E. in Applied Chemistry from Each China University of Science and Technology in 2014. He then moved to The University of Akron. During his M.S. work with Dr. Toshikazu Miyoshi, he focused on structural characterization of carbon fiber precursors during thermal stabilization with solid-state NMR. He is currently working towards his Ph.D. in Washington University in St. Louis with Dr. Michael L. Gross. His research interest is to develop and apply novel mass spectrometry-based approaches in characterizing protein high order structures.

Mengru Mira Zhang was born in Daqing, China and received her B.E. degree in 2014 at East China University of Science and Technology. In 2013, she moved to Ohio and joined the Department of Polymer Science at the University of Akron under the supervision of Dr.

Li Jia, focusing on organometallic synthesis and its catalytic application for novel polymers. After obtaining her M.S. degree in 2015, she decided to pursue her Ph.D. degree in Dr. Michael L. Gross lab at Washington University in St. Louis with interests in developing and utilizing multiple biophysical methods to address different biological questions.

Michael L. Gross is a chemist who has worked independently in mass spectrometry since 1968. He began his career at the University of Nebraska - Lincoln, where he was distinguished professor of chemistry and director of an NSF Center for Mass Spectrometry until 1994. He then moved to Washington University in St. Louis as professor of chemistry, immunology, medicine and principal investigator of the WU NIH NIGMS Mass Spectrometry Research Resource. During his career of 50+ years, he has authored and coauthored over 650 publications and book chapters. His primary research interests have evolved to structural proteomics and MS-based biophysics.

Abbreviations

$^1O_2$
singlet oxygen

3D
three dimensional

5-IAF
5-idoacetamidofluorescein

6-Cl-IMP
6-Chloropurine riboside 5'-monophosphate

Aβ
amyloid beta

ADH
adipic acid dihydrazide

AFM
atomic force microscopy

Ala
alanine

aMB
apo-myoglobin

ANB-NOS
N-5-azido-2-nitrobenzoyloxysuccinimide

APEX
ascorbate peroxidase

Arg
arginine

Asn
asparagine

Asp
aspartic acid

αSyn
alpha-synuclein

β2m
β-2-microglobulin

BAMG
bis(succinimidyl)-3-azidomethylglutarate

BDC
N-benzyl-N'-3-dimethylaminopropylcarbodiimide

BDP-NHP
N-hydroxyphthalamide ester of biotin aspartate proline

BHD
benzhydrazide

BME
b-mercaptoethanol

BS3
Bis(Sulfosuccinimidyl)suberate

C. elegans
Caenorhabditis elegans

CaM
calmodulin

CASP
critical assesment of protein structure presiction

CBDPS
cyanurbiotindimercaptopropionyl succinimide

CD
circular dichroism

CDR
complementarity determining region

chloramine T
N-chloro-4-methyl-benzenesulfonamide

CID
collision induced dissociation

CL-MS
covalent labeling MS

Cryo-EM
cryogenic electron microscopy

Cys
cysteine

DEPC
diethylpyrocarbonate

di-UB
di-ubiquitin

DMP
dimethyl pimelimidate

DMS
dimethyl suberimidate

DMTMM
4-(4,6-dimethoxy-1,3,5-triazin-2-yl)-4-methyl-morpholinium chloride

DSBU
disuccinimidyl dibutyric urea

DSG
disuccinimidyl glutarate

DSS
disuccinimidyl suberate

DSSO
disuccinimidyl sulfoxide

DTBP
dimethyl 3,3′-dithiobispropionimidate

DTNB
5,5'-dithiobis-(2-nitrobenzoic acid)

DTSSP
3,3'-dithiobis(sulfosuccinimidylpropionate)

DTT
Dithiothreitol

E. Coli
Escherichia coli

eaq^-
hydrated electrons

ECD
electron capture dissociation

EDC
1-ethyl-3-(3-(dimethylamino)propyl)carbodiimide

EDD
electron detachment dissociation

EDTA
ethylenediaminetetraacetic acid

EGF
epidermal growth factor

EGFR
human epidermal growth factor receptor

eIF3
yeast initiation factor 3

ELISA
enzyme linked immunosorbent assay

EPR
electron paramagnetic resonance

ESI
electrospray ionization

ETD
electron transfer dissociation

EThcD
electron transfer higher energy dissociation

FAB
fast atom bombardment

FDR
false discoverer rate

Fe-BABE
Fe-(S)-1-(p-bromoacetimidobenzyl)-EDTA

FMO
Fenna-Matthews-Olson

FPOP
fast photochemical oxidation of proteins

FRET
Förster Resonance Energy Transfer

FTICR
Fourier-transform ion cyclotron resonance

FT-IR
fourier transform infrared spectroscopy

GA
glycinamide

GEE
glycine ethyl ester

Glu
glutamic acid

Glu
glutamine

GLUTs
human glucose transporters

Gly
glycine

g-ray
gamma ray

H_2O*
activated water

HBx
hepatitis B virus X protein

HDX
hydrogen deuterium exchange

hERα
human estrogen receptor alpha

His
histidine

hMB
holo-myoglobin

HNB
2-Hydroxy-5-nitrobenzyl-bromide

HNSB
dimethyl(2-hydroxy-5-nitrobenzyl)sulfonium bromide

holo-CaM
calcium-bound calmodulin

HOS
higher order structure

HRP
horseradish peroxidase

hVKOR
human vitamin K epoxide reductase

IAM
iodoacetamide

ICAT
isotope-coded affinity tag

IgG1
human Immunoglobulin G subclass 1 antibody

IL-6R
human interleukin-6 receptor α-chain

Ile
isoleucine

IMPDH
human type II inosine 5’-monophosphate dehydrogenase

iodogen
1,3,4,6-tetra-chloro-3a,6a-diphenyl-glycouril

IRMPD
infrared multiphoton dissociation

ITC
isothermal titration calorimetry

kethoxal
3-ethoxy-1,1-dihydroxy-2-butanone

LC
liquid chromatography

Leu
leucine

LITPOMS
ligand titration, fast photochemical oxidation of proteins and mass spectrometry

Lys
lysine

m/z
mass to charge ratio

mAb
Monoclonal antibodies

MALDI
matrix-assisted laser desorption ionization

MCO
metal-catalyzed oxidation

Melarsen oxide
p-(4,6-diamino-1,3,5-triazin-2-yl)aminophenylarsonous acid

MES
2-(N-Morpholino) ethanesulfonic acid

Met
methionine

MMTS
methyl methanethiosulfonate

MS
mass spectrometry

MS/MS
tandem MS

MURR1
mouse U2af1-rs1 region1

N-AcO-AAF
N-acetoxy-N-acetyl-2-aminofluorene

NAI
N-acetylimidazole

NBS
N-bromosuccinimide

NCS
N-chlorosuccinimide

NEM
N-ethylmaleimide

NHS-ester
N-Hydroxysuccinimide ester

NMR
nuclear magnetic resonance

NTCB
2-nitro-5-thiocyanobenzoic acid

PAL
photoaffinity labeling

***p*-bromophenacyl bromide**
2-bromo-1-(4-bromophenyl)ethenone

PD
plasma desorption

PDB
protein data bank

PDH
pimelic acid dihydrazide

PF
protection factor

Phe
phenylalanine

PIR
protein interaction reporter

PLIMB
plasma induced modification of biomolecules

PLIMSTEX

protein–ligand interactions by mass spectrometry, titration, and H/D exchange

PLP
pyridoxal-5’-phosphate

POSE
protein oxidation of sialic acid environment

PPIs
protein-protein interactions

Pro
proline

PrP
prion protein

PSII
photosystem II

PTM
post translational modification

ReACT
real-time analysis for cross-linked peptides technology

RMSD
root mean square deviation

ROS
reactive oxygen species

SASA
solvent accessible surface area

Ser
serine

SID
surface induced dissociation

SOD
Superoxide dimustase

SPR
surface plasmon resonance

sulfo-SDA
sulfosuccinimidyl 4,4'-azipentanoate

SUPREX
stability of unpurified proteins from rates of H/D exchange

TBHP
t-butylhydroperoxide

TECP
tris(2-carboxyethyl)phosphine

Thr
theronine

ThT
thioflaven T

TNBS
2,4,6-Trinitrobenzenesulfonic acid

TNM
tetranitromethane

TOF
time-of-flight

TPDs
3-trifluoromethyl-3-phenyldiazirines

TPO
thyroid peroxidase

Trp
tryptophan

Tyr
tyrosine

UBA
ubiquitin associated domain of USP5

Ugi
PBS2 uracil-DNA glycosylase inhibitor

Ung
uracil-DNA glycosylase

UPS5
ubiquitin specific protease 5

UV
ultra-violet

UVPD
ultraviolet photodissociation

Val
valine

WRK
Woodward's reagent K

XL-MS
Cross-linking mass spectrometry

XO
xanthine oxidase

ZnF-UBP
Zn-finger ubiquitin-binding domain of USP5

References

1. Lodish H; Berk A; Kaiser CA; Krieger M; Scott MP; Bretscher A; Ploegh H; Matsudaira P, Molecular cell biology. Macmillan: 2008.
2. Anfinsen CB; Haber E; Sela M; White FH, THE KINETICS OF FORMATION OF NATIVE RIBONUCLEASE DURING OXIDATION OF THE REDUCED POLYPEPTIDE CHAIN. Proceedings of the National Academy of Sciences 1961, 47 (9), 1309–1314.
3. Fermi G; Perutz MF; Shaanan B; Fourme R, The crystal structure of human deoxyhaemoglobin at 1.74 Å resolution. Journal of Molecular Biology 1984, 175 (2), 159–174. [PubMed: 6726807]
4. Mathews CKVH, K. E.; Appling DR; Anthony-Cahill SJ, Biochemistry. Pearson: 2013.
5. FRUTON JS, Early Theories of Protein Structure. Annals of the New York Academy of Sciences 1979, 325 (1), 1–20.
6. Sanger F; Tuppy H, The amino-acid sequence in the phenylalanyl chain of insulin. 1. The identification of lower peptides from partial hydrolysates. Biochemical Journal 1951, 49 (4), 463. [PubMed: 14886310]
7. Sanger F, The Arrangement of Amino Acids in Proteins In Advances in Protein Chemistry, Anson ML; Bailey K; Edsall JT, Eds. Academic Press: 1952; Vol. 7, pp 1–67. [PubMed: 14933251]
8. Baker EN; Hubbard RE, Hydrogen bonding in globular proteins. Progress in Biophysics and Molecular Biology 1984, 44 (2), 97–179. [PubMed: 6385134]
9. Fersht AR; Shi J-P; Knill-Jones J; Lowe DM; Wilkinson AJ; Blow DM; Brick P; Carter P; Waye MMY; Winter G, Hydrogen bonding and biological specificity analysed by protein engineering. Nature 1985, 314 (6008), 235–238. [PubMed: 3845322]
10. Waldburger CD; Schildbach JF; Sauer RT, Are buried salt bridges important for protein stability and conformational specificity? Nature Structural Biology 1995, 2 (2), 122–128. [PubMed: 7749916]
11. Kumar S; Nussinov R, Salt bridge stability in monomeric proteins11Edited by J. M. Thornton. Journal of Molecular Biology 1999, 293 (5), 1241–1255. [PubMed: 10547298]
12. Privalov PL; Gill SJ, Stability of Protein Structure and Hydrophobic Interaction In Advances in Protein Chemistry, Anfinsen CB; Edsall JT; Richards FM; Eisenberg DS, Eds. Academic Press: 1988; Vol. 39, pp 191–234. [PubMed: 3072868]
13. Baldwin RL, Temperature dependence of the hydrophobic interaction in protein folding. Proceedings of the National Academy of Sciences 1986, 83 (21), 8069–8072.
14. Burley S; Petsko G, Aromatic-aromatic interaction: a mechanism of protein structure stabilization. Science 1985, 229 (4708), 23–28. [PubMed: 3892686]

15. Gallivan JP; Dougherty DA, Cation-π interactions in structural biology. Proceedings of the National Academy of Sciences 1999, 96 (17), 9459–9464.
16. Roth CM; Neal BL; Lenhoff AM, Van der Waals interactions involving proteins. Biophysical Journal 1996, 70 (2), 977–987. [PubMed: 8789115]
17. Betz SF, Disulfide bonds and the stability of globular proteins. Protein Science 1993, 2 (10), 1551–1558. [PubMed: 8251931]
18. Wedemeyer WJ; Welker E; Narayan M; Scheraga HA, Disulfide Bonds and Protein Folding. Biochemistry 2000, 39 (15), 4207–4216. [PubMed: 10757967]
19. Doig AJ; Sternberg MJE, Side-chain conformational entropy in protein folding. Protein Science 1995, 4 (11), 2247–2251. [PubMed: 8563620]
20. Frederick KK; Marlow MS; Valentine KG; Wand AJ, Conformational entropy in molecular recognition by proteins. Nature 2007, 448, 325. [PubMed: 17637663]
21. Tzeng S-R; Kalodimos CG, Protein activity regulation by conformational entropy. Nature 2012, 488, 236. [PubMed: 22801505]
22. Kendrew JC; Bodo G; Dintzis HM; Parrish RG; Wyckoff H; Phillips DC, A Three-Dimensional Model of the Myoglobin Molecule Obtained by X-Ray Analysis. Nature 1958, 181 (4610), 662–666. [PubMed: 13517261]
23. Perutz MF; Rossmann MG; Cullis AF; Muirhead H; Will G; North ACT, Structure of Hæmoglobin: A Three-Dimensional Fourier Synthesis at 5.5-Å. Resolution, Obtained by X-Ray Analysis. Nature 1960, 185 (4711), 416–422. [PubMed: 18990801]
24. Kuboniwa H; Tjandra N; Grzesiek S; Ren H; Klee CB; Bax A, Solution structure of calcium-free calmodulin. Nature Structural Biology 1995, 2, 768. [PubMed: 7552748]
25. Drenth J, Principles of protein X-ray crystallography. Springer Science & Business Media: 2007.
26. McPherson A, Introduction to protein crystallization. Methods 2004, 34 (3), 254–265. [PubMed: 15325645]
27. McPherson A; Gavira JA, Introduction to protein crystallization. Acta Crystallographica Section F 2014, 70 (1), 2–20.
28. Billeter M, Comparison of protein structures determined by NMR in solution and by X-ray diffraction in single crystals. Quarterly Reviews of Biophysics 1992, 25 (3), 325–377. [PubMed: 1470680]
29. Garbuzynskiy SO; Melnik BS; Lobanov MY; Finkelstein AV; Galzitskaya OV, Comparison of X-ray and NMR structures: Is there a systematic difference in residue contacts between X-ray- and NMR-resolved protein structures? Proteins: Structure, Function, and Bioinformatics 2005, 60 (1), 139–147.
30. Wüthrich K, NMR in biological research: peptides and proteins. North-Holland Amsterdam: 1976.
31. Wuthrich K, Protein structure determination in solution by nuclear magnetic resonance spectroscopy. Science 1989, 243 (4887), 45–50. [PubMed: 2911719]
32. Wüthrich K, The way to NMR structures of proteins. Nature Structural Biology 2001, 8 (11), 923–925. [PubMed: 11685234]
33. Bax A; Grzesiek S, Methodological advances in protein NMR. Accounts of Chemical Research 1993, 26 (4), 131–138.
34. Cavanagh J; Fairbrother WJ; Palmer AG III; Skelton NJ, Protein NMR spectroscopy: principles and practice. Elsevier: 1995.
35. Williamson MP; Havel TF; Wüthrich K, Solution conformation of proteinase inhibitor IIA from bull seminal plasma by 1H nuclear magnetic resonance and distance geometry. Journal of Molecular Biology 1985, 182 (2), 295–315. [PubMed: 3839023]
36. Wüthrich K, NMR with proteins and nucleic acids. Europhysics News 1986, 17 (1), 11–13.
37. Mainz A; Religa TL; Sprangers R; Linser R; Kay LE; Reif B, NMR Spectroscopy of Soluble Protein Complexes at One Mega-Dalton and Beyond. Angewandte Chemie International Edition 2013, 52 (33), 8746–8751. [PubMed: 23873792]
38. Ishima R; Torchia DA, Protein dynamics from NMR. Nature Structural Biology 2000, 7 (9), 740–743. [PubMed: 10966641]

39. Andronesi OC; Becker S; Seidel K; Heise H; Young HS; Baldus M, Determination of Membrane Protein Structure and Dynamics by Magic-Angle-Spinning Solid-State NMR Spectroscopy. Journal of the American Chemical Society 2005, 127 (37), 12965–12974. [PubMed: 16159291]
40. Tuttle MD; Comellas G; Nieuwkoop AJ; Covell DJ; Berthold DA; Kloepper KD; Courtney JM; Kim JK; Barclay AM; Kendall A; Wan W; Stubbs G; Schwieters CD; Lee VMY; George JM; Rienstra CM, Solid-state NMR structure of a pathogenic fibril of full-length human α-synuclein. Nature Structural &Amp; Molecular Biology 2016, 23, 409.
41. Castellani F; van Rossum B; Diehl A; Schubert M; Rehbein K; Oschkinat H, Structure of a protein determined by solid-state magic-angle-spinning NMR spectroscopy. Nature 2002, 420 (6911), 99–102.
42. Baldus M, Solid-State NMR Spectroscopy: Molecular Structure and Organization at the Atomic Level. Angewandte Chemie International Edition 2006, 45 (8), 1186–1188. [PubMed: 16463311]
43. Kline AD; Braun W; Wüthrich K, Determination of the complete three-dimensional structure of the α-amylase inhibitor tendamistat in aqueous solution by nuclear magnetic resonance and distance geometry. Journal of Molecular Biology 1988, 204 (3), 675–724. [PubMed: 3265733]
44. Yee AA; Savchenko A; Ignachenko A; Lukin J; Xu X; Skarina T; Evdokimova E; Liu CS; Semesi A; Guido V, NMR and X-ray crystallography, complementary tools in structural proteomics of small proteins. Journal of the American Chemical Society 2005, 127 (47), 16512–16517. [PubMed: 16305238]
45. DataBank, P. https://www.rcsb.org/stats/summary.
46. Bai X.-c.; McMullan G; Scheres SHW, How cryo-EM is revolutionizing structural biology. Trends in Biochemical Sciences 2015, 40 (1), 49–57. [PubMed: 25544475]
47. Cheng Y, Single-Particle Cryo-EM at Crystallographic Resolution. Cell 2015, 161 (3), 450–457. [PubMed: 25910205]
48. Dubochet J; McDowall AW, VITRIFICATION OF PURE WATER FOR ELECTRON MICROSCOPY. Journal of Microscopy 1981, 124 (3), 3–4.
49. Knapek E, Properties of organic specimens and their supports at 4 K under irradiation in an electron microscope. Ultramicroscopy 1982, 10 (1), 71–86. [PubMed: 7135625]
50. Frank J, Averaging of low exposure electron micrographs of non-periodic objects. Ultramicroscopy 1975, 1 (2), 159–162. [PubMed: 1236029]
51. Henderson R; Baldwin JM; Ceska TA; Zemlin F; Beckmann E; Downing KH, Model for the structure of bacteriorhodopsin based on high-resolution electron cryo-microscopy. Journal of Molecular Biology 1990, 213 (4), 899–929. [PubMed: 2359127]
52. Yu X; Jin L; Zhou ZH, 3.88 Å structure of cytoplasmic polyhedrosis virus by cryo-electron microscopy. Nature 2008, 453, 415. [PubMed: 18449192]
53. Zhang X; Jin L; Fang Q; Hui WH; Zhou ZH, 3.3 Å Cryo-EM Structure of a Nonenveloped Virus Reveals a Priming Mechanism for Cell Entry. Cell 2010, 141 (3), 472–482. [PubMed: 20398923]
54. Merk A; Bartesaghi A; Banerjee S; Falconieri V; Rao P; Davis MI; Pragani R; Boxer MB; Earl LA; Milne JLS; Subramaniam S, Breaking Cryo-EM Resolution Barriers to Facilitate Drug Discovery. Cell 2016, 165 (7), 1698–1707. [PubMed: 27238019]
55. Matadeen R; Patwardhan A; Gowen B; Orlova EV; Pape T; Cuff M; Mueller F; Brimacombe R; van Heel M, The Escherichia coli large ribosomal subunit at 7.5 Å resolution. Structure 1999, 7 (12), 1575–1583. [PubMed: 10647188]
56. Jomaa A; Boehringer D; Leibundgut M; Ban N, Structures of the E. coli translating ribosome with SRP and its receptor and with the translocon. Nature Communications 2016, 7, 10471.
57. Du Y; Duc NM; Rasmussen SGF; Hilger D; Kubiak X; Wang L; Bohon J; Kim HR; Wegrecki M; Asuru A; Jeong KM; Lee J; Chance MR; Lodowski DT; Kobilka BK; Chung KY, Assembly of a GPCR-G Protein Complex. Cell 2019, 177 (5), 1232–1242.e11. [PubMed: 31080064]
58. Thompson RF; Walker M; Siebert CA; Muench SP; Ranson NA, An introduction to sample preparation and imaging by cryo-electron microscopy for structural biology. Methods 2016, 100, 3–15. [PubMed: 26931652]
59. Provencher SW; Gloeckner J, Estimation of globular protein secondary structure from circular dichroism. Biochemistry 1981, 20 (1), 33–37. [PubMed: 7470476]

60. Greenfield NJ, Using circular dichroism spectra to estimate protein secondary structure. Nature Protocols 2006, 1 (6), 2876–2890. [PubMed: 17406547]
61. Oladepo SA; Xiong K; Hong Z; Asher SA; Handen J; Lednev IK, UV Resonance Raman Investigations of Peptide and Protein Structure and Dynamics. Chemical Reviews 2012, 112 (5), 2604–2628. [PubMed: 22335827]
62. Jackson M; Mantsch HH, The Use and Misuse of FTIR Spectroscopy in the Determination of Protein Structure. Critical Reviews in Biochemistry and Molecular Biology 1995, 30 (2), 95–120. [PubMed: 7656562]
63. KONG J; YU S, Fourier Transform Infrared Spectroscopic Analysis of Protein Secondary Structures. Acta Biochimica et Biophysica Sinica 2007, 39 (8), 549–559. [PubMed: 17687489]
64. Noble JE; Bailey MJA, Chapter 8 Quantitation of Protein In Methods in Enzymology, Burgess RR; Deutscher MP, Eds. Academic Press: 2009; Vol. 463, pp 73–95. [PubMed: 19892168]
65. Eftink MR, Fluorescence Techniques for Studying Protein Structure In Methods of Biochemical Analysis, Suelter CH, Ed. 1991; Vol. 35, pp 127–205. [PubMed: 2002770]
66. Royer CA, Probing Protein Folding and Conformational Transitions with Fluorescence. Chemical Reviews 2006, 106 (5), 1769–1784. [PubMed: 16683754]
67. Piston DW; Kremers G-J, Fluorescent protein FRET: the good, the bad and the ugly. Trends in Biochemical Sciences 2007, 32 (9), 407–414. [PubMed: 17764955]
68. Jachimska B; Wasilewska M; Adamczyk Z, Characterization of Globular Protein Solutions by Dynamic Light Scattering, Electrophoretic Mobility, and Viscosity Measurements. Langmuir 2008, 24 (13), 6866–6872. [PubMed: 18512882]
69. Stetefeld J; McKenna SA; Patel TR, Dynamic light scattering: a practical guide and applications in biomedical sciences. Biophysical Reviews 2016, 8 (4), 409–427. [PubMed: 28510011]
70. Wen J; Arakawa T; Philo JS, Size-Exclusion Chromatography with On-Line Light-Scattering, Absorbance, and Refractive Index Detectors for Studying Proteins and Their Interactions. Analytical Biochemistry 1996, 240 (2), 155–166. [PubMed: 8811899]
71. Krause F, Das magnetische Elektronenmikroskop und seine Anwendung in der Biologie. Naturwissenschaften 1937, 25 (51), 817–825.
72. Brenner S; Horne RW, A negative staining method for high resolution electron microscopy of viruses. Biochimica et Biophysica Acta 1959, 34, 103–110. [PubMed: 13804200]
73. Müller DJ; Engel A, Atomic force microscopy and spectroscopy of native membrane proteins. Nature Protocols 2007, 2, 2191. [PubMed: 17853875]
74. Wiseman T; Williston S; Brandts JF; Lin L-N, Rapid measurement of binding constants and heats of binding using a new titration calorimeter. Analytical Biochemistry 1989, 179 (1), 131–137. [PubMed: 2757186]
75. Leavitt S; Freire E, Direct measurement of protein binding energetics by isothermal titration calorimetry. Current Opinion in Structural Biology 2001, 11 (5), 560–566. [PubMed: 11785756]
76. Johnsson B; Löfås S; Lindquist G, Immobilization of proteins to a carboxymethyldextran-modified gold surface for biospecific interaction analysis in surface plasmon resonance sensors. Analytical Biochemistry 1991, 198 (2), 268–277. [PubMed: 1724720]
77. Smith EA; Thomas WD; Kiessling LL; Corn RM, Surface Plasmon Resonance Imaging Studies of Protein-Carbohydrate Interactions. Journal of the American Chemical Society 2003, 125 (20), 6140–6148. [PubMed: 12785845]
78. Baker D; Sali A, Protein Structure Prediction and Structural Genomics. Science 2001, 294 (5540), 93–96. [PubMed: 11588250]
79. Zhang Y, Progress and challenges in protein structure prediction. Current Opinion in Structural Biology 2008, 18 (3), 342–348. [PubMed: 18436442]
80. Kihara D, Protein structure prediction. Springer: 2014.
81. Guzzo AV, The Influence of Amino Acid Sequence on Protein Structure. Biophysical Journal 1965, 5 (6), 809–822. [PubMed: 5884309]
82. Prothero JW, Correlation between the distribution of amino acids and alpha helices. Biophysical Journal 1966, 6 (3), 367–370. [PubMed: 5962284]

83. Chou PY; Fasman GD, Prediction of protein conformation. Biochemistry 1974, 13 (2), 222–245. [PubMed: 4358940]
84. Ginalski K, Comparative modeling for protein structure prediction. Current Opinion in Structural Biology 2006, 16 (2), 172–177. [PubMed: 16510277]
85. Zhexin X, Advances in Homology Protein Structure Modeling. Current Protein & Peptide Science 2006, 7 (3), 217–227. [PubMed: 16787261]
86. Bowie JU; Eisenberg D, An evolutionary approach to folding small alpha-helical proteins that uses sequence information and an empirical guiding fitness function. Proceedings of the National Academy of Sciences 1994, 91 (10), 4436–4440.
87. Lee J; Freddolino PL; Zhang Y, Ab Initio Protein Structure Prediction In From Protein Structure to Function with Bioinformatics, Rigden J, D., Ed. Springer Netherlands: Dordrecht, 2017; pp 3–35.
88. Bradley P; Misura KMS; Baker D, Toward High-Resolution de Novo Structure Prediction for Small Proteins. Science 2005, 309 (5742), 1868–1871. [PubMed: 16166519]
89. Marks DS; Hopf TA; Sander C, Protein structure prediction from sequence variation. Nature Biotechnology 2012, 30, 1072.
90. Moult J; Fidelis K; Kryshtafovych A; Schwede T; Tramontano A, Critical assessment of methods of protein structure prediction (CASP)—Round XII. Proteins: Structure, Function, and Bioinformatics 2018, 86 (S1), 7–15.
91. Munson MSB; Field FH, Chemical Ionization Mass Spectrometry. I. General Introduction. Journal of the American Chemical Society 1966, 88 (12), 2621–2630.
92. Dole M; Mack LL; Hines RL; Mobley RC; Ferguson LD; Alice MB, Molecular Beams of Macroions. The Journal of Chemical Physics 1968, 49 (5), 2240–2249.
93. Winkler HU; Beckey HD, Field desorption mass spectrometry of amino acids. Organic Mass Spectrometry 1972, 6 (6), 655–660.
94. Mumma RO; Vastola FJ, Analysis of organic salts by laser ionization mass spectrometry. Sulfonates, sulfates and thiosulfates. Organic Mass Spectrometry 1972, 6 (12), 1373–1376.
95. Posthumus MA; Kistemaker PG; Meuzelaar HLC; Ten Noever de Brauw MC, Laser desorption-mass spectrometry of polar nonvolatile bio-organic molecules. Analytical Chemistry 1978, 50 (7), 985–991.
96. Torgerson DF; Skowronski RP; Macfarlane RD, New approach to the mass spectroscopy of non-volatile compounds. Biochemical and Biophysical Research Communications 1974, 60 (2), 616–621. [PubMed: 4417794]
97. Benninghoven A; Jaspers D; Sichtermann W, Secondary-ion emission of amino acids. Applied physics 1976, 11 (1), 35–39.
98. Barber M; Bordoli RS; Sedgwick RD; Tyler AN, Fast atom bombardment of solids (F.A.B.): a new ion source for mass spectrometry. Journal of the Chemical Society, Chemical Communications 1981, (7), 325–327.
99. Barber M; Bordoli RS; Elliott GJ; Sedgwick RD; Tyler AN, Fast atom bombardment mass spectrometry. Analytical Chemistry 1982, 54 (4), 645–657.
100. Karas M; Bachmann D; Hillenkamp F, Influence of the wavelength in high-irradiance ultraviolet laser desorption mass spectrometry of organic molecules. Analytical Chemistry 1985, 57 (14), 2935–2939.
101. Karas M; Bahr U; Gießmann U, Matrix-assisted laser desorption ionization mass spectrometry. Mass Spectrometry Reviews 1991, 10 (5), 335–357.
102. Sundqvist B; Kamensky I; Håkansson P; Kjellberg J; Salehpour M; Widdiyasekera S; Fohlman J; Peterson PA; Roepstorff P, Californium-252 plasma desorption time of flight mass spectroscopy of proteins. Biomedical Mass Spectrometry 1984, 11 (5), 242–257. [PubMed: 6378264]
103. Sundqvist B; Roepstorff P; Fohlman J; Hedin A; Hakansson P; Kamensky I; Lindberg M; Salehpour M; Sawe G, Molecular weight determinations of proteins by californium plasma desorption mass spectrometry. Science 1984, 226 (4675), 696–698. [PubMed: 6387912]
104. Barber M; Green BN; Jennings KR, The analysis of small proteins in the molecular weight range 10–24 kDa by magnetic sector mass spectrometry. Rapid Communications in Mass Spectrometry 1987, 1 (5), 80–83. [PubMed: 2980331]

105. Tanaka K; Waki H; Ido Y; Akita S; Yoshida Y; Yoshida T; Matsuo T, Protein and polymer analyses up to m/z 100 000 by laser ionization time-of-flight mass spectrometry. Rapid Communications in Mass Spectrometry 1988, 2 (8), 151–153.

106. Karas M; Hillenkamp F, Laser desorption ionization of proteins with molecular masses exceeding 10,000 daltons. Analytical Chemistry 1988, 60 (20), 2299–2301. [PubMed: 3239801]

107. Fenn J; Mann M; Meng C; Wong S; Whitehouse C, Electrospray ionization for mass spectrometry of large biomolecules. Science 1989, 246 (4926), 64–71. [PubMed: 2675315]

108. Whitehouse CM; Dreyer RN; Yamashita M; Fenn JB, Electrospray interface for liquid chromatographs and mass spectrometers. Analytical Chemistry 1985, 57 (3), 675–679. [PubMed: 2581476]

109. Wilm MS; Mann M, Electrospray and Taylor-Cone theory, Dole's beam of macromolecules at last? International Journal of Mass Spectrometry and Ion Processes 1994, 136 (2), 167–180.

110. Wilm M; Mann M, Analytical Properties of the Nanoelectrospray Ion Source. Analytical Chemistry 1996, 68 (1), 1–8. [PubMed: 8779426]

111. Paul W; Steinwedel H, Ein neues massenspektrometer ohne magnetfeld. Zeitschrift für Naturforschung A 1953, 8 (7), 448–450.

112. Johnson EG; Nier AO, Angular Aberrations in Sector Shaped Electromagnetic Lenses for Focusing Beams of Charged Particles. Physical Review 1953, 91 (1), 10–17.

113. Gross ML, [6] Tandem mass spectrometry: Multisector magnetic instruments In Methods in Enzymology, Academic Press: 1990; Vol. 193, pp 131–153.

114. Gross ML; Chess EK; Lyon PA; Crow FW; Evans S; Tudge H, Triple analyzer mass spectrometry for high resolution MS/MS studies. International Journal of Mass Spectrometry and Ion Physics 1982, 42 (4), 243–254.

115. McLafferty FW; Todd PJ; McGilvery DC; Baldwin MA, Collisional activation and metastable ion characteristics. 73. High-resolution tandem mass spectrometer (MS/MS) of increased sensitivity and mass range. Journal of the American Chemical Society 1980, 102 (10), 3360–3363.

116. Bateman RH; Brown J; Lefevere M; Flammang R; Van Haverbeke Y, Applications in gaseous ion and neutral chemistry using a six-sector mass spectrometer. International Journal of Mass Spectrometry and Ion Processes 1992, 115 (2), 205–218.

117. Wiley WC; McLaren IH, Time-of-Flight Mass Spectrometer with Improved Resolution. Review of Scientific Instruments 1955, 26 (12), 1150–1157.

118. Mamyrin B; Karataev V; Shmikk D; Zagulin V, The mass-reflectron, a new nonmagnetic time-of-flight mass spectrometer with high resolution. Zh. Eksp. Teor. Fiz 1973, 64, 82–89.

119. Guilhaus M; Selby D; Mlynski V, Orthogonal acceleration time-of-flight mass spectrometry. Mass Spectrometry Reviews 2000, 19 (2), 65–107. [PubMed: 10795088]

120. Wolfgang P; Helmut S, Apparatus for separating charged particles of different specific charges. Google Patents: 1960.

121. Comisarow MB; Marshall AG, Fourier transform ion cyclotron resonance spectroscopy. Chemical Physics Letters 1974, 25 (2), 282–283.

122. Makarov A, Electrostatic Axially Harmonic Orbital Trapping: A High-Performance Technique of Mass Analysis. Analytical Chemistry 2000, 72 (6), 1156–1162. [PubMed: 10740853]

123. Zubarev RA; Makarov A, Orbitrap Mass Spectrometry. Analytical Chemistry 2013, 85 (11), 5288–5296. [PubMed: 23590404]

124. Morris HR; Paxton T; Dell A; Langhorne J; Berg M; Bordoli RS; Hoyes J; Bateman RH, High Sensitivity Collisionally-activated Decomposition Tandem Mass Spectrometry on a Novel Quadrupole/Orthogonal-acceleration Time-of-flight Mass Spectrometer. Rapid Communications in Mass Spectrometry 1996, 10 (8), 889–896. [PubMed: 8777321]

125. Hu Q; Noll RJ; Li H; Makarov A; Hardman M; Graham Cooks R, The Orbitrap: a new mass spectrometer. Journal of Mass Spectrometry 2005, 40 (4), 430–443. [PubMed: 15838939]

126. Sleno L; Volmer DA, Ion activation methods for tandem mass spectrometry. Journal of mass spectrometry 2004, 39 (10), 1091–1112. [PubMed: 15481084]

127. Jennings KR, Collision-induced decompositions of aromatic molecular ions. International Journal of Mass Spectrometry and Ion Physics 1968, 1 (3), 227–235.

128. Mitchell Wells J; McLuckey SA, Collision-Induced Dissociation (CID) of Peptides and Proteins In Methods in Enzymology, Academic Press: 2005; Vol. 402, pp 148–185. [PubMed: 16401509]

129. Gross ML; McCrery D; Crow F; Tomer KB; Pope MR; Ciuffetti LM; Knoche HW; Daly JM; Dunkle LD, The structure of the toxin from helminthosporium carbonum. Tetrahedron Letters 1982, 23 (51), 5381–5384.

130. Hunt DF; Yates JR; Shabanowitz J; Winston S; Hauer CR, Protein sequencing by tandem mass spectrometry. Proceedings of the National Academy of Sciences 1986, 83 (17), 6233–6237.

131. Biemann K; Papayannopoulos IA, Amino acid sequencing of proteins. Accounts of Chemical Research 1994, 27 (11), 370–378.

132. Mabud MA; Dekrey MJ; Graham Cooks R, Surface-induced dissociation of molecular ions. International Journal of Mass Spectrometry and Ion Processes 1985, 67 (3), 285–294.

133. Chorush RA; Little DP; Beu SC; Wood TD; McLafferty FW, Surface-Induced Dissociation of Multiply-Protonated Proteins. Analytical Chemistry 1995, 67 (6), 1042–1046. [PubMed: 7536399]

134. Syka JEP; Coon JJ; Schroeder MJ; Shabanowitz J; Hunt DF, Peptide and protein sequence analysis by electron transfer dissociation mass spectrometry. Proceedings of the National Academy of Sciences of the United States of America 2004, 101 (26), 9528–9533. [PubMed: 15210983]

135. Zubarev RA; Kelleher NL; McLafferty FW, Electron Capture Dissociation of Multiply Charged Protein Cations. A Nonergodic Process. Journal of the American Chemical Society 1998, 120 (13), 3265–3266.

136. Budnik BA; Haselmann KF; Zubarev RA, Electron detachment dissociation of peptide di-anions: an electron–hole recombination phenomenon. Chemical Physics Letters 2001, 342 (3-4), 299–302.

137. Bowers WD; Delbert SS; Hunter RL; McIver RT, Fragmentation of oligopeptide ions using ultraviolet laser radiation and Fourier transform mass spectrometry. Journal of the American Chemical Society 1984, 106 (23), 7288–7289.

138. Shaw JB; Li W; Holden DD; Zhang Y; Griep-Raming J; Fellers RT; Early BP; Thomas PM; Kelleher NL; Brodbelt JS, Complete Protein Characterization Using Top-Down Mass Spectrometry and Ultraviolet Photodissociation. Journal of the American Chemical Society 2013, 135 (34), 12646–12651. [PubMed: 23697802]

139. Little DP; Speir JP; Senko MW; O'Connor PB; McLafferty FW, Infrared Multiphoton Dissociation of Large Multiply Charged Ions for Biomolecule Sequencing. Analytical Chemistry 1994, 66 (18), 2809–2815. [PubMed: 7526742]

140. Brodbelt JS, Ion Activation Methods for Peptides and Proteins. Analytical Chemistry 2016, 88 (1), 30–51. [PubMed: 26630359]

141. Domon B; Aebersold R, Mass Spectrometry and Protein Analysis. Science 2006, 312 (5771), 212–217. [PubMed: 16614208]

142. Dančík V; Addona TA; Clauser KR; Vath JE; Pevzner PA, De novo peptide sequencing via tandem mass spectrometry. Journal of computational biology 1999, 6 (3-4), 327–342. [PubMed: 10582570]

143. Edman P, Method for determination of the amino acid sequence in peptides. Acta chem. scand 1950, 4 (7), 283–293.

144. Mann M; Jensen ON, Proteomic analysis of post-translational modifications. Nature Biotechnology 2003, 21 (3), 255–261.

145. McLachlin DT; Chait BT, Analysis of phosphorylated proteins and peptides by mass spectrometry. Current Opinion in Chemical Biology 2001, 5 (5), 591–602. [PubMed: 11578935]

146. Nørregaard Jensen O, Modification-specific proteomics: characterization of post-translational modifications by mass spectrometry. Current Opinion in Chemical Biology 2004, 8 (1), 33–41. [PubMed: 15036154]

147. Witze ES; Old WM; Resing KA; Ahn NG, Mapping protein post-translational modifications with mass spectrometry. Nature Methods 2007, 4 (10), 798–806. [PubMed: 17901869]

148. Hao P; Adav SS; Gallart-Palau X; Sze SK, Recent advances in mass spectrometric analysis of protein deamidation. Mass Spectrometry Reviews 2017, 36 (6), 677–692. [PubMed: 26763661]

149. Loo JA, Studying noncovalent protein complexes by electrospray ionization mass spectrometry. Mass Spectrometry Reviews 1997, 16 (1), 1–23. [PubMed: 9414489]

150. Hernández H; Robinson CV, Determining the stoichiometry and interactions of macromolecular assemblies from mass spectrometry. Nature Protocols 2007, 2, 715. [PubMed: 17406634]

151. Benesch JLP; Ruotolo BT; Simmons DA; Robinson CV, Protein Complexes in the Gas Phase: Technology for Structural Genomics and Proteomics. Chemical Reviews 2007, 107 (8), 3544–3567. [PubMed: 17649985]

152. Laganowsky A; Reading E; Hopper JTS; Robinson CV, Mass spectrometry of intact membrane protein complexes. Nature Protocols 2013, 8, 639. [PubMed: 23471109]

153. Boeri Erba E; Petosa C, The emerging role of native mass spectrometry in characterizing the structure and dynamics of macromolecular complexes. Protein Science 2015, 24 (8), 1176–1192. [PubMed: 25676284]

154. Ruotolo BT; Benesch JLP; Sandercock AM; Hyung S-J; Robinson CV, Ion mobility–mass spectrometry analysis of large protein complexes. Nature Protocols 2008, 3, 1139. [PubMed: 18600219]

155. Uetrecht C; Rose RJ; van Duijn E; Lorenzen K; Heck AJR, Ion mobility mass spectrometry of proteins and protein assemblies. Chemical Society Reviews 2010, 39 (5), 1633–1655. [PubMed: 20419213]

156. Zhong Y; Hyung S-J; Ruotolo BT, Ion mobility–mass spectrometry for structural proteomics. Expert Review of Proteomics 2012, 9 (1), 47–58. [PubMed: 22292823]

157. Sinz A, Chemical cross-linking and mass spectrometry to map three-dimensional protein structures and protein–protein interactions. Mass Spectrometry Reviews 2006, 25 (4), 663–682. [PubMed: 16477643]

158. Leitner A, Cross-linking and other structural proteomics techniques: how chemistry is enabling mass spectrometry applications in structural biology. Chemical Science 2016, 7 (8), 4792–4803. [PubMed: 30155128]

159. Leitner A; Walzthoeni T; Kahraman A; Herzog F; Rinner O; Beck M; Aebersold R, Probing Native Protein Structures by Chemical Cross-linking, Mass Spectrometry, and Bioinformatics. Molecular & Cellular Proteomics 2010, 9 (8), 1634–1649. [PubMed: 20360032]

160. Galas DJ; Schmitz A, DNAase footprinting a simple method for the detection of protein-DNA binding specificity. Nucleic Acids Research 1978, 5 (9), 3157–3170. [PubMed: 212715]

161. Sheshberadaran H; Payne LG, Protein antigen-monoclonal antibody contact sites investigated by limited proteolysis of monoclonal antibody-bound antigen: protein “footprinting”. Proceedings of the National Academy of Sciences 1988, 85 (1), 1–5.

162. Fontana A; de Laureto PP; Spolaore B; Frare E; Picotti P; Zambonin M, Probing protein structure by limited proteolysis. ACTA BIOCHIMICA POLONICA-ENGLISH EDITION- 2004, 51, 299–322.

163. Schopper S; Kahraman A; Leuenberger P; Feng Y; Piazza I; Müller O; Boersema PJ; Picotti P, Measuring protein structural changes on a proteome-wide scale using limited proteolysis-coupled mass spectrometry. Nature Protocols 2017, 12, 2391. [PubMed: 29072706]

164. Ermácora MR; Delfino JM; Cuenoud B; Schepartz A; Fox RO, Conformation-dependent cleavage of staphylococcal nuclease with a disulfide-linked iron chelate. Proceedings of the National Academy of Sciences 1992, 89 (14), 6383–6387.

165. Konermann L; Pan J; Liu Y-H, Hydrogen exchange mass spectrometry for studying protein structure and dynamics. Chemical Society Reviews 2011, 40 (3), 1224–1234. [PubMed: 21173980]

166. Wold F, In vivo chemical modification of proteins (post-translational modification). Annual review of biochemistry 1981, 50 (1), 783–814.

167. Krishna RG; Wold F, Post-Translational Modifications of Proteins In Methods in Protein Sequence Analysis, Imahori K; Sakiyama F, Eds. Springer US: Boston, MA, 1993; pp 167–172.

168. Deribe YL; Pawson T; Dikic I, Post-translational modifications in signal integration. Nature Structural &Amp; Molecular Biology 2010, 17, 666.

169. Mendoza VL; Vachet RW, Probing protein structure by amino acid-specific covalent labeling and mass spectrometry. Mass Spectrometry Reviews 2009, 28 (5), 785–815. [PubMed: 19016300]

170. Guozhong XMRC, Hydroxyl Radical-Mediated Modification of Proteins as Probes for Structural Proteomics. Chem. Rev 2007, 107, 3514–3543. [PubMed: 17683160]

171. Chait BT, Mass Spectrometry: Bottom-Up or Top-Down? Science 2006, 314 (5796), 65–66. [PubMed: 17023639]

172. Kelleher NL; Lin HY; Valaskovic GA; Aaserud DJ; Fridriksson EK; McLafferty FW, Top Down versus Bottom Up Protein Characterization by Tandem High-Resolution Mass Spectrometry. Journal of the American Chemical Society 1999, 121 (4), 806–812.

173. Zhang Y; Fonslow BR; Shan B; Baek M-C; Yates JR, Protein Analysis by Shotgun/Bottom-up Proteomics. Chemical Reviews 2013, 113 (4), 2343–2394. [PubMed: 23438204]

174. Kelleher NL, Peer Reviewed: Top-Down Proteomics. Analytical Chemistry 2004, 76 (11), 196 A–203 A.

175. Siuti N; Kelleher NL, Decoding protein modifications using top-down mass spectrometry. Nature Methods 2007, 4, 817. [PubMed: 17901871]

176. Toby TK; Fornelli L; Kelleher NL, Progress in Top-Down Proteomics and the Analysis of Proteoforms. Annual Review of Analytical Chemistry 2016, 9 (1), 499–519.

177. Cui W; Rohrs HW; Gross ML, Top-down mass spectrometry: recent developments, applications and perspectives. Analyst 2011, 136 (19), 3854–3864. [PubMed: 21826297]

178. Compton PD; Zamdborg L; Thomas PM; Kelleher NL, On the Scalability and Requirements of Whole Protein Mass Spectrometry. Analytical Chemistry 2011, 83 (17), 6868–6874. [PubMed: 21744800]

179. Kruppa GH; Schoeniger J; Young MM, A top down approach to protein structural studies using chemical cross-linking and Fourier transform mass spectrometry. Rapid Communications in Mass Spectrometry 2003, 17 (2), 155–162. [PubMed: 12512095]

180. Novak P; Kruppa GH; Young MM; Schoeniger J, A Top-down method for the determination of residue-specific solvent accessibility in proteins. Journal of Mass Spectrometry 2004, 39 (3), 322–328. [PubMed: 15039940]

181. Chen J; Cui W; Giblin D; Gross ML, New Protein Footprinting: Fast Photochemical Iodination Combined with Top-Down and Bottom-Up Mass Spectrometry. Journal of The American Society for Mass Spectrometry 2012, 23 (8), 1306–1318. [PubMed: 22669760]

182. Hvidt A; Linderstrøm-Lang K, Exchange of hydrogen atoms in insulin with deuterium atoms in aqueous solutions. Biochimica et biophysica acta 1954, 14 (4), 574. [PubMed: 13198919]

183. Englander SW; Mayne L; Bai Y; Sosnick TR, Hydrogen exchange: The modern legacy of Linderstrøm-Lang. Protein Science 1997, 6 (5), 1101–1109. [PubMed: 9144782]

184. Linderstrøm-Lang K, The pH-dependence of the deuterium exchange of insulin. Biochimica et Biophysica Acta 1955, 18, 308. [PubMed: 13276391]

185. Berger A; Linderstrøm-Lang K, Deuterium exchange of poly-dl-alanine in aqueous solution. Archives of Biochemistry and Biophysics 1957, 69, 106–118. [PubMed: 13445185]

186. Linderstrøm-Lang K, Symposium on Protein Structure. Methuen & Co. Ltd: London, 1958.

187. Hvidt A; Nielsen SO, Hydrogen Exchange in Proteins In Advances in Protein Chemistry, Anfinsen CB; Anson ML; Edsall JT; Richards FM, Eds. Academic Press: 1966; Vol. 21, pp 287–386. [PubMed: 5333290]

188. Hvidt A; Johansen G; LinderstrØM-Lang K, 3 - DEUTERIUM AND 18O EXCHANGE In The Composition, Structure and Reactivity of Proteins, Alexander P; Block RJ, Eds. Pergamon: 1960; pp 101–130.

189. Englander SW, Hydrogen exchange and mass spectrometry: A historical perspective. Journal of The American Society for Mass Spectrometry 2006, 17 (11), 1481–1489.

190. Englander JJ; Calhoun DB; Englander SW, Measurement and calibration of peptide group hydrogen-deuterium exchange by ultraviolet spectrophotometry. Analytical Biochemistry 1979, 92 (2), 517–524. [PubMed: 443552]

191. Nielsen SO, Hydrogen-deuterium exchange in N-methylacetamide. Biochimica et Biophysica Acta 1960, 37 (1), 146–147. [PubMed: 14427099]

192. Blout ER; De Loze C; Asadourian A, The Deuterium Exchange of Water-soluble Polypeptides and Proteins as Measured by Infrared Spectroscopy. Journal of the American Chemical Society 1961, 83 (8), 1895–1900.

193. Kossiakoff AA, Protein dynamics investigated by the neutron diffraction–hydrogen exchange technique. Nature 1982, 296 (5859), 713–721. [PubMed: 7070514]

194. Saunders M; Wishnia A; Kirkwood JG, THE NUCLEAR MAGNETIC RESONANCE SPECTRUM OF RIBONUCLEASE1. Journal of the American Chemical Society 1957, 79 (12), 3289–3290.

195. Saunders M; Wishnia A, NUCLEAR MAGNETIC RESONANCE SPECTRA OF PROTEINS. Annals of the New York Academy of Sciences 1958, 70 (4), 870–874.

196. Wishnia A; Saunders M, The Nature of the Slowly Exchanging Protons of Ribonuclease. Journal of the American Chemical Society 1962, 84 (22), 4235–4239.

197. Glickson JD; McDonald CC; Phillips WD, Assignment of tryptophan indole NH proton resonances of lysozyme. Biochemical and Biophysical Research Communications 1969, 35 (4), 492–498. [PubMed: 4306956]

198. Wagner G; Wüthrich K, Amide proton exchange and surface conformation of the basic pancreatic trypsin inhibitor in solution: Studies with two-dimensional nuclear magnetic resonance. Journal of Molecular Biology 1982, 160 (2), 343–361. [PubMed: 6184480]

199. Schanda P; Brutscher B, Very Fast Two-Dimensional NMR Spectroscopy for Real-Time Investigation of Dynamic Events in Proteins on the Time Scale of Seconds. Journal of the American Chemical Society 2005, 127 (22), 8014–8015. [PubMed: 15926816]

200. Englander SW; Kallenbach NR, Hydrogen exchange and structural dynamics of proteins and nucleic acids. Quarterly Reviews of Biophysics 1983, 16 (4), 521–655. [PubMed: 6204354]

201. Englander SW; Sosnick TR; Englander JJ; Mayne L, Mechanisms and uses of hydrogen exchange. Current Opinion in Structural Biology 1996, 6 (1), 18–23. [PubMed: 8696968]

202. Paterson Y; Englander S; Roder H, An antibody binding site on cytochrome c defined by hydrogen exchange and two-dimensional NMR. Science 1990, 249 (4970), 755–759. [PubMed: 1697101]

203. Katta V; Chait BT; Carr S, Conformational changes in proteins probed by hydrogen-exchange electrospray-ionization mass spectrometry. Rapid Communications in Mass Spectrometry 1991, 5 (4), 214–217. [PubMed: 1666528]

204. Zhang Z; Smith DL, Determination of amide hydrogen exchange by mass spectrometry: A new tool for protein structure elucidation. Protein Science 1993, 2 (4), 522–531. [PubMed: 8390883]

205. Englander SW; N W Downer a.; Teitelbaum H, Hydrogen Exchange. Annual Review of Biochemistry 1972, 41 (1), 903–924.

206. Bai Y; Milne JS; Mayne L; Englander SW, Primary structure effects on peptide group hydrogen exchange. Proteins: Structure, Function, and Bioinformatics 1993, 17 (1), 75–86.

207. Smith DL; Deng Y; Zhang Z, Probing the Non-covalent Structure of Proteins by Amide Hydrogen Exchange and Mass Spectrometry. Journal of Mass Spectrometry 1997, 32 (2), 135–146. [PubMed: 9102198]

208. Pauling L; Corey RB; Branson HR, The structure of proteins: Two hydrogen-bonded helical configurations of the polypeptide chain. Proceedings of the National Academy of Sciences 1951, 37 (4), 205–211.

209. Konermann L; Tong X; Pan Y, Protein structure and dynamics studied by mass spectrometry: H/D exchange, hydroxyl radical labeling, and related approaches. Journal of Mass Spectrometry 2008, 43 (8), 1021–1036. [PubMed: 18523973]

210. Chalmers MJ; Busby SA; Pascal BD; West GM; Griffin PR, Differential hydrogen/deuterium exchange mass spectrometry analysis of protein–ligand interactions. Expert Review of Proteomics 2011, 8 (1), 43–59. [PubMed: 21329427]

211. Masson GR; Burke JE; Ahn NG; Anand GS; Borchers C; Brier S; Bou-Assaf GM; Engen JR; Englander SW; Faber J; Garlish R; Griffin PR; Gross ML; Guttman M; Hamuro Y; Heck AJR; Houde D; Iacob RE; Jørgensen TJD; Kaltashov IA; Klinman JP; Konermann L; Man P; Mayne L; Pascal BD; Reichmann D; Skehel M; Snijder J; Strutzenberg TS; Underbakke ES; Wagner C; Wales TE; Walters BT; Weis DD; Wilson DJ; Wintrode PL; Zhang Z; Zheng J; Schriemer DC;

Rand KD, Recommendations for performing, interpreting and reporting hydrogen deuterium exchange mass spectrometry (HDX-MS) experiments. Nature Methods 2019, 16 (7), 595–602. [PubMed: 31249422]

212. Rosa JJ; Richards FM, An experimental procedure for increasing the structural resolution of chemical hydrogen-exchange measurements on proteins: Application to ribonuclease S peptide. Journal of Molecular Biology 1979, 133 (3), 399–416. [PubMed: 43900]
213. Englander JJ; Rogero JR; Englander SW, Protein hydrogen exchange studied by the fragment separation method. Analytical Biochemistry 1985, 147 (1), 234–244. [PubMed: 2992314]
214. Jørgensen TJD; Gårdsvoll H; Ploug M; Roepstorff P, Intramolecular Migration of Amide Hydrogens in Protonated Peptides upon Collisional Activation. Journal of the American Chemical Society 2005, 127 (8), 2785–2793. [PubMed: 15725037]
215. Jørgensen TJD; Bache N; Roepstorff P; Gårdsvoll H; Ploug M, Collisional Activation by MALDI Tandem Time-of-flight Mass Spectrometry Induces Intramolecular Migration of Amide Hydrogens in Protonated Peptides. Molecular & Cellular Proteomics 2005, 4 (12), 1910–1919. [PubMed: 16127176]
216. Rand KD; Adams CM; Zubarev RA; Jørgensen TJD, Electron Capture Dissociation Proceeds with a Low Degree of Intramolecular Migration of Peptide Amide Hydrogens. Journal of the American Chemical Society 2008, 130 (4), 1341–1349. [PubMed: 18171065]
217. Zehl M; Rand KD; Jensen ON; Jørgensen TJD, Electron Transfer Dissociation Facilitates the Measurement of Deuterium Incorporation into Selectively Labeled Peptides with Single Residue Resolution. Journal of the American Chemical Society 2008, 130 (51), 17453–17459. [PubMed: 19035774]
218. Pan J; Han J; Borchers CH; Konermann L, Hydrogen/Deuterium Exchange Mass Spectrometry with Top-Down Electron Capture Dissociation for Characterizing Structural Transitions of a 17 kDa Protein. Journal of the American Chemical Society 2009, 131 (35), 12801–12808. [PubMed: 19670873]
219. Hamuro Y; E SY, Determination of Backbone Amide Hydrogen Exchange Rates of Cytochrome c Using Partially Scrambled Electron Transfer Dissociation Data. Journal of The American Society for Mass Spectrometry 2018, 29 (5), 989–1001. [PubMed: 29500740]
220. Kan Z-Y; Walters BT; Mayne L; Englander SW, Protein hydrogen exchange at residue resolution by proteolytic fragmentation mass spectrometry analysis. Proceedings of the National Academy of Sciences 2013, 110 (41), 16438–16443.
221. Hamuro Y; Zhang T, High-Resolution HDX-MS of Cytochrome c Using Pepsin/Fungal Protease Type XIII Mixed Bed Column. Journal of The American Society for Mass Spectrometry 2019, 30 (2), 227–234. [PubMed: 30374663]
222. López-Ferrer D; Petritis K; Lourette NM; Clowers B; Hixson KK; Heibeck T; Prior DC; Paša-Tolić L; Camp DG; Belov ME; Smith RD, On-line Digestion System for Protein Characterization and Proteome Analysis. Analytical Chemistry 2008, 80 (23), 8930–8936. [PubMed: 19551971]
223. Jones LM; Zhang H; Vidavsky I; Gross ML, Online, High-Pressure Digestion System for Protein Characterization by Hydrogen/Deuterium Exchange and Mass Spectrometry. Analytical Chemistry 2010, 82 (4), 1171–1174. [PubMed: 20095571]
224. Rand KD; Zehl M; Jensen ON; Jørgensen TJD, Protein Hydrogen Exchange Measured at Single-Residue Resolution by Electron Transfer Dissociation Mass Spectrometry. Analytical Chemistry 2009, 81 (14), 5577–5584. [PubMed: 19601649]
225. Gessner C; Steinchen W; Bédard S; Skinner J, J.; Woods VL; Walsh TJ; Bange G; Pantazatos DP, Computational method allowing Hydrogen-Deuterium Exchange Mass Spectrometry at single amide Resolution. Scientific Reports 2017, 7 (1), 3789. [PubMed: 28630467]
226. Saltzberg DJ; Broughton HB; Pellarin R; Chalmers MJ; Espada A; Dodge JA; Pascal BD; Griffin PR; Humblet C; Sali A, A Residue-Resolved Bayesian Approach to Quantitative Interpretation of Hydrogen–Deuterium Exchange from Mass Spectrometry: Application to Characterizing Protein–Ligand Interactions. The Journal of Physical Chemistry B 2017, 121 (15), 3493–3501. [PubMed: 27807976]

227. Jansson ET; Lai Y-H; Santiago JG; Zare RN, Rapid Hydrogen–Deuterium Exchange in Liquid Droplets. Journal of the American Chemical Society 2017, 139 (20), 6851–6854. [PubMed: 28481522]

228. Rand KD; Pringle SD; Murphy JP; Fadgen KE; Brown J; Engen JR, Gas-Phase Hydrogen/Deuterium Exchange in a Traveling Wave Ion Guide for the Examination of Protein Conformations. Analytical Chemistry 2009, 81 (24), 10019–10028. [PubMed: 19921790]

229. Mistarz Ulrik H.; Brown Jeffery M.; Haselmann Kim F.; Rand Kasper D., Probing the Binding Interfaces of Protein Complexes Using Gas-Phase H/D Exchange Mass Spectrometry. Structure 2016, 24 (2), 310–318. [PubMed: 26749447]

230. Uppal SS; Beasley SE; Scian M; Guttman M, Gas-Phase Hydrogen/Deuterium Exchange for Distinguishing Isomeric Carbohydrate Ions. Analytical Chemistry 2017, 89 (8), 4737–4742. [PubMed: 28304155]

231. Powell KD; Ghaemmaghami S; Wang MZ; Ma L; Oas TG; Fitzgerald MC, A General Mass Spectrometry-Based Assay for the Quantitation of Protein–Ligand Binding Interactions in Solution. Journal of the American Chemical Society 2002, 124 (35), 10256–10257. [PubMed: 12197709]

232. Zhu MM; Rempel DL; Du Z; Gross ML, Quantification of Protein–Ligand Interactions by Mass Spectrometry, Titration, and H/D Exchange: PLIMSTEX. Journal of the American Chemical Society 2003, 125 (18), 5252–5253. [PubMed: 12720418]

233. Wang H; Rempel DL; Giblin D; Frieden C; Gross ML, Peptide-Level Interactions between Proteins and Small-Molecule Drug Candidates by Two Hydrogen–Deuterium Exchange MS-Based Methods: The Example of Apolipoprotein E3. Analytical Chemistry 2017, 89 (20), 10687–10695. [PubMed: 28901129]

234. Rey M; Mrázek H; Pompach P; Novák P; Pelosi L; Brandolin G; Forest E; Havlíček V; Man P, Effective Removal of Nonionic Detergents in Protein Mass Spectrometry, Hydrogen/Deuterium Exchange, and Proteomics. Analytical Chemistry 2010, 82 (12), 5107–5116. [PubMed: 20507168]

235. Anderson KW; Gallagher ES; Hudgens JW, Automated Removal of Phospholipids from Membrane Proteins for H/D Exchange Mass Spectrometry Workflows. Analytical Chemistry 2018, 90 (11), 6409–6412. [PubMed: 29723469]

236. Möller IR; Slivacka M; Hausner J; Nielsen AK; Pospíšilová E; Merkle PS; Lišková R; Polák M; Loland CJ; Kádek A; Man P; Rand KD, Improving the Sequence Coverage of Integral Membrane Proteins during Hydrogen/Deuterium Exchange Mass Spectrometry Experiments. Analytical Chemistry 2019, 91 (17), 10970–10978. [PubMed: 31408320]

237. Jensen PF; Comamala G; Trelle MB; Madsen JB; Jørgensen TJD; Rand KD, Removal of N-Linked Glycosylations at Acidic pH by PNGase A Facilitates Hydrogen/Deuterium Exchange Mass Spectrometry Analysis of N-Linked Glycoproteins. Analytical Chemistry 2016, 88 (24), 12479–12488. [PubMed: 28193043]

238. Hamuro Y; Coales SJ; Southern MR; Nemeth-Cawley JF; Stranz DD; Griffin PR, Rapid analysis of protein structure and dynamics by hydrogen/deuterium exchange mass spectrometry. J Biomol Tech 2003, 14 (3), 171–182. [PubMed: 13678147]

239. Weis DD; Engen JR; Kass IJ, Semi-automated data processing of hydrogen exchange mass spectra using HX-Express. Journal of The American Society for Mass Spectrometry 2006, 17 (12), 1700–1703. [PubMed: 16931036]

240. Pascal BD; Willis S; Lauer JL; Landgraf RR; West GM; Marciano D; Novick S; Goswami D; Chalmers MJ; Griffin PR, HDX Workbench: Software for the Analysis of H/D Exchange MS Data. Journal of The American Society for Mass Spectrometry 2012, 23 (9), 1512–1521. [PubMed: 22692830]

241. Palmblad M; Buijs J; Håkansson P, Automatic analysis of hydrogen/deuterium exchange mass spectra of peptides and proteins using calculations of isotopic distributions. Journal of the American Society for Mass Spectrometry 2001, 12 (11), 1153–1162. [PubMed: 11720389]

242. Zhang Z, Large-Scale Identification and Quantification of Covalent Modifications in Therapeutic Proteins. Analytical Chemistry 2009, 81 (20), 8354–8364. [PubMed: 19764700]

243. Zhang Z; Zhang A; Xiao G, Improved Protein Hydrogen/Deuterium Exchange Mass Spectrometry Platform with Fully Automated Data Processing. Analytical Chemistry 2012, 84 (11), 4942–4949. [PubMed: 22571272]

244. Pascal BD; Chalmers MJ; Busby SA; Griffin PR, HD desktop: An integrated platform for the analysis and visualization of H/D exchange data. Journal of the American Society for Mass Spectrometry 2009, 20 (4), 601–610. [PubMed: 19135386]

245. Lou X; Kirchner M; Renard BY; Köthe U; Boppel S; Graf C; Lee C-T; Steen JAJ; Steen H; Mayer MP; Hamprecht FA, Deuteration distribution estimation with improved sequence coverage for HX/MS experiments. Bioinformatics 2010, 26 (12), 1535–1541. [PubMed: 20439256]

246. Kan Z-Y; Mayne L; Sevugan Chetty P; Englander SW, ExMS: Data Analysis for HX-MS Experiments. Journal of The American Society for Mass Spectrometry 2011, 22 (11), 1906. [PubMed: 21952778]

247. Liu S; Liu L; Uzuner U; Zhou X; Gu M; Shi W; Zhang Y; Dai SY; Yuan JS, HDX-analyzer: a novel package for statistical analysis of protein structure dynamics. BMC bioinformatics 2011, 12 Suppl 1 (Suppl 1), S43–S43. [PubMed: 21342575]

248. Miller DE; Prasannan CB; Villar MT; Fenton AW; Artigues A, HDXFinder: Automated Analysis and Data Reporting of Deuterium/Hydrogen Exchange Mass Spectrometry. Journal of The American Society for Mass Spectrometry 2012, 23 (2), 425–429. [PubMed: 22083588]

249. Rey M; Sarpe V; Burns KM; Buse J; Baker Charles A. H.; van Dijk M; Wordeman L; Bonvin Alexandre M. J. J.; Schriemer David C., Mass Spec Studio for Integrative Structural Biology. Structure 2014, 22 (10), 1538–1548. [PubMed: 25242457]

250. Kavan D; Man P, MSTools—Web based application for visualization and presentation of HXMS data. International Journal of Mass Spectrometry 2011, 302 (1), 53–58.

251. Hourdel V; Volant S; O'Brien DP; Chenal A; Chamot-Rooke J; Dillies M-A; Brier S, MEMHDX: an interactive tool to expedite the statistical validation and visualization of large HDX-MS datasets. Bioinformatics (Oxford, England) 2016, 32 (22), 3413–3419.

252. Lau AMC; Ahdash Z; Martens C; Politis A, Deuteros: software for rapid analysis and visualization of data from differential hydrogen deuterium exchange-mass spectrometry. Bioinformatics 2019, 35 (17), 3171–3173. [PubMed: 30649183]

253. Bouyssié D; Lesne J; Locard-Paulet M; Albigot R; Burlet-Schiltz O; Marcoux J, HDX-Viewer: interactive 3D visualization of hydrogen–deuterium exchange data. Bioinformatics 2019.

254. Pirrone GF; Iacob RE; Engen JR, Applications of Hydrogen/Deuterium Exchange MS from 2012 to 2014. Analytical Chemistry 2015, 87 (1), 99–118. [PubMed: 25398026]

255. Engen JR; Wales TE, Analytical Aspects of Hydrogen Exchange Mass Spectrometry. Annual Review of Analytical Chemistry 2015, 8 (1), 127–148.

256. Marciano DP; Dharmarajan V; Griffin PR, HDX-MS guided drug discovery: small molecules and biopharmaceuticals. Current Opinion in Structural Biology 2014, 28, 105–111. [PubMed: 25179005]

257. Wei H; Mo J; Tao L; Russell RJ; Tymiak AA; Chen G; Iacob RE; Engen JR, Hydrogen/deuterium exchange mass spectrometry for probing higher order structure of protein therapeutics: methodology and applications. Drug Discovery Today 2014, 19 (1), 95–102. [PubMed: 23928097]

258. Deng B; Lento C; Wilson DJ, Hydrogen deuterium exchange mass spectrometry in biopharmaceutical discovery and development – A review. Analytica Chimica Acta 2016, 940, 8–20. [PubMed: 27662755]

259. Masson GR; Jenkins ML; Burke JE, An overview of hydrogen deuterium exchange mass spectrometry (HDX-MS) in drug discovery. Expert Opinion on Drug Discovery 2017, 12 (10), 981–994. [PubMed: 28770632]

260. Englander SW; Mayne L; Kan Z-Y; Hu W, Protein Folding—How and Why: By Hydrogen Exchange, Fragment Separation, and Mass Spectrometry. Annual Review of Biophysics 2016, 45 (1), 135–152.

261. Georgescauld F; Wales TE; Engen JR, Hydrogen deuterium exchange mass spectrometry applied to chaperones and chaperone-assisted protein folding. Expert Review of Proteomics 2019, 16 (7), 613–625. [PubMed: 31215268]

262. Gallagher ES; Hudgens JW, Chapter Fourteen - Mapping Protein–Ligand Interactions with Proteolytic Fragmentation, Hydrogen/Deuterium Exchange-Mass Spectrometry In Methods in Enzymology, Kelman Z, Ed. Academic Press: 2016; Vol. 566, pp 357–404. [PubMed: 26791987]
263. Percy AJ; Rey M; Burns KM; Schriemer DC, Probing protein interactions with hydrogen/deuterium exchange and mass spectrometry—A review. Analytica Chimica Acta 2012, 721, 7–21. [PubMed: 22405295]
264. Harrison RA; Engen JR, Conformational insight into multi-protein signaling assemblies by hydrogen–deuterium exchange mass spectrometry. Current Opinion in Structural Biology 2016, 41, 187–193. [PubMed: 27552080]
265. Engen JR, Analysis of Protein Conformation and Dynamics by Hydrogen/Deuterium Exchange MS. Analytical Chemistry 2009, 81 (19), 7870–7875. [PubMed: 19788312]
266. Kochert BA; Iacob RE; Wales TE; Makriyannis A; Engen JR, Hydrogen-Deuterium Exchange Mass Spectrometry to Study Protein Complexes In Protein Complex Assembly: Methods and Protocols, Marsh JA, Ed. Springer New York: New York, NY, 2018; pp 153–171.
267. Englander JJ; Del Mar C; Li W; Englander SW; Kim JS; Stranz DD; Hamuro Y; Woods VL, Protein structure change studied by hydrogen-deuterium exchange, functional labeling, and mass spectrometry. Proceedings of the National Academy of Sciences 2003, 100 (12), 7057–7062.
268. Vadas O; Jenkins ML; Dornan GL; Burke JE, Chapter Seven - Using Hydrogen–Deuterium Exchange Mass Spectrometry to Examine Protein–Membrane Interactions In Methods in Enzymology, Gelb MH, Ed. Academic Press: 2017; Vol. 583, pp 143–172. [PubMed: 28063489]
269. Rand KD; Zehl M; Jørgensen TJD, Measuring the Hydrogen/Deuterium Exchange of Proteins at High Spatial Resolution by Mass Spectrometry: Overcoming Gas-Phase Hydrogen/Deuterium Scrambling. Accounts of Chemical Research 2014, 47 (10), 3018–3027. [PubMed: 25171396]
270. Baslé E; Joubert N; Pucheault M, Protein Chemical Modification on Endogenous Amino Acids. Chemistry & Biology 2010, 17 (3), 213–227. [PubMed: 20338513]
271. Lundblad RL, Chemical reagents for protein modification. CRC press: 2014.
272. Spicer CD; Davis BG, Selective chemical protein modification. Nature Communications 2014, 5 (1), 4740.
273. Boutureira O; Bernardes GJL, Advances in Chemical Protein Modification. Chemical Reviews 2015, 115 (5), 2174–2195. [PubMed: 25700113]
274. Leitner A, A review of the role of chemical modification methods in contemporary mass spectrometry-based proteomics research. Analytica Chimica Acta 2018, 1000, 2–19. [PubMed: 29289310]
275. Bauer RA, Covalent inhibitors in drug discovery: from accidental discoveries to avoided liabilities and designed therapies. Drug Discovery Today 2015, 20 (9), 1061–1073. [PubMed: 26002380]
276. Lonsdale R; Ward RA, Structure-based design of targeted covalent inhibitors. Chemical Society Reviews 2018, 47 (11), 3816–3830. [PubMed: 29620097]
277. Mukherjee H; Grimster NP, Beyond cysteine: recent developments in the area of targeted covalent inhibition. Current Opinion in Chemical Biology 2018, 44, 30–38. [PubMed: 29857316]
278. Tamura T; Hamachi I, Chemistry for Covalent Modification of Endogenous/Native Proteins: From Test Tubes to Complex Biological Systems. Journal of the American Chemical Society 2019, 141 (7), 2782–2799. [PubMed: 30592612]
279. Giles NM; Giles GI; Jacob C, Multiple roles of cysteine in biocatalysis. Biochemical and Biophysical Research Communications 2003, 300 (1), 1–4. [PubMed: 12480511]
280. Giron P; Dayon L; Sanchez J-C, Cysteine tagging for MS-based proteomics. Mass Spectrometry Reviews 2011, 30 (3), 366–395. [PubMed: 21500242]
281. Wu X; Liang H; O'Hara KA; Yalowich JC; Hasinoff BB, Thiol-Modulated Mechanisms of the Cytotoxicity of Thimerosal and Inhibition of DNA Topoisomerase IIα. Chemical Research in Toxicology 2008, 21 (2), 483–493. [PubMed: 18197631]
282. Smolka MB; Zhou H; Purkayastha S; Aebersold R, Optimization of the Isotope-Coded Affinity Tag-Labeling Procedure for Quantitative Proteome Analysis. Analytical Biochemistry 2001, 297 (1), 25–31. [PubMed: 11567524]

283. Smythe CV, THE REACTION OF IODOACETATE AND OF IODOACETAMIDE WITH VARIOUS SULFHYDRYL GROUPS, WITH UREASE, AND WITH YEAST PREPARATIONS. Journal of Biological Chemistry 1936, 114 (3), 601–612.

284. Anson ML, THE REACTIONS OF IODINE AND IODOACETAMIDE WITH NATIVE EGG ALBUMIN. The Journal of General Physiology 1940, 23 (3), 321–331. [PubMed: 19873158]

285. Schroeder EF; Woodward GE; Platt ME, THE RELATION OF SULFHYDRYL TO INHIBITION OF YEAST FERMENTATION BY IODOACETIC ACID. Journal of Biological Chemistry 1933, 101 (1), 133–144.

286. Pasquarello C; Sanchez J-C; Hochstrasser DF; Corthals GL, N-t-butyliodoacetamide and iodoacetanilide: two new cysteine alkylating reagents for relative quantitation of proteins. Rapid Communications in Mass Spectrometry 2004, 18 (1), 117–127. [PubMed: 14689568]

287. Gundlach HG; Stein WH; Moore S, The Nature of the Amino Acid Residues Involved in the Inactivation of Ribonuclease by Iodoacetate. Journal of Biological Chemistry 1959, 234 (7), 1754–1760. [PubMed: 13672958]

288. Heinrikson RL; Stein WH; Crestfield AM; Moore S, The Reactivities of the Histidine Residues at the Active Site of Ribonuclease toward Halo Acids of Different Structures. Journal of Biological Chemistry 1965, 240 (7), 2921–2934. [PubMed: 14342316]

289. Gurd FRN, [62] Carboxymethylation In Methods in Enzymology, Academic Press: 1967; Vol. 11, pp 532–541.

290. Gundlach HG; Moore S; Stein WH, The Reaction of Iodoacetate with Methionine. Journal of Biological Chemistry 1959, 234 (7), 1761–1764. [PubMed: 13672959]

291. Whitehurst CB; Soderblom EJ; West ML; Hernandez R; Goshe MB; Brown DT, Location and Role of Free Cysteinyl Residues in the Sindbis Virus E1 and E2 Glycoproteins. Journal of Virology 2007, 81 (12), 6231–6240. [PubMed: 17409163]

292. Britto PJ; Knipling L; Wolff J, The Local Electrostatic Environment Determines Cysteine Reactivity of Tubulin. Journal of Biological Chemistry 2002, 277 (32), 29018–29027. [PubMed: 12023292]

293. Korman S; Clarke HT, CARBOXYMETHYLAMINO ACIDS AND PEPTIDES. Journal of Biological Chemistry 1956, 221 (1), 113–132. [PubMed: 13345804]

294. Dahl KH; McKinley-McKee JS, The reactivity of affinity labels: A kinetic study of the reaction of alkyl halides with thiolate anions—a model reaction for protein alkylation. Bioorganic Chemistry 1981, 10 (3), 329–341.

295. Plapp BV, [25] Application of affinity labeling for studying structure and function of enzymes In Methods in Enzymology, Purich DL, Ed. Academic Press: 1982; Vol. 87, pp 469–499. [PubMed: 7176925]

296. Tedaldi LM; Smith MEB; Nathani RI; Baker JR, Bromomaleimides: new reagents for the selective and reversible modification of cysteine. Chemical Communications 2009, (43), 6583–6585. [PubMed: 19865657]

297. Smith MEB; Schumacher FF; Ryan CP; Tedaldi LM; Papaioannou D; Waksman G; Caddick S; Baker JR, Protein Modification, Bioconjugation, and Disulfide Bridging Using Bromomaleimides. Journal of the American Chemical Society 2010, 132 (6), 1960–1965. [PubMed: 20092331]

298. Ryan CP; Smith MEB; Schumacher FF; Grohmann D; Papaioannou D; Waksman G; Werner F; Baker JR; Caddick S, Tunable reagents for multi-functional bioconjugation: reversible or permanent chemical modification of proteins and peptides by control of maleimide hydrolysis. Chemical Communications 2011, 47 (19), 5452–5454. [PubMed: 21465057]

299. Gregory JD, The Stability of N-Ethylmaleimide and its Reaction with Sulfhydryl Groups. Journal of the American Chemical Society 1955, 77 (14), 3922–3923.

300. Leslie J, Spectral shifts in the reaction of N-ethylmaleimide with proteins. Analytical Biochemistry 1965, 10 (1), 162–167. [PubMed: 14287860]

301. Gorin G; Martic PA; Doughty G, Kinetics of the reaction of N-ethylmaleimide with cysteine and some congeners. Archives of Biochemistry and Biophysics 1966, 115 (3), 593–597. [PubMed: 5970483]

302. Smyth DG; Nagamatsu A; Fruton JS, Some Reactions of N-Ethylmaleimide1. Journal of the American Chemical Society 1960, 82 (17), 4600–4604.

303. Bednar RA, Reactivity and pH dependence of thiol conjugation to N-ethylmaleimide: detection of a conformational change in chalcone isomerase. Biochemistry 1990, 29 (15), 3684–3690. [PubMed: 2340265]

304. Apuy JL; Park Z-Y; Swartz PD; Dangott LJ; Russell DH; Baldwin TO, Pulsed-Alkylation Mass Spectrometry for the Study of Protein Folding and Dynamics: Development and Application to the Study of a Folding/Unfolding Intermediate of Bacterial Luciferase. Biochemistry 2001, 40 (50), 15153–15163. [PubMed: 11735398]

305. Antonino LC; Straub K; Wu JC, Probing the Active Site of Human IMP Dehydrogenase Using Halogenated Purine Riboside 5'-Monophosphates and Covalent Modification Reagents. Biochemistry 1994, 33 (7), 1760–1765. [PubMed: 7906543]

306. Toutchkine A; Kraynov V; Hahn K, Solvent-Sensitive Dyes to Report Protein Conformational Changes in Living Cells. Journal of the American Chemical Society 2003, 125 (14), 4132–4145. [PubMed: 12670235]

307. Garrett SC; Hodgson L; Rybin A; Toutchkine A; Hahn KM; Lawrence DS; Bresnick AR, A Biosensor of S100A4 Metastasis Factor Activation: Inhibitor Screening and Cellular Activation Dynamics. Biochemistry 2008, 47 (3), 986–996. [PubMed: 18154362]

308. Embaby AM; Schoffelen S; Kofoed C; Meldal M; Diness F, Rational Tuning of Fluorobenzene Probes for Cysteine-Selective Protein Modification. Angewandte Chemie 2018, 130 (27), 8154–8158.

309. Chumsae C; Gaza-Bulseco G; Liu H, Identification and Localization of Unpaired Cysteine Residues in Monoclonal Antibodies by Fluorescence Labeling and Mass Spectrometry. Analytical Chemistry 2009, 81 (15), 6449–6457. [PubMed: 19572546]

310. Everett EA; Falick AM; Reich NO, Identification of a critical cysteine in EcoRI DNA methyltransferase by mass spectrometry. Journal of Biological Chemistry 1990, 265 (29), 17713–9. [PubMed: 2170393]

311. Hess DT; Matsumoto A; Kim S-O; Marshall HE; Stamler JS, Protein S-nitrosylation: purview and parameters. Nature Reviews Molecular Cell Biology 2005, 6 (2), 150–166. [PubMed: 15688001]

312. Torta F; Usuelli V; Malgaroli A; Bachi A, Proteomic analysis of protein S-nitrosylation. PROTEOMICS 2008, 8 (21), 4484–4494. [PubMed: 18846506]

313. Smith S; Kyte J, Assessment of the number of free cysteines and isolation and identification of cysteine-containing peptides from acetylcholine receptor. Appendix: Reversible modification of cysteine with cyanogen bromide. Biochemistry 1989, 28 (8), 3481–3482.

314. Xu K; Zhang Y; Tang B; Laskin J; Roach PJ; Chen H, Study of Highly Selective and Efficient Thiol Derivatization Using Selenium Reagents by Mass Spectrometry. Analytical Chemistry 2010, 82 (16), 6926–6932. [PubMed: 20704382]

315. Wang Z; Zhang Y; Zhang H; Harrington PB; Chen H, Fast and Selective Modification of Thiol Proteins/Peptides by N-(Phenylseleno)phthalimide. Journal of The American Society for Mass Spectrometry 2012, 23 (3), 520–529. [PubMed: 22223263]

316. Ellman GL, Tissue sulfhydryl groups. Archives of Biochemistry and Biophysics 1959, 82 (1), 70–77. [PubMed: 13650640]

317. Grassetti DR; Murray JF, Determination of sulfhydryl groups with 2,2′- or 4,4′-dithiodipyridine. Archives of Biochemistry and Biophysics 1967, 119, 41–49. [PubMed: 6052434]

318. Friedman M, Application of the S-Pyridylethylation Reaction to the Elucidation of the Structures and Functions of Proteins. Journal of Protein Chemistry 2001, 20 (6), 431–453. [PubMed: 11760118]

319. Kleinova M; Belgacem O; Pock K; Rizzi A; Buchacher A; Allmaier G, Characterization of cysteinylation of pharmaceutical-grade human serum albumin by electrospray ionization mass spectrometry and low-energy collision-induced dissociation tandem mass spectrometry. Rapid Communications in Mass Spectrometry 2005, 19 (20), 2965–2973. [PubMed: 16178042]

320. LoPachin RM; Gavin T; Geohagen BC; Das S, Neurotoxic Mechanisms of Electrophilic Type-2 Alkenes: Soft–Soft Interactions Described by Quantum Mechanical Parameters. Toxicological Sciences 2007, 98 (2), 561–570. [PubMed: 17519395]

321. Farnworth AJ, The reactivity of the cystine linkages in wool towards reducing agents. Biochemical Journal 1955, 60 (4), 626–635. [PubMed: 13249957]
322. Lindley H; Cranston RW, The reactivity of the disulphide bonds of wool. Biochemical Journal 1974, 139 (3), 515–523. [PubMed: 4408385]
323. Hiskey RG; Harpp DN, Chemistry of Aliphatic Disulfides: VII. Cyanide Cleavage in the Presence of Thiocyanates. Journal of the American Chemical Society 1964, 86 (10), 2014–2018.
324. Neumann H; Smith RA, Cleavage of the disulfide bonds of cystine and oxidized glutathione by phosphorothioate. Archives of Biochemistry and Biophysics 1967, 122 (2), 354–361. [PubMed: 6066243]
325. Lukesh JC; Palte MJ; Raines RT, A Potent, Versatile Disulfide-Reducing Agent from Aspartic Acid. Journal of the American Chemical Society 2012, 134 (9), 4057–4059. [PubMed: 22353145]
326. Singh R; Lamoureux GV; Lees WJ; Whitesides GM, [14] Reagents for rapid reduction of disulfide bonds In Methods in Enzymology, Academic Press: 1995; Vol. 251, pp 167–173. [PubMed: 7651195]
327. Duane Brown W, Reduction of protein disulfide bonds by sodium borohydride. Biochimica et Biophysica Acta 1960, 44, 365–367.
328. Simpson SD; Young L, Biochemical studies of toxic agents. 1. Experiments with radioactive 2:3-dimercaptopropanol (British Anti-Lewisite). Biochemical Journal 1950, 46 (5), 634–640. [PubMed: 15420205]
329. Evans RM; Fraser JB; Owen LN, 61. Dithiols. Part III. Derivatives of polyhydric alcohols. Journal of the Chemical Society (Resumed) 1949, (0), 248–255.
330. Cleland WW, Dithiothreitol, a New Protective Reagent for SH Groups*. Biochemistry 1964, 3 (4), 480–482. [PubMed: 14192894]
331. Stevens R; Stevens L; Price NC, The stabilities of various thiol compounds used in protein purifications. Biochemical Education 1983, 11 (2), 70–70.
332. Iyer KS; Klee WA, Direct Spectrophotometric Measurement of the Rate of Reduction of Disulfide Bonds: THE REACTIVITY OF THE DISULFIDE BONDS OF BOVINE α-LACTALBUMIN. Journal of Biological Chemistry 1973, 248 (2), 707–710. [PubMed: 4734333]
333. Burns JA; Butler JC; Moran J; Whitesides GM, Selective reduction of disulfides by tris(2-carboxyethyl)phosphine. The Journal of Organic Chemistry 1991, 56 (8), 2648–2650.
334. Vâlcu C-M; Schlink K, Reduction of proteins during sample preparation and two-dimensional gel electrophoresis of woody plant samples. PROTEOMICS 2006, 6 (5), 1599–1605. [PubMed: 16456882]
335. Hong R; Nisonoff A, Relative Labilities of the Two Types of Interchain Disulfide Bond of Rabbit γG-Immunoglobulin. Journal of Biological Chemistry 1965, 240 (10), 3883–3891. [PubMed: 4158501]
336. Humphreys DP; Heywood SP; Henry A; Ait-Lhadj L; Antoniw P; Palframan R; Greenslade KJ; Carrington B; Reeks DG; Bowering LC; West S; Brand HA, Alternative antibody Fab′ fragment PEGylation strategies: combination of strong reducing agents, disruption of the interchain disulphide bond and disulphide engineering. Protein Engineering, Design and Selection 2007, 20 (5), 227–234.
337. Kraj A; Brouwer H-J; Reinhoud N; Chervet J-P, A novel electrochemical method for efficient reduction of disulfide bonds in peptides and proteins prior to MS detection. Analytical and Bioanalytical Chemistry 2013, 405 (29), 9311–9320. [PubMed: 24077854]
338. Mysling S; Salbo R; Ploug M; Jørgensen TJD, Electrochemical Reduction of Disulfide-Containing Proteins for Hydrogen/Deuterium Exchange Monitored by Mass Spectrometry. Analytical Chemistry 2014, 86 (1), 340–345. [PubMed: 24251601]
339. Palego L; Betti L; Rossi A; Giannaccini G, Tryptophan Biochemistry: Structural, Nutritional, Metabolic, and Medical Aspects in Humans. Journal of Amino Acids 2016, 2016, 13.
340. Painter RG; Sage HJ; Tanford C, Contributions of heavy and light chains of rabbit immunoglobulin G to antibody activity. I. Binding studies on isolated heavy and light chains. Biochemistry 1972, 11 (8), 1327–1337. [PubMed: 4623250]

341. Schibli DJ; Epand RF; Vogel HJ; Epand RM, Tryptophan-rich antimicrobial peptides: comparative properties and membrane interactions. Biochemistry and Cell Biology 2002, 80 (5), 667–677. [PubMed: 12440706]

342. Al-Abdul-Wahid MS; DeMill CM; Serwin MB; Prosser RS; Stewart BA, Effect of juxtamembrane tryptophans on the immersion depth of Synaptobrevin, an integral vesicle membrane protein. Biochimica et Biophysica Acta (BBA) - Biomembranes 2012, 1818 (12), 2994–2999. [PubMed: 22846509]

343. Herbst DA; Boll B; Zocher G; Stehle T; Heide L, Structural Basis of the Interaction of MbtH-like Proteins, Putative Regulators of Nonribosomal Peptide Biosynthesis, with Adenylating Enzymes. Journal of Biological Chemistry 2013, 288 (3), 1991–2003. [PubMed: 23192349]

344. Chen Y; Barkley MD, Toward Understanding Tryptophan Fluorescence in Proteins. Biochemistry 1998, 37 (28), 9976–9982. [PubMed: 9665702]

345. Vivian JT; Callis PR, Mechanisms of Tryptophan Fluorescence Shifts in Proteins. Biophysical Journal 2001, 80 (5), 2093–2109. [PubMed: 11325713]

346. MEYBECK A; WINDLE JJ, An EPR study of peptides after UV irradiation. Photochemistry and photobiology 1969, 10 (1), 1–12. [PubMed: 4308919]

347. SANTUS R; GROSSWEINER LI, PRIMARY PRODUCTS IN THE FLASH PHOTOLYSIS OF TRYPTOPHAN*. Photochemistry and Photobiology 1972, 15 (1), 101–105.

348. Ananthaswamy HN; Eisenstark A, NEAR-UV-INDUCED BREAKS IN PHAGE DNA: SENSITIZATION BY HYDROGEN PEROXIDE (A TRYPTOPHAN PHOTOPRODUCT). Photochemistry and Photobiology 1976, 24 (5), 439–442. [PubMed: 981345]

349. Szajdzinska-Pietek E; Bednarek J; Plonka A, Electron spin resonance studies on tryptophan photolysis in frozen micellar systems of anionic surfactants. Journal of Photochemistry and Photobiology A: Chemistry 1993, 75 (2), 131–136.

350. Angiolillo PJ; Vanderkooi JM, Hydrogen Atoms Are Produced When Tryptophan within a Protein Is Irradiated with Ultraviolet Light. Photochemistry and Photobiology 1996, 64 (3), 492–495. [PubMed: 8806227]

351. Barnes S; Shonsey Erin M.; Eliuk Shannon M.; Stella D; Barrett K; Srivastava Om P.; Kim H; Renfrow Matthew B., High-resolution mass spectrometry analysis of protein oxidations and resultant loss of function. Biochemical Society Transactions 2008, 36 (5), 1037–1044. [PubMed: 18793185]

352. Freinbichler W; Colivicchi MA; Stefanini C; Bianchi L; Ballini C; Misini B; Weinberger P; Linert W; Varešlija D; Tipton KF; Della Corte L, Highly reactive oxygen species: detection, formation, and possible functions. Cellular and Molecular Life Sciences 2011, 68 (12), 2067–2079. [PubMed: 21533983]

353. Previero A; Coletti-Previero MA; Cavadore J-C, A reversible chemical modification of the tryptophan residue. Biochimica et Biophysica Acta (BBA) - Protein Structure 1967, 147 (3), 453–461.

354. Foettinger A; Melmer M; Leitner A; Lindner W, Reaction of the Indole Group with Malondialdehyde: Application for the Derivatization of Tryptophan Residues in Peptides. Bioconjugate Chemistry 2007, 18 (5), 1678–1683. [PubMed: 17705413]

355. Sturm M; Leitner A; Lindner W, Development of an Indole-Based Chemically Cleavable Linker Concept for Immobilizing Bait Compounds for Protein Pull-Down Experiments. Bioconjugate Chemistry 2011, 22 (2), 211–217. [PubMed: 21247093]

356. Koshland DE; Karkhanis YD; Latham HG, An Environmentally-Sensitive Reagent with Selectivity for the Tryptophan Residue in Proteins. Journal of the American Chemical Society 1964, 86 (7), 1448–1450.

357. Horton HR; Koshland DE, A Highly Reactive Colored Reagent with Selectivity for the Tryptophan Residue in Proteins. 2-Hydroxy-5-nitrobenzyl Bromide1. Journal of the American Chemical Society 1965, 87 (5), 1126–1132. [PubMed: 14284628]

358. Loudon GM; Koshland DE, The Chemistry of a Reporter Group: 2-Hydroxy-5-nitrobenzyl Bromide. Journal of Biological Chemistry 1970, 245 (9), 2247–2254. [PubMed: 5442270]

359. Horton HR; Tucker WP, Dimethyl(2-hydroxy-5-nitrobenzyl)sulfonium Salts: WATER-SOLUBLE ENVIRONMENTALLY SENSITIVE PROTEIN REAGENTS. Journal of Biological Chemistry 1970, 245 (13), 3397–3401. [PubMed: 5459643]

360. Horton HR; Kelly H; Koshland DE, Environmentally Sensitive Protein Reagents: 2-METHOXY-5-NITROBENZYL BROMIDE. Journal of Biological Chemistry 1965, 240 (2), 722–724. [PubMed: 14275127]

361. Robert Horton H; Young G, 2-Acetoxy-5-nitrobenzyl chloride: A reagent designed to introduce a reporter group near the active site of chymotrypsin. Biochimica et Biophysica Acta (BBA) - Protein Structure 1969, 194 (1), 272–278.

362. Strohalm M; Kodíček M; Pechar M, Tryptophan modification by 2-hydroxy-5-nitrobenzyl bromide studied by MALDI-TOF mass spectrometry. Biochemical and Biophysical Research Communications 2003, 312 (3), 811–816. [PubMed: 14680838]

363. Strohalm M; Šantrůček J; Hynek R; Kodíček M, Analysis of tryptophan surface accessibility in proteins by MALDI-TOF mass spectrometry. Biochemical and Biophysical Research Communications 2004, 323 (4), 1134–1138. [PubMed: 15451414]

364. Peyser YM; Muhlrad A; Werber MM, Tryptophan-130 is the most reactive tryptophan residue in rabbit skeletal myosin subfragment-1. FEBS Letters 1990, 259 (2), 346–348. [PubMed: 2294025]

365. Xu Y; Strickland EC; Fitzgerald MC, Thermodynamic Analysis of Protein Folding and Stability Using a Tryptophan Modification Protocol. Analytical Chemistry 2014, 86 (14), 7041–7048. [PubMed: 24896224]

366. Patchornik A; Lawson WB; Witkop B, SELECTIVE CLEAVAGE OF PEPTIDE BONDS. II. THE TRYPTOPHYL PEPTIDE BOND AND THE CLEAVAGE OF GLUCAGON1. Journal of the American Chemical Society 1958, 80 (17), 4747–4748.

367. Spande TF; Witkop B, [58] Determination of the tryptophan content of proteins with N-bromosuccinimide In Methods in Enzymology, Academic Press: 1967; Vol. 11, pp 498–506.

368. Takahashi T; Hiramoto S; Wato S.-i.; Nishimoto T; Wada Y; Nagai K; Yamaguchi H, Identification of Essential Amino Acid Residues of an α-Amylase Inhibitor from Phaseolus vulgaris White Kidney Beans1. The Journal of Biochemistry 1999, 126 (5), 838–844. [PubMed: 10544275]

369. Padrines M; Rabaud M; Bieth JG, Oxidized α1-proteinase-formula> inhibitor: a fast-acting inhibitor of human pancreatic elastase. Biochimica et Biophysica Acta (BBA) - Protein Structure and Molecular Enzymology 1992, 1118 (2), 174–178. [PubMed: 1730036]

370. Lischwe MA; Sung MT, Use of N-chlorosuccinimide/urea for the selective cleavage of tryptophanyl peptide bonds in proteins. Cytochrome c. Journal of Biological Chemistry 1977, 252 (14), 4976–80. [PubMed: 194900]

371. Smith BJ, Chemical Cleavage of Proteins at Tryptophan Residues In The Protein Protocols Handbook, Walker JM, Ed. Humana Press: Totowa, NJ, 1996; pp 375–380.

372. Scoffone E; Fontana A; Rocchi R, Sulfenyl halides as modifying reagents for polypeptides and proteins. I. Modification of tryptophan residues. Biochemistry 1968, 7 (3), 971–979. [PubMed: 4297965]

373. Wilchek M; Miron T, The conversion of tryptophan to 2-thioltryptophan in peptides and proteins. Biochemical and Biophysical Research Communications 1972, 47 (5), 1015–1020. [PubMed: 5029854]

374. ZHANG J-G; REID GE; MORITZ RL; WARD LD; SIMPSON RJ, Specific covalent modification of the tryptophan residues in murine interleukin-6. European Journal of Biochemistry 1993, 217 (1), 53–59. [PubMed: 8223586]

375. Zhang Z; Ostanin K; Van Etten RL, Covalent modification and site-directed mutagenesis of an active site tryptophan of human prostatic acid phosphatase. ACTA BIOCHIMICA POLONICA-ENGLISH EDITION- 1997, 44, 659–672.

376. Spande TF; Green NM; Witkop B, The Reactivity toward N-Bromosuccinimide of Tryptophan in Enzymes, Zymogens, and Inhibited Enzymes*. Biochemistry 1966, 5 (6), 1926–1933. [PubMed: 5963434]

377. INOKUCHI N; TAKAHASHI T; YOSHIMOTO A; IRIE M, N-Bromosuccinimide Oxidation of a Glucoamylase from Aspergillus saitoi. The Journal of Biochemistry 1982, 91 (5), 1661–1668. [PubMed: 6807973]

378. Ohnishi M; Kawagishi T; Hiromi K, Stopped-flow chemical modification with N-bromosuccinimide: A good probe for changes in the microenvironment of the Trp 62 residue of chicken egg white lysozyme. Archives of Biochemistry and Biophysics 1989, 272 (1), 46–51. [PubMed: 2735767]

379. Jiang Y; Ma D, Regioselective acylation at the 5- or 6-position of l-tryptophan derivatives. Tetrahedron Letters 2002, 43 (39), 7013–7015.

380. Hawkins Clare L.; Pattison David I.; Stanley Naomi R.; Davies Michael J., Tryptophan residues are targets in hypothiocyanous acid-mediated protein oxidation. Biochemical Journal 2008, 416 (3), 441–452. [PubMed: 18652572]

381. Edwards RA; Jickling G; Turner RJ, The Light-induced Reactions of Tryptophan with Halocompounds¶. Photochemistry and Photobiology 2002, 75 (4), 362–368. [PubMed: 12003125]

382. Rall SC; Cole RD, Amino Acid Sequence and Sequence Variability of the Amino-terminal Regions of Lysine-rich Histones. Journal of Biological Chemistry 1971, 246 (23), 7175–7190. [PubMed: 5167020]

383. Bogan AA; Thorn KS, Anatomy of hot spots in protein interfaces. Journal of Molecular Biology 1998, 280 (1), 1–9. [PubMed: 9653027]

384. Abello N; Kerstjens HAM; Postma DS; Bischoff R, Protein Tyrosine Nitration: Selectivity, Physicochemical and Biological Consequences, Denitration, and Proteomics Methods for the Identification of Tyrosine-Nitrated Proteins. Journal of Proteome Research 2009, 8 (7), 3222–3238. [PubMed: 19415921]

385. Castro L; Demicheli V; Tórtora V; Radi R, Mitochondrial protein tyrosine nitration. Free Radical Research 2011, 45 (1), 37–52. [PubMed: 20942571]

386. Aslan M; Dogan S, Proteomic detection of nitroproteins as potential biomarkers for cardiovascular disease. Journal of Proteomics 2011, 74 (11), 2274–2288. [PubMed: 21640858]

387. Radi R, Protein Tyrosine Nitration: Biochemical Mechanisms and Structural Basis of Functional Effects. Accounts of Chemical Research 2013, 46 (2), 550–559. [PubMed: 23157446]

388. Monigatti F; Hekking B; Steen H, Protein sulfation analysis—A primer. Biochimica et Biophysica Acta (BBA) - Proteins and Proteomics 2006, 1764 (12), 1904–1913. [PubMed: 16952486]

389. Stone MJ; Chuang S; Hou X; Shoham M; Zhu JZ, Tyrosine sulfation: an increasingly recognised post-translational modification of secreted proteins. New Biotechnology 2009, 25 (5), 299–317. [PubMed: 19658209]

390. Machida K; Mayer BJ; Nollau P, Profiling the Global Tyrosine Phosphorylation State. Molecular & Cellular Proteomics 2003, 2 (4), 215–233. [PubMed: 12754303]

391. Leitner A; Sturm M; Lindner W, Tools for analyzing the phosphoproteome and other phosphorylated biomolecules: A review. Analytica Chimica Acta 2011, 703 (1), 19–30. [PubMed: 21843671]

392. Dushek O; Goyette J; van der Merwe PA, Non-catalytic tyrosine-phosphorylated receptors. Immunological Reviews 2012, 250 (1), 258–276. [PubMed: 23046135]

393. Hunter T, Why nature chose phosphate to modify proteins. Philosophical Transactions of the Royal Society B: Biological Sciences 2012, 367 (1602), 2513–2516.

394. Johnson TB; Kohmann EF, STUDIES ON NITRATED PROTEINS: I. THE DETERMINATION OF THE STRUCTURE OF NITROTYROSINE. Journal of the American Chemical Society 1915, 37 (8), 1863–1884.

395. Wormall A, THE IMMUNOLOGICAL SPECIFICITY OF CHEMICALLY ALTERED PROTEINS. HALOGENATED AND NITRATED PROTEINS 1930, 51 (2), 295–317.

396. Riordan JF; Sokolovsky M; Vallee BL, Tetranitromethane. A Reagent for the Nitration of Tyrosine and Tyrosyl Residues of Proteins1. Journal of the American Chemical Society 1966, 88 (17), 4104–4105.

397. Sokolovsky M; Harell D; Riordan JF, Reaction of tetranitromethane with sulfhydryl groups in proteins. Biochemistry 1969, 8 (12), 4740–4745. [PubMed: 4904041]

398. Riordan JF; Vallee BL, [44] Nitration with tetranitromethane In Methods in Enzymology, Academic Press: 1972; Vol. 25, pp 515–521. [PubMed: 23014433]

399. Rabani J; Mulac WA; Matheson MS, The Pulse Radiolysis of Aqueous Tetranitromethane.1 I. Rate Constants and the Extinction Coefficient of eaq-. II. Oxygenated Solutions. The Journal of Physical Chemistry 1965, 69 (1), 53–70.

400. Cuatrecasas P; Fuchs S; Anfinsen CB, The Tyrosyl Residues at the Active Site of Staphylococcal Nuclease: MODIFICATIONS BY TETRANITROMETHANE. Journal of Biological Chemistry 1968, 243 (18), 4787–4798. [PubMed: 5687721]

401. Palamalai V; Miyagi M, Mechanism of glyceraldehyde-3-phosphate dehydrogenase inactivation by tyrosine nitration. Protein Science 2010, 19 (2), 255–262. [PubMed: 20014444]

402. Doyle RJ; Bello J; Roholt OA, Probable protein crosslinking with tetranitromethane. Biochimica et Biophysica Acta (BBA) - Protein Structure 1968, 160 (2), 274–276.

403. Boesel RW; Carpenter FH, Crosslinking during the nitration of bovine insulin with tetranitromethane. Biochemical and Biophysical Research Communications 1970, 38 (4), 678–682. [PubMed: 5462700]

404. Kunkel GR; Mehrabian M; Martinson HG, Contact-site cross-linking agents. Molecular and cellular biochemistry 1981, 34 (1), 3–13. [PubMed: 6112663]

405. CUTFIELD SM; DODSON GG; RONCO N; CUTFIELD JF, Preparation and activity of nitrated insulin dimer. International Journal of Peptide and Protein Research 1986, 27 (4), 335–343. [PubMed: 3519486]

406. Ploug M; Rahbek-Nielsen H; Ellis V; Roepstorff P; Dano K, Chemical Modification of the Urokinase-Type Plasminogen Activator and Its Receptor Using Tetranitromethane. Evidence for the Involvement of Specific Tyrosine Residues in Both Molecules during Receptor-Ligand Interaction. Biochemistry 1995, 34 (39), 12524–12534. [PubMed: 7548000]

407. Šantrůček J; Strohalm M; Kadlčík V; Hynek R; Kodíček M, Tyrosine residues modification studied by MALDI-TOF mass spectrometry. Biochemical and Biophysical Research Communications 2004, 323 (4), 1151–1156. [PubMed: 15451417]

408. Greenacre SAB; Ischiropoulos H, Tyrosine nitration: Localisation, quantification, consequences for protein function and signal transduction. Free Radical Research 2001, 34 (6), 541–581. [PubMed: 11697033]

409. Ischiropoulos H, Biological selectivity and functional aspects of protein tyrosine nitration. Biochemical and Biophysical Research Communications 2003, 305 (3), 776–783. [PubMed: 12763060]

410. Lennon CW; Cox HD; Hennelly SP; Chelmo SJ; McGuirl MA, Probing Structural Differences in Prion Protein Isoforms by Tyrosine Nitration. Biochemistry 2007, 46 (16), 4850–4860. [PubMed: 17397138]

411. Matters D; Cooper HJ; McDonnell L; Iniesta J; Heptinstall J; Derrick P; Walton D; Peterson I, Mass spectrometry in demonstrating the site-specific nitration of hen egg white lysozyme by an improved electrochemical method. Analytical Biochemistry 2006, 356 (2), 171–181. [PubMed: 16899211]

412. Qiao L; Lu Y; Liu B; Girault HH, Copper-Catalyzed Tyrosine Nitration. Journal of the American Chemical Society 2011, 133 (49), 19823–19831. [PubMed: 22046951]

413. Chapman EM; Skanse BN; Evans RD, Treatment of Hyperthyroidism with Radioactive Iodine. Radiology 1948, 51 (4), 558–563. [PubMed: 18893289]

414. Banks WA; Niehoff ML; Ponzio NM; Erickson MA; Zalcman SS, Pharmacokinetics and modeling of immune cell trafficking: quantifying differential influences of target tissues versus lymphocytes in SJL and lipopolysaccharide-treated mice. Journal of Neuroinflammation 2012, 9 (1), 231. [PubMed: 23034075]

415. Hunter WM; Greenwood FC, Preparation of Iodine-131 Labelled Human Growth Hormone of High Specific Activity. Nature 1962, 194 (4827), 495–496. [PubMed: 14450081]

416. GREENWOOD F; HUNTER W; GLOVER J, THE PREPARATION OF 131I-LABELLED HUMAN GROWTH HORMONE OF HIGH SPECIFIC RADIOACTIVITY. Biochemical Journal 1963, 89 (1), 114–123. [PubMed: 14097352]
417. McConahey PJ; Dixon FJ, [11] Radioiodination of proteins by the use of the chloramine-T method In Methods in Enzymology, Academic Press: 1980; Vol. 70, pp 210–213. [PubMed: 7421589]
418. McFarlane AS, Efficient Trace-labelling of Proteins with Iodine. Nature 1958, 182 (4627), 53–53.
419. Angeles Contreras M; Bale WF; Spar IL, [22] Iodine monochloride (ICI) iodination techniques In Methods in Enzymology, Academic Press: 1983; Vol. 92, pp 277–292. [PubMed: 6855615]
420. Salacinski PRP; McLean C; Sykes JEC; Clement-Jones VV; Lowry PJ, Iodination of proteins, glycoproteins, and peptides using a solid-phase oxidizing agent, 1,3,4,6-tetrachloro-3α,6α-diphenyl glycoluril (Iodogen). Analytical Biochemistry 1981, 117 (1), 136–146. [PubMed: 7316186]
421. Marchalonis JJ, An enzymic method for the trace iodination of immunoglobulins and other proteins. Biochemical Journal 1969, 113 (2), 299–305. [PubMed: 4185494]
422. Liou Y-C; Davies PL; Jia Z, Crystallization and preliminary X-ray analysis of insect antifreeze protein from the beetle Tenebrio molitor. Acta Crystallographica Section D: Biological Crystallography 2000, 56 (3), 354–356. [PubMed: 10713525]
423. Koshland ME; Englberger FM; Erwin MJ; Gaddone SM, Modification of Amino Acid Residues in Anti-p-azobenzenearsonic Acid Antibody during Extensive Iodination. Journal of Biological Chemistry 1963, 238 (4), 1343–1348. [PubMed: 14034956]
424. Hobba GD; Forbes BE; Parkinson EJ; Francis GL; Wallace JC, The Insulin-like Growth Factor (IGF) Binding Site of Bovine Insulin-like Growth Factor Binding Protein-2 (bIGFBP-2) Probed by Iodination. Journal of Biological Chemistry 1996, 271 (48), 30529–30536. [PubMed: 8940022]
425. Simpson RT; Riordan JF; Vallee BL, Functional Tyrosyl Residues in the Active Center of Bovine Pancreatic Carboxypeptidase A*. Biochemistry 1963, 2 (3), 616–622. [PubMed: 14069557]
426. Riordan JF; Wacker WEC; Vallee BL, N-Acetylimidazole: A Reagent for Determination of “Free” Tyrosyl Residues of Proteins*. Biochemistry 1965, 4 (9), 1758–1765.
427. Houston LL; Walsh K, Transient inactivation of trypsin by mild acetylation with N-acetylimidazole. Biochemistry 1970, 9 (1), 156–166. [PubMed: 5460783]
428. Riordan JF; Vallee BL, [42] O-Acetyltyrosine In Methods in Enzymology, Academic Press: 1972; Vol. 25, pp 500–506. [PubMed: 23014431]
429. Koltun WL; Dexter RN; Clark RE; Gurd FRN, Coördination Complexes and Catalytic Properties of Proteins and Related Substances. I. Effect of Cupric and Zinc Ions on the Hydrolysis of p-Nitrophenyl Acetate by Imidazole1. Journal of the American Chemical Society 1958, 80 (16), 4188–4194.
430. Fife TH; Natarajan R; Werner MH, Effect of the leaving group in the hydrolysis of N-acylimidazoles. The hydroxide ion, water, and general-base catalyzed hydrolysis of N-acyl-4(5)-nitroimidazoles. The Journal of Organic Chemistry 1987, 52 (5), 740–746.
431. Zappacosta F; Ingallinella P; Scaloni A; Pessi A; Bianchi E; Sollazzo M; Tramontano A; Marino G; Pucci P, Surface topology of Minibody by selective chemical modifications and mass spectrometry. Protein Science 1997, 6 (9), 1901–1909. [PubMed: 9300490]
432. Irie M; Miyasaka T; Arakawa K, 3-Acetoxy-1-acetyl-5-methylpyrazole, a Novel Acetylating Reagent of Protein. The Journal of Biochemistry 1972, 72 (1), 65–72. [PubMed: 5069750]
433. Adackaparayil M; Smith JH, Preparation and reactivity of a new spin label reagent. The Journal of Organic Chemistry 1977, 42 (9), 1655–1656.
434. Fraenkel-Conrat H; Colloms M, Reactivity of tobacco mosaic virus and its protein toward acetic anhydride. Biochemistry 1967, 6 (9), 2740–2745. [PubMed: 6069710]
435. Kurihara K; Horinishi H; Shibata K, Reactions of cyanuric halides with proteins I. Bound tyrosine residues of insulin and lysozyme as identified with cyanuric fluoride. Biochimica et Biophysica Acta 1963, 74, 678–687. [PubMed: 14078931]
436. Gorbunoff MJ, [43] Cyanuration In Methods in Enzymology, Academic Press: 1972; Vol. 25, pp 506–514. [PubMed: 23014432]

437. Riordan JF; Vallee BL, [45] Diazonium salts as specific reagents and probes of protein conformation In Methods in Enzymology, Academic Press: 1972; Vol. 25, pp 521–531. [PubMed: 23014434]

438. Jones MW; Mantovani G; Blindauer CA; Ryan SM; Wang X; Brayden DJ; Haddleton DM, Direct Peptide Bioconjugation/PEGylation at Tyrosine with Linear and Branched Polymeric Diazonium Salts. Journal of the American Chemical Society 2012, 134 (17), 7406–7413. [PubMed: 22494012]

439. Qu N; Li F; Shao B; Shao J; Zhai G; Wang F; Zhu B-Z, The Unexpected and Exceptionally Facile Chemical Modification of the Phenolic Hydroxyl Group of Tyrosine by Polyhalogenated Quinones under Physiological Conditions. Chemical Research in Toxicology 2016, 29 (10), 1699–1705. [PubMed: 27611113]

440. Liao TH; Ting RS; Yeung JE, Reactivity of tyrosine in bovine pancreatic deoxyribonuclease with p-nitrobenzenesulfonyl fluoride. Journal of Biological Chemistry 1982, 257 (10), 5637–5644. [PubMed: 7068611]

441. Gitlin G; Bayer EA; Wilchek M, Studies on the biotin-binding sites of avidin and streptavidin. Tyrosine residues are involved in the binding site. Biochemical Journal 1990, 269 (2), 527–530. [PubMed: 2386489]

442. Murachi T; Inagami T; Yasui M, Evidence for Alkylphosphorylation of Tyrosyl Residues of Stem Bromelain by Diisopropylphosphorofluoridate*. Biochemistry 1965, 4 (12), 2815–2825. [PubMed: 5880690]

443. Means GE; Wu H-L, The reactive tyrosine residue of human serum albumin: Characterization of its reaction with diisopropylfluorophosphate. Archives of Biochemistry and Biophysics 1979, 194 (2), 526–530. [PubMed: 443818]

444. Awad-Elkarim A; Means GE, The reactivity of p-nitrophenyl acetate with serum albumins. Comparative biochemistry and physiology. B, Comparative biochemistry 1988, 91 (2), 267–272. [PubMed: 3197397]

445. Sato S; Nakamura K; Nakamura H, Tyrosine-Specific Chemical Modification with in Situ Hemin-Activated Luminol Derivatives. ACS Chemical Biology 2015, 10 (11), 2633–2640. [PubMed: 26356088]

446. Fraenkel-Conrat H; Olcott HS, ESTERIFICATION OF PROTEINS WITH ALCOHOLS OF LOW MOLECULAR WEIGHT. Journal of Biological Chemistry 1945, 161 (1), 259–268. [PubMed: 21005732]

447. Erlanger BF; Vratsanos SM; Wassermann N; Cooper AG, A chemical investigation of the active center of pepsin. Biochemical and Biophysical Research Communications 1966, 23 (3), 243–245. [PubMed: 5335664]

448. Gross E; Morell JL, Evidence for an Active Carboxyl Group in Pepsin. Journal of Biological Chemistry 1966, 241 (15), 3638–3639. [PubMed: 5331581]

449. Kemp DS; Chien SW, A New Peptide Coupling Reagent. Journal of the American Chemical Society 1967, 89 (11), 2743–2745. [PubMed: 6043804]

450. Chibnall AC; Mangan JL; Rees MW, Studies on the amide and C-terminal residues in proteins. 3. The esterification of proteins. Biochemical Journal 1958, 68 (1), 114–118. [PubMed: 13522585]

451. Doscher MS; Wilcox PE, Chemical Derivatives of α-Chymotrypsinogen: IV. A COMPARISON OF THE REACTIONS OF α-CHYMOTRYPSINOGEN AND OF SIMPLE CARBOXYLIC ACIDS WITH DIAZOACETAMIDE. Journal of Biological Chemistry 1961, 236 (5), 1328–1337. [PubMed: 13723984]

452. Delpierre GR; Fruton JS, Inactivation of pepsin by diphenyldiazomethane. Proceedings of the National Academy of Sciences 1965, 54 (4), 1161–1167.

453. Rajagopalan TG; Stein WH; Moore S, The Inactivation of Pepsin by Diazoacetylnorleucine Methyl Ester. Journal of Biological Chemistry 1966, 241 (18), 4295–4297. [PubMed: 5332481]

454. Mix KA; Raines RT, Optimized Diazo Scaffold for Protein Esterification. Organic Letters 2015, 17 (10), 2358–2361. [PubMed: 25938936]

455. Woodward RB; Olofson RA; Mayer H, A NEW SYNTHESIS OF PEPTIDES. Journal of the American Chemical Society 1961, 83 (4), 1010–1012.

456. Bodlaender P; Feinstein G; Shaw E, Use of isoxazolium salts for carboxyl group modification in proteins. Trypsin. Biochemistry 1969, 8 (12), 4941–4949. [PubMed: 5365787]

457. Feinstein G; Bodlaender P; Shaw E, Modification of essential carboxylic acid side chains of trypsin. Biochemistry 1969, 8 (12), 4949–4955. [PubMed: 5365788]

458. Komissarov AA; Romanova DV; Debabov VG, Complete Inactivation of Escherichia coli Uridine Phosphorylase by Modification of Asp5 with Woodward's Reagent K. Journal of Biological Chemistry 1995, 270 (17), 10050–10055. [PubMed: 7730307]

459. Martín-Gago P; Fansa EK; Winzker M; Murarka S; Janning P; Schultz-Fademrecht C; Baumann M; Wittinghofer A; Waldmann H, Covalent Protein Labeling at Glutamic Acids. Cell Chemical Biology 2017, 24 (5), 589–597.e5. [PubMed: 28434875]

460. Sheehan JC; Hlavka JJ, The Use of Water-Soluble and Basic Carbodiimides in Peptide Synthesis. The Journal of Organic Chemistry 1956, 21 (4), 439–441.

461. Franzblau C; Gallop PM; Seifter S, The presence in collagen of γ-glutamyl peptide linkages. Biopolymers 1963, 1 (1), 79–97.

462. Goodfriend TL; Levine L; Fasman GD, Antibodies to Bradykinin and Angiotensin: A Use of Carbodiimides in Immunology. Science 1964, 144 (3624), 1344–1346. [PubMed: 14171526]

463. Riehm JP; Scheraga HA, Structural Studies of Ribonuclease. XXI. The Reaction between Ribonuclease and a Water-Soluble Carbodiimide*. Biochemistry 1966, 5 (1), 99–115. [PubMed: 5938958]

464. Hoare DG; Koshland DE, A Procedure for the Selective Modification of Carboxyl Groups in Proteins. Journal of the American Chemical Society 1966, 88 (9), 2057–2058.

465. Hoare DG; Koshland DE, A Method for the Quantitative Modification and Estimation of Carboxylic Acid Groups in Proteins. Journal of Biological Chemistry 1967, 242 (10), 2447–2453. [PubMed: 6026234]

466. Carraway KL; Koshland DE, [56] Carbodiimide modification of proteins In Methods in Enzymology, Academic Press: 1972; Vol. 25, pp 616–623. [PubMed: 23014445]

467. Akashi S; Niitsu U; Yuji R; Ide H; Hirayama K, Investigation of the interaction between enzyme and inhibitor by the combination of chemical modification, electrospray ionization mass spectrometry and frit-fast atom bombardment liquid chromatography/mass spectrometry. Biological Mass Spectrometry 1993, 22 (2), 124–132. [PubMed: 8448221]

468. Sanderson RJ; Mosbaugh DW, Identification of Specific Carboxyl Groups on Uracil-DNA Glycosylase Inhibitor Protein That Are Required for Activity. Journal of Biological Chemistry 1996, 271 (46), 29170–29181. [PubMed: 8910574]

469. Wen J; Zhang H; Gross ML; Blankenship RE, Membrane orientation of the FMO antenna protein from Chlorobaculum tepidum as determined by mass spectrometry-based footprinting. Proceedings of the National Academy of Sciences 2009, 106 (15), 6134–6139.

470. Zhang H; Liu H; Blankenship RE; Gross ML, Isotope-Encoded Carboxyl Group Footprinting for Mass Spectrometry-Based Protein Conformational Studies. Journal of The American Society for Mass Spectrometry 2016, 27 (1), 178–181. [PubMed: 26384685]

471. Guo C; Cheng M; Gross ML, Protein-Metal-Ion Interactions Studied by Mass Spectrometry-Based Footprinting with Isotope-Encoded Benzhydrazide. Analytical Chemistry 2019, 91 (2), 1416–1423. [PubMed: 30495934]

472. Prell JS; O'Brien JT; Steill JD; Oomens J; Williams ER, Structures of Protonated Dipeptides: The Role of Arginine in Stabilizing Salt Bridges. Journal of the American Chemical Society 2009, 131 (32), 11442–11449. [PubMed: 19624125]

473. Donald JE; Kulp DW; DeGrado WF, Salt bridges: Geometrically specific, designable interactions. Proteins: Structure, Function, and Bioinformatics 2011, 79 (3), 898–915.

474. Migliori V; Phalke S; Bezzi M; Guccione E, Arginine/lysine–methyl/methyl switches: biochemical role of histone arginine methylation in transcriptional regulation. Epigenomics 2010, 2 (1), 119–137. [PubMed: 22122749]

475. Boisvert F-M; Chénard CA; Richard S, Protein Interfaces in Signaling Regulated by Arginine Methylation. Science's STKE 2005, 2005 (271), re2–re2.

476. Fitch CA; Platzer G; Okon M; Garcia-Moreno E, B.; McIntosh LP, Arginine: Its pKa value revisited. Protein Science 2015, 24 (5), 752–761. [PubMed: 25808204]

477. Takahashi K, The Reaction of Phenylglyoxal with Arginine Residues in Proteins. Journal of Biological Chemistry 1968, 243 (23), 6171–6179. [PubMed: 5723461]

478. Riordan JF, Arginyl residues and anion binding sites in proteins. Molecular and Cellular Biochemistry 1979, 26 (2), 71–92. [PubMed: 388184]

479. Cheung S-T; Fonda ML, Reaction of phenylglyoxal with arginine. The effect of buffers and pH. Biochemical and Biophysical Research Communications 1979, 90 (3), 940–947. [PubMed: 41527]

480. Eun HM; Miles EW, Reaction of phenylglyoxal and {p-hydroxyphenyl} glyoxal with arginines and cysteines in the. alpha. subunit of tryptophan synthase. Biochemistry 1984, 23 (26), 6484–6491. [PubMed: 6397226]

481. Borders CL; Pearson LJ; McLaughlin AE; Gustafson ME; Vasiloff J; An FY; Morgan DJ, 4-hydroxy-3-nitrophenylglyoxal. A chromophoric reagent for arginyl residues in proteins. Biochimica et Biophysica Acta (BBA) - Enzymology 1979, 568 (2), 491–495.

482. Yamasaki RB; Shimer DA; Feeney RE, Colorimetric determination of arginine residues in proteins by p-nitrophenylglyoxal. Analytical Biochemistry 1981, 111 (2), 220–226. [PubMed: 7247020]

483. Politz SM; Noller HF; McWhirter PD, Ribonucleic acid-protein cross-linking in Escherichia coli ribosomes:(4-azidophenyl) glyoxal, a novel heterobifunctional reagent. Biochemistry 1981, 20 (2), 372–378. [PubMed: 7008843]

484. Krell T; Pitt AR; Coggins JR, The use of electrospray mass spectrometry to identify an essential arginine residue in type II dehydroquinases. FEBS Letters 1995, 360 (1), 93–96. [PubMed: 7875309]

485. Wood TD; Guan Z; Borders CL; Chen LH; Kenyon GL; McLafferty FW, Creatine kinase: Essential arginine residues at the nucleotide binding site identified by chemical modification and high-resolution tandem mass spectrometry. Proceedings of the National Academy of Sciences 1998, 95 (7), 3362–3365.

486. Yankeelov JA; Mitchell CD; Crawford TH, Simple trimerization of 2,3-butanedione yielding a selective reagent for the modification of arginine in proteins. Journal of the American Chemical Society 1968, 90 (6), 1664–1666. [PubMed: 5636807]

487. Riordan JF, Functional arginyl residues in carboxypeptidase A. Modification with butanedione. Biochemistry 1973, 12 (20), 3915–3923. [PubMed: 4355543]

488. Leitner A; Lindner W, Probing of arginine residues in peptides and proteins using selective tagging and electrospray ionization mass spectrometry. Journal of mass spectrometry 2003, 38 (8), 891–899. [PubMed: 12938110]

489. Leitner A; Lindner W, Effects of an arginine-selective tagging procedure on the fragmentation behavior of peptides studied by electrospray ionization tandem mass spectrometry (ESI-MS/MS). Analytica Chimica Acta 2005, 528 (2), 165–173.

490. Leitner A; Lindner W, Functional Probing of Arginine Residues in Proteins Using Mass Spectrometry and an Arginine-Specific Covalent Tagging Concept. Analytical Chemistry 2005, 77 (14), 4481–4488. [PubMed: 16013863]

491. Leitner A; Amon S; Rizzi A; Lindner W, Use of the arginine-specific butanedione/phenylboronic acid tag for analysis of peptides and protein digests using matrix-assisted laser desorption/ionization mass spectrometry. Rapid Communications in Mass Spectrometry 2007, 21 (7), 1321–1330. [PubMed: 17340573]

492. Stensland M; Holm A; Kiehne A; Fleckenstein B, Targeted analysis of protein citrullination using chemical modification and tandem mass spectrometry. Rapid Communications in Mass Spectrometry: An International Journal Devoted to the Rapid Dissemination of Up-to-the-Minute Research in Mass Spectrometry 2009, 23 (17), 2754–2762.

493. De Ceuleneer M; De Wit V; Van Steendam K; Van Nieuwerburgh F; Tilleman K; Deforce D, Modification of citrulline residues with 2, 3-butanedione facilitates their detection by liquid chromatography/mass spectrometry. Rapid Communications in Mass Spectrometry 2011, 25 (11), 1536–1542. [PubMed: 21594927]

494. Toi K; Bynum E; Norris E; Itano HA, Studies on the Chemical Modification of Arginine: I. THE REACTION OF 1,2-CYCLOHEXANEDIONE WITH ARGININE AND ARGINYL

RESIDUES OF PROTEINS. Journal of Biological Chemistry 1967, 242 (5), 1036–1043. [PubMed: 6020430]

495. Patthy L; Smith EL, Reversible modification of arginine residues. Application to sequence studies by restriction of tryptic hydrolysis to lysine residues. Journal of Biological Chemistry 1975, 250 (2), 557–64. [PubMed: 234432]
496. Patthy L; Smith EL, Identification of functional arginine residues in ribonuclease A and lysozyme. Journal of Biological Chemistry 1975, 250 (2), 565–9. [PubMed: 1112778]
497. Suckau D; Mak M; Przybylski M, Protein surface topology-probing by selective chemical modification and mass spectrometric peptide mapping. Proceedings of the National Academy of Sciences 1992, 89 (12), 5630–5634.
498. Litt M, Structural studies on transfer ribonucleic acid. I. Labeling of exposed guanine sites in yeast phenylalanine transfer ribonucleic acid with kethoxal. Biochemistry 1969, 8 (8), 3249–3253. [PubMed: 4897332]
499. Quarrier S; Martin JS; Davis-Neulander L; Beauregard A; Laederach A, Evaluation of the information content of RNA structure mapping data for secondary structure prediction. RNA 2010, 16 (6), 1108–1117. [PubMed: 20413617]
500. Delihas N; Zorn GA; Strobel E, The reaction of Escherichia coli ribosomes with kethoxal. Biochimie 1973, 55 (10), 1227–1234. [PubMed: 4602331]
501. Iijima H; Patrzyc H; Bello J, Modification of amino acids and bovine pancreatic ribonuclease a by kethoxal. Biochimica et Biophysica Acta (BBA) - Protein Structure 1977, 491 (1), 305–316.
502. Akinsiku OT; Yu ET; Fabris D, Mass spectrometric investigation of protein alkylation by the RNA footprinting probe kethoxal. Journal of Mass Spectrometry 2005, 40 (10), 1372–1381. [PubMed: 16237662]
503. Itano HA; Gottlieb AJ, Blocking of tryptic cleavage of arginyl bonds by the chemical modification of the guanido group with benzil. Biochemical and Biophysical Research Communications 1963, 12 (5), 405–408. [PubMed: 14070354]
504. Foettinger A; Leitner A; Lindner W, Derivatisation of arginine residues with malondialdehyde for the analysis of peptides and protein digests by LC-ESI-MS/MS. Journal of mass spectrometry 2006, 41 (5), 623–632. [PubMed: 16541401]
505. Leitner A; Foettinger A; Lindner W, Improving fragmentation of poorly fragmenting peptides and phosphopeptides during collision-induced dissociation by malondialdehyde modification of arginine residues. Journal of Mass Spectrometry 2007, 42 (7), 950–959. [PubMed: 17539043]
506. Onofrejova L; Leitner A; Lindner W, Malondialdehyde tagging improves the analysis of arginine oligomers and arginine-containing dendrimers by HPLC-MS. Journal of Separation Science 2008, 31 (3), 499–506. [PubMed: 18210380]
507. Gao Y; Wang Y, Site-Selective Modifications of Arginine Residues in Human Hemoglobin Induced by Methylglyoxal. Biochemistry 2006, 45 (51), 15654–15660. [PubMed: 17176087]
508. Klöpfer A; Spanneberg R; Glomb MA, Formation of Arginine Modifications in a Model System of Nα-tert-Butoxycarbonyl (Boc)-Arginine with Methylglyoxal. Journal of Agricultural and Food Chemistry 2011, 59 (1), 394–401. [PubMed: 21126021]
509. TAKAHASHI K, Specific Modification of Arginine Residues in Proteins with Ninhydrin1. The Journal of Biochemistry 1976, 80 (5), 1173–1176. [PubMed: 826523]
510. Boppana VK; Rhodes GR, High-performance liquid chromatographic determination of an arginine-containing octapeptide antagonist of vasopressin in human plasma by means of a selective post-column reaction with fluorescence detection. Journal of Chromatography A 1990, 507, 79–84.
511. Schneider F, Histidine in Enzyme Active Centers. Angewandte Chemie International Edition in English 1978, 17 (8), 583–592.
512. Hoffman KW; Romei MG; Londergan CH, A New Raman Spectroscopic Probe of Both the Protonation State and Noncovalent Interactions of Histidine Residues. The Journal of Physical Chemistry A 2013, 117 (29), 5987–5996. [PubMed: 23451758]
513. Gromiha MM; Selvaraj S, Inter-residue interactions in protein folding and stability. Progress in Biophysics and Molecular Biology 2004, 86 (2), 235–277. [PubMed: 15288760]

514. Krupenko SA; Vlasov AP; Wagner C, On the Role of Conserved Histidine 106 in 10-Formyltetrahydrofolate Dehydrogenase Catalysis: CONNECTION BETWEEN HYDROLASE AND DEHYDROGENASE MECHANISMS. Journal of Biological Chemistry 2001, 276 (26), 24030–24037. [PubMed: 11320079]

515. Barnard EA; Stein WD, The histidine residue in the active centre of ribonuclease: I. A specific reaction with bromoacetic acid. Journal of Molecular Biology 1959, 1 (4), 339–349.

516. Nigen AM; Keim P; Marshall RC; Morrow JS; Gurd FRN, Carbon 13 Nuclear Magnetic Resonance Spectroscopy of Myoglobins and Ribonuclease A Carboxymethylated with Enriched [2–13C]Bromoacetate. Journal of Biological Chemistry 1972, 247 (12), 4100–4102. [PubMed: 5033404]

517. Plapp BV, Mechanisms of Carboxymethylation of Bovine Pancreatic Nucleases by Haloacetates and Tosylglycolate. Journal of Biological Chemistry 1973, 248 (14), 4896–4900. [PubMed: 4736883]

518. Wieghardt T; Goren HJ, The reactivity of imidazole nitrogens in histidine to alkylation. Bioorganic Chemistry 1975, 4 (1), 30–40.

519. Lennette EP; Plapp BV, Kinetics of carboxymethylation of histidine hydantoin. Biochemistry 1979, 18 (18), 3933–3938. [PubMed: 39589]

520. Malinowski DP; Fridovich I, Subunit association and side-chain reactivities of bovine erythrocyte superoxide dismutase in denaturing solvents. Biochemistry 1979, 18 (23), 5055–5060. [PubMed: 115491]

521. Postnikova GB; Moiseeva SA; Shekhovtsova EA, The Main Role of Inner Histidines in the Molecular Mechanism of Myoglobin Oxidation Catalyzed by Copper Compounds. Inorganic Chemistry 2010, 49 (4), 1347–1354. [PubMed: 20088488]

522. Lin MC; Stein WH; Moore S, Further Studies on the Alkylation of the Histidine Residues at the Active Site of Pancreatic Ribonuclease. Journal of Biological Chemistry 1968, 243 (23), 6167–6170. [PubMed: 5723460]

523. PINCUS MR; HUMMEL CF; BRANDT-RAUF PW; CARTY RP, Enthalpic and entropic determinants for the specificity of alkylation of the histidine-12 residue of ribonuclease A by four bromoacetamido nucleoside affinity labels and bromoacetamide. International Journal of Peptide and Protein Research 1990, 36 (1), 56–66. [PubMed: 2401600]

524. Anderton BH; Rabin BR, Alkylation Studies on a Reactive Histidine in Pig Heart Malate Dehydrogenase. European Journal of Biochemistry 1970, 15 (3), 568–573. [PubMed: 4318422]

525. Nakagawa Y; Bender ML, Modification of .alpha.-chymotrypsin by methyl p-nitrobenzenesulfonate. Journal of the American Chemical Society 1969, 91 (6), 1566–1567. [PubMed: 5776264]

526. Nakagawa Y; Bender ML, Methylation of histidine-57 in α-chymotrypsin by methyl ρ-nitrobenzenesulfonate. New approach to enzyme modification. Biochemistry 1970, 9 (2), 259–267. [PubMed: 5460940]

527. Volwerk JJ; Pieterson WA; De Haas GH, Phospholipase A2 and its zymogen from porcine pancreas. VI. Histidine at the active site of phospholipase A2. Biochemistry 1974, 13 (7), 1446–1454. [PubMed: 4856505]

528. Roberts MF; Deems RA; Mincey TC; Dennis EA, Chemical modification of the histidine residue in phospholipase A2 (Naja naja naja). A case of half-site reactivity. Journal of Biological Chemistry 1977, 252 (7), 2405–11. [PubMed: 14964]

529. Marchi-Salvador DP; Fernandes CAH; Silveira LB; Soares AM; Fontes MRM, Crystal structure of a phospholipase A2 homolog complexed with p-bromophenacyl bromide reveals important structural changes associated with the inhibition of myotoxic activity. Biochimica et Biophysica Acta (BBA) - Proteins and Proteomics 2009, 1794 (11), 1583–1590. [PubMed: 19616648]

530. Blacklow B; Escoubas P; Nicholson GM, Characterisation of the heterotrimeric presynaptic phospholipase A2 neurotoxin complex from the venom of the common death adder (Acanthophis antarcticus). Biochemical Pharmacology 2010, 80 (2), 277–287. [PubMed: 20361942]

531. Hullán L; Szontágh T; Turtóczky I; Fedorcsák I, The inactivation of trypsin by diethyl pyrocarbonate. Acta chemica Scandinavica 1965, 19 (10), 2440–2441. [PubMed: 5859482]

532. Fedorcsak I; Ehrenberg L, Effects of diethyl pyrocarbonate and methyl methanesulfonate on nucleic acids and nucleases. Acta Chem Scand 1966, 20 (1), 107–112. [PubMed: 5933521]

533. Rosen C-G; Fedorcsák I, Studies on the action of diethyl pyrocarbonate on proteins. Biochimica et Biophysica Acta (BBA)-General Subjects 1966, 130 (2), 401–405. [PubMed: 5972850]

534. Holbrook JJ; Ingram VA, Ionic properties of an essential histidine residue in pig heart lactate dehydrogenase. Biochemical Journal 1973, 131 (4), 729–738. [PubMed: 4352913]

535. Mendoza VL; Vachet RW, Protein Surface Mapping Using Diethylpyrocarbonate with Mass Spectrometric Detection. Analytical Chemistry 2008, 80 (8), 2895–2904. [PubMed: 18338903]

536. Hnízda A; Šantrůček J; Šanda M; Strohalm M; Kodíček M, Reactivity of histidine and lysine side-chains with diethylpyrocarbonate — A method to identify surface exposed residues in proteins. Journal of Biochemical and Biophysical Methods 2008, 70 (6), 1091–1097. [PubMed: 17765977]

537. Muhirad AH, G.; Toth G, Effect of diethylpyr-ocarbonate on proteins. I. Reaction of diethylpyrocarbonate with amino acids. Acta Biochim. Biophys. Acad. Sci. Hung 1967, 2, 19–29.

538. Miles EW, [41] Modification of histidyl residues in proteins by diethylpyrocarbonate In Methods in Enzymology, Academic Press: 1977; Vol. 47, pp 431–442. [PubMed: 22021]

539. Melchior WB; Fahrney D, Ethoxyformylation of proteins. Reaction of ethoxyformic anhydride with .alpha.-chymotrypsin, pepsin, and pancreatic ribonuclease at pH 4. Biochemistry 1970, 9 (2), 251–258. [PubMed: 4904867]

540. Kalkum M; Przybylski M; Glocker MO, Structure Characterization of Functional Histidine Residues and Carbethoxylated Derivatives in Peptides and Proteins by Mass Spectrometry. Bioconjugate Chemistry 1998, 9 (2), 226–235. [PubMed: 9548538]

541. Limpikirati P; Pan X; Vachet RW, Covalent Labeling with Diethylpyrocarbonate: Sensitive to the Residue Microenvironment, Providing Improved Analysis of Protein Higher Order Structure by Mass Spectrometry. Analytical Chemistry 2019, 91 (13), 8516–8523. [PubMed: 31150223]

542. Foti S; Marletta D; Saletti R; Petrone G; Daolio S, Fast-atom bombardment mass spectrometry of peptide derivatives with diethylpyrocarbonate. Rapid Communications in Mass Spectrometry 1991, 5 (7), 336–339.

543. Glocker MO; Kalkum M; Yamamoto R; Schreurs J, Selective Biochemical Modification of Functional Residues in Recombinant Human Macrophage Colony-Stimulating Factor β (rhM-CSF β): Identification by Mass Spectrometry. Biochemistry 1996, 35 (46), 14625–14633. [PubMed: 8931561]

544. Dage JL; Sun H; Halsall HB, Determination of Diethylpyrocarbonate-Modified Amino Acid Residues in α1-Acid Glycoprotein by High-Performance Liquid Chromatography Electrospray Ionization–Mass Spectrometry and Matrix-Assisted Laser Desorption/Ionization Time-of-Flight–Mass Spectrometry. Analytical Biochemistry 1998, 257 (2), 176–185. [PubMed: 9514787]

545. Srikanth R; Mendoza VL; Bridgewater JD; Zhang G; Vachet RW, Copper Binding to β-2-Microglobulin and Its Pre-Amyloid Oligomers. Biochemistry 2009, 48 (41), 9871–9881. [PubMed: 19754160]

546. Mendoza VL; Antwi K; Barón-Rodríguez MA; Blanco C; Vachet RW, Structure of the Preamyloid Dimer of β-2-Microglobulin from Covalent Labeling and Mass Spectrometry. Biochemistry 2010, 49 (7), 1522–1532. [PubMed: 20088607]

547. Zhou Y; Vachet RW, Diethylpyrocarbonate Labeling for the Structural Analysis of Proteins: Label Scrambling in Solution and How to Avoid It. Journal of The American Society for Mass Spectrometry 2012, 23 (5), 899–907. [PubMed: 22351293]

548. Zhou Y; Vachet RW, Increased Protein Structural Resolution from Diethylpyrocarbonate-based Covalent Labeling and Mass Spectrometric Detection. Journal of The American Society for Mass Spectrometry 2012, 23 (4), 708–717. [PubMed: 22298289]

549. Joshi PN; Rai V, Single-site labeling of histidine in proteins, on-demand reversibility, and traceless metal-free protein purification. Chemical Communications 2019, 55 (8), 1100–1103. [PubMed: 30620346]

550. Riordan JF; Vallee BL, [66] Acetylation In Methods in Enzymology, Academic Press: 1967; Vol. 11, pp 565–570.

551. Scholten A; Visser NFC; van den Heuvel RHH; Heck AJR, Analysis of protein-protein interaction surfaces using a combination of efficient lysine acetylation and nanoLC-MALDI-MS/MS applied to the E9:Im9 bacteriotoxin—immunity protein complex. Journal of The American Society for Mass Spectrometry 2006, 17 (7), 983–994. [PubMed: 16713291]

552. Miyazaki K; Tsugita A, C-terminal sequencing method for proteins in polyacrylamide gel by the reaction of acetic anhydride. Proteomics 2006, 6 (7), 2026–2033. [PubMed: 16552787]

553. Fraenkel-Conrat H, [11] Methods for investigating the essential groups for enzyme activity In Methods in Enzymology, Academic Press: 1957; Vol. 4, pp 247–269.

554. Ohguro H; Palczewski K; Walsh KA; Johnson RS, Topographic study of arrestin using differential chemical modifications and hydrogen/deuterium exchange. Protein Science 1994, 3 (12), 2428–2434. [PubMed: 7756996]

555. Bennett KL; Smith SV; Lambrecht RM; Truscott RJW; Sheil MM, Rapid Characterization of Chemically-Modified Proteins by Electrospray Mass Spectrometry. Bioconjugate Chemistry 1996, 7 (1), 16–22. [PubMed: 8741986]

556. Fligge TA; Kast J; Bruns K; Przybylski M, Direct monitoring of protein–chemical reactions utilising nanoelectrospray mass spectrometry. Journal of the American Society for Mass Spectrometry 1999, 10 (2), 112–118. [PubMed: 9926405]

557. Bothner B; Schneemann A; Marshall D; Reddy V; Johnson JE; Siuzdak G, Crystallographically identical virus capsids display different properties in solution. Nature Structural Biology 1999, 6 (2), 114–116. [PubMed: 10048920]

558. Izumi S; Kaneko H; Yamazaki T; Hirata T; Kominami S, Membrane Topology of Guinea Pig Cytochrome P450 17α Revealed by a Combination of Chemical Modifications and Mass Spectrometry. Biochemistry 2003, 42 (49), 14663–14669. [PubMed: 14661979]

559. Smith CM; Gafken PR; Zhang Z; Gottschling DE; Smith JB; Smith DL, Mass spectrometric quantification of acetylation at specific lysines within the amino-terminal tail of histone H4. Analytical Biochemistry 2003, 316 (1), 23–33. [PubMed: 12694723]

560. D'Ambrosio C; Talamo F; Vitale RM; Amodeo P; Tell G; Ferrara L; Scaloni A, Probing the Dimeric Structure of Porcine Aminoacylase 1 by Mass Spectrometric and Modeling Procedures. Biochemistry 2003, 42 (15), 4430–4443. [PubMed: 12693939]

561. Turner BT; Sabo TM; Wilding D; Maurer MC, Mapping of factor XIII solvent accessibility as a function of activation state using chemical modification methods. Biochemistry 2004, 43 (30), 9755–9765. [PubMed: 15274630]

562. Gong B; Ramos A; Vázquez-Fernández E; Silva CJ; Alonso J; Liu Z; Requena JR, Probing structural differences between PrPC and PrPSc by surface nitration and acetylation: evidence of conformational change in the C-terminus. Biochemistry 2011, 50 (22), 4963–4972. [PubMed: 21526750]

563. Steiner RF; Albaugh S; Fenselau C; Murphy C; Vestling M, A mass spectrometry method for mapping the interface topography of interacting proteins, illustrated by the melittin-calmodulin system. Analytical Biochemistry 1991, 196 (1), 120–125. [PubMed: 1888025]

564. Klotz IM, [68] Succinylation In Methods in Enzymology, Academic Press: 1967; Vol. 11, pp 576–580.

565. Meighen EA; Nicoli MZ; Hastings JW, Hybridization of bacterial luciferase with a variant produced by chemical modification. Biochemistry 1971, 10 (22), 4062–4068. [PubMed: 5161030]

566. Nagel GM; Schachman H, Cooperative interactions in hybrids of aspartate transcarbamylase containing succinylated regulatory polypeptide chains. Biochemistry 1975, 14 (14), 3195–3203. [PubMed: 1096938]

567. ROSSI A; MENEZES LC; PUDLES J, Yeast Hexokinase A European Journal of Biochemistry 1975, 59 (2), 423–432. [PubMed: 1253]

568. SCHWENKE KD; ZIRWER D; GAST K; GÖRNITZ E; LINOW K-J; GUEGUEN J, Changes of the oligomeric structure of legumin from pea (Pisum sativum L.) after succinylation. European Journal of Biochemistry 1990, 194 (2), 621–627. [PubMed: 2269287]

569. Klapper MH; Klotz IM, [46] Acylation with dicarboxylic acid anhydrides In Methods in Enzymology, Academic Press: 1972; Vol. 25, pp 531–536. [PubMed: 23014435]

570. Przybylski M; Glocker MO; Nestel U; Schnaible V; Blüggel M; Diederichs K; Weckesser J; Schad M; Schmid A; Welte W; Benz R, X-ray crystallographic and mass spectrometric structure determination and functional characterization of succinylated porin from rhodobacter capsulatus: Implications for ion selectivity and single-channel conductance. Protein Science 1996, 5 (8), 1477–1489. [PubMed: 8844839]

571. Gould AR; Norton RS, Chemical modification of cationic groups in the polypeptide cardiac stimulant anthopleurin-A. Toxicon 1995, 33 (2), 187–199. [PubMed: 7597722]

572. Becker L; McLeod RS; Marcovina SM; Yao Z; Koschinsky ML, Identification of a Critical Lysine Residue in Apolipoprotein B-100 That Mediates Noncovalent Interaction with Apolipoprotein(a). Journal of Biological Chemistry 2001, 276 (39), 36155–36162. [PubMed: 11473115]

573. Ehrhard B; Misselwitz R; Welfle K; Hausdorf G; Glaser RW; Schneider-Mergener J; Welfle H, Chemical Modification of Recombinant HIV-1 Capsid Protein p24 Leads to the Release of a Hidden Epitope Prior to Changes of the Overall Folding of the Protein. Biochemistry 1996, 35 (28), 9097–9105. [PubMed: 8703914]

574. Paetzel M; Strynadka NCJ; Tschantz WR; Casareno R; Bullinger PR; Dalbey RE, Use of Site-directed Chemical Modification to Study an Essential Lysine in Escherichia coli Leader Peptidase. Journal of Biological Chemistry 1997, 272 (15), 9994–10003. [PubMed: 9092541]

575. Neurath AR; Debnath AK; Strick N; Li Y-Y; Lin K; Jiang S, Blocking of CD4 cell receptors for the human immunodeficiency virus type 1 (HIV-1) by chemically modified bovine milk proteins: Potential for AIDS prophylaxis. Journal of Molecular Recognition 1995, 8 (5), 304–316. [PubMed: 8619951]

576. O'Brien AM; Smith AT; Ó'Fágáin C, Effects of phthalic anhydride modification on horseradish peroxidase stability and activity. Biotechnology and Bioengineering 2003, 81 (2), 233–240. [PubMed: 12451559]

577. Lindh CH; Jönsson BAG, Human Hemoglobin Adducts Following Exposure to Hexahydrophthalic Anhydride and Methylhexahydrophthalic Anhydride. Toxicology and Applied Pharmacology 1998, 153 (2), 152–160. [PubMed: 9878586]

578. Kristiansson MH; Jönsson BAG; Lindh CH, Mass Spectrometric Characterization of Human Hemoglobin Adducts Formed in Vitro by Hexahydrophthalic Anhydride. Chemical Research in Toxicology 2002, 15 (4), 562–569. [PubMed: 11952343]

579. Jonsson BAG; Wishnok JS; Skipper PL; Stillwell WG; Tannenbaum SR, Lysine Adducts Between Methyltetrahydrophthalic Anhydride and Collagen in Guinea Pig Lung. Toxicology and Applied Pharmacology 1995, 135 (1), 156–162. [PubMed: 7482535]

580. Swart PJ; Kuipers EM; Smit C; Van Der Strate BWA; Harmsen MC; Meijer DKF, Lactoferrin In Advances in Lactoferrin Research, Spik G; Legrand D; Mazurier J; Pierce A; Perraudin J-P, Eds. Springer US: Boston, MA, 1998; pp 205–213.

581. Alcalde M; Plou FJ; Teresa Martín M; Valdés I; Méndez E; Ballesteros A, Succinylation of cyclodextrin glycosyltransferase from Thermoanaerobacter sp. 501 enhances its transferase activity using starch as donor. Journal of Biotechnology 2001, 86 (1), 71–80. [PubMed: 11223146]

582. SWART PJ, M. E. K., SMIT C, PAUWELS R, DE BÉTHUNE MP, DE CLERCQ E, MEIJER DKF, HUISMAN JG, Antiviral Effects of Milk Proteins: Acylation Results in Polyanionic Compounds with Potent Activity against Human Immunodeficiency Virus Types 1 and 2 in Vitro. AIDS Research and Human Retroviruses 1996, 12 (9), 769–775. [PubMed: 8738428]

583. Pool CT; Thompson TE, Methods for Dual, Site-Specific Derivatization of Bovine Pancreatic Trypsin Inhibitor: Trypsin Protection of Lysine-15 and Attachment of Fatty Acids or Hydrophobic Peptides at the N-Terminus. Bioconjugate Chemistry 1999, 10 (2), 221–230. [PubMed: 10077471]

584. Makoff AJ; Malcolm ADB, Properties of methyl acetimidate and its use as a protein-modifying reagent. Biochemical Journal 1981, 193 (1), 245–249. [PubMed: 7305926]

585. SEKIGUCHI T; OSHIRO S; GOINGO EM; NOSOH Y, Chemical Modification of ε-Amino Groups in Glutamine Synthetase from Bacillus stearothermophilus with Ethyl Acetimidate. The Journal of Biochemistry 1979, 85 (1), 75–78. [PubMed: 33165]

586. Zoltobrocki M; Kim JC; Plapp BV, Activity of liver alcohol dehydrogenase with various substituents on the amino groups. Biochemistry 1974, 13 (5), 899–903. [PubMed: 4360354]

587. Thumm M; Hoenes J; Pfleiderer G, S-methylthioacetimidate is a new reagent for the amidination of proteins at low pH. Biochimica et Biophysica Acta (BBA) - General Subjects 1987, 923 (2), 263–267.

588. Rack M, Effects of chemical modification of amino groups by two different imidoesters on voltage-clamped nerve fibres of the frog. Pflügers Archiv 1985, 404 (2), 126–130. [PubMed: 2409524]

589. Jaffee EG; Lauber MA; Running WE; Reilly JP, In Vitro and In Vivo Chemical Labeling of Ribosomal Proteins: A Quantitative Comparison. Analytical Chemistry 2012, 84 (21), 9355–9361. [PubMed: 23020143]

590. Whiteley NM; Berg HC, Amidination of the outer and inner surfaces of the human erythrocyte membrane. Journal of Molecular Biology 1974, 87 (3), 541–561. [PubMed: 4444035]

591. Janecki DJ; Beardsley RL; Reilly JP, Probing Protein Tertiary Structure with Amidination. Analytical Chemistry 2005, 77 (22), 7274–7281. [PubMed: 16285675]

592. Browne DT; Kent SBH, Formation of non-amidine products in the chemical modification of horse liver alcohol dehydrogenase with imido esters. Biochemical and Biophysical Research Communications 1975, 67 (1), 133–138. [PubMed: 1010]

593. Blumberg S; Vallee BL, Superactivation of thermolysin by acylation with amino acid N-hydroxysuccinimide esters. Biochemistry 1975, 14 (11), 2410–2419. [PubMed: 237533]

594. Staros JV, N-hydroxysulfosuccinimide active esters: bis(N-hydroxysulfosuccinimide) esters of two dicarboxylic acids are hydrophilic, membrane-impermeant, protein cross-linkers. Biochemistry 1982, 21 (17), 3950–3955. [PubMed: 7126526]

595. Staros JV, Membrane-impermeant crosslinking reagents: probes of the structure and dynamics of membrane proteins. Accounts of Chemical Research 1988, 21 (12), 435–441.

596. Kalkhof S; Sinz A, Chances and pitfalls of chemical cross-linking with amine-reactive N-hydroxysuccinimide esters. Analytical and Bioanalytical Chemistry 2008, 392 (1), 305–312. [PubMed: 18724398]

597. Wilchek M; Bayer EA, [2] Introduction to avidin-biotin technology In Methods in Enzymology, Wilchek M; Bayer EA, Eds. Academic Press: 1990; Vol. 184, pp 5–13. [PubMed: 2201884]

598. Bayer EA; Wilchek M, [14] Protein biotinylation In Methods in Enzymology, Wilchek M; Bayer EA, Eds. Academic Press: 1990; Vol. 184, pp 138–160. [PubMed: 2388567]

599. Liu Y; Kvaratskhelia M; Hess S; Qu Y; Zou Y, Modulation of Replication Protein A Function by Its Hyperphosphorylation-induced Conformational Change Involving DNA Binding Domain B. Journal of Biological Chemistry 2005, 280 (38), 32775–32783. [PubMed: 16006651]

600. Knock SL; Miller BT; Blankenship JE; Nagle GT; Smith JS; Kurosky A, N-acylation of Aplysia egg-laying hormone with biotin. Characterization of bioactive and inactive derivatives. Journal of Biological Chemistry 1991, 266 (36), 24413–9. [PubMed: 1761543]

601. Shell SM; Hess S; Kvaratskhelia M; Zou Y, Mass Spectrometric Identification of Lysines Involved in the Interaction of Human Replication Protein A with Single-Stranded DNA. Biochemistry 2005, 44 (3), 971–978. [PubMed: 15654753]

602. Gabant G; Augier J; Armengaud J, Assessment of solvent residues accessibility using three Sulfo-NHS-biotin reagents in parallel: application to footprint changes of a methyltransferase upon binding its substrate. Journal of Mass Spectrometry 2008, 43 (3), 360–370. [PubMed: 17968972]

603. Dreger M; Leung BW; Brownlee GG; Deng T, A quantitative strategy to detect changes in accessibility of protein regions to chemical modification on heterodimerization. Protein Science 2009, 18 (7), 1448–1458. [PubMed: 19517532]

604. Ori A; Free P; Courty J; Wilkinson MC; Fernig DG, Identification of Heparin-binding Sites in Proteins by Selective Labeling. Molecular & Cellular Proteomics 2009, 8 (10), 2256–2265. [PubMed: 19567366]

605. Bolton AE; Hunter WM, The labelling of proteins to high specific radioactivities by conjugation to a 125I-containing acylating agent. Application to the radioimmunoassay. Biochemical Journal 1973, 133 (3), 529–538. [PubMed: 4733239]

606. Harmon CM; Luce P; Beth AH; Abumrad NA, Labeling of adipocyte membranes by sulfo-N-succinimidyl derivatives of long-chain fatty acids: Inhibition of fatty acid transport. The Journal of Membrane Biology 1991, 121 (3), 261–268. [PubMed: 1865490]

607. OKUYAMA T; SATAKE K, On the preparation and properties of 2, 4, 6-trinitrophenyl-amino acids and-peptides. The Journal of Biochemistry 1960, 47 (4), 454–466.

608. Habeeb AFSA, Determination of free amino groups in proteins by trinitrobenzenesulfonic acid. Analytical Biochemistry 1966, 14 (3), 328–336. [PubMed: 4161471]

609. Fields R, [38] The rapid determination of amino groups with TNBS In Methods in Enzymology, Academic Press: 1972; Vol. 25, pp 464–468. [PubMed: 23014427]

610. Yang CC; Chang LS, Studies on the status of lysine residues in phospholipase A2 from Naja naja atra (Taiwan cobra) snake venom. Biochemical Journal 1989, 262 (3), 855–860. [PubMed: 2511834]

611. Komatsu H; Emoto Y; Tawada K, Half-stoichiometric trinitrophenylation of myosin subfragment 1 in the presence of pyrophosphate or adenosine diphosphate. Journal of Biological Chemistry 1993, 268 (11), 7799–7808. [PubMed: 8385121]

612. Chang L.-s.; Lin S.-r.; Chang C.-c., Probing Calcium Ion-Induced Conformational Changes of Taiwan Cobra Phospholipase A2 by Trinitrophenylation of Lysine Residues. Journal of Protein Chemistry 1997, 16 (1), 51–57. [PubMed: 9055207]

613. Gevaert K; Goethals M; Martens L; Van Damme J; Staes A; Thomas GR; Vandekerckhove J, Exploring proteomes and analyzing protein processing by mass spectrometric identification of sorted N-terminal peptides. Nature Biotechnology 2003, 21 (5), 566–569.

614. Kluger R; Tsui W-C, Methyl acetyl phosphate. A small anionic acetylating agent. The Journal of Organic Chemistry 1980, 45 (13), 2723–2724.

615. Ueno H; Pospischil MA; Manning JM, Methyl acetyl phosphate as a covalent probe for anion-binding sites in human and bovine hemoglobins. Journal of Biological Chemistry 1989, 264 (21), 12344–12351. [PubMed: 2745446]

616. Xu ASL; Labotka RJ; London RE, Acetylation of Human Hemoglobin by Methyl Acetylphosphate: EVIDENCE OF BROAD REGIO-SELECTIVITY REVEALED BY NMR STUDIES. Journal of Biological Chemistry 1999, 274 (38), 26629–26632. [PubMed: 10480863]

617. Raibekas AA; Bures EJ; Siska CC; Kohno T; Latypov RF; Kerwin BA, Anion Binding and Controlled Aggregation of Human Interleukin-1 Receptor Antagonist. Biochemistry 2005, 44 (29), 9871–9879. [PubMed: 16026159]

618. Anderson BM; Anderson CD; Churchich JE, Inhibition of glutamic dehydrogenase by pyridoxal 5'-phosphate. Biochemistry 1966, 5 (9), 2893–2900. [PubMed: 5961876]

619. Cole SCJ; Yon RJ, Active-site-directed inactivation of wheat-germ aspartate transcarbamoylase by pyridoxal 5′-phosphate. Biochemical Journal 1987, 248 (2), 403–408. [PubMed: 3435454]

620. Gui-Shan X; Jun-Mei Z, Conformational changes at the active site of bovine pancreatic RNase A at low concentrations of guanidine hydrochloride probed by pyridoxal 5′-phosphate. Biochimica et Biophysica Acta (BBA) - Protein Structure and Molecular Enzymology 1996, 1294 (1), 1–7. [PubMed: 8639708]

621. Ahmed SA; McPhie P; Miles EW, A Thermally Induced Reversible Conformational Transition of the Tryptophan Synthase Subunit Probed by the Spectroscopic Properties of Pyridoxal Phosphate and by Enzymatic Activity. Journal of Biological Chemistry 1996, 271 (15), 8612–8617. [PubMed: 8621491]

622. Sanger F; Tuppy H, The amino-acid sequence in the phenylalanyl chain of insulin. 1. The identification of lower peptides from partial hydrolysates. Biochemical Journal 1951, 49 (4), 463–481. [PubMed: 14886310]

623. Brautigan DL; Ferguson-Miller S; Margoliash E, Definition of cytochrome c binding domains by chemical modification. I. Reaction with 4-chloro-3,5-dinitrobenzoate and chromatographic separation of singly substituted derivatives. Journal of Biological Chemistry 1978, 253 (1), 130–139. [PubMed: 201614]

624. Stark GR, [53] Modification of proteins with cyanate In Methods in Enzymology, Academic Press: 1972; Vol. 25, pp 579–584. [PubMed: 23014442]

625. Means GE; Feeney RE, Reductive Alkylation of Proteins. Analytical Biochemistry 1995, 224 (1), 1–16. [PubMed: 7710054]

626. Rayment I, [12] Reductive alkylation of lysine residues to alter crystallization properties of proteins In Methods in Enzymology, Academic Press: 1997; Vol. 276, pp 171–179.

627. Day JF; Thorpe SR; Baynes JW, Nonenzymatically glucosylated albumin. In vitro preparation and isolation from normal human serum. Journal of Biological Chemistry 1979, 254 (3), 595–597. [PubMed: 762083]

628. Gurd FRN, [34a] Carboxymethylation In Methods in Enzymology, Academic Press: 1972; Vol. 25, pp 424–438. [PubMed: 23014423]

629. Jones WC Jr; Rothgeb TM; Gurd FR, Specific enrichment with carbon-13 of the methionine methyl groups of sperm whale myoglobin. Journal of the American Chemical Society 1975, 97 (13), 3875–3877. [PubMed: 1141593]

630. Degen J; Kyte J, The purification of peptides which contain methionine residues. Analytical Biochemistry 1978, 89 (2), 529–539. [PubMed: 569447]

631. Houghten RA; Glaser CB; Li CH, Human somatotropin: Reaction with hydrogen peroxide. Archives of Biochemistry and Biophysics 1977, 178 (2), 350–355. [PubMed: 556925]

632. Mizzer JP; Thorpe C, An essential methionine in pig kidney general acyl-CoA dehydrogenase. Biochemistry 1980, 19 (24), 5500–5504. [PubMed: 7459327]

633. Gross E, [27] The cyanogen bromide reaction In Methods in Enzymology, Academic Press: 1967; Vol. 11, pp 238–255.

634. Moerman PP; Sergeant K; Debyser G; Devreese B; Samyn B, A new chemical approach to differentiate carboxy terminal peptide fragments in cyanogen bromide digests of proteins. Journal of Proteomics 2010, 73 (8), 1454–1460. [PubMed: 20153848]

635. McLoughlin SM; Mazur MT; Miller LM; Yin J; Liu F; Walsh CT; Kelleher NL, Chemoenzymatic Approaches for Streamlined Detection of Active Site Modifications on Thiotemplate Assembly Lines Using Mass Spectrometry. Biochemistry 2005, 44 (43), 14159–14169. [PubMed: 16245932]

636. Reid GE; Roberts KD; Simpson RJ; O'Hair RAJ, Selective Identification and Quantitative Analysis of Methionine Containing Peptides by Charge Derivatization and Tandem Mass Spectrometry. Journal of the American Society for Mass Spectrometry 2005, 16 (7), 1131–1150. [PubMed: 15923125]

637. Savige WE; Fontana A, [43] Interconversion of methionine and methionine sulfoxide In Methods in Enzymology, Academic Press: 1977; Vol. 47, pp 453–459. [PubMed: 927198]

638. Levine RL; Mosoni L; Berlett BS; Stadtman ER, Methionine residues as endogenous antioxidants in proteins. Proceedings of the National Academy of Sciences 1996, 93 (26), 15036–15040.

639. West GM; Tang L; Fitzgerald MC, Thermodynamic Analysis of Protein Stability and Ligand Binding Using a Chemical Modification- and Mass Spectrometry-Based Strategy. Analytical Chemistry 2008, 80 (11), 4175–4185. [PubMed: 18457414]

640. Steen P. V. d.; Rudd PM; Dwek RA; Opdenakker G, Concepts and Principles of O-Linked Glycosylation. Critical Reviews in Biochemistry and Molecular Biology 1998, 33 (3), 151–208. [PubMed: 9673446]

641. Prescher JA; Bertozzi CR, Chemical Technologies for Probing Glycans. Cell 2006, 126 (5), 851–854. [PubMed: 16959565]

642. North SJ; Hitchen PG; Haslam SM; Dell A, Mass spectrometry in the analysis of N-linked and O-linked glycans. Current Opinion in Structural Biology 2009, 19 (5), 498–506. [PubMed: 19577919]

643. Cohen P, The origins of protein phosphorylation. Nature Cell Biology 2002, 4 (5), E127–E130. [PubMed: 11988757]

644. Lockridge O; Xue W; Gaydess A; Grigoryan H; Ding S-J; Schopfer LM; Hinrichs SH; Masson P, Pseudo-esterase Activity of Human Albumin: SLOW TURNOVER ON TYROSINE 411 AND STABLE ACETYLATION OF 82 RESIDUES INCLUDING 59 LYSINES. Journal of Biological Chemistry 2008, 283 (33), 22582–22590. [PubMed: 18577514]

645. Means GE; Bender ML, Acetylation of human serum albumin by p-nitrophenyl acetate. Biochemistry 1975, 14 (22), 4989–4994. [PubMed: 241394]

646. Jabusch JR; Deutsch HF, Localization of lysines acetylated in ubiquitin reacted with p-nitrophenyl acetate. Archives of Biochemistry and Biophysics 1985, 238 (1), 170–177. [PubMed: 2984995]

647. Chelius D; Shaler TA, Capture of Peptides with N-Terminal Serine and Threonine: A Sequence-Specific Chemical Method for Peptide Mixture Simplification. Bioconjugate Chemistry 2003, 14 (1), 205–211. [PubMed: 12526710]

648. Loo RRO; Loo JA, Matrix-Assisted Laser Desorption/Ionization-Mass Spectrometry of Hydrophobic Proteins in Mixtures Using Formic Acid, Perfluorooctanoic Acid, and Sorbitol. Analytical Chemistry 2007, 79 (3), 1115–1125. [PubMed: 17263344]

649. Robinson NE, Protein deamidation. Proceedings of the National Academy of Sciences 2002, 99 (8), 5283–5288.

650. Won J-I; Meagher RJ; Barron AE, Characterization of Glutamine Deamidation in a Long, Repetitive Protein Polymer via Bioconjugate Capillary Electrophoresis. Biomacromolecules 2004, 5 (2), 618–627. [PubMed: 15003029]

651. Lomant AJ; Fairbanks G, Chemical probes of extended biological structures: synthesis and properties of the cleavable protein cross-linking reagent [35S] dithiobis (succinimidyl propionate). Journal of molecular biology 1976, 104 (1), 243–261. [PubMed: 957432]

652. Cuatrecasas P; Anfinsen CB, [31] Affinity chromatography In Methods in enzymology, Elsevier: 1971; Vol. 22, pp 345–378.

653. Scientific, T., Thermo scientific crosslinking technical handbook. Waltham (USA): Thermo Scientific 2012.

654. Hermanson GT; Giese R, Bioconjugate techniques. Journal of Chromatography-A incl Cumulative Indexes 1996, 746 (2), 303–303.

655. Iacobucci C; Piotrowski C; Aebersold R; Amaral BC; Andrews P; Bernfur K; Borchers C; Brodie NI; Bruce JE; Cao Y, First Community-Wide, Comparative Cross-Linking Mass Spectrometry Study. Analytical chemistry 2019, 91 (11), 6953–6961. [PubMed: 31045356]

656. Bragg P; Hou C, Subunit composition, function, and spatial arrangement in the Ca2+-and Mg2+-activated adenosine triphosphatases of Escherichia coli and Salmonella typhimurium. Archives of biochemistry and biophysics 1975, 167 (1), 311–321. [PubMed: 124154]

657. Merkley ED; Rysavy S; Kahraman A; Hafen RP; Daggett V; Adkins JN, Distance restraints from crosslinking mass spectrometry: mining a molecular dynamics simulation database to evaluate lysine–lysine distances. Protein science 2014, 23 (6), 747–759. [PubMed: 24639379]

658. Yu C; Huang L, Cross-linking mass spectrometry: an emerging technology for interactomics and structural biology. Analytical chemistry 2017, 90 (1), 144–165. [PubMed: 29160693]

659. Kao A; Chiu C.-l.; Vellucci D; Yang Y; Patel VR; Guan S; Randall A; Baldi P; Rychnovsky SD; Huang L, Development of a novel cross-linking strategy for fast and accurate identification of cross-linked peptides of protein complexes. Molecular & Cellular Proteomics 2011, 10 (1), M110. 002212.

660. Petrotchenko EV; Serpa JJ; Borchers CH, An isotopically coded CID-cleavable biotinylated cross-linker for structural proteomics. Molecular & Cellular Proteomics 2011, 10 (2), M110. 001420.

661. Müller MQ; Dreiocker F; Ihling CH; Schäfer M; Sinz A, Cleavable cross-linker for protein structure analysis: reliable identification of cross-linking products by tandem MS. Analytical chemistry 2010, 82 (16), 6958–6968. [PubMed: 20704385]

662. Weisbrod CR; Chavez JD; Eng JK; Yang L; Zheng C; Bruce JE, In vivo protein interaction network identified with a novel real-time cross-linked peptide identification strategy. Journal of proteome research 2013, 12 (4), 1569–1579. [PubMed: 23413883]

663. Hartman FC; Wold F, Bifunctional Reagents. Cross-Linking of Pancreatic Ribonuclease with a Diimido Ester1. Journal of the American Chemical Society 1966, 88 (16), 3890–3891.

664. Hunter M; Ludwig M, The reaction of imidoesters with proteins and related small molecules. Journal of the American Chemical Society 1962, 84 (18), 3491–3504.

665. Browne DT; Kent SB, Formation of non-amidine products in the reaction of primary amines with imido esters. Biochemical and biophysical research communications 1975, 67 (1), 126–132. [PubMed: 1009]

666. Grabarek Z; Gergely J, Zero-length crosslinking procedure with the use of active esters. Analytical Biochemistry 1990, 185 (1), 131–135. [PubMed: 2344038]

667. Sinz A, Chemical cross-linking and mass spectrometry to map three-dimensional protein structures and protein–protein interactions. Mass spectrometry reviews 2006, 25 (4), 663–682. [PubMed: 16477643]

668. Novak P; Kruppa GH, Intra-molecular cross-linking of acidic residues for protein structure studies. European Journal of Mass Spectrometry 2008, 14 (6), 355–365. [PubMed: 19136724]

669. Leitner A; Joachimiak LA; Unverdorben P; Walzthoeni T; Frydman J; Förster F; Aebersold R, Chemical cross-linking/mass spectrometry targeting acidic residues in proteins and protein complexes. Proceedings of the National Academy of Sciences 2014, 111 (26), 9455–9460.

670. Zhang X; Wang J-H; Tan D; Li Q; Li M; Gong Z; Tang C; Liu Z; Dong M-Q; Lei X, Carboxylate-Selective Chemical Cross-Linkers for Mass Spectrometric Analysis of Protein Structures. Analytical Chemistry 2018, 90 (2), 1195–1201. [PubMed: 29251911]

671. Smyth DG; Blumenfeld O; Konigsberg W, Reactions of N-ethylmaleimide with peptides and amino acids. Biochemical Journal 1964, 91 (3), 589. [PubMed: 5840721]

672. Gorin G; Martic P; Doughty G, Kinetics of the reaction of N-ethylmaleimide with cysteine and some congeners. Archives of biochemistry and biophysics 1966, 115 (3), 593–597. [PubMed: 5970483]

673. Brewer CF; Riehm JP, Evidence for possible nonspecific reactions between N-ethylmaleimide and proteins. Analytical Biochemistry 1967, 18 (2), 248–255.

674. Gilchrist TL; Rees CW, Carbenes, nitrenes and arynes. 1969.

675. Brunner J, New photolabeling and crosslinking methods. Annual review of biochemistry 1993, 62 (1), 483–514.

676. Suchanek M; Radzikowska A; Thiele C, Photo-leucine and photo-methionine allow identification of protein-protein interactions in living cells. Nature methods 2005, 2 (4), 261. [PubMed: 15782218]

677. Lewis RV; Roberts MF; Dennis EA; Allison WS, Photoactivated heterobifunctional cross-linking reagents which demonstrate the aggregation state of phospholipase A2. Biochemistry 1977, 16 (25), 5650–5654. [PubMed: 921957]

678. Li X; Li Z; Xie B; Sharp JS, Improved Identification and Relative Quantification of Sites of Peptide and Protein Oxidation for Hydroxyl Radical Footprinting. Journal of The American Society for Mass Spectrometry 2013, 24 (11), 1767–1776. [PubMed: 24014150]

679. Dudev T; Lim C, Competition among Metal Ions for Protein Binding Sites: Determinants of Metal Ion Selectivity in Proteins. Chemical Reviews 2014, 114 (1), 538–556. [PubMed: 24040963]

680. Tainer JA; Roberts VA; Getzoff ED, Protein metal-binding sites. Current Opinion in Biotechnology 1992, 3 (4), 378–387. [PubMed: 1368439]

681. Bowman SEJ; Bridwell-Rabb J; Drennan CL, Metalloprotein Crystallography: More than a Structure. Accounts of Chemical Research 2016, 49 (4), 695–702. [PubMed: 26975689]

682. Bertini G; Gray H; Gray HB; Stiefel E; Valentine JS; Stiefel EI, Biological inorganic chemistry: structure and reactivity. University Science Books: 2007.

683. Gregory DS; Martin ACR; Cheetham JC; Rees AR, The prediction and characterization of metal binding sites in proteins. Protein Engineering, Design and Selection 1993, 6 (1), 29–35.

684. Xu H; Xu DC; Wang Y, Natural Indices for the Chemical Hardness/Softness of Metal Cations and Ligands. ACS Omega 2017, 2 (10), 7185–7193. [PubMed: 31457297]

685. Carlton DD; Schug KA, A review on the interrogation of peptide–metal interactions using electrospray ionization-mass spectrometry. Analytica Chimica Acta 2011, 686 (1), 19–39. [PubMed: 21237305]

686. Sung Y.-h.; Rospigliosi C; Eliezer D, NMR mapping of copper binding sites in alpha-synuclein. Biochimica et Biophysica Acta (BBA) - Proteins and Proteomics 2006, 1764 (1), 5–12. [PubMed: 16338184]

687. Zhang Q; Dai X; Cong Y; Zhang J; Chen D-H; Dougherty MT; Wang J; Ludtke Steven J.; Schmid Michael F.; Chiu W, Cryo-EM Structure of a Molluscan Hemocyanin Suggests Its Allosteric Mechanism. Structure 2013, 21 (4), 604–613. [PubMed: 23541894]

688. Carter KP; Young AM; Palmer AE, Fluorescent Sensors for Measuring Metal Ions in Living Systems. Chemical Reviews 2014, 114 (8), 4564–4601. [PubMed: 24588137]

689. Huang RY; Rempel DL; Gross ML, HD exchange and PLIMSTEX determine the affinities and order of binding of Ca2+ with troponin C. Biochemistry 2011, 50 (24), 5426–35. [PubMed: 21574565]

690. Liu XR; Zhang MM; Rempel DL; Gross ML, A Single Approach Reveals the Composite Conformational Changes, Order of Binding, and Affinities for Calcium Binding to Calmodulin. Analytical Chemistry 2019, 91 (9), 5508–5512. [PubMed: 30963760]

691. Zhang Hao, B. C. G., Jones Lisa M., Vidavsky Ilan, and Gross Michael L., Fast Photochemical Oxidation of Proteins for Comparing Structures of Protein-Ligand Complexes: The Calmodulin-Peptide Model System. Anal. Chem 2011, 83, 311–318. [PubMed: 21142124]

692. Qin K; Yang Y; Mastrangelo P; Westaway D, Mapping Cu(II) Binding Sites in Prion Proteins by Diethyl Pyrocarbonate Modification and Matrix-assisted Laser Desorption Ionization-Time of Flight (MALDI-TOF) Mass Spectrometric Footprinting. Journal of Biological Chemistry 2002, 277 (3), 1981–1990. [PubMed: 11698407]

693. Burns CS; Aronoff-Spencer E; Legname G; Prusiner SB; Antholine WE; Gerfen GJ; Peisach J; Millhauser GL, Copper coordination in the full-length, recombinant prion protein. Biochemistry 2003, 42 (22), 6794–6803. [PubMed: 12779334]

694. Qin K; Coomaraswamy J; Mastrangelo P; Yang Y; Lugowski S; Petromilli C; Prusiner SB; Fraser PE; Goldberg JM; Chakrabartty A; Westaway D, The PrP-like Protein Doppel Binds Copper. Journal of Biological Chemistry 2003, 278 (11), 8888–8896. [PubMed: 12482851]

695. Narindrasorasak S; Kulkarni P; Deschamps P; She Y-M; Sarkar B, Characterization and Copper Binding Properties of Human COMMD1 (MURR1). Biochemistry 2007, 46 (11), 3116–3128. [PubMed: 17309234]

696. Zhao H; Waite JH, Proteins in Load-Bearing Junctions: The Histidine-Rich Metal-Binding Protein of Mussel Byssus. Biochemistry 2006, 45 (47), 14223–14231. [PubMed: 17115717]

697. Binolfi A; Lamberto GR; Duran R; Quintanar L; Bertoncini CW; Souza JM; Cerveñansky C; Zweckstetter M; Griesinger C; Fernández CO, Site-Specific Interactions of Cu(II) with α and β-Synuclein: Bridging the Molecular Gap between Metal Binding and Aggregation. Journal of the American Chemical Society 2008, 130 (35), 11801–11812. [PubMed: 18693689]

698. Srabani K; Das KP, Interaction of Cu+2 with α-Crystallin: A Biophysical and Mass Spectrometric Study. Protein & Peptide Letters 2018, 25 (3), 275–284. [PubMed: 29298644]

699. Ginotra YP; Kulkarni PP, Solution Structure of Physiological Cu(His)2: Novel Considerations into Imidazole Coordination. Inorganic Chemistry 2009, 48 (15), 7000–7002. [PubMed: 19722687]

700. Miller J; McLachlan AD; Klug A, Repetitive zinc-binding domains in the protein transcription factor IIIA from Xenopus oocytes. The EMBO Journal 1985, 4 (6), 1609–1614. [PubMed: 4040853]

701. Gonzalez de Peredo A; Saint-Pierre C; Adrait A; Jacquamet L; Latour J-M; Michaud-Soret I; Forest E, Identification of the Two Zinc-Bound Cysteines in the Ferric Uptake Regulation Protein from Escherichia coli: Chemical Modification and Mass Spectrometry Analysis. Biochemistry 1999, 38 (26), 8582–8589. [PubMed: 10387106]

702. Apuy JL; Chen X; Russell DH; Baldwin TO; Giedroc DP, Ratiometric Pulsed Alkylation/Mass Spectrometry of the Cysteine Pairs in Individual Zinc Fingers of MRE-Binding Transcription Factor-1 (MTF-1) as a Probe of Zinc Chelate Stability. Biochemistry 2001, 40 (50), 15164–15175. [PubMed: 11735399]

703. Atsriku C; Scott GK; Benz CC; Baldwin MA, Reactivity of zinc finger cysteines: Chemical modifications within labile zinc fingers in estrogen receptor. Journal of the American Society for Mass Spectrometry 2005, 16 (12), 2017–2026. [PubMed: 16246571]

704. Larabee JL; Hocker JR; Hanas JS, Mechanisms of Aurothiomalate–Cys2His2 Zinc Finger Interactions. Chemical Research in Toxicology 2005, 18 (12), 1943–1954. [PubMed: 16359185]

705. Larabee JL; Hocker JR; Hanas JS, Cys redox reactions and metal binding of a Cys2His2 zinc finger. Archives of Biochemistry and Biophysics 2005, 434 (1), 139–149. [PubMed: 15629117]

706. Walter ED; Stevens DJ; Visconte MP; Millhauser GL, The Prion Protein is a Combined Zinc and Copper Binding Protein: Zn2+ Alters the Distribution of Cu2+ Coordination Modes. Journal of the American Chemical Society 2007, 129 (50), 15440–15441. [PubMed: 18034490]

707. Karmakar S; Das KP, Identification of Histidine Residues Involved in Zn2+ Binding to αA- and αB-Crystallin by Chemical Modification and MALDI TOF Mass Spectrometry. The Protein Journal 2012, 31 (7), 623–640. [PubMed: 22890888]

708. Chen S-H; Russell WK; Russell DH, Combining Chemical Labeling, Bottom-Up and Top-Down Ion-Mobility Mass Spectrometry To Identify Metal-Binding Sites of Partially Metalated Metallothionein. Analytical Chemistry 2013, 85 (6), 3229–3237. [PubMed: 23421923]

709. Puljung Michael C.; Zagotta William N., Labeling of Specific Cysteines in Proteins Using Reversible Metal Protection. Biophysical Journal 2011, 100 (10), 2513–2521. [PubMed: 21575586]

710. Ramakrishnan D; Xing W; Beran RK; Chemuru S; Rohrs H; Niedziela-Majka A; Marchand B; Mehra U; Zábranský A; Doležal M; Hubálek M; Pichová I; Gross ML; Kwon HJ; Fletcher SP, Hepatitis B Virus X Protein Function Requires Zinc Binding. Journal of Virology 2019, 93 (16), e00250–19. [PubMed: 31167910]

711. Clapham DE, Calcium signaling. Cell 1995, 80 (2), 259–268. [PubMed: 7834745]

712. Clapham DE, Calcium Signaling. Cell 2007, 131 (6), 1047–1058. [PubMed: 18083096]

713. Gifford Jessica L.; Walsh Michael P.; Vogel Hans J., Structures and metal-ion-binding properties of the Ca2+-binding helix–loop–helix EF-hand motifs. Biochemical Journal 2007, 405 (2), 199–221. [PubMed: 17590154]

714. Zhang H; Wen J; Huang RYC; Blankenship RE; Gross ML, Mass spectrometry-based carboxyl footprinting of proteins: Method evaluation. International Journal of Mass Spectrometry 2012, 312, 78–86. [PubMed: 22408386]

715. Narumi R; Yamamoto T; Inoue A; Arata T, Substrate-induced conformational changes in sarcoplasmic reticulum Ca2+-ATPase probed by surface modification using diethylpyrocarbonate with mass spectrometry. FEBS Letters 2012, 586 (19), 3172–3178. [PubMed: 22771786]

716. Senguen FT; Grabarek Z, X-ray Structures of Magnesium and Manganese Complexes with the N-Terminal Domain of Calmodulin: Insights into the Mechanism and Specificity of Metal Ion Binding to an EF-Hand. Biochemistry 2012, 51 (31), 6182–6194. [PubMed: 22803592]

717. Gorman JJ; Wallis TP; Pitt JJ, Protein disulfide bond determination by mass spectrometry. Mass Spectrometry Reviews 2002, 21 (3), 183–216. [PubMed: 12476442]

718. Xia Y; Cooks RG, Plasma Induced Oxidative Cleavage of Disulfide Bonds in Polypeptides during Nanoelectrospray Ionization. Analytical Chemistry 2010, 82 (7), 2856–2864. [PubMed: 20196567]

719. Wang Y; Lu Q; Wu S-L; Karger BL; Hancock WS, Characterization and Comparison of Disulfide Linkages and Scrambling Patterns in Therapeutic Monoclonal Antibodies: Using LC-MS with Electron Transfer Dissociation. Analytical Chemistry 2011, 83 (8), 3133–3140. [PubMed: 21428412]

720. Liu F; van Breukelen B; Heck AJR, Facilitating Protein Disulfide Mapping by a Combination of Pepsin Digestion, Electron Transfer Higher Energy Dissociation (EThcD), and a Dedicated Search Algorithm SlinkS. Molecular & Cellular Proteomics 2014, 13 (10), 2776–2786. [PubMed: 24980484]

721. Agarwal A; Diedrich JK; Julian RR, Direct Elucidation of Disulfide Bond Partners Using Ultraviolet Photodissociation Mass Spectrometry. Analytical Chemistry 2011, 83 (17), 6455–6458. [PubMed: 21797266]

722. Quick MM; Crittenden CM; Rosenberg JA; Brodbelt JS, Characterization of Disulfide Linkages in Proteins by 193 nm Ultraviolet Photodissociation (UVPD) Mass Spectrometry. Analytical Chemistry 2018, 90 (14), 8523–8530. [PubMed: 29902373]

723. Zhang Y; Dewald HD; Chen H, Online Mass Spectrometric Analysis of Proteins/Peptides Following Electrolytic Cleavage of Disulfide Bonds. Journal of Proteome Research 2011, 10 (3), 1293–1304. [PubMed: 21197958]

724. Echterbille J; Quinton L; Gilles N; De Pauw E, Ion Mobility Mass Spectrometry as a Potential Tool To Assign Disulfide Bonds Arrangements in Peptides with Multiple Disulfide Bridges. Analytical Chemistry 2013, 85 (9), 4405–4413. [PubMed: 23509902]

725. Choi S; Jeong J; Na S; Lee HS; Kim H-Y; Lee K-J; Paek E, New Algorithm for the Identification of Intact Disulfide Linkages Based on Fragmentation Characteristics in Tandem Mass Spectra. Journal of Proteome Research 2010, 9 (1), 626–635. [PubMed: 19902913]

726. Huang SY; Chen SF; Chen CH; Huang HW; Wu WG; Sung WC, Global Disulfide Bond Profiling for Crude Snake Venom Using Dimethyl Labeling Coupled with Mass Spectrometry and RADAR Algorithm. Analytical Chemistry 2014, 86 (17), 8742–8750. [PubMed: 25138527]

727. Morris HR; Pucci P, A new method for rapid assignment of S-S bridges in proteins. Biochemical and Biophysical Research Communications 1985, 126 (3), 1122–1128. [PubMed: 3919720]

728. Smith DL; Zhou Z, [20] Strategies for locating disulfide bonds in proteins In Methods in Enzymology, Academic Press: 1990; Vol. 193, pp 374–389. [PubMed: 2074827]

729. Zaluzec EJ; Gage DA; Watson JT, Quantitative assessment of cysteine and cystine in peptides and proteins following organomercurial derivatization and analysis by matrix-assisted laser desorption ionization mass spectrometry. Journal of the American Society for Mass Spectrometry 1994, 5 (5), 359–366. [PubMed: 24222590]

730. Zaluzec EJ; Gage DA; Watson JT, Matrix-Assisted Laser Desorption Ionization Mass Spectrometry: Applications in Peptide and Protein Characterization. Protein Expression and Purification 1995, 6 (2), 109–123. [PubMed: 7606158]

731. Wu J; Gage DA; Watson JT, A Strategy to Locate Cysteine Residues in Proteins by Specific Chemical Cleavage Followed by Matrix-Assisted Laser Desorption/Ionization Time-of-Flight Mass Spectrometry. Analytical Biochemistry 1996, 235 (2), 161–174. [PubMed: 8833324]

732. Jacobson GR; Schaffer MH; Stark GR; Vanaman TC, Specific Chemical Cleavage in High Yield at the Amino Peptide Bonds of Cysteine and Cystine Residues. Journal of Biological Chemistry 1973, 248 (19), 6583–6591. [PubMed: 4583259]

733. Barbirz S; Jakob U; Glocker MO, Mass Spectrometry Unravels Disulfide Bond Formation as the Mechanism That Activates a Molecular Chaperone. Journal of Biological Chemistry 2000, 275 (25), 18759–18766. [PubMed: 10764757]

734. Abo M; Li C; Weerapana E, Isotopically-Labeled Iodoacetamide-Alkyne Probes for Quantitative Cysteine-Reactivity Profiling. Molecular Pharmaceutics 2018, 15 (3), 743–749. [PubMed: 29172527]

735. Weerapana E; Wang C; Simon GM; Richter F; Khare S; Dillon MBD; Bachovchin DA; Mowen K; Baker D; Cravatt BF, Quantitative reactivity profiling predicts functional cysteines in proteomes. Nature 2010, 468 (7325), 790–795. [PubMed: 21085121]

736. Chalker JM; Bernardes GJL; Lin YA; Davis BG, Chemical Modification of Proteins at Cysteine: Opportunities in Chemistry and Biology. Chemistry – An Asian Journal 2009, 4 (5), 630–640.

737. Glocker MO; Arbogast B; Schreurs J; Deinzer ML, Assignment of the inter- and intramolecular disulfide linkages in recombinant human macrophage colony stimulating factor using fast atom bombardment mass spectrometry. Biochemistry 1993, 32 (2), 482–488. [PubMed: 8422357]

738. Li KS; Chen G; Mo J; Huang RYC; Deyanova EG; Beno BR; O'Neil SR; Tymiak AA; Gross ML, Orthogonal Mass Spectrometry-Based Footprinting for Epitope Mapping and Structural Characterization: The IL-6 Receptor upon Binding of Protein Therapeutics. Analytical Chemistry 2017, 89 (14), 7742–7749. [PubMed: 28621526]

739. Kaur P; Tomechko S; Kiselar J; Shi W; Deperalta G; Wecksler AT; Gokulrangan G; Ling V; Chance MR, Characterizing monoclonal antibody structure by carbodiimide/GEE footprinting. mAbs 2014, 6 (6), 1486–1499. [PubMed: 25484052]

740. Kaur P; Kiselar J; Shi W; Yang S; Chance MR, Covalent Labeling Techniques for Characterizing Higher Order Structure of Monoclonal Antibodies In State-of-the-Art and Emerging Technologies for Therapeutic Monoclonal Antibody Characterization Volume 3. Defining the Next Generation of Analytical and Biophysical Techniques, American Chemical Society: 2015; Vol. 1202, pp 45–73.

741. Wecksler AT; Kalo MS; Deperalta G, Mapping of Fab-1:VEGF Interface Using Carboxyl Group Footprinting Mass Spectrometry. Journal of The American Society for Mass Spectrometry 2015, 26 (12), 2077–2080. [PubMed: 26419770]

742. Kaur P; Tomechko SE; Kiselar J; Shi W; Deperalta G; Wecksler AT; Gokulrangan G; Ling V; Chance MR, Characterizing monoclonal antibody structure by carboxyl group footprinting. mAbs 2015, 7 (3), 540–552. [PubMed: 25933350]

743. Pan LY; Salas-Solano O; Valliere-Douglass JF, Localized conformational interrogation of antibody and antibody-drug conjugates by site-specific carboxyl group footprinting. mAbs 2017, 9 (2), 307–318. [PubMed: 27929747]

744. Underbakke ES; Zhu Y; Kiessling LL, Protein Footprinting in a Complex Milieu: Identifying the Interaction Surfaces of the Chemotaxis Adaptor Protein CheW. Journal of Molecular Biology 2011, 409 (4), 483–495. [PubMed: 21463637]

745. Underbakke ES; Zhu Y; Kiessling LL, Isotope-Coded Affinity Tags with Tunable Reactivities for Protein Footprinting. Angewandte Chemie International Edition 2008, 47 (50), 9677–9680. [PubMed: 18979478]

746. Gygi SP; Rist B; Gerber SA; Turecek F; Gelb MH; Aebersold R, Quantitative analysis of complex protein mixtures using isotope-coded affinity tags. Nature Biotechnology 1999, 17 (10), 994–999.

747. Aebersold R; Goodlett DR, Mass Spectrometry in Proteomics. Chemical Reviews 2001, 101 (2), 269–296. [PubMed: 11712248]

748. Mendoza VL; Barón-Rodríguez MA; Blanco C; Vachet RW, Structural Insights into the Pre-Amyloid Tetramer of β-2-Microglobulin from Covalent Labeling and Mass Spectrometry. Biochemistry 2011, 50 (31), 6711–6722. [PubMed: 21718071]

749. Liu T; Marcinko TM; Kiefer PA; Vachet RW, Using Covalent Labeling and Mass Spectrometry To Study Protein Binding Sites of Amyloid Inhibiting Molecules. Analytical Chemistry 2017, 89 (21), 11583–11591. [PubMed: 29028328]

750. Shrivastava S; Nuffer JH; Siegel RW; Dordick JS, Position-Specific Chemical Modification and Quantitative Proteomics Disclose Protein Orientation Adsorbed on Silica Nanoparticles. Nano Letters 2012, 12 (3), 1583–1587. [PubMed: 22296027]

751. Thyparambil AA; Wei Y; Wu Y; Latour RA, Determination of orientation and adsorption-induced changes in the tertiary structure of proteins on material surfaces by chemical modification and peptide mapping. Acta Biomaterialia 2014, 10 (6), 2404–2414. [PubMed: 24486912]

752. Tollefson EJ; Allen CR; Chong G; Zhang X; Rozanov ND; Bautista A; Cerda JJ; Pedersen JA; Murphy CJ; Carlson EE; Hernandez R, Preferential Binding of Cytochrome c to Anionic Ligand-Coated Gold Nanoparticles: A Complementary Computational and Experimental Approach. ACS Nano 2019, 13 (6), 6856–6866. [PubMed: 31082259]

753. Yang B; Wu Y-J; Zhu M; Fan S-B; Lin J; Zhang K; Li S; Chi H; Li Y-X; Chen H-F, Identification of cross-linked peptides from complex samples. Nature methods 2012, 9 (9), 904. [PubMed: 22772728]

754. Rinner O; Seebacher J; Walzthoeni T; Mueller LN; Beck M; Schmidt A; Mueller M; Aebersold R, Identification of cross-linked peptides from large sequence databases. Nature methods 2008, 5 (4), 315. [PubMed: 18327264]

755. Liu F; Rijkers DT; Post H; Heck AJ, Proteome-wide profiling of protein assemblies by cross-linking mass spectrometry. Nature methods 2015, 12 (12), 1179. [PubMed: 26414014]

756. Götze M; Pettelkau J; Schaks S; Bosse K; Ihling CH; Krauth F; Fritzsche R; Kühn U; Sinz A, StavroX—a software for analyzing crosslinked products in protein interaction studies. Journal of the American Society for Mass Spectrometry 2012, 23 (1), 76–87. [PubMed: 22038510]

757. Young MM; Tang N; Hempel JC; Oshiro CM; Taylor EW; Kuntz ID; Gibson BW; Dollinger G, High throughput protein fold identification by using experimental constraints derived from intramolecular cross-links and mass spectrometry. Proceedings of the National Academy of Sciences 2000, 97 (11), 5802–5806.

758. Alber F; Dokudovskaya S; Veenhoff LM; Zhang W; Kipper J; Devos D; Suprapto A; Karni-Schmidt O; Williams R; Chait BT, The molecular architecture of the nuclear pore complex. Nature 2007, 450 (7170), 695. [PubMed: 18046406]

759. Shi Y; Fernandez-Martinez J; Tjioe E; Pellarin R; Kim SJ; Williams R; Schneidman-Duhovny D; Sali A; Rout MP; Chait BT, Structural characterization by cross-linking reveals the detailed architecture of a coatomer-related heptameric module from the nuclear pore complex. Molecular & Cellular Proteomics 2014, 13 (11), 2927–2943. [PubMed: 25161197]

760. Erzberger JP; Stengel F; Pellarin R; Zhang S; Schaefer T; Aylett CH; Cimermančič P; Boehringer D; Sali A; Aebersold R, Molecular architecture of the 40S· eIF1· eIF3 translation initiation complex. Cell 2014, 158 (5), 1123–1135. [PubMed: 25171412]

761. Herzog F; Kahraman A; Boehringer D; Mak R; Bracher A; Walzthoeni T; Leitner A; Beck M; Hartl F-U; Ban N; Malmström L; Aebersold R, Structural Probing of a Protein Phosphatase 2A Network by Chemical Cross-Linking and Mass Spectrometry. Science 2012, 337 (6100), 1348–1352. [PubMed: 22984071]

762. Hofmann T; Fischer AW; Meiler J; Kalkhof S, Protein structure prediction guided by crosslinking restraints–A systematic evaluation of the impact of the crosslinking spacer length. Methods 2015, 89, 79–90. [PubMed: 25986934]

763. Gutierrez CB; Yu C; Novitsky EJ; Huszagh AS; Rychnovsky SD; Huang L, Developing an Acidic Residue Reactive and Sulfoxide-Containing MS-Cleavable Homobifunctional Cross-Linker for Probing Protein–Protein Interactions. Analytical chemistry 2016, 88 (16), 8315–8322. [PubMed: 27417384]

764. Belsom A; Mudd G; Giese S; Auer M; Rappsilber J, Complementary benzophenone cross-linking/mass spectrometry photochemistry. Analytical chemistry 2017, 89 (10), 5319–5324. [PubMed: 28430416]

765. Belsom A; Schneider M; Fischer L; Brock O; Rappsilber J, Serum albumin domain structures in human blood serum by mass spectrometry and computational biology. Molecular & Cellular Proteomics 2016, 15 (3), 1105–1116. [PubMed: 26385339]

766. Leitner A; Faini M; Stengel F; Aebersold R, Crosslinking and Mass Spectrometry: An Integrated Technology to Understand the Structure and Function of Molecular Machines. Trends in Biochemical Sciences 2016, 41 (1), 20–32. [PubMed: 26654279]

767. Schneider M; Belsom A; Rappsilber J, Protein Tertiary Structure by Crosslinking/Mass Spectrometry. Trends in Biochemical Sciences 2018, 43 (3), 157–169. [PubMed: 29395654]

768. Zhang MM; Beno BR; Huang RYC; Adhikari J; Deyanova EG; Li J; Chen G; Gross ML, An Integrated Approach for Determining a Protein-Protein Binding Interface in Solution and an Evaluation of HDX Kinetics for Adjudicating Candidate Docking Models. Analytical Chemistry 2019.

769. Komolov KE; Du Y; Duc NM; Betz RM; Rodrigues JPGLM; Leib RD; Patra D; Skiniotis G; Adams CM; Dror RO; Chung KY; Kobilka BK; Benovic JL, Structural and Functional Analysis of a β2-Adrenergic Receptor Complex with GRK5. Cell 2017, 169 (3), 407–421.e16. [PubMed: 28431242]

770. Lin S-J; Chen Y-F; Hsu K-C; Chen Y-L; Ko T-P; Lo C-F; Wang H-C; Wang H-C, Structural Insights to the Heterotetrameric Interaction between the Vibrio parahaemolyticus PirAvp and PirBvp Toxins and Activation of the Cry-Like Pore-Forming Domain. Toxins 2019, 11 (4), 233.

771. Xu H; Hsu P-H; Zhang L; Tsai M-D; Freitas MA, Database Search Algorithm for Identification of Intact Cross-Links in Proteins and Peptides Using Tandem Mass Spectrometry. Journal of Proteome Research 2010, 9 (7), 3384–3393. [PubMed: 20469931]

772. Yang B; Wu Y-J; Zhu M; Fan S-B; Lin J; Zhang K; Li S; Chi H; Li Y-X; Chen H-F; Luo S-K; Ding Y-H; Wang L-H; Hao Z; Xiu L-Y; Chen S; Ye K; He S-M; Dong M-Q, Identification of cross-linked peptides from complex samples. Nature Methods 2012, 9, 904. [PubMed: 22772728]

773. Liu F; Lössl P; Scheltema R; Viner R; Heck AJR, Optimized fragmentation schemes and data analysis strategies for proteome-wide cross-link identification. Nature Communications 2017, 8, 15473.

774. Tan D; Li Q; Zhang M-J; Liu C; Ma C; Zhang P; Ding Y-H; Fan S-B; Tao L; Yang B; Li X; Ma S; Liu J; Feng B; Liu X; Wang H-W; He S-M; Gao N; Ye K; Dong M-Q; Lei X, Trifunctional cross-linker for mapping protein-protein interaction networks and comparing protein conformational states. eLife 2016, 5, e12509. [PubMed: 26952210]

775. Yu C; Huang L, Cross-Linking Mass Spectrometry: An Emerging Technology for Interactomics and Structural Biology. Analytical Chemistry 2018, 90 (1), 144–165. [PubMed: 29160693]

776. Liu F; Rijkers DTS; Post H; Heck AJR, Proteome-wide profiling of protein assemblies by cross-linking mass spectrometry. Nature Methods 2015, 12, 1179. [PubMed: 26414014]

777. Konermann L; Simmons DA, Protein-folding kinetics and mechanisms studied by pulse-labeling and mass spectrometry. Mass Spectrometry Reviews 2003, 22 (1), 1–26. [PubMed: 12768602]

778. Happersberger HP; Stapleton J; Cowgill C; Glocker MO, Characterization of the folding pathway of recombinant human macrophage-colony stimulating-factor β (rhM-CSF β) by bis-cysteinyl modification and mass spectrometry. Proteins: Structure, Function, and Bioinformatics 1998, 33 (S2), 50–62.

779. Smith DJ; Kenyon GL, Nonessentiality of the Active Sulfhydryl Group of Rabbit Muscle Creatine Kinase. Journal of Biological Chemistry 1974, 249 (10), 3317–3318. [PubMed: 4364425]

780. Feng Z; Butler MC; Alam SL; Loh SN, On the nature of conformational openings: native and unfolded-state hydrogen and thiol-disulfide exchange studies of ferric aquomyoglobin 11Edited by P. E. Wright. Journal of Molecular Biology 2001, 314 (1), 153–166. [PubMed: 11724540]

781. Ha J-H; Loh SN, Changes in side chain packing during apomyoglobin folding characterized by pulsed thiol-disulfide exchange. Nature Structural Biology 1998, 5 (8), 730–737. [PubMed: 9699638]

782. Feng Z; Ha J-H; Loh SN, Identifying the Site of Initial Tertiary Structure Disruption during Apomyoglobin Unfolding. Biochemistry 1999, 38 (44), 14433–14439. [PubMed: 10545165]

783. Jha SK; Udgaonkar JB, Exploring the Cooperativity of the Fast Folding Reaction of a Small Protein Using Pulsed Thiol Labeling and Mass Spectrometry. Journal of Biological Chemistry 2007, 282 (52), 37479–37491. [PubMed: 17959598]

784. Han H; McLuckey SA, Selective Covalent Bond Formation in Polypeptide Ions via Gas-Phase Ion/Ion Reaction Chemistry. Journal of the American Chemical Society 2009, 131 (36), 12884–12885. [PubMed: 19702304]

785. Mentinova M; McLuckey SA, Covalent Modification of Gaseous Peptide Ions with N-Hydroxysuccinimide Ester Reagent Ions. Journal of the American Chemical Society 2010, 132 (51), 18248–18257. [PubMed: 21128662]

786. Peng Z; McGee WM; Bu J; Barefoot NZ; McLuckey SA, Gas Phase Reactivity of Carboxylates with N-Hydroxysuccinimide Esters. Journal of The American Society for Mass Spectrometry 2015, 26 (1), 174–180. [PubMed: 25338221]

787. Peng Z; Pilo AL; Luongo CA; McLuckey SA, Gas-Phase Amidation of Carboxylic Acids with Woodward's Reagent K Ions. Journal of The American Society for Mass Spectrometry 2015, 26 (10), 1686–1694. [PubMed: 26122523]

788. Mourão Márcio A.; Hakim Joe B.; Schnell S, Connecting the Dots: The Effects of Macromolecular Crowding on Cell Physiology. Biophysical Journal 2014, 107 (12), 2761–2766. [PubMed: 25517143]

789. Guin D; Gruebele M, Weak Chemical Interactions That Drive Protein Evolution: Crowding, Sticking, and Quinary Structure in Folding and Function. Chemical Reviews 2019.

790. Xue L; Karpenko IA; Hiblot J; Johnsson K, Imaging and manipulating proteins in live cells through covalent labeling. Nature Chemical Biology 2015, 11, 917. [PubMed: 26575238]

791. Chen I; Ting AY, Site-specific labeling of proteins with small molecules in live cells. Current Opinion in Biotechnology 2005, 16 (1), 35–40. [PubMed: 15722013]

792. Jing C; Cornish VW, Chemical Tags for Labeling Proteins Inside Living Cells. Accounts of Chemical Research 2011, 44 (9), 784–792. [PubMed: 21879706]

793. Griffin BA; Adams SR; Tsien RY, Specific Covalent Labeling of Recombinant Protein Molecules Inside Live Cells. Science 1998, 281 (5374), 269–272. [PubMed: 9657724]

794. Marks KM; Braun PD; Nolan GP, A general approach for chemical labeling and rapid, spatially controlled protein inactivation. Proceedings of the National Academy of Sciences of the United States of America 2004, 101 (27), 9982–9987. [PubMed: 15218100]

795. Takaoka Y; Ojida A; Hamachi I, Protein Organic Chemistry and Applications for Labeling and Engineering in Live-Cell Systems. Angewandte Chemie International Edition 2013, 52 (15), 4088–4106. [PubMed: 23426903]

796. Szymański W; Beierle JM; Kistemaker HAV; Velema WA; Feringa BL, Reversible Photocontrol of Biological Systems by the Incorporation of Molecular Photoswitches. Chemical Reviews 2013, 113 (8), 6114–6178. [PubMed: 23614556]

797. Angel TE; Aryal UK; Hengel SM; Baker ES; Kelly RT; Robinson EW; Smith RD, Mass spectrometry-based proteomics: existing capabilities and future directions. Chemical Society Reviews 2012, 41 (10), 3912–3928. [PubMed: 22498958]

798. Sechi S; Oda Y, Quantitative proteomics using mass spectrometry. Current Opinion in Chemical Biology 2003, 7 (1), 70–77. [PubMed: 12547429]

799. Birkemeyer C; Luedemann A; Wagner C; Erban A; Kopka J, Metabolome analysis: the potential of in vivo labeling with stable isotopes for metabolite profiling. Trends in Biotechnology 2005, 23 (1), 28–33. [PubMed: 15629855]

800. Selenko P; Wagner G, Looking into live cells with in-cell NMR spectroscopy. Journal of Structural Biology 2007, 158 (2), 244–253. [PubMed: 17502240]

801. Sakakibara D; Sasaki A; Ikeya T; Hamatsu J; Hanashima T; Mishima M; Yoshimasu M; Hayashi N; Mikawa T; Wälchli M; Smith BO; Shirakawa M; Güntert P; Ito Y, Protein structure determination in living cells by in-cell NMR spectroscopy. Nature 2009, 458 (7234), 102–105. [PubMed: 19262674]

802. Sinz A, The advancement of chemical cross-linking and mass spectrometry for structural proteomics: from single proteins to protein interaction networks. Expert Review of Proteomics 2014, 11 (6), 733–743. [PubMed: 25227871]

803. Chavez JD; Bruce JE, Chemical cross-linking with mass spectrometry: a tool for systems structural biology. Current opinion in chemical biology 2019, 48, 8–18. [PubMed: 30172868]

804. Zhang H; Tang X; Munske GR; Tolic N; Anderson GA; Bruce JE, Identification of protein-protein interactions and topologies in living cells with chemical cross-linking and mass spectrometry. Molecular & Cellular Proteomics 2009, 8 (3), 409–420. [PubMed: 18936057]

805. Chavez JD; Weisbrod CR; Zheng C; Eng JK; Bruce JE, Protein interactions, post-translational modifications and topologies in human cells. Molecular & Cellular Proteomics 2013, 12 (5), 1451–1467. [PubMed: 23354917]

806. Zheng C; Yang L; Hoopmann MR; Eng JK; Tang X; Weisbrod CR; Bruce JE, Cross-linking measurements of in vivo protein complex topologies. Molecular & Cellular Proteomics 2011, 10 (10), M110. 006841.

807. Navare AT; Chavez JD; Zheng C; Weisbrod CR; Eng JK; Siehnel R; Singh PK; Manoil C; Bruce JE, Probing the protein interaction network of Pseudomonas aeruginosa cells by chemical cross-linking mass spectrometry. Structure 2015, 23 (4), 762–773. [PubMed: 25800553]

808. Wu X; Chavez JD; Schweppe DK; Zheng C; Weisbrod CR; Eng JK; Murali A; Lee SA; Ramage E; Gallagher LA, In vivo protein interaction network analysis reveals porin-localized antibiotic inactivation in Acinetobacter baumannii strain AB5075. Nature communications 2016, 7, 13414.

809. Zhong X; Navare AT; Chavez JD; Eng JK; Schweppe DK; Bruce JE, Large-scale and targeted quantitative cross-linking MS using isotope-labeled protein interaction reporter (PIR) cross-linkers. Journal of proteome research 2016, 16 (2), 720–727. [PubMed: 28152603]

810. de Jong L; de Koning EA; Roseboom W; Buncherd H; Wanner MJ; Dapic I; Jansen PJ; van Maarseveen JH; Corthals GL; Lewis PJ, In-Culture Cross-Linking of Bacterial Cells Reveals Large-Scale Dynamic Protein–Protein Interactions at the Peptide Level. Journal of proteome research 2017, 16 (7), 2457–2471. [PubMed: 28516784]

811. Kaake RM; Wang X; Burke A; Yu C; Kandur W; Yang Y; Novtisky EJ; Second T; Duan J; Kao A, A new in vivo cross-linking mass spectrometry platform to define protein–protein interactions in living cells. Molecular & Cellular Proteomics 2014, 13 (12), 3533–3543. [PubMed: 25253489]

812. Liu F; Lössl P; Rabbitts BM; Balaban RS; Heck AJ, The interactome of intact mitochondria by cross-linking mass spectrometry provides evidence for coexisting respiratory supercomplexes. Molecular & Cellular Proteomics 2018, 17 (2), 216–232. [PubMed: 29222160]

813. Liu H; Zhang H; Niedzwiedzki DM; Prado M; He G; Gross ML; Blankenship RE, Phycobilisomes Supply Excitations to Both Photosystems in a Megacomplex in Cyanobacteria. Science 2013, 342 (6162), 1104–1107. [PubMed: 24288334]

814. Liu H; Weisz DA; Zhang MM; Cheng M; Zhang B; Zhang H; Gerstenecker GS; Pakrasi HB; Gross ML; Blankenship RE, Phycobilisomes Harbor FNRL in Cyanobacteria. mBio 2019, 10 (2), e00669–19. [PubMed: 31015331]

815. Liu F; Heck AJ, Interrogating the architecture of protein assemblies and protein interaction networks by cross-linking mass spectrometry. Current opinion in structural biology 2015, 35, 100–108. [PubMed: 26615471]

816. Shen G; Cui W; Zhang H; Zhou F; Huang W; Liu Q; Yang Y; Li S; Bowman GR; Sadler JE; Gross ML; Li W, Warfarin traps human vitamin K epoxide reductase in an intermediate state during electron transfer. Nature Structural &Amp; Molecular Biology 2016, 24, 69.

817. Calabrese AN; Radford SE, Mass spectrometry-enabled structural biology of membrane proteins. Methods 2018, 147, 187–205. [PubMed: 29510247]

818. Bolla JR; Agasid MT; Mehmood S; Robinson CV, Membrane Protein–Lipid Interactions Probed Using Mass Spectrometry. Annual Review of Biochemistry 2019, 88 (1), 85–111.

819. Leney AC; Heck AJR, Native Mass Spectrometry: What is in the Name? Journal of The American Society for Mass Spectrometry 2017, 28 (1), 5–13.

820. Shen G; Li S; Cui W; Liu S; Yang Y; Gross M; Li W, Membrane Protein Structure in Live Cells: Methodology for Studying Drug Interaction by Mass Spectrometry-Based Footprinting. Biochemistry 2018, 57 (3), 286–294. [PubMed: 29192498]

821. Li K Mass Spectrometry-based Strategies for Protein Characterization: Amyloid Formation, Protein-Ligand Interactions and Structures of Membrane Proteins in Live Cells Dissertation, Washington University in St. Louis, 2018.

822. Rouillon C; Zhou M; Zhang J; Politis A; Beilsten-Edmands V; Cannone G; Graham S; Robinson CV; Spagnolo L; White MF, Structure of the CRISPR interference complex CSM reveals key similarities with cascade. Molecular cell 2013, 52 (1), 124–134. [PubMed: 24119402]

823. Bui KH; von Appen A; DiGuilio AL; Ori A; Sparks L; Mackmull M-T; Bock T; Hagen W; Andrés-Pons A; Glavy JS, Integrated structural analysis of the human nuclear pore complex scaffold. Cell 2013, 155 (6), 1233–1243. [PubMed: 24315095]

824. Lasker K; Förster F; Bohn S; Walzthoeni T; Villa E; Unverdorben P; Beck F; Aebersold R; Sali A; Baumeister W, Molecular architecture of the 26S proteasome holocomplex determined by an integrative approach. Proceedings of the National Academy of Sciences 2012, 109 (5), 1380–1387.

825. Greber BJ; Boehringer D; Leitner A; Bieri P; Voigts-Hoffmann F; Erzberger JP; Leibundgut M; Aebersold R; Ban N, Architecture of the large subunit of the mammalian mitochondrial ribosome. Nature 2014, 505 (7484), 515. [PubMed: 24362565]

826. Kar UK; Simonian M; Whitelegge JP, Integral membrane proteins: bottom-up, top-down and structural proteomics. Expert Rev Proteomics 2017, 14 (8), 715–723. [PubMed: 28737967]

827. Weisz DA; Gross ML; Pakrasi HB, The Use of Advanced Mass Spectrometry to Dissect the Life-Cycle of Photosystem II. Front Plant Sci 2016, 7.

828. Hurt E; Beck M, Towards understanding nuclear pore complex architecture and dynamics in the age of integrative structural analysis. Curr Opin Cell Biol 2015, 34, 31–38. [PubMed: 25938906]

829. Sinz A; Arlt C; Chorev D; Sharon M, Chemical cross-linking and native mass spectrometry: A fruitful combination for structural biology. Protein Science 2015, 24 (8), 1193–1209. [PubMed: 25970732]

830. Politis A; Schmidt C; Tjioe E; Sandercock AM; Lasker K; Gordiyenko Y; Russel D; Sali A; Robinson CV, Topological models of heteromeric protein assemblies from mass spectrometry: application to the yeast eIF3: eIF5 complex. Chemistry & biology 2015, 22 (1), 117–128. [PubMed: 25544043]

831. Robinson PJ; Trnka MJ; Bushnell DA; Davis RE; Mattei P-J; Burlingame AL; Kornberg RD, Structure of a Complete Mediator-RNA Polymerase II Pre-Initiation Complex. Cell 2016, 166 (6), 1411–1422.e16. [PubMed: 27610567]

832. Schmidt C; Macpherson JA; Lau AM; Tan KW; Fraternali F; Politis A, Surface Accessibility and Dynamics of Macromolecular Assemblies Probed by Covalent Labeling Mass Spectrometry and Integrative Modeling. Analytical Chemistry 2017, 89 (3), 1459–1468. [PubMed: 28208298]

833. Liu WH; Roemer SC; Zhou Y; Shen Z-J; Dennehey BK; Balsbaugh JL; Liddle JC; Nemkov T; Ahn NG; Hansen KC, The Cac1 subunit of histone chaperone CAF-1 organizes CAF-1-H3/H4 architecture and tetramerizes histones. Elife 2016, 5, e18023. [PubMed: 27690308]

834. Mysling S; Kristensen KK; Larsson M; Beigneux AP; Gårdsvoll H; Fong LG; Bensadouen A; Jørgensen TJ; Young SG; Ploug M, The acidic domain of the endothelial membrane protein GPIHBP1 stabilizes lipoprotein lipase activity by preventing unfolding of its catalytic domain. Elife 2016, 5, e12095. [PubMed: 26725083]

835. Zanphorlin LM; Lima TB; Wong MJ; Balbuena TS; Minetti CA; Remeta DP; Young JC; Barbosa LR; Gozzo FC; Ramos CH, Heat shock protein 90 kDa (Hsp90) has a second functional interaction site with the mitochondrial import receptor Tom70. Journal of Biological Chemistry 2016, 291 (36), 18620–18631. [PubMed: 27402847]

836. Aprahamian ML; Lindert S, Utility of Covalent Labeling Mass Spectrometry Data in Protein Structure Prediction with Rosetta. Journal of Chemical Theory and Computation 2019, 15 (5), 3410–3424. [PubMed: 30946594]

837. Kaltashov IA; Bobst CE; Abzalimov RR; Berkowitz SA; Houde D, Conformation and Dynamics of Biopharmaceuticals: Transition of Mass Spectrometry-Based Tools from Academe to Industry. Journal of the American Society for Mass Spectrometry 2010, 21 (3), 323–337. [PubMed: 19963397]

838. Gau B; Garai K; Frieden C; Gross ML, Mass Spectrometry-Based Protein Footprinting Characterizes the Structures of Oligomeric Apolipoprotein E2, E3, and E4. Biochemistry 2011, 50 (38), 8117–8126. [PubMed: 21848287]

839. Liu T; Limpikirati P; Vachet RW, Synergistic Structural Information from Covalent Labeling and Hydrogen–Deuterium Exchange Mass Spectrometry for Protein–Ligand Interactions. Analytical Chemistry 2019.

840. Hager-Braun C; Tomer KB, Characterization of the Tertiary Structure of Soluble CD4 Bound to Glycosylated Full-Length HIVgp120 by Chemical Modification of Arginine Residues and Mass Spectrometric Analysis. Biochemistry 2002, 41 (6), 1759–1766. [PubMed: 11827520]

841. Hambly DM; Gross ML, Laser flash photolysis of hydrogen peroxide to oxidize protein solvent-accessible residues on the microsecond timescale. J Am Soc Mass Spectrom 2005, 16 (12), 2057–63. [PubMed: 16263307]

842. Murphy Michael P., How mitochondria produce reactive oxygen species. Biochemical Journal 2009, 417 (1), 1–13. [PubMed: 19061483]

843. Apel K; Hirt H, REACTIVE OXYGEN SPECIES: Metabolism, Oxidative Stress, and Signal Transduction. Annual Review of Plant Biology 2004, 55 (1), 373–399.

844. D'Autréaux B; Toledano MB, ROS as signalling molecules: mechanisms that generate specificity in ROS homeostasis. Nature Reviews Molecular Cell Biology 2007, 8, 813. [PubMed: 17848967]

845. Takamoto K; Chance MR, RADIOLYTIC PROTEIN FOOTPRINTING WITH MASS SPECTROMETRY TO PROBE THE STRUCTURE OF MACROMOLECULAR COMPLEXES. Annual Review of Biophysics and Biomolecular Structure 2006, 35 (1), 251–276.

846. Buxton GV; Greenstock CL; Helman WP; Ross AB, Critical Review of rate constants for reactions of hydrated electrons, hydrogen atoms and hydroxyl radicals (·OH/·O− in Aqueous Solution. Journal of Physical and Chemical Reference Data 1988, 17 (2), 513–886.

847. Garrison WM, Reaction mechanisms in the radiolysis of peptides, polypeptides, and proteins. Chemical Reviews 1987, 87 (2), 381–398.

848. Fenton HJH, LXXIII.—Oxidation of tartaric acid in presence of iron. Journal of the Chemical Society, Transactions 1894, 65 (0), 899–910.

849. Masarwa A; Rachmilovich-Calis S; Meyerstein N; Meyerstein D, Oxidation of organic substrates in aerated aqueous solutions by the Fenton reagent. Coordination Chemistry Reviews 2005, 249 (17), 1937–1943.

850. Kryatov SV; Rybak-Akimova EV; Schindler S, Kinetics and Mechanisms of Formation and Reactivity of Non-heme Iron Oxygen Intermediates. Chemical Reviews 2005, 105 (6), 2175–2226. [PubMed: 15941212]

851. Goldstein S; Meyerstein D; Czapski G, The Fenton reagents. Free Radical Biology and Medicine 1993, 15 (4), 435–445. [PubMed: 8225025]

852. Sawyer DT; Sobkowiak A; Matsushita T, Metal [MLx; M = Fe, Cu, Co, Mn]/Hydroperoxide-Induced Activation of Dioxygen for the Oxygenation of Hydrocarbons: Oxygenated Fenton Chemistry. Accounts of Chemical Research 1996, 29 (9), 409–416.

853. Haber F; Weiss J, Über die Katalyse des Hydroperoxydes. Naturwissenschaften 1932, 20 (51), 948–950.

854. Haber F; Weiss J; Pope WJ, The catalytic decomposition of hydrogen peroxide by iron salts. Proceedings of the Royal Society of London. Series A - Mathematical and Physical Sciences 1934, 147 (861), 332–351.

855. Barb WG; Baxendale JH; George P; Hargrave KR, Reactions of ferrous and ferric ions with hydrogen peroxide. Part I.—The ferrous ion reaction. Transactions of the Faraday Society 1951, 47 (0), 462–500.

856. Barb WG; Baxendale JH; George P; Hargrave KR, Reactions of ferrous and ferric ions with hydrogen peroxide. Part II.—The ferric ion reaction. Transactions of the Faraday Society 1951, 47 (0), 591–616.

857. Tullius T; Dombroski B, Iron(II) EDTA used to measure the helical twist along any DNA molecule. Science 1985, 230 (4726), 679–681. [PubMed: 2996145]

858. Tullius TD; Dombroski BA, Hydroxyl radical "footprinting": high-resolution information about DNA-protein contacts and application to lambda repressor and Cro protein. Proceedings of the National Academy of Sciences 1986, 83 (15), 5469–5473.

859. Pogozelski WK; McNeese TJ; Tullius TD, What Species Is Responsible for Strand Scission in the Reaction of [FeIIEDTA]2- and H2O2 with DNA? Journal of the American Chemical Society 1995, 117 (24), 6428–6433.

860. Baron CP; Refsgaard HHF; Skibsted LH; Andersen ML, Oxidation of bovine serum albumin initiated by the Fenton reaction—effect of EDTA, tert-butylhydroperoxide and tetrahydrofuran. Free Radical Research 2006, 40 (4), 409–417. [PubMed: 16517506]

861. Tullius TD; Greenbaum JA, Mapping nucleic acid structure by hydroxyl radical cleavage. Current Opinion in Chemical Biology 2005, 9 (2), 127–134. [PubMed: 15811796]

862. Heyduk E; Heyduk T, Mapping Protein Domains Involved in Macromolecular Interactions: A Novel Protein Footprinting Approach. Biochemistry 1994, 33 (32), 9643–9650. [PubMed: 8068641]

863. Sharp JS; Becker JM; Hettich RL, Protein surface mapping by chemical oxidation: Structural analysis by mass spectrometry. Analytical Biochemistry 2003, 313 (2), 216–225. [PubMed: 12605858]

864. Monroe EB; Heien ML, Electrochemical Generation of Hydroxyl Radicals for Examining Protein Structure. Analytical Chemistry 2013, 85 (13), 6185–6189. [PubMed: 23777226]

865. Rana TM; Meares CF, Specific cleavage of a protein by an attached iron chelate. Journal of the American Chemical Society 1990, 112 (6), 2457–2458.

866. Rana TM; Meares CF, Iron chelate mediated proteolysis: protein structure dependence. Journal of the American Chemical Society 1991, 113 (5), 1859–1861.

867. Rana TM; Meares CF, Transfer of oxygen from an artificial protease to peptide carbon during proteolysis. Proceedings of the National Academy of Sciences 1991, 88 (23), 10578–10582.

868. Heilek GM; Noller HF, Site-Directed Hydroxyl Radical Probing of the rRNA Neighborhood of Ribosomal Protein S5. Science 1996, 272 (5268), 1659–1662. [PubMed: 8658142]

869. Lancaster L; Kiel MC; Kaji A; Noller HF, Orientation of Ribosome Recycling Factor in the Ribosome from Directed Hydroxyl Radical Probing. Cell 2002, 111 (1), 129–140. [PubMed: 12372306]

870. Duval M; Marenna A; Chevalier C; Marzi S, Site-Directed Chemical Probing to map transient RNA/protein interactions. Methods 2017, 117, 48–58. [PubMed: 28027957]

871. Cheal SM; Ng M; Barrios B; Miao Z; Kalani AK; Meares CF, Mapping Protein–Protein Interactions by Localized Oxidation: Consequences of the Reach of Hydroxyl Radical. Biochemistry 2009, 48 (21), 4577–4586. [PubMed: 19354299]

872. Li Q; Xie Y; Xu G; Lebrilla CB, Identification of potential sialic acid binding proteins on cell membranes by proximity chemical labeling. Chemical Science 2019, 10 (24), 6199–6209. [PubMed: 31360427]

873. Zhu Y; Guo T; Park JE; Li X; Meng W; Datta A; Bern M; Lim SK; Sze SK, Elucidating in Vivo Structural Dynamics in Integral Membrane Protein by Hydroxyl Radical Footprinting. Molecular & Cellular Proteomics 2009, 8 (8), 1999–2010. [PubMed: 19473960]

874. Petit A; Mwale F; Tkaczyk C; Antoniou J; Zukor DJ; Huk OL, Induction of protein oxidation by cobalt and chromium ions in human U937 macrophages. Biomaterials 2005, 26 (21), 4416–4422. [PubMed: 15701370]

875. Bridgewater JD; Lim J; Vachet RW, Transition Metal–Peptide Binding Studied by Metal-Catalyzed Oxidation Reactions and Mass Spectrometry. Analytical Chemistry 2006, 78 (7), 2432–2438. [PubMed: 16579630]

876. Lim J; Vachet RW, Development of a Methodology Based on Metal-Catalyzed Oxidation Reactions and Mass Spectrometry To Determine the Metal Binding Sites in Copper Metalloproteins. Analytical Chemistry 2003, 75 (5), 1164–1172. [PubMed: 12641237]

877. Lim J; Vachet RW, Using Mass Spectrometry To Study Copper–Protein Binding under Native and Non-Native Conditions: β-2-Microglobulin. Analytical Chemistry 2004, 76 (13), 3498–3504. [PubMed: 15228316]

878. Gau BC; Sharp JS; Rempel DL; Gross ML, Fast Photochemical Oxidation of Protein Footprints Faster than Protein Unfolding. Analytical Chemistry 2009, 81 (16), 6563–6571. [PubMed: 20337372]

879. Shcherbakova I; Mitra S; Beer RH; Brenowitz M, Fast Fenton footprinting: a laboratory-based method for the time-resolved analysis of DNA, RNA and proteins. Nucleic Acids Research 2006, 34 (6), e48–e48. [PubMed: 16582097]

880. Sclavi B; Sullivan M; Chance MR; Brenowitz M; Woodson SA, RNA Folding at Millisecond Intervals by Synchrotron Hydroxyl Radical Footprinting. Science 1998, 279 (5358), 1940–1943. [PubMed: 9506944]

881. Sclavi B; Woodson S; Sullivan M; Chance MR; Brenowitz M, Time-resolved synchrotron X-ray “footprinting”, a new approach to the study of nucleic acid structure and function: application to protein-DNA interactions and RNA folding 1 1 Edited by D. E. Draper. Journal of Molecular Biology 1997, 266 (1), 144–159. [PubMed: 9054977]

882. Chance MR; Sclavi B; Woodson SA; Brenowitz M, Examining the conformational dynamics of macromolecules with time-resolved synchrotron X-ray ‘footprinting’. Structure 1997, 5 (7), 865–869. [PubMed: 9261085]

883. Sclavi B; Woodson S; Sullivan M; Chance M; Brenowitz M, [19] Following the folding of RNA with time-resolved synchrotron X-ray footprinting In Methods in Enzymology, Academic Press: 1998; Vol. 295, pp 379–402. [PubMed: 9750229]

884. Maleknia SD; Brenowitz M; Chance MR, Millisecond Radiolytic Modification of Peptides by Synchrotron X-rays Identified by Mass Spectrometry. Analytical Chemistry 1999, 71 (18), 3965–3973. [PubMed: 10500483]

885. Simic MG, [2] Pulse radiolysis in study of oxygen radicals In Methods in Enzymology, Academic Press: 1990; Vol. 186, pp 89–100. [PubMed: 2172727]

886. Gupta S; Sullivan M; Toomey J; Kiselar J; Chance MR, The Beamline X28C of the Center for Synchrotron Biosciences: a National Resource for Biomolecular Structure and Dynamics Experiments Using Synchrotron Footprinting. Journal of Synchrotron Radiation 2007, 14 (3), 233–243. [PubMed: 17435298]

887. Asuru A; Farquhar ER; Sullivan M; Abel D; Toomey J; Chance MR; Bohon J, The XFP (17-BM) beamline for X-ray footprinting at NSLS-II. Journal of Synchrotron Radiation 2019, 26 (4), 1388–1399. [PubMed: 31274468]

888. Weeks JL; Matheson MS, The Primary Quantum Yield of Hydrogen Peroxide Decomposition1. Journal of the American Chemical Society 1956, 78 (7), 1273–1278.

889. Dainton FS, The Primary Quantum Yield in the Photolysis of Hydrogen Peroxide at 3130 Å. and the Primary Radical Yield in the X- and γ-Radiolysis of Water. Journal of the American Chemical Society 1956, 78 (7), 1278–1279.

890. Sharp JS; Becker JM; Hettich RL, Analysis of Protein Solvent Accessible Surfaces by Photochemical Oxidation and Mass Spectrometry. Analytical Chemistry 2004, 76 (3), 672–683. [PubMed: 14750862]

891. Aye TT; Low TY; Sze SK, Nanosecond Laser-Induced Photochemical Oxidation Method for Protein Surface Mapping with Mass Spectrometry. Analytical Chemistry 2005, 77 (18), 5814–5822. [PubMed: 16159110]

892. Hambly DM; Gross ML, Cold Chemical Oxidation of Proteins. Analytical Chemistry 2009, 81 (17), 7235–7242. [PubMed: 19715356]

893. Jiawei Chen DLR, and Michael L Gross, Temperature Jump and Fast Photochemical Oxidation Probe Submillisecond Protein Folding. J. Am. Chem. Soc 2010, 132, 15502–15504. [PubMed: 20958033]

894. Chen J; Rempel DL; Gau BC; Gross ML, Fast Photochemical Oxidation of Proteins and Mass Spectrometry Follow Submillisecond Protein Folding at the Amino-Acid Level. Journal of the American Chemical Society 2012, 134 (45), 18724–18731. [PubMed: 23075429]

895. Zhang Y; Rempel DL; Zhang H; Gross ML, An Improved Fast Photochemical Oxidation of Proteins (FPOP) Platform for Protein Therapeutics. Journal of The American Society for Mass Spectrometry 2015, 26 (3), 526–529. [PubMed: 25519854]

896. Liu XR; Zhang MM; Zhang B; Rempel DL; Gross ML, Hydroxyl-Radical Reaction Pathways for the Fast Photochemical Oxidation of Proteins Platform As Revealed by 18O Isotopic Labeling. Analytical Chemistry 2019, 91 (14), 9238–9245. [PubMed: 31241913]

897. Vahidi S; Konermann L, Probing the Time Scale of FPOP (Fast Photochemical Oxidation of Proteins): Radical Reactions Extend Over Tens of Milliseconds. Journal of The American Society for Mass Spectrometry 2016, 27 (7), 1156–1164. [PubMed: 27067899]

898. Sheng Y; Capri J; Waring A; Valentine JS; Whitelegge J, Exposure of Solvent-Inaccessible Regions in the Amyloidogenic Protein Human SOD1 Determined by Hydroxyl Radical Footprinting. Journal of The American Society for Mass Spectrometry 2019, 30 (2), 218–226. [PubMed: 30328005]

899. Maleknia SD; Chance MR; Downard KM, Electrospray-assisted modification of proteins: a radical probe of protein structure. Rapid Communications in Mass Spectrometry 1999, 13 (23), 2352–2358. [PubMed: 10567934]

900. Maleknia SD; Wong JWH; Downard KM, Photochemical and electrophysical production of radicals on millisecond timescales to probe the structure, dynamics and interactions of proteins. Photochemical & Photobiological Sciences 2004, 3 (8), 741–748. [PubMed: 15295629]

901. Maleknia SD; Downard KM, Advances in radical probe mass spectrometry for protein footprinting in chemical biology applications. Chemical Society Reviews 2014, 43 (10), 3244–3258. [PubMed: 24590115]

902. Thomas MC; Mitchell TW; Blanksby SJ, Ozonolysis of Phospholipid Double Bonds during Electrospray Ionization: A New Tool for Structure Determination. Journal of the American Chemical Society 2006, 128 (1), 58–59. [PubMed: 16390120]

903. Wong JWH; Maleknia SD; Downard KM, Study of the Ribonuclease–S-Protein–Peptide Complex Using a Radical Probe and Electrospray Ionization Mass Spectrometry. Analytical Chemistry 2003, 75 (7), 1557–1563. [PubMed: 12705585]

904. Wong JWH; Maleknia SD; Downard KM, Hydroxyl radical probe of the calmodulin-melittin complex interface by electrospray ionization mass spectrometry. Journal of the American Society for Mass Spectrometry 2005, 16 (2), 225–233. [PubMed: 15694772]

905. Maleknia SD; Downard KM, On-plate deposition of oxidized proteins to facilitate protein footprinting studies by radical probe mass spectrometry. Rapid Communications in Mass Spectrometry 2012, 26 (19), 2311–2318. [PubMed: 22956323]

906. Lin H; Kitova EN; Johnson MA; Eugenio L; Ng KKS; Klassen JS, Electrospray Ionization-Induced Protein Unfolding. Journal of The American Society for Mass Spectrometry 2012, 23 (12), 2122–2131. [PubMed: 22993046]

907. Minkoff BB; Blatz JM; Choudhury FA; Benjamin D; Shohet JL; Sussman MR, Plasma-Generated OH Radical Production for Analyzing Three-Dimensional Structure in Protein Therapeutics. Scientific Reports 2017, 7 (1), 12946. [PubMed: 29021557]

908. LaVerne JA, OH Radicals and Oxidizing Products in the Gamma Radiolysis of Water. Radiation Research 2000, 153 (2), 196–200, 5. [PubMed: 10629619]

909. Hayes JJ; Kam L; Tullius TD, [56] Footprinting protein-DNA complexes with γ-rays In Methods in Enzymology, Academic Press: 1990; Vol. 186, pp 545–549. [PubMed: 2172714]

910. Nukuna BN; Sun G; Anderson VE, Hydroxyl radical oxidation of cytochrome c by aerobic radiolysis. Free Radical Biology and Medicine 2004, 37 (8), 1203–1213. [PubMed: 15451060]

911. Xu G; Kiselar J; He Q; Chance MR, Secondary Reactions and Strategies To Improve Quantitative Protein Footprinting. Analytical Chemistry 2005, 77 (10), 3029–3037. [PubMed: 15889890]

912. Xu G; Chance MR, Radiolytic modification and reactivity of amino acid residues serving as structural probes for protein footprinting. Analytical chemistry 2005, 77 (14), 4549–4555. [PubMed: 16013872]

913. Sharp JS; Tomer KB, Effects of Anion Proximity in Peptide Primary Sequence on the Rate and Mechanism of Leucine Oxidation. Analytical Chemistry 2006, 78 (14), 4885–4893. [PubMed: 16841907]

914. Tong X; Wren JC; Konermann L, Effects of Protein Concentration on the Extent of γ-Ray-Mediated Oxidative Labeling Studied by Electrospray Mass Spectrometry. Analytical Chemistry 2007, 79 (16), 6376–6382. [PubMed: 17628115]

915. Sharp JS; Tomer KB, Analysis of the Oxidative Damage-Induced Conformational Changes of Apo- and Holocalmodulin by Dose-Dependent Protein Oxidative Surface Mapping. Biophysical Journal 2007, 92 (5), 1682–1692. [PubMed: 17158574]

916. Tong X; Wren JC; Konermann L, γ-Ray-Mediated Oxidative Labeling for Detecting Protein Conformational Changes by Electrospray Mass Spectrometry. Analytical Chemistry 2008, 80 (6), 2222–2231. [PubMed: 18260674]

917. Fang X; Mark G; von Sonntag C, OH radical formation by ultrasound in aqueous solutions Part I: the chemistry underlying the terephthalate dosimeter. Ultrasonics Sonochemistry 1996, 3 (1), 57–63.

918. Mark G; Tauber A; Laupert R; Schuchmann H-P; Schulz D; Mues A; von Sonntag C, OH-radical formation by ultrasound in aqueous solution – Part II: Terephthalate and Fricke dosimetry and the influence of various conditions on the sonolytic yield. Ultrasonics Sonochemistry 1998, 5 (2), 41–52. [PubMed: 11270336]

919. Spotheim-Maurizot M; Charlier M; Sabattier R, DNA Radiolysis by Fast Neutrons. International Journal of Radiation Biology 1990, 57 (2), 301–313. [PubMed: 1968496]

920. Spotheim-Maurizot M; Franchet J; Sabattier R; Charlier M, DNA Radiolysis by Fast Neutrons. II. Oxygen, Thiols and Ionic Strength Effects. International Journal of Radiation Biology 1991, 59 (6), 1313–1324. [PubMed: 1677378]

921. Franchet-Beuzit J; Spotheim-Maurizot M; Sabattier R; Blazy-Baudras B; Charlier M, Radiolytic footprinting. .beta. Rays, .gamma. photons, and fast neutrons probe DNA-protein interactions. Biochemistry 1993, 32 (8), 2104–2110. [PubMed: 8383534]

922. King PA; Jamison E; Strahs D; Anderson VE; Brenowitz M, 'Footprinting' proteins on DNA with peroxonitrous acid. Nucleic Acids Research 1993, 21 (10), 2473–2478. [PubMed: 8389444]

923. Coddington JW; Hurst JK; Lymar SV, Hydroxyl Radical Formation during Peroxynitrous Acid Decomposition. Journal of the American Chemical Society 1999, 121 (11), 2438–2443.

924. Watson C; Janik I; Zhuang T; Charvátová O; Woods RJ; Sharp JS, Pulsed Electron Beam Water Radiolysis for Submicrosecond Hydroxyl Radical Protein Footprinting. Analytical Chemistry 2009, 81 (7), 2496–2505. [PubMed: 19265387]

925. Chaulk SG; Pezacki JP; MacMillan AM, Studies of RNA Cleavage by Photolysis of N-Hydroxypyridine-2(1H)-thione. A New Photochemical Footprinting Method. Biochemistry 2000, 39 (34), 10448–10453. [PubMed: 10956035]

926. Kelly JJ; Chernov BK; Tovstanovsky I; Mirzabekov AD; Bavykin SG, Radical-generating coordination complexes as tools for rapid and effective fragmentation and fluorescent labeling of nucleic acids for microchip hybridization. Analytical Biochemistry 2002, 311 (2), 103–118. [PubMed: 12470669]

927. McClintock CS; Hettich RL, Experimental Approach to Controllably Vary Protein Oxidation While Minimizing Electrode Adsorption for Boron-Doped Diamond Electrochemical Surface Mapping Applications. Analytical Chemistry 2013, 85 (1), 213–219. [PubMed: 23210708]

928. Xu G; Takamoto K; Chance MR, Radiolytic Modification of Basic Amino Acid Residues in Peptides: Probes for Examining Protein–Protein Interactions. Analytical Chemistry 2003, 75 (24), 6995–7007. [PubMed: 14670063]

929. Xu G; Chance MR, Radiolytic Modification of Acidic Amino Acid Residues in Peptides: Probes for Examining Protein–Protein Interactions. Analytical Chemistry 2004, 76 (5), 1213–1221. [PubMed: 14987073]

930. Xu G; Chance MR, Radiolytic Modification of Sulfur-Containing Amino Acid Residues in Model Peptides: Fundamental Studies for Protein Footprinting. Analytical Chemistry 2005, 77 (8), 2437–2449. [PubMed: 15828779]

931. Karmakar T; Balasubramanian S, Elucidating the interaction of H2O2 with polar amino acids – Quantum chemical calculations. Chemical Physics Letters 2014, 613, 5–9.

932. Davies M; Dean R; Davies D, Radical-Mediated Protein Oxidation: From Chemistry to Medicine 1997 Oxford University Press: New York, NY.

933. Xiao R; Liu K; Bai L; Minakata D; Seo Y; Göktaş RK; Dionysiou DD; Tang C-J; Wei Z; Spinney R, Inactivation of pathogenic microorganisms by sulfate radical: Present and future. Chemical Engineering Journal 2019.

934. Davies MJ, Protein oxidation and peroxidation. Biochemical Journal 2016, 473 (7), 805–825. [PubMed: 27026395]

935. Fancy DA; Kodadek T, Chemistry for the analysis of protein–protein interactions: rapid and efficient cross-linking triggered by long wavelength light. Proceedings of the National Academy of Sciences 1999, 96 (11), 6020–6024.

936. Borsarelli CD; Falomir-Lockhart LJ; Ostatna V; Fauerbach JA; Hsiao H-H; Urlaub H; Paleček E; Jares-Erijman EA; Jovin TM, Biophysical properties and cellular toxicity of covalent crosslinked oligomers of α-synuclein formed by photoinduced side-chain tyrosyl radicals. Free Radical Biology and Medicine 2012, 53 (4), 1004–1015. [PubMed: 22771470]

937. Rayshell M; Ross J; Werbin H, Evidence that N-acetoxy-N-acetyl-2-aminofluorene crosslinks DNA to protein by a free radical mechanism. Carcinogenesis 1983, 4 (5), 501–507. [PubMed: 6342830]

938. Bridgewater JD; Vachet RW, Using microwave-assisted metal-catalyzed oxidation reactions and mass spectrometry to increase the rate at which the copper-binding sites of a protein are determined. Analytical chemistry 2005, 77 (14), 4649–4653. [PubMed: 16013884]

939. Bridgewater JD; Lim J; Vachet RW, Using metal-catalyzed oxidation reactions and mass spectrometry to identify amino acid residues within 10 Å of the metal in Cu-binding proteins. Journal of the American Society for Mass Spectrometry 2006, 17 (11), 1552–1559. [PubMed: 16872838]

940. Bridgewater JD; Vachet RW, Metal-catalyzed oxidation reactions and mass spectrometry: The roles of ascorbate and different oxidizing agents in determining Cu–protein-binding sites. Analytical biochemistry 2005, 341 (1), 122–130. [PubMed: 15866536]

941. Gau BC; Chen H; Zhang Y; Gross ML, Sulfate radical anion as a new reagent for fast photochemical oxidation of proteins. Analytical chemistry 2010, 82 (18), 7821–7827. [PubMed: 20738105]

942. Davies MJ; Gilbert BC; McCleland CW; Thomas CB; Young J, E.s.r. evidence for the multiplicity of side-chain oxidation pathways in the acid-catalysed decomposition of substituted hydroxycyclohexadienyl radicals. Journal of the Chemical Society, Chemical Communications 1984, (15), 966–967.

943. Davies MJ; Gilbert BC; Norman ROC, Electron spin resonance. Part 67. Oxidation of aliphatic sulphides and sulphoxides by the sulphate radical anion ($SO_4^{-\cdot}$) and of aliphatic radicals by the peroxydisulphate anion ($S_2O_8^{2-}$). Journal of the Chemical Society, Perkin Transactions 2 1984, (3), 503–509.

944. Rustgi SM; Riesz P, An E.S.R. and Spin-trapping Study of the Reactions of the $\dot{S}O_4^-$ Radical with Protein and Nucleic Acid Constituents. International Journal of Radiation Biology and Related Studies in Physics, Chemistry and Medicine 1978, 34 (4), 301–316.

945. Lu Y; Zhang H; Niedzwiedzki DM; Jiang J; Blankenship RE; Gross ML, Fast Photochemical Oxidation of Proteins Maps the Topology of Intrinsic Membrane Proteins: Light-Harvesting Complex 2 in a Nanodisc. Analytical Chemistry 2016, 88 (17), 8827–8834. [PubMed: 27500903]

946. Medinas DB; Cerchiaro G; Trindade DF; Augusto O, The carbonate radical and related oxidants derived from bicarbonate buffer. IUBMB Life 2007, 59 (4–5), 255–62. [PubMed: 17505962]

947. Sankarapandi S; Zweier JL, Bicarbonate Is Required for the Peroxidase Function of Cu,Zn-Superoxide Dismutase at Physiological pH. Journal of Biological Chemistry 1999, 274 (3), 1226–1232. [PubMed: 9880490]

948. Hodgson EK; Fridovich I, The mechanism of the activity-dependent luminescence of xanthine oxidase. Arch Biochem Biophys 1976, 172 (1), 202–5. [PubMed: 1252075]

949. Augusto O; Bonini MG; Amanso AM; Linares E; Santos CC; De Menezes SL, Nitrogen dioxide and carbonate radical anion: two emerging radicals in biology. Free Radic Biol Med 2002, 32 (9), 841–59. [PubMed: 11978486]

950. Radi R, Nitric oxide, oxidants, and protein tyrosine nitration. Proceedings of the National Academy of Sciences of the United States of America 2004, 101 (12), 4003–4008. [PubMed: 15020765]

951. Paviani V; Queiroz RF; Marques EF; Di Mascio P; Augusto O, Production of lysozyme and lysozyme-superoxide dismutase dimers bound by a ditryptophan cross-link in carbonate radical-treated lysozyme. Free Radical Biology and Medicine 2015, 89, 72–82. [PubMed: 26197052]

952. Gebicka L; Didik J; Gebicki J, Reactions of heme proteins with carbonate radical anion. Res Chem Intermediat 2009, 35 (4), 401–409.

953. Shafirovich V; Dourandin A; Huang WD; Geacintov NE, The carbonate radical is a site-selective oxidizing agent of guanine in double-stranded oligonucleotides. Journal of Biological Chemistry 2001, 276 (27), 24621–24626. [PubMed: 11320091]

954. Chen SN; Hoffman MZ, Rate constants for the reaction of the carbonate radical with compounds of biochemical interest in neutral aqueous solution. Radiat Res 1973, 56 (1), 40–7. [PubMed: 4743729]

955. Medinas DB; Gozzo FC; Santos LF; Iglesias AH; Augusto O, A ditryptophan cross-link is responsible for the covalent dimerization of human superoxide dismutase 1 during its bicarbonate-dependent peroxidase activity. Free Radical Biology and Medicine 2010, 49 (6), 1046–1053. [PubMed: 20600836]

956. Coelho FR; Iqbal A; Linares E; Silva DF; Lima FS; Cuccovia IM; Augusto O, Oxidation of the tryptophan 32 residue of human superoxide dismutase 1 caused by its bicarbonate-dependent peroxidase activity triggers the non-amyloid aggregation of the enzyme. Journal of Biological Chemistry 2014, 289 (44), 30690–30701. [PubMed: 25237191]

957. Zhang MM; Rempel DL; Gross ML, A Fast Photochemical Oxidation of Proteins (FPOP) platform for free-radical reactions: the carbonate radical anion with peptides and proteins. Free Radical Biology and Medicine 2019, 131, 126–132. [PubMed: 30502457]

958. Chen S.-n.; Hoffman MZ, Rate Constants for the Reaction of the Carbonate Radical with Compounds of Biochemical Interest in Neutral Aqueous Solution. Radiation Research 1973, 56 (1), 40–47. [PubMed: 4743729]

959. Huie RE; Clifton CL; Neta P, Electron-Transfer Reaction-Rates and Equilibria of the Carbonate and Sulfate Radical-Anions. Radiation Physics and Chemistry 1991, 38 (5), 477–481.

960. Paulsen S, 3.3-Dialkyl-diazacyclopropen-(1). Angewandte Chemie 1960, 72 (21), 781–782.

961. Smith RA; Knowles JR, Aryldiazirines. Potential reagents for photolabeling of biological receptor sites. Journal of the American Chemical Society 1973, 95 (15), 5072–5073. [PubMed: 4741289]

962. Nicholas RA, Purification of the membrane-spanning tryptic peptides of the. alpha. polypeptide from (sodium and potassium ion)-activated adenosine triphosphatase labeled with 1-tritiospiro [adamantane-4, 1'-diazirine]. Biochemistry 1984, 23 (5), 888–898. [PubMed: 6324857]

963. Farley RA, Identification of hydrophobic regions of the calcium-transport ATPase from sarcoplasmic reticulum after photochemical labeling with adamantane diazirine. The International journal of biochemistry 1983, 15 (12), 1423–1427. [PubMed: 6228448]

964. Xi J; Liu R; Rossi MJ; Yang J; Loll PJ; Dailey WP; Eckenhoff RG, Photoactive analogues of the haloether anesthetics provide high-resolution features from low-affinity interactions. ACS chemical biology 2006, 1 (6), 377–384. [PubMed: 17163775]

965. Gomes AF; Gozzo FC, Chemical cross-linking with a diazirine photoactivatable cross-linker investigated by MALDI-and ESI-MS/MS. Journal of mass spectrometry 2010, 45 (8), 892–899. [PubMed: 20635431]

966. Richards FM; Lamed R; Wynn R; Patel D; Olack G, Methylene as a possible universal footprinting reagent that will include hydrophobic surface areas: Overview and feasibility: Properties of diazirine as a precursor. Protein Science 2000, 9 (12), 2506–2517. [PubMed: 11206072]

967. Jumper CC; Schriemer DC, Mass spectrometry of laser-initiated carbene reactions for protein topographic analysis. Analytical chemistry 2011, 83 (8), 2913–2920. [PubMed: 21425771]

968. Jumper CC; Bomgarden R; Rogers J; Etienne C; Schriemer DC, High-resolution mapping of carbene-based protein footprints. Analytical chemistry 2012, 84 (10), 4411–4418. [PubMed: 22480364]

969. Ziemianowicz DS; Bomgarden R; Etienne C; Schriemer DC, Amino acid insertion frequencies arising from photoproducts generated using aliphatic diazirines. Journal of the American Society for Mass Spectrometry 2017, 28 (10), 2011–2021. [PubMed: 28799075]

970. Blencowe A; Hayes W, Development and application of diazirines in biological and synthetic macromolecular systems. Soft Matter 2005, 1 (3), 178–205. [PubMed: 32646075]

971. Hu Y; Guo T; Ye X; Li Q; Guo M; Liu H; Wu Z, Dye adsorption by resins: Effect of ionic strength on hydrophobic and electrostatic interactions. Chemical Engineering Journal 2013, 228, 392–397.

972. Christen RP; Nomikos SI; Smith ET, Probing protein electrostatic interactions through temperature/reduction potential profiles. JBIC Journal of Biological Inorganic Chemistry 1996, 1 (6), 515–522.

973. Zhang B; Rempel DL; Gross ML, Protein Footprinting by Carbenes on a Fast Photochemical Oxidation of Proteins (FPOP) Platform. Journal of The American Society for Mass Spectrometry 2016, 27 (3), 552–555. [PubMed: 26679355]

974. Manzi L; Barrow AS; Scott D; Layfield R; Wright TG; Moses JE; Oldham NJ, Carbene footprinting accurately maps binding sites in protein–ligand and protein–protein interactions. Nature communications 2016, 7, 13288.

975. Irikura KK; Goddard W III; Beauchamp J, Singlet-triplet gaps in substituted carbenes CXY (X, Y= H, fluoro, chloro, bromo, iodo, silyl). Journal of the American Chemical Society 1992, 114 (1), 48–51.

976. Horspool WM; Lenci F, CRC Handbook of Organic Photochemistry and Photobiology, Volumes 1 & 2 CRC press: 2003.

977. Das J, Aliphatic diazirines as photoaffinity probes for proteins: recent developments. Chemical reviews 2011, 111 (8), 4405–4417. [PubMed: 21466226]

978. Bourissou D; Guerret O; Gabbai FP; Bertrand G, Stable carbenes. Chemical Reviews 2000, 100 (1), 39–92. [PubMed: 11749234]

979. Richards CA Jr; Kim S-J; Yamaguchi Y; Schaefer HF III, Dimethylcarbene: a singlet ground state? Journal of the American Chemical Society 1995, 117 (40), 10104–10107.

980. Bertrand G, Carbene chemistry: from fleeting intermediates to powerful reagents. CRC Press: 2002.

981. Chan KJ; O'Hagan D, The rare fluorinated natural products and biotechnological prospects for fluorine enzymology In Methods in enzymology, Elsevier: 2012; Vol. 516, pp 219–235. [PubMed: 23034231]

982. O'Hagan D, Understanding organofluorine chemistry. An introduction to the C–F bond. Chemical Society Reviews 2008, 37 (2), 308–319. [PubMed: 18197347]

983. Shannon RD, Revised effective ionic radii and systematic studies of interatomic distances in halides and chalcogenides. Acta crystallographica section A: crystal physics, diffraction, theoretical and general crystallography 1976, 32 (5), 751–767.

984. Müller K; Faeh C; Diederich F, Fluorine in pharmaceuticals: looking beyond intuition. Science 2007, 317 (5846), 1881–1886. [PubMed: 17901324]

985. Wofsy L; Metzger H; Singer S, Affinity labeling—a general method for labeling the active sites of antibody and enzyme molecules. Biochemistry 1962, 1 (6), 1031–1039. [PubMed: 14001461]

986. Brunner J; Senn H; Richards F, 3-Trifluoromethyl-3-phenyldiazirine. A new carbene generating group for photolabeling reagents. Journal of Biological Chemistry 1980, 255 (8), 3313–3318. [PubMed: 7364745]

987. Emeleus H; Haszeldine R, 623. Organometallic fluorine compounds. Part I. The synthesis of trifluoromethyl and pentafluoroethyl mercurials. Journal of the Chemical Society (Resumed) 1949, 2948–2952.

988. Naumann D; Kischkewitz J, Trifluormethylierungsreaktionen von Te(CF3)2 mit halogenbenzolen und methylbenzolen [1]. Journal of Fluorine Chemistry 1990, 47 (2), 283–299.

989. Lane SI; Oexler EV; Staricco EH, The Gas-Phase Reaction of Cf3 Radicals with C6f5h in the Temperature-Range 373–658-K. Int J Chem Kinet 1991, 23 (5), 361–367.

990. Charpentier J; Früh N; Togni A, Electrophilic Trifluoromethylation by Use of Hypervalent Iodine Reagents. Chemical Reviews 2015, 115 (2), 650–682. [PubMed: 25152082]

991. Teruo U; Sumi I, Power-variable trifluoromethylating agents, (trifluoromethyl)dibenzothio- and -selenophenium salt system. Tetrahedron Letters 1990, 31 (25), 3579–3582.

992. Mizuta S; Verhoog S; Engle KM; Khotavivattana T; O'duill M; Wheelhouse K; Rassias G; Médebielle M; Gouverneur V. r., Catalytic hydrotrifluoromethylation of unactivated alkenes. Journal of the American Chemical Society 2013, 135 (7), 2505–2508. [PubMed: 23373772]

993. Mizuta S; Engle KM; Verhoog S; Galicia-López O; O'Duill M; Médebielle M; Wheelhouse K; Rassias G; Thompson AL; Gouverneur V, Trifluoromethylation of allylsilanes under photoredox catalysis. Organic letters 2013, 15 (6), 1250–1253. [PubMed: 23465076]

994. Chaabouni S; Simonet F; François A; Abid S; Galaup C; Chassaing S, 3-Trifluoromethylated Coumarins and Carbostyrils by Radical Trifluoromethylation of ortho-Functionalized Cinnamic Esters. European Journal of Organic Chemistry 2017, 2017 (2), 271–277.

995. Langlois BR; Laurent E; Roidot N, Trifluoromethylation of aromatic compounds with sodium trifluoromethanesulfinate under oxidative conditions. Tetrahedron Letters 1991, 32 (51), 7525–7528.

996. Ji Y; Brueckl T; Baxter RD; Fujiwara Y; Seiple IB; Su S; Blackmond DG; Baran PS, Innate CH trifluoromethylation of heterocycles. Proceedings of the National Academy of Sciences 2011, 108 (35), 14411–14415.

997. Fujiwara Y; Dixon JA; O'Hara F; Funder ED; Dixon DD; Rodriguez RA; Baxter RD; Herle B; Sach N; Collins MR, Practical and innate carbon–hydrogen functionalization of heterocycles. Nature 2012, 492 (7427), 95. [PubMed: 23201691]

998. Fennewald JC; Lipshutz BH, Trifluoromethylation of heterocycles in water at room temperature. Green Chemistry 2014, 16 (3), 1097–1100. [PubMed: 24839397]

999. Cheng M; Zhang B; Cui W; Gross ML, Laser-Initiated Radical Trifluoromethylation of Peptides and Proteins: Application to Mass-Spectrometry-Based Protein Footprinting. Angewandte Chemie International Edition 2017, 56 (45), 14007–14010. [PubMed: 28901679]

1000. Winkler R, Iodine—a potential antioxidant and the role of Iodine/Iodide in health and disease. Natural Science 2015, 7 (12), 548.

1001. Cavalieri RR, Iodine metabolism and thyroid physiology: current concepts. Thyroid 1997, 7 (2), 177–181. [PubMed: 9133680]

1002. Soundarrajan M; Kopp PA, Thyroid Hormone Biosynthesis and Physiology In Thyroid Disease and Reproduction, Springer: 2019; pp 1–17.

1003. Kessler J; Obinger C; Eales G, Factors influencing the study of peroxidase-generated iodine species and implications for thyroglobulin synthesis. Thyroid 2008, 18 (7), 769–774. [PubMed: 18631006]

1004. Rousset B; Dupuy C; Miot F; Dumont J, Thyroid hormone synthesis and secretion In Endotext [Internet], MDText. com, Inc: 2015.

1005. Verma S; Kumar GP; Laloraya M; Singh A, Activation of iodine into a free-radical intermediate by superoxide: a physiologically significant step in the iodination of tyrosine. Biochemical and biophysical research communications 1990, 170 (3), 1026–1034. [PubMed: 2167666]

1006. Goldsmith SJ In Radioimmunoassay: Review of basic principles, Seminars in nuclear medicine, Elsevier: 1975; pp 125–152.

1007. Béhé M; Gotthardt M; Behr TM, Chapter 20 - Radioiodination of Proteins and Peptides In Cell Biology (Third Edition), Celis JE, Ed. Academic Press: Burlington, 2006; pp 149–154.

1008. Caldwell HD; Kromhout J; Schachter J, Purification and partial characterization of the major outer membrane protein of Chlamydia trachomatis. Infection and immunity 1981, 31 (3), 1161–1176. [PubMed: 7228399]

1009. Hatch TP; Vance D; Al-Hossainy E, Identification of a major envelope protein in Chlamydia spp. Journal of bacteriology 1981, 146 (1), 426–429. [PubMed: 7217005]

1010. Rupp WD; Prusoff WH, Photochemistry of iodouracil. II Effects of sulfur compounds, ethanol and oxygen. Biochemical and biophysical research communications 1965, 18 (2), 158–164. [PubMed: 14282011]

1011. Watanabe T; Bando T; Xu Y; Tashiro R; Sugiyama H, Efficient Generation of 2 '-Deoxyuridin-5-yl at 5 '-(G/C) AAXUXU-3 '(X= Br, I) Sequences in Duplex DNA under UV Irradiation. Journal of the American Chemical Society 2005, 127 (1), 44–45. [PubMed: 15631440]

1012. Xu Y; Sugiyama H, Photochemical approach to probing different DNA structures. Angewandte Chemie International Edition 2006, 45 (9), 1354–1362. [PubMed: 16416452]

1013. Dai X; Song D; Liu K; Su H, Photoinduced C—I bond homolysis of 5-iodouracil: A singlet predissociation pathway. The Journal of chemical physics 2017, 146 (2), 025103. [PubMed: 28088146]

1014. Ly T; Julian RR, Residue-specific radical-directed dissociation of whole proteins in the gas phase. Journal of the American Chemical Society 2008, 130 (1), 351–358. [PubMed: 18078340]

1015. Ly T; Julian RR, Elucidating the tertiary structure of protein ions in vacuo with site specific photoinitiated radical reactions. Journal of the American Chemical Society 2010, 132 (25), 8602–8609. [PubMed: 20524634]

1016. Tao Y; Quebbemann NR; Julian RR, Discriminating D-amino acid-containing peptide epimers by radical-directed dissociation mass spectrometry. Analytical chemistry 2012, 84 (15), 6814–6820. [PubMed: 22812429]

1017. Ranka K; Zhao N; Yu L; Stanton JF; Polfer NC, Radical Rearrangement Chemistry in Ultraviolet Photodissociation of Iodotyrosine Systems: Insights from Metastable Dissociation, Infrared Ion Spectroscopy, and Reaction Pathway Calculations. Journal of The American Society for Mass Spectrometry 2018, 29 (9), 1791–1801. [PubMed: 29845561]

1018. Li CH, Kinetics of reactions between iodine and histidine. Journal of the American Chemical Society 1944, 66 (2), 225–227.

1019. Chen J; Rempel DL; Gross ML, Temperature jump and fast photochemical oxidation probe submillisecond protein folding. Journal of the American Chemical Society 2010, 132 (44), 15502–15504. [PubMed: 20958033]

1020. Li KS; Rempel DL; Gross ML, Conformational-Sensitive Fast Photochemical Oxidation of Proteins and Mass Spectrometry Characterize Amyloid Beta 1–42 Aggregation. Journal of the American Chemical Society 2016, 138 (37), 12090–12098. [PubMed: 27568528]

1021. KÖHler G; Milstein C, Continuous cultures of fused cells secreting antibody of predefined specificity. Nature 1975, 256 (5517), 495–497. [PubMed: 1172191]

1022. Coons AH; Creech HJ; Jones RN, Immunological Properties of an Antibody Containing a Fluorescent Group. Proceedings of the Society for Experimental Biology and Medicine 1941, 47 (2), 200–202.

1023. Engvall E; Perlmann P, Enzyme-Linked Immunosorbent Assay, Elisa. III. Quantitation of Specific Antibodies by Enzyme-Labeled Anti-Immunoglobulin in Antigen-Coated Tubes 1972, 109 (1), 129–135.

1024. Burnette WN, "Western Blotting": Electrophoretic transfer of proteins from sodium dodecyl sulfate-polyacrylamide gels to unmodified nitrocellulose and radiographic detection with

antibody and radioiodinated protein A. Analytical Biochemistry 1981, 112 (2), 195–203. [PubMed: 6266278]

1025. Adams GP; Weiner LM, Monoclonal antibody therapy of cancer. Nature Biotechnology 2005, 23, 1147.

1026. Scott AM; Wolchok JD; Old LJ, Antibody therapy of cancer. Nature Reviews Cancer 2012, 12, 278. [PubMed: 22437872]

1027. Wang W; Singh S; Zeng DL; King K; Nema S, Antibody structure, instability, and formulation. Journal of Pharmaceutical Sciences 2007, 96 (1), 1–26. [PubMed: 16998873]

1028. Tonegawa S, Somatic generation of antibody diversity. Nature 1983, 302 (5909), 575–581. [PubMed: 6300689]

1029. Van Regenmortel MHV, Mapping Epitope Structure and Activity: From One-Dimensional Prediction to Four-Dimensional Description of Antigenic Specificity. Methods 1996, 9 (3), 465–472. [PubMed: 8812702]

1030. Barlow DJ; Edwards MS; Thornton JM, Continuous and discontinuous protein antigenic determinants. Nature 1986, 322 (6081), 747–748. [PubMed: 2427953]

1031. Amit A; Mariuzza R; Phillips S; Poljak R, Three-dimensional structure of an antigen-antibody complex at 2.8 A resolution. Science 1986, 233 (4765), 747–753. [PubMed: 2426778]

1032. Mayer M; Meyer B, Characterization of Ligand Binding by Saturation Transfer Difference NMR Spectroscopy. Angewandte Chemie International Edition 1999, 38 (12), 1784–1788. [PubMed: 29711196]

1033. Cunningham B; Wells J, High-resolution epitope mapping of hGH-receptor interactions by alanine-scanning mutagenesis. Science 1989, 244 (4908), 1081–1085. [PubMed: 2471267]

1034. Geysen HM; Meloen RH; Barteling SJ, Use of peptide synthesis to probe viral antigens for epitopes to a resolution of a single amino acid. Proceedings of the National Academy of Sciences 1984, 81 (13), 3998–4002.

1035. Chen J; Marechal V; Levine AJ, Mapping of the p53 and mdm-2 interaction domains. Molecular and Cellular Biology 1993, 13 (7), 4107–4114. [PubMed: 7686617]

1036. Suckau D; Köhl J; Karwath G; Schneider K; Casaretto M; Bitter-Suermann D; Przybylski M, Molecular epitope identification by limited proteolysis of an immobilized antigen-antibody complex and mass spectrometric peptide mapping. Proceedings of the National Academy of Sciences 1990, 87 (24), 9848–9852.

1037. Zhao Y; Chait BT, Protein Epitope Mapping By Mass Spectrometry. Analytical Chemistry 1994, 66 (21), 3723–3726. [PubMed: 7528478]

1038. Opuni KFM; Al-Majdoub M; Yefremova Y; El-Kased RF; Koy C; Glocker MO, Mass spectrometric epitope mapping. Mass Spectrometry Reviews 2018, 37 (2), 229–241. [PubMed: 27403762]

1039. Macht M; Fiedler W; Kürzinger K; Przybylski M, Mass Spectrometric Mapping of Protein Epitope Structures of Myocardial Infarct Markers Myoglobin and Troponin T. Biochemistry 1996, 35 (49), 15633–15639. [PubMed: 8961925]

1040. Al-Majdoub M; Opuni KFM; Koy C; Glocker MO, Facile Fabrication and Instant Application of Miniaturized Antibody-Decorated Affinity Columns for Higher-Order Structure and Functional Characterization of TRIM21 Epitope Peptides. Analytical Chemistry 2013, 85 (21), 10479–10487. [PubMed: 24094071]

1041. Baerga-Ortiz A; Hughes CA; Mandell JG; Komives EA, Epitope mapping of a monoclonal antibody against human thrombin by H/D-exchange mass spectrometry reveals selection of a diverse sequence in a highly conserved protein. Protein Science 2002, 11 (6), 1300–1308. [PubMed: 12021429]

1042. Zhang H-M; Kazazic S; Schaub TM; Tipton JD; Emmett MR; Marshall AG, Enhanced Digestion Efficiency, Peptide Ionization Efficiency, and Sequence Resolution for Protein Hydrogen/Deuterium Exchange Monitored by Fourier Transform Ion Cyclotron Resonance Mass Spectrometry. Analytical Chemistry 2008, 80 (23), 9034–9041. [PubMed: 19551977]

1043. Johnson Daniel J. D.; Adams Ty E.; Li W; Huntington James A., Crystal structure of wild-type human thrombin in the Na+-free state. Biochemical Journal 2005, 392 (1), 21–28. [PubMed: 16201969]

1044. Jones LM; Sperry JB; Carroll JA; Gross ML, Fast Photochemical Oxidation of Proteins for Epitope Mapping. Analytical Chemistry 2011, 83 (20), 7657–7661. [PubMed: 21894996]

1045. Yan Y; Chen G; Wei H; Huang RY-C; Mo J; Rempel DL; Tymiak AA; Gross ML, Fast Photochemical Oxidation of Proteins (FPOP) Maps the Epitope of EGFR Binding to Adnectin. Journal of The American Society for Mass Spectrometry 2014, 25 (12), 2084–2092. [PubMed: 25267085]

1046. Zhang Y; Wecksler AT; Molina P; Deperalta G; Gross ML, Mapping the Binding Interface of VEGF and a Monoclonal Antibody Fab-1 Fragment with Fast Photochemical Oxidation of Proteins (FPOP) and Mass Spectrometry. Journal of The American Society for Mass Spectrometry 2017, 28 (5), 850–858. [PubMed: 28255747]

1047. Li X; Grant OC; Ito K; Wallace A; Wang S; Zhao P; Wells L; Lu S; Woods RJ; Sharp JS, Structural Analysis of the Glycosylated Intact HIV-1 gp120–b12 Antibody Complex Using Hydroxyl Radical Protein Footprinting. Biochemistry 2017, 56 (7), 957–970. [PubMed: 28102671]

1048. Li J; Wei H; Krystek SR; Bond D; Brender TM; Cohen D; Feiner J; Hamacher N; Harshman J; Huang RYC; Julien SH; Lin Z; Moore K; Mueller L; Noriega C; Sejwal P; Sheppard P; Stevens B; Chen G; Tymiak AA; Gross ML; Schneeweis LA, Mapping the Energetic Epitope of an Antibody/Interleukin-23 Interaction with Hydrogen/Deuterium Exchange, Fast Photochemical Oxidation of Proteins Mass Spectrometry, and Alanine Shave Mutagenesis. Analytical Chemistry 2017, 89 (4), 2250–2258. [PubMed: 28193005]

1049. Xie B; Sharp JS, Hydroxyl Radical Dosimetry for High Flux Hydroxyl Radical Protein Footprinting Applications Using a Simple Optical Detection Method. Analytical Chemistry 2015, 87 (21), 10719–10723. [PubMed: 26455423]

1050. Niu B; Mackness BC; Rempel DL; Zhang H; Cui W; Matthews CR; Zitzewitz JA; Gross ML, Incorporation of a Reporter Peptide in FPOP Compensates for Adventitious Scavengers and Permits Time-Dependent Measurements. J Am Soc Mass Spectrom 2017, 28 (2), 389–392. [PubMed: 27924496]

1051. Levinthal C, Are there pathways for protein folding? J. Chim. Phys 1968, 65, 44–45.

1052. Anfinsen CB, Principles that Govern the Folding of Protein Chains. Science 1973, 181 (4096), 223–230. [PubMed: 4124164]

1053. Dill KA, Dominant forces in protein folding. Biochemistry 1990, 29 (31), 7133–7155. [PubMed: 2207096]

1054. Leopold PE; Montal M; Onuchic JN, Protein folding funnels: a kinetic approach to the sequence-structure relationship. Proceedings of the National Academy of Sciences 1992, 89 (18), 8721–8725.

1055. Dill KA; Chan HS, From Levinthal to pathways to funnels. Nature Structural Biology 1997, 4 (1), 10–19. [PubMed: 8989315]

1056. Moult J, A decade of CASP: progress, bottlenecks and prognosis in protein structure prediction. Current Opinion in Structural Biology 2005, 15 (3), 285–289. [PubMed: 15939584]

1057. Dobson CM, Protein folding and misfolding. Nature 2003, 426 (6968), 884–890. [PubMed: 14685248]

1058. Dill KA; MacCallum JL, The Protein-Folding Problem, 50 Years On. Science 2012, 338 (6110), 1042–1046. [PubMed: 23180855]

1059. Englander SW; Mayne L, The nature of protein folding pathways. Proceedings of the National Academy of Sciences 2014, 111 (45), 15873–15880.

1060. Roder H; Maki K; Cheng H, Early Events in Protein Folding Explored by Rapid Mixing Methods. Chemical Reviews 2006, 106 (5), 1836–1861. [PubMed: 16683757]

1061. Ballew RM; Sabelko J; Gruebele M, Direct observation of fast protein folding: the initial collapse of apomyoglobin. Proceedings of the National Academy of Sciences 1996, 93 (12), 5759–5764.

1062. Gruebele M; Sabelko J; Ballew R; Ervin J, Laser Temperature Jump Induced Protein Refolding. Accounts of Chemical Research 1998, 31 (11), 699–707.

1063. Jones CM; Henry ER; Hu Y; Chan CK; Luck SD; Bhuyan A; Roder H; Hofrichter J; Eaton WA, Fast events in protein folding initiated by nanosecond laser photolysis. Proceedings of the

National Academy of Sciences of the United States of America 1993, 90 (24), 11860–11864. [PubMed: 8265638]

1064. Chan C-K; Hu Y; Takahashi S; Rousseau DL; Eaton WA; Hofrichter J, Submillisecond protein folding kinetics studied by ultrarapid mixing. Proceedings of the National Academy of Sciences 1997, 94 (5), 1779–1784.

1065. Jeong B-S; Dyer RB, Proton Transport Mechanism of M2 Proton Channel Studied by Laser-Induced pH Jump. Journal of the American Chemical Society 2017, 139 (19), 6621–6628. [PubMed: 28467842]

1066. Charlier C; Alderson TR; Courtney JM; Ying J; Anfinrud P; Bax A, Study of protein folding under native conditions by rapidly switching the hydrostatic pressure inside an NMR sample cell. Proceedings of the National Academy of Sciences 2018, 115 (18), E4169–E4178.

1067. Eaton WA; Muñoz V; Thompson PA; Henry ER; Hofrichter J, Kinetics and Dynamics of Loops, α-Helices, β-Hairpins, and Fast-Folding Proteins. Accounts of Chemical Research 1998, 31 (11), 745–753.

1068. Mayor U; Johnson CM; Daggett V; Fersht AR, Protein folding and unfolding in microseconds to nanoseconds by experiment and simulation. Proceedings of the National Academy of Sciences 2000, 97 (25), 13518–13522.

1069. Jennings P; Wright P, Formation of a molten globule intermediate early in the kinetic folding pathway of apomyoglobin. Science 1993, 262 (5135), 892–896. [PubMed: 8235610]

1070. Barth A, Infrared spectroscopy of proteins. Biochimica et Biophysica Acta (BBA) - Bioenergetics 2007, 1767 (9), 1073–1101. [PubMed: 17692815]

1071. Udgaonkar JB; Baldwin RL, NMR evidence for an early framework intermediate on the folding pathway of ribonuclease A. Nature 1988, 335 (6192), 694–699. [PubMed: 2845278]

1072. Roder H; Elöve GA; Englander SW, Structural characterization of folding intermediates in cytochrome c by H-exchange labelling and proton NMR. Nature 1988, 335 (6192), 700–704. [PubMed: 2845279]

1073. Dyer RB; Gai F; Woodruff WH; Gilmanshin R; Callender RH, Infrared Studies of Fast Events in Protein Folding. Accounts of Chemical Research 1998, 31 (11), 709–716.

1074. Deniz AA; Laurence TA; Beligere GS; Dahan M; Martin AB; Chemla DS; Dawson PE; Schultz PG; Weiss S, Single-molecule protein folding: Diffusion fluorescence resonance energy transfer studies of the denaturation of chymotrypsin inhibitor 2. Proceedings of the National Academy of Sciences 2000, 97 (10), 5179–5184.

1075. Itzhaki LS; Otzen DE; Fersht AR, The Structure of the Transition State for Folding of Chymotrypsin Inhibitor 2 Analysed by Protein Engineering Methods: Evidence for a Nucleation-condensation Mechanism for Protein Folding. Journal of Molecular Biology 1995, 254 (2), 260–288. [PubMed: 7490748]

1076. Chowdhury SK; Katta V; Chait BT, Probing conformational changes in proteins by mass spectrometry. Journal of the American Chemical Society 1990, 112 (24), 9012–9013.

1077. Simmons DA; Konermann L, Characterization of Transient Protein Folding Intermediates during Myoglobin Reconstitution by Time-Resolved Electrospray Mass Spectrometry with On-Line Isotopic Pulse Labeling. Biochemistry 2002, 41 (6), 1906–1914. [PubMed: 11827537]

1078. Katta V; Chait BT, Hydrogen/deuterium exchange electrospray ionization mass spectrometry: a method for probing protein conformational changes in solution. Journal of the American Chemical Society 1993, 115 (14), 6317–6321.

1079. Miranker A; Robinson C; Radford S; Aplin R; Dobson C, Detection of transient protein folding populations by mass spectrometry. Science 1993, 262 (5135), 896–900. [PubMed: 8235611]

1080. Kragelund BB; Robinson CV; Knudsen J; Dobson CM; Poulsen FM, Folding of a four-helix bundle: studies of acyl-coenzyme A binding protein. Biochemistry 1995, 34 (21), 7217–7224. [PubMed: 7766632]

1081. Maleknia SD; Downard KM, Unfolding of apomyoglobin helices by synchrotron radiolysis and mass spectrometry. European Journal of Biochemistry 2001, 268 (21), 5578–5588. [PubMed: 11683881]

1082. Poor TA; Jones LM; Sood A; Leser GP; Plasencia MD; Rempel DL; Jardetzky TS; Woods RJ; Gross ML; Lamb RA, Probing the paramyxovirus fusion (F) protein-refolding event from pre- to

postfusion by oxidative footprinting. Proceedings of the National Academy of Sciences 2014, 111 (25), E2596–E2605.

1083. Calabrese AN; Ault JR; Radford SE; Ashcroft AE, Using hydroxyl radical footprinting to explore the free energy landscape of protein folding. Methods 2015, 89, 38–44. [PubMed: 25746386]

1084. Stocks BB; Konermann L, Structural Characterization of Short-Lived Protein Unfolding Intermediates by Laser-Induced Oxidative Labeling and Mass Spectrometry. Analytical Chemistry 2009, 81 (1), 20–27. [PubMed: 19055350]

1085. Stocks BB; Konermann L, Time-Dependent Changes in Side-Chain Solvent Accessibility during Cytochrome c Folding Probed by Pulsed Oxidative Labeling and Mass Spectrometry. Journal of Molecular Biology 2010, 398 (2), 362–373. [PubMed: 20230834]

1086. Stocks BB; Rezvanpour A; Shaw GS; Konermann L, Temporal Development of Protein Structure during S100A11 Folding and Dimerization Probed by Oxidative Labeling and Mass Spectrometry. Journal of Molecular Biology 2011, 409 (4), 669–679. [PubMed: 21515281]

1087. Pan Y; Brown L; Konermann L, Kinetic Folding Mechanism of an Integral Membrane Protein Examined by Pulsed Oxidative Labeling and Mass Spectrometry. Journal of Molecular Biology 2011, 410 (1), 146–158. [PubMed: 21570983]

1088. Vahidi S; Stocks BB; Liaghati-Mobarhan Y; Konermann L, Submillisecond Protein Folding Events Monitored by Rapid Mixing and Mass Spectrometry-Based Oxidative Labeling. Analytical Chemistry 2013, 85 (18), 8618–8625. [PubMed: 23841479]

1089. Wu L; Lapidus LJ, Combining Ultrarapid Mixing with Photochemical Oxidation to Probe Protein Folding. Analytical Chemistry 2013, 85 (10), 4920–4924. [PubMed: 23593999]

1090. Mortensen DN; Williams ER, Theta-Glass Capillaries in Electrospray Ionization: Rapid Mixing and Short Droplet Lifetimes. Analytical Chemistry 2014, 86 (18), 9315–9321. [PubMed: 25160559]

1091. Mortensen DN; Williams ER, Ultrafast (1 μs) Mixing and Fast Protein Folding in Nanodrops Monitored by Mass Spectrometry. Journal of the American Chemical Society 2016, 138 (10), 3453–3460. [PubMed: 26902747]

1092. Braak H; Tredici KD; Rüb U; de Vos RAI; Jansen Steur ENH; Braak E, Staging of brain pathology related to sporadic Parkinson's disease. Neurobiology of Aging 2003, 24 (2), 197–211. [PubMed: 12498954]

1093. Goedert M; Spillantini MG; Del Tredici K; Braak H, 100 years of Lewy pathology. Nature Reviews Neurology 2012, 9, 13.

1094. Lewy F, Paralysis agitans. I. Pathologische anatomie. Handbuch der neurologie 1912.

1095. Berchtold NC; Cotman CW, Evolution in the Conceptualization of Dementia and Alzheimer's Disease: Greco-Roman Period to the 1960s. Neurobiology of Aging 1998, 19 (3), 173–189. [PubMed: 9661992]

1096. Hamley IW, The Amyloid Beta Peptide: A Chemist's Perspective. Role in Alzheimer's and Fibrillization. Chemical Reviews 2012, 112 (10), 5147–5192. [PubMed: 22813427]

1097. Vos T; Allen C; Arora M; Barber RM; Bhutta ZA; Brown A; Carter A; Casey DC; Charlson FJ; Chen AZ; Coggeshall M; Cornaby L; Dandona L; Dicker DJ; Dilegge T; Erskine HE; Ferrari AJ; Fitzmaurice C; Fleming T; Forouzanfar MH; Fullman N; Gething PW; Goldberg EM; Graetz N; Haagsma JA; Hay SI; Johnson CO; Kassebaum NJ; Kawashima T; Kemmer L; Khalil IA; Kinfu Y; Kyu HH; Leung J; Liang X; Lim SS; Lopez AD; Lozano R; Marczak L; Mensah GA; Mokdad AH; Naghavi M; Nguyen G; Nsoesie E; Olsen H; Pigott DM; Pinho C; Rankin Z; Reinig N; Salomon JA; Sandar L; Smith A; Stanaway J; Steiner C; Teeple S; Thomas BA; Troeger C; Wagner JA; Wang H; Wanga V; Whiteford HA; Zoeckler L; Abajobir AA; Abate KH; Abbafati C; Abbas KM; Abd-Allah F; Abraham B; Abubakar I; Abu-Raddad LJ; Abu-Rmeileh NME; Ackerman IN; Adebiyi AO; Ademi Z; Adou AK; Afanvi KA; Agardh EE; Agarwal A; Kiadaliri AA; Ahmadieh H; Ajala ON; Akinyemi RO; Akseer N; Al-Aly Z; Alam K; Alam NKM; Aldhahri SF; Alegretti MA; Alemu ZA; Alexander LT; Alhabib S; Ali R; Alkerwi A. a.; Alla F; Allebeck P; Al-Raddadi R; Alsharif U; Altirkawi KA; Alvis-Guzman N; Amare AT; Amberbir A; Amini H; Ammar W; Amrock SM; Andersen HH; Anderson GM; Anderson BO; Antonio CAT; Aregay AF; Ärnlöv J; Artaman A; Asayesh H; Assadi R; Atique S; Avokpaho EFGA; Awasthi A; Quintanilla BPA; Azzopardi P; Bacha U; Badawi A; Balakrishnan K; Banerjee A; Barac A;

Barker-Collo SL; Bärnighausen T; Barregard L; Barrero LH; Basu A; Bazargan-Hejazi S; Beghi E; Bell B; Bell ML; Bennett DA; Bensenor IM; Benzian H; Berhane A; Bernabé E; Betsu BD; Beyene AS; Bhala N; Bhatt S; Biadgilign S; Bienhoff K; Bikbov B; Biryukov S; Bisanzio D; Bjertness E; Blore J; Borschmann R; Boufous S; Brainin M; Brazinova A; Breitborde NJK; Brown J; Buchbinder R; Buckle GC; Butt ZA; Calabria B; Campos-Nonato IR; Campuzano JC; Carabin H; Cárdenas R; Carpenter DO; Carrero JJ; Castañeda-Orjuela CA; Rivas JC; Catalá-López F; Chang J-C; Chiang PP-C; Chibueze CE; Chisumpa VH; Choi J-YJ; Chowdhury R; Christensen H; Christopher DJ; Ciobanu LG; Cirillo M; Coates MM; Colquhoun SM; Cooper C; Cortinovis M; Crump JA; Damtew SA; Dandona R; Daoud F; Dargan PI; das Neves J; Davey G; Davis AC; Leo DD; Degenhardt L; Gobbo LCD; Dellavalle RP; Deribe K; Deribew A; Derrett S; Jarlais DCD; Dharmaratne SD; Dhillon PK; Diaz-Torné C; Ding EL; Driscoll TR; Duan L; Dubey M; Duncan BB; Ebrahimi H; Ellenbogen RG; Elyazar I; Endres M; Endries AY; Ermakov SP; Eshrati B; Estep K; Farid TA; Farinha C. S. e. S.; Faro A; Farvid MS; Farzadfar F; Feigin VL; Felson DT; Fereshtehnejad S-M; Fernandes JG; Fernandes JC; Fischer F; Fitchett JRA; Foreman K; Fowkes FGR; Fox J; Franklin RC; Friedman J; Frostad J; Fürst T; Futran ND; Gabbe B; Ganguly P; Gankpé FG; Gebre T; Gebrehiwot TT; Gebremedhin AT; Geleijnse JM; Gessner BD; Gibney KB; Ginawi IAM; Giref AZ; Giroud M; Gishu MD; Giussani G; Glaser E; Godwin WW; Gomez-Dantes H; Gona P; Goodridge A; Gopalani SV; Gotay CC; Goto A; Gouda HN; Grainger R; Greaves F; Guillemin F; Guo Y; Gupta R; Gupta R; Gupta V; Gutiérrez RA; Haile D; Hailu AD; Hailu GB; Halasa YA; Hamadeh RR; Hamidi S; Hammami M; Hancock J; Handal AJ; Hankey GJ; Hao Y; Harb HL; Harikrishnan S; Haro JM; Havmoeller R; Hay RJ; Heredia-Pi IB; Heydarpour P; Hoek HW; Horino M; Horita N; Hosgood HD; Hoy DG; Htet AS; Huang H; Huang JJ; Huynh C; Iannarone M; Iburg KM; Innos K; Inoue M; Iyer VJ; Jacobsen KH; Jahanmehr N; Jakovljevic MB; Javanbakht M; Jayaraman SP; Jayatilleke AU; Jee SH; Jeemon P; Jensen PN; Jiang Y; Jibat T; Jimenez-Corona A; Jin Y; Jonas JB; Kabir Z; Kalkonde Y; Kamal R; Kan H; Karch A; Karema CK; Karimkhani C; Kasaeian A; Kaul A; Kawakami N; Keiyoro PN; Kemp AH; Keren A; Kesavachandran CN; Khader YS; Khan AR; Khan EA; Khang Y-H; Khera S; Khoja TAM; Khubchandani J; Kieling C; Kim P; Kim C.-i.; Kim D; Kim YJ; Kissoon N; Knibbs LD; Knudsen AK; Kokubo Y; Kolte D; Kopec JA; Kosen S; Kotsakis GA; Koul PA; Koyanagi A; Kravchenko M; Defo BK; Bicer BK; Kudom AA; Kuipers EJ; Kumar GA; Kutz M; Kwan GF; Lal A; Lalloo R; Lallukka T; Lam H; Lam JO; Langan SM; Larsson A; Lavados PM; Leasher JL; Leigh J; Leung R; Levi M; Li Y; Li Y; Liang J; Liu S; Liu Y; Lloyd BK; Lo WD; Logroscino G; Looker KJ; Lotufo PA; Lunevicius R; Lyons RA; Mackay MT; Magdy M; Razek AE; Mahdavi M; Majdan M; Majeed A; Malekzadeh R; Marcenes W; Margolis DJ; Martinez-Raga J; Masiye F; Massano J; McGarvey ST; McGrath JJ; McKee M; McMahon BJ; Meaney PA; Mehari A; Mejia-Rodriguez F; Mekonnen AB; Melaku YA; Memiah P; Memish ZA; Mendoza W; Meretoja A; Meretoja TJ; Mhimbira FA; Millear A; Miller TR; Mills EJ; Mirarefin M; Mitchell PB; Mock CN; Mohammadi A; Mohammed S; Monasta L; Hernandez JCM; Montico M; Mooney MD; Moradi-Lakeh M; Morawska L; Mueller UO; Mullany E; Mumford JE; Murdoch ME; Nachega JB; Nagel G; Naheed A; Naldi L; Nangia V; Newton JN; Ng M; Ngalesoni FN; Nguyen QL; Nisar MI; Pete PMN; Nolla JM; Norheim OF; Norman RE; Norrving B; Nunes BP; Ogbo FA; Oh I-H; Ohkubo T; Olivares PR; Olusanya BO; Olusanya JO; Ortiz A; Osman M; Ota E; Pa M; Park E-K; Parsaeian M; de Azeredo Passos VM; Caicedo AJP; Patten SB; Patton GC; Pereira DM; Perez-Padilla R; Perico N; Pesudovs K; Petzold M; Phillips MR; Piel FB; Pillay JD; Pishgar F; Plass D; Platts-Mills JA; Polinder S; Pond CD; Popova S; Poulton RG; Pourmalek F; Prabhakaran D; Prasad NM; Qorbani M; Rabiee RHS; Radfar A; Rafay A; Rahimi K; Rahimi-Movaghar V; Rahman M; Rahman MHU; Rahman SU; Rai RK; Rajsic S; Ram U; Rao P; Refaat AH; Reitsma MB; Remuzzi G; Resnikoff S; Reynolds A; Ribeiro AL; Blancas MJR; Roba HS; Rojas-Rueda D; Ronfani L; Roshandel G; Roth GA; Rothenbacher D; Roy A; Sagar R; Sahathevan R; Sanabria JR; Sanchez-Niño MD; Santos IS; Santos JV; Sarmiento-Suarez R; Sartorius B; Satpathy M; Savic M; Sawhney M; Schaub MP; Schmidt MI; Schneider IJC; Schöttker B; Schwebel DC; Scott JG; Seedat S; Sepanlou SG; Servan-Mori EE; Shackelford KA; Shaheen A; Shaikh MA; Sharma R; Sharma U; Shen J; Shepard DS; Sheth KN; Shibuya K; Shin M-J; Shiri R; Shiue I; Shrime MG; Sigfusdottir ID; Silva DAS; Silveira DGA; Singh A; Singh JA; Singh OP; Singh PK; Sivonda A; Skirbekk V; Skogen JC; Sligar A; Sliwa K; Soljak M; Søreide K; Sorensen RJD; Soriano JB; Sposato LA; Sreeramareddy CT; Stathopoulou V; Steel N; Stein DJ; Steiner TJ; Steinke S; Stovner L; Stroumpoulis K; Sunguya BF; Sur P;

Swaminathan S; Sykes BL; Szoeke CEI; Tabarés-Seisdedos R; Takala JS; Tandon N; Tanne D; Tavakkoli M; Taye B; Taylor HR; Ao BJT; Tedla BA; Terkawi AS; Thomson AJ; Thorne-Lyman AL; Thrift AG; Thurston GD; Tobe-Gai R; Tonelli M; Topor-Madry R; Topouzis F; Tran BX; Truelsen T; Dimbuene ZT; Tsilimbaris M; Tura AK; Tuzcu EM; Tyrovolas S; Ukwaja KN; Undurraga EA; Uneke CJ; Uthman OA; van Gool CH; Varakin YY; Vasankari T; Venketasubramanian N; Verma RK; Violante FS; Vladimirov SK; Vlassov VV; Vollset SE; Wagner GR; Waller SG; Wang L; Watkins DA; Weichenthal S; Weiderpass E; Weintraub RG; Werdecker A; Westerman R; White RA; Williams HC; Wiysonge CS; Wolfe CDA; Won S; Woodbrook R; Wubshet M; Xavier D; Xu G; Yadav AK; Yan LL; Yano Y; Yaseri M; Ye P; Yebyo HG; Yip P; Yonemoto N; Yoon S-J; Younis MZ; Yu C; Zaidi Z; Zaki MES; Zeeb H; Zhou M; Zodpey S; Zuhlke LJ; Murray CJL, Global, regional, and national incidence, prevalence, and years lived with disability for 310 diseases and injuries, 1990–2015: a systematic analysis for the Global Burden of Disease Study 2015. The Lancet 2016, 388 (10053), 1545–1602.

1098. Hardy J; Selkoe DJ, The Amyloid Hypothesis of Alzheimer's Disease: Progress and Problems on the Road to Therapeutics. Science 2002, 297 (5580), 353–356. [PubMed: 12130773]

1099. Chiti F; Dobson CM, Protein Misfolding, Functional Amyloid, and Human Disease. Annual Review of Biochemistry 2006, 75 (1), 333–366.

1100. Lührs T; Ritter C; Adrian M; Riek-Loher D; Bohrmann B; Döbeli H; Schubert D; Riek R, 3D structure of Alzheimer's amyloid-β(1–42) fibrils. Proceedings of the National Academy of Sciences of the United States of America 2005, 102 (48), 17342–17347. [PubMed: 16293696]

1101. Petkova AT; Ishii Y; Balbach JJ; Antzutkin ON; Leapman RD; Delaglio F; Tycko R, A structural model for Alzheimer's β-amyloid fibrils based on experimental constraints from solid state NMR. Proceedings of the National Academy of Sciences 2002, 99 (26), 16742–16747.

1102. Sawaya MR; Sambashivan S; Nelson R; Ivanova MI; Sievers SA; Apostol MI; Thompson MJ; Balbirnie M; Wiltzius JJW; McFarlane HT; Madsen AØ; Riekel C; Eisenberg D, Atomic structures of amyloid cross-β spines reveal varied steric zippers. Nature 2007, 447, 453. [PubMed: 17468747]

1103. Miller Y; Ma B; Tsai C-J; Nussinov R, Hollow core of Alzheimer's Aβ42 amyloid observed by cryoEM is relevant at physiological pH. Proceedings of the National Academy of Sciences 2010, 107 (32), 14128–14133.

1104. Gremer L; Schölzel D; Schenk C; Reinartz E; Labahn J; Ravelli RBG; Tusche M; Lopez-Iglesias C; Hoyer W; Heise H; Willbold D; Schröder GF, Fibril structure of amyloid-β(1–42) by cryo–electron microscopy. Science 2017, 358 (6359), 116–119. [PubMed: 28882996]

1105. Economou NJ; Giammona MJ; Do TD; Zheng X; Teplow DB; Buratto SK; Bowers MT, Amyloid β-Protein Assembly and Alzheimer's Disease: Dodecamers of Aβ42, but Not of Aβ40, Seed Fibril Formation. Journal of the American Chemical Society 2016, 138 (6), 1772–1775. [PubMed: 26839237]

1106. Levine H III, Thioflavine T interaction with synthetic Alzheimer's disease β-amyloid peptides: Detection of amyloid aggregation in solution. Protein Science 1993, 2 (3), 404–410. [PubMed: 8453378]

1107. Biancalana M; Koide S, Molecular mechanism of Thioflavin-T binding to amyloid fibrils. Biochimica et Biophysica Acta (BBA) - Proteins and Proteomics 2010, 1804 (7), 1405–1412. [PubMed: 20399286]

1108. Groenning M, Binding mode of Thioflavin T and other molecular probes in the context of amyloid fibrils—current status. Journal of Chemical Biology 2010, 3 (1), 1–18. [PubMed: 19693614]

1109. Wolfe LS; Calabrese MF; Nath A; Blaho DV; Miranker AD; Xiong Y, Protein-induced photophysical changes to the amyloid indicator dye thioflavin T. Proceedings of the National Academy of Sciences 2010, 107 (39), 16863–16868.

1110. Stoeckli M; Staab D; Staufenbiel M; Wiederhold K-H; Signor L, Molecular imaging of amyloid β peptides in mouse brain sections using mass spectrometry. Analytical Biochemistry 2002, 311 (1), 33–39. [PubMed: 12441150]

1111. Bernstein SL; Dupuis NF; Lazo ND; Wyttenbach T; Condron MM; Bitan G; Teplow DB; Shea J-E; Ruotolo BT; Robinson CV; Bowers MT, Amyloid-β protein oligomerization and the

importance of tetramers and dodecamers in the aetiology of Alzheimer's disease. Nature Chemistry 2009, 1, 326.

1112. Kheterpal I; Zhou S; Cook KD; Wetzel R, Aβ amyloid fibrils possess a core structure highly resistant to hydrogen exchange. Proceedings of the National Academy of Sciences 2000, 97 (25), 13597–13601.

1113. Kheterpal I; Lashuel HA; Hartley DM; Walz T; Lansbury PT; Wetzel R, Aβ Protofibrils Possess a Stable Core Structure Resistant to Hydrogen Exchange. Biochemistry 2003, 42 (48), 14092–14098. [PubMed: 14640676]

1114. Zhang Y; Rempel DL; Zhang J; Sharma AK; Mirica LM; Gross ML, Pulsed hydrogen–deuterium exchange mass spectrometry probes conformational changes in amyloid beta (Aβ) peptide aggregation. Proceedings of the National Academy of Sciences 2013, 110 (36), 14604–14609.

1115. Pan J; Han J; Borchers CH; Konermann L, Conformer-Specific Hydrogen Exchange Analysis of Aβ(1–42) Oligomers by Top-Down Electron Capture Dissociation Mass Spectrometry. Analytical Chemistry 2011, 83 (13), 5386–5393. [PubMed: 21635007]

1116. Pan J; Han J; Borchers CH; Konermann L, Structure and Dynamics of Small Soluble Aβ(1–40) Oligomers Studied by Top-Down Hydrogen Exchange Mass Spectrometry. Biochemistry 2012, 51 (17), 3694–3703. [PubMed: 22486153]

1117. Stoeckli M; Knochenmuss R; McCombie G; Mueller D; Rohner T; Staab D; Wiederhold KH, MALDI MS Imaging of Amyloid In Methods in Enzymology, Academic Press: 2006; Vol. 412, pp 94–106. [PubMed: 17046654]

1118. Grasso G, The use of mass spectrometry to study amyloid-β peptides. Mass Spectrometry Reviews 2011, 30 (3), 347–365. [PubMed: 21500241]

1119. Hoffmann W; von Helden G; Pagel K, Ion mobility-mass spectrometry and orthogonal gas-phase techniques to study amyloid formation and inhibition. Current Opinion in Structural Biology 2017, 46, 7–15. [PubMed: 28343095]

1120. Klinger AL; Kiselar J; Ilchenko S; Komatsu H; Chance MR; Axelsen PH, A Synchrotron-Based Hydroxyl Radical Footprinting Analysis of Amyloid Fibrils and Prefibrillar Intermediates with Residue-Specific Resolution. Biochemistry 2014, 53 (49), 7724–7734. [PubMed: 25382225]

1121. Williams M, Daviter Tina, Protein-Ligand Interactions Methods and Applications. Humana Press: New York, 2013.

1122. Rossi AM; Taylor CW, Analysis of protein-ligand interactions by fluorescence polarization. Nature Protocols 2011, 6, 365. [PubMed: 21372817]

1123. Yan Y; Marriott G, Analysis of protein interactions using fluorescence technologies. Current Opinion in Chemical Biology 2003, 7 (5), 635–640. [PubMed: 14580569]

1124. Paolini S; Tanfani F; Fini C; Bertoli E; Paolo P, Porcine odorant-binding protein: structural stability and ligand affinities measured by Fourier-transform infrared spectroscopy and fluorescence spectroscopy. Biochimica et Biophysica Acta (BBA) - Protein Structure and Molecular Enzymology 1999, 1431 (1), 179–188. [PubMed: 10209290]

1125. Meyer B; Peters T, NMR Spectroscopy Techniques for Screening and Identifying Ligand Binding to Protein Receptors. Angewandte Chemie International Edition 2003, 42 (8), 864–890. [PubMed: 12596167]

1126. Willets KA; Duyne RPV, Localized Surface Plasmon Resonance Spectroscopy and Sensing. Annual Review of Physical Chemistry 2007, 58 (1), 267–297.

1127. Kitova EN; El-Hawiet A; Schnier PD; Klassen JS, Reliable Determinations of Protein–Ligand Interactions by Direct ESI-MS Measurements. Are We There Yet? Journal of The American Society for Mass Spectrometry 2012, 23 (3), 431–441. [PubMed: 22270873]

1128. Powell KD; Fitzgerald MC, Measurements of Protein Stability by H/D Exchange and Matrix-Assisted Laser Desorption/Ionization Mass Spectrometry Using Picomoles of Material. Analytical Chemistry 2001, 73 (14), 3300–3304. [PubMed: 11476229]

1129. Liu XR; Zhang MM; Rempel DL; Gross ML, Protein-Ligand Interaction by Ligand Titration, Fast Photochemical Oxidation of Proteins and Mass Spectrometry: LITPOMS. Journal of The American Society for Mass Spectrometry 2019, 30 (2), 213–217. [PubMed: 30484077]

1130. Katta V; Chait BT, Observation of the heme-globin complex in native myoglobin by electrospray-ionization mass spectrometry. Journal of the American Chemical Society 1991, 113 (22), 8534–8535.

1131. Ganem B; Li YT; Henion JD, Detection of noncovalent receptor-ligand complexes by mass spectrometry. Journal of the American Chemical Society 1991, 113 (16), 6294–6296.

1132. Daniel JM; Friess SD; Rajagopalan S; Wendt S; Zenobi R, Quantitative determination of noncovalent binding interactions using soft ionization mass spectrometry. International Journal of Mass Spectrometry 2002, 216 (1), 1–27.

1133. Loo RRO; Goodlett DR; Smith RD; Loo JA, Observation of a noncovalent ribonuclease S-protein/S-peptide complex by electrospray ionization mass spectrometry. Journal of the American Chemical Society 1993, 115 (10), 4391–4392.

1134. Ayed A; Krutchinsky AN; Ens W; Standing KG; Duckworth HW, Quantitative evaluation of protein–protein and ligand–protein equilibria of a large allosteric enzyme by electrospray ionization time-of-flight mass spectrometry. Rapid Communications in Mass Spectrometry 1998, 12 (7), 339–344. [PubMed: 9554114]

1135. Liu J; Konermann L, Protein–Protein Binding Affinities in Solution Determined by Electrospray Mass Spectrometry. Journal of The American Society for Mass Spectrometry 2011, 22 (3), 408–417. [PubMed: 21472560]

1136. Loo JA; Hu P; McConnell P; Mueller WT; Sawyer TK; Thanabal V, A study of Src SH2 domain protein-phosphopeptide binding interactions by electrospray ionization mass spectrometry. Journal of the American Society for Mass Spectrometry 1997, 8 (3), 234–243.

1137. Greig MJ; Gaus H; Cummins LL; Sasmor H; Griffey RH, Measurement of Macromolecular Binding Using Electrospray Mass Spectrometry. Determination of Dissociation Constants for Oligonucleotide: Serum Albumin Complexes. Journal of the American Chemical Society 1995, 117 (43), 10765–10766.

1138. Jecklin MC; Schauer S; Dumelin CE; Zenobi R, Label-free determination of protein–ligand binding constants using mass spectrometry and validation using surface plasmon resonance and isothermal titration calorimetry. Journal of Molecular Recognition 2009, 22 (4), 319–329. [PubMed: 19373858]

1139. Jørgensen TJD; Roepstorff P; Heck AJR, Direct Determination of Solution Binding Constants for Noncovalent Complexes between Bacterial Cell Wall Peptide Analogues and Vancomycin Group Antibiotics by Electrospray Ionization Mass Spectrometry. Analytical Chemistry 1998, 70 (20), 4427–4432.

1140. Griffey RH; Sannes-Lowery KA; Drader JJ; Mohan V; Swayze EE; Hofstadler SA, Characterization of Low-Affinity Complexes between RNA and Small Molecules Using Electrospray Ionization Mass Spectrometry. Journal of the American Chemical Society 2000, 122 (41), 9933–9938.

1141. Wang W; Kitova EN; Klassen JS, Influence of Solution and Gas Phase Processes on Protein–Carbohydrate Binding Affinities Determined by Nanoelectrospray Fourier Transform Ion Cyclotron Resonance Mass Spectrometry. Analytical Chemistry 2003, 75 (19), 4945–4955. [PubMed: 14708765]

1142. El-Hawiet A; Kitova EN; Liu L; Klassen JS, Quantifying Labile Protein–Ligand Interactions Using Electrospray Ionization Mass Spectrometry. Journal of the American Society for Mass Spectrometry 2010, 21 (11), 1893–1899. [PubMed: 20801056]

1143. Wang Y; Park H; Lin H; Kitova EN; Klassen JS, Multipronged ESI–MS Approach for Studying Glycan-Binding Protein Interactions with Glycoproteins. Analytical Chemistry 2019, 91 (3), 2140–2147. [PubMed: 30624066]

1144. Nguyen GTH; Tran TN; Podgorski MN; Bell SG; Supuran CT; Donald WA, Nanoscale Ion Emitters in Native Mass Spectrometry for Measuring Ligand–Protein Binding Affinities. ACS Central Science 2019, 5 (2), 308–318. [PubMed: 30834319]

1145. Ghaemmaghami S; Fitzgerald MC; Oas TG, A quantitative, high-throughput screen for protein stability. Proceedings of the National Academy of Sciences 2000, 97 (15), 8296–8301.

1146. Tang L; Hopper ED; Tong Y; Sadowsky JD; Peterson KJ; Gellman SH; Fitzgerald MC, H/D Exchange- and Mass Spectrometry-Based Strategy for the Thermodynamic Analysis of Protein–Ligand Binding. Analytical Chemistry 2007, 79 (15), 5869–5877. [PubMed: 17580981]

1147. Liu XR; Zhang MM; Rempel DL; Gross ML, A Single Approach Reveals the Composite Conformational Changes, Order of Binding, and Affinities for Calcium Binding to Calmodulin. Analytical Chemistry 2019.

1148. Zhao L; Lai L; Zhang Z, How calcium ion binding induces the conformational transition of the calmodulin N-terminal domain—an atomic level characterization. Physical Chemistry Chemical Physics 2019, 21 (36), 19795–19804. [PubMed: 31482888]

1149. Ottinger LM; Tullius TD, High-Resolution in Vivo Footprinting of a Protein–DNA Complex Using γ-Radiation. Journal of the American Chemical Society 2000, 122 (24), 5901–5902.

1150. Adilakshmi T; Soper SFC; Woodson SA, Chapter 12 - Structural Analysis of RNA in Living Cells by In Vivo Synchrotron X-Ray Footprinting In Methods in Enzymology, Academic Press: 2009; Vol. 468, pp 239–258. [PubMed: 20946773]

1151. Clatterbuck Soper Sarah F.; Dator Romel P.; Limbach Patrick A.; Woodson Sarah A., In Vivo X-Ray Footprinting of Pre-30S Ribosomes Reveals Chaperone-Dependent Remodeling of Late Assembly Intermediates. Molecular Cell 2013, 52 (4), 506–516. [PubMed: 24207057]

1152. Adilakshmi T; Lease RA; Woodson SA, Hydroxyl radical footprinting in vivo: mapping macromolecular structures with synchrotron radiation. Nucleic Acids Research 2006, 34 (8), e64–e64. [PubMed: 16682443]

1153. Hulscher RM; Bohon J; Rappé MC; Gupta S; D'Mello R; Sullivan M; Ralston CY; Chance MR; Woodson SA, Probing the structure of ribosome assembly intermediates in vivo using DMS and hydroxyl radical footprinting. Methods 2016, 103, 49–56. [PubMed: 27016143]

1154. Espino JA; Mali VS; Jones LM, In Cell Footprinting Coupled with Mass Spectrometry for the Structural Analysis of Proteins in Live Cells. Analytical Chemistry 2015, 87 (15), 7971–7978. [PubMed: 26146849]

1155. Rinas A; Mali VS; Espino JA; Jones LM, Development of a Microflow System for In-Cell Footprinting Coupled with Mass Spectrometry. Analytical Chemistry 2016, 88 (20), 10052–10058. [PubMed: 27681498]

1156. Espino JA; Jones LM, Illuminating Biological Interactions with in Vivo Protein Footprinting. Analytical Chemistry 2019, 91 (10), 6577–6584. [PubMed: 31025855]

1157. Zhu Y; Serra A; Guo T; Park JE; Zhong Q; Sze SK, Application of Nanosecond Laser Photolysis Protein Footprinting to Study EGFR Activation by EGF in Cells. Journal of Proteome Research 2017, 16 (6), 2282–2293. [PubMed: 28452222]

1158. Rhee H-W; Zou P; Udeshi ND; Martell JD; Mootha VK; Carr SA; Ting AY, Proteomic Mapping of Mitochondria in Living Cells via Spatially Restricted Enzymatic Tagging. Science 2013, 339 (6125), 1328–1331. [PubMed: 23371551]

1159. Han S; Li J; Ting AY, Proximity labeling: spatially resolved proteomic mapping for neurobiology. Current Opinion in Neurobiology 2018, 50, 17–23. [PubMed: 29125959]

1160. Mortensen A; Skibsted LH, Importance of Carotenoid Structure in Radical-Scavenging Reactions. Journal of Agricultural and Food Chemistry 1997, 45 (8), 2970–2977.

1161. Mayer G; Bendayan M, Biotinyl–Tyramide: A Novel Approach for Electron Microscopic Immunocytochemistry. Journal of Histochemistry & Cytochemistry 1997, 45 (11), 1449–1454. [PubMed: 9358846]

1162. Lam SS; Martell JD; Kamer KJ; Deerinck TJ; Ellisman MH; Mootha VK; Ting AY, Directed evolution of APEX2 for electron microscopy and proximity labeling. Nature Methods 2015, 12 (1), 51–54. [PubMed: 25419960]

1163. Loh KH; Stawski PS; Draycott AS; Udeshi ND; Lehrman EK; Wilton DK; Svinkina T; Deerinck TJ; Ellisman MH; Stevens B; Carr SA; Ting AY, Proteomic Analysis of Unbounded Cellular Compartments: Synaptic Clefts. Cell 2016, 166 (5), 1295–1307.e21. [PubMed: 27565350]

1164. Lee S-Y; Kang M-G; Shin S; Kwak C; Kwon T; Seo JK; Kim J-S; Rhee H-W, Architecture Mapping of the Inner Mitochondrial Membrane Proteome by Chemical Tools in Live Cells. Journal of the American Chemical Society 2017, 139 (10), 3651–3662. [PubMed: 28156110]

1165. Shen Y; Lange O; Delaglio F; Rossi P; Aramini JM; Liu G; Eletsky A; Wu Y; Singarapu KK; Lemak A; Ignatchenko A; Arrowsmith CH; Szyperski T; Montelione GT; Baker D; Bax A, Consistent blind protein structure generation from NMR chemical shift data. Proceedings of the National Academy of Sciences 2008, 105 (12), 4685–4690.

1166. Huang W; Ravikumar KM; Parisien M; Yang S, Theoretical modeling of multiprotein complexes by iSPOT: Integration of small-angle X-ray scattering, hydroxyl radical footprinting, and computational docking. Journal of Structural Biology 2016, 196 (3), 340–349. [PubMed: 27496803]

1167. DiMaio F; Tyka MD; Baker ML; Chiu W; Baker D, Refinement of Protein Structures into Low-Resolution Density Maps Using Rosetta. Journal of Molecular Biology 2009, 392 (1), 181–190. [PubMed: 19596339]

1168. DiMaio F; Song Y; Li X; Brunner MJ; Xu C; Conticello V; Egelman E; Marlovits TC; Cheng Y; Baker D, Atomic-accuracy models from 4.5-Å cryo-electron microscopy data with density-guided iterative local refinement. Nature Methods 2015, 12, 361. [PubMed: 25707030]

1169. Alexander NS; Stein RA; Koteiche HA; Kaufmann KW; McHaourab HS; Meiler J, RosettaEPR: Rotamer Library for Spin Label Structure and Dynamics. PLOS ONE 2013, 8 (9), e72851. [PubMed: 24039810]

1170. Walzthoeni T; Joachimiak LA; Rosenberger G; Röst HL; Malmström L; Leitner A; Frydman J; Aebersold R, xTract: software for characterizing conformational changes of protein complexes by quantitative cross-linking mass spectrometry. Nature Methods 2015, 12, 1185. [PubMed: 26501516]

1171. Gerega SK; Downard KM, PROXIMO—a new docking algorithm to model protein complexes using data from radical probe mass spectrometry (RP-MS). Bioinformatics 2006, 22 (14), 1702–1709. [PubMed: 16679333]

1172. Huang W; Ravikumar Krishnakumar M.; Chance Mark R.; Yang S, Quantitative Mapping of Protein Structure by Hydroxyl Radical Footprinting-Mediated Structural Mass Spectrometry: A Protection Factor Analysis. Biophysical Journal 2015, 108 (1), 107–115. [PubMed: 25564857]

1173. Huang W; Peng Y; Kiselar J; Zhao X; Albaqami A; Mendez D; Chen Y; Chakravarthy S; Gupta S; Ralston C; Kao H-Y; Chance MR; Yang S, Multidomain architecture of estrogen receptor reveals interfacial cross-talk between its DNA-binding and ligand-binding domains. Nature Communications 2018, 9 (1), 3520.

1174. Xie B; Sood A; Woods RJ; Sharp JS, Quantitative Protein Topography Measurements by High Resolution Hydroxyl Radical Protein Footprinting Enable Accurate Molecular Model Selection. Scientific Reports 2017, 7 (1), 4552. [PubMed: 28674401]

1175. Aprahamian ML; Chea EE; Jones LM; Lindert S, Rosetta Protein Structure Prediction from Hydroxyl Radical Protein Footprinting Mass Spectrometry Data. Analytical Chemistry 2018, 90 (12), 7721–7729. [PubMed: 29874044]

1176. Seffernick JT; Harvey SR; Wysocki VH; Lindert S, Predicting Protein Complex Structure from Surface-Induced Dissociation Mass Spectrometry Data. ACS Central Science 2019, 5 (8), 1330–1341. [PubMed: 31482115]

1177. Nosaka Y; Nosaka AY, Generation and Detection of Reactive Oxygen Species in Photocatalysis. Chemical Reviews 2017, 117 (17), 11302–11336. [PubMed: 28777548]

1178. Weisz DA; Gross ML; Pakrasi HB, Reactive oxygen species leave a damage trail that reveals water channels in Photosystem II. Science Advances 2017, 3 (11), eaao3013. [PubMed: 29159285]

1179. Loll B; Kern J; Saenger W; Zouni A; Biesiadka J, Towards complete cofactor arrangement in the 3.0 Å resolution structure of photosystem II. Nature 2005, 438 (7070), 1040–1044. [PubMed: 16355230]

1180. Chaplin M, Do we underestimate the importance of water in cell biology? Nature Reviews Molecular Cell Biology 2006, 7 (11), 861–866. [PubMed: 16955076]

1181. Ball P, Water as an Active Constituent in Cell Biology. Chemical Reviews 2008, 108 (1), 74–108. [PubMed: 18095715]

1182. Jiang J-S; Brünger AT, Protein Hydration Observed by X-ray Diffraction: Solvation Properties of Penicillopepsin and Neuraminidase Crystal Structures. Journal of Molecular Biology 1994, 243 (1), 100–115. [PubMed: 7932732]

1183. Persson E; Halle B, Nanosecond to Microsecond Protein Dynamics Probed by Magnetic Relaxation Dispersion of Buried Water Molecules. Journal of the American Chemical Society 2008, 130 (5), 1774–1787. [PubMed: 18183977]

1184. Gupta S; D'Mello R; Chance MR, Structure and dynamics of protein waters revealed by radiolysis and mass spectrometry. Proceedings of the National Academy of Sciences 2012, 109 (37), 14882–14887.

1185. Angel TE; Chance MR; Palczewski K, Conserved waters mediate structural and functional activation of family A (rhodopsin-like) G protein-coupled receptors. Proceedings of the National Academy of Sciences 2009, 106 (21), 8555–8560.

1186. Orban T; Gupta S; Palczewski K; Chance MR, Visualizing Water Molecules in Transmembrane Proteins Using Radiolytic Labeling Methods. Biochemistry 2010, 49 (5), 827–834. [PubMed: 20047303]

1187. Kleene R; Schachner M, Glycans and neural cell interactions. Nature Reviews Neuroscience 2004, 5 (3), 195–208. [PubMed: 14976519]

1188. Blixt O; Head S; Mondala T; Scanlan C; Huflejt ME; Alvarez R; Bryan MC; Fazio F; Calarese D; Stevens J; Razi N; Stevens DJ; Skehel JJ; van Die I; Burton DR; Wilson IA; Cummings R; Bovin N; Wong C-H; Paulson JC, Printed covalent glycan array for ligand profiling of diverse glycan binding proteins. Proceedings of the National Academy of Sciences of the United States of America 2004, 101 (49), 17033–17038. [PubMed: 15563589]

1189. Cheng M; Zhang B; Cui W; Gross ML, Laser-Initiated Radical Trifluoromethylation of Peptides and Proteins: Application to Mass-Spectrometry-Based Protein Footprinting. Angewandte Chemie International Edition 2017, 56 (45), 14007–14010. [PubMed: 28901679]

1190. Bavro Vassiliy N.; Gupta S; Ralston C, Oxidative footprinting in the study of structure and function of membrane proteins: current state and perspectives. Biochemical Society Transactions 2015, 43 (5), 983–994. [PubMed: 26517913]

1191. Mummadisetti MP; Frankel LK; Bellamy HD; Sallans L; Goettert JS; Brylinski M; Limbach PA; Bricker TM, Use of protein cross-linking and radiolytic footprinting to elucidate PsbP and PsbQ interactions within higher plant Photosystem II. Proceedings of the National Academy of Sciences 2014, 111 (45), 16178–16183.

1192. Shum W-K; Maleknia SD; Downard KM, Onset of oxidative damage in α-crystallin by radical probe mass spectrometry. Analytical Biochemistry 2005, 344 (2), 247–256. [PubMed: 16091281]

1193. Hart KM; Ho CMW; Dutta S; Gross ML; Bowman GR, Modelling proteins' hidden conformations to predict antibiotic resistance. Nature Communications 2016, 7, 12965.

1194. Loizos N; Darst SA, Mapping protein–ligand interactions by footprinting, a radical idea. Structure 1998, 6 (6), 691–695. [PubMed: 9655829]

1195. Chalmers MJ; Busby SA; Pascal BD; He Y; Hendrickson CL; Marshall AG; Griffin PR, Probing Protein Ligand Interactions by Automated Hydrogen/Deuterium Exchange Mass Spectrometry. Analytical Chemistry 2006, 78 (4), 1005–1014. [PubMed: 16478090]

1196. Iacob RE; Murphy JP III; Engen JR, Ion mobility adds an additional dimension to mass spectrometric analysis of solution-phase hydrogen/deuterium exchange. Rapid Communications in Mass Spectrometry 2008, 22 (18), 2898–2904. [PubMed: 18727141]

1197. Nishimura C; Dyson HJ; Wright PE, Enhanced picture of protein-folding intermediates using organic solvents in H/D exchange and quench-flow experiments. Proceedings of the National Academy of Sciences of the United States of America 2005, 102 (13), 4765–4770. [PubMed: 15769860]

1198. Zhang Z, Retention Time Alignment of LC/MS Data by a Divide-and-Conquer Algorithm. Journal of The American Society for Mass Spectrometry 2012, 23 (4), 764–772. [PubMed: 22298290]

1199. Claesen J; Burzykowski T, Computational methods and challenges in hydrogen/deuterium exchange mass spectrometry. Mass Spectrometry Reviews 2017, 36 (5), 649–667. [PubMed: 27602546]

1200. Denisov IG; Sligar SG, Nanodiscs in Membrane Biochemistry and Biophysics. Chemical Reviews 2017, 117 (6), 4669–4713. [PubMed: 28177242]

1201. Popot J-L, Amphipols, Nanodiscs, and Fluorinated Surfactants: Three Nonconventional Approaches to Studying Membrane Proteins in Aqueous Solutions. Annual Review of Biochemistry 2010, 79 (1), 737–775.

1202. Manzi L; Barrow AS; Hopper JTS; Kaminska R; Kleanthous C; Robinson CV; Moses JE; Oldham NJ, Carbene Footprinting Reveals Binding Interfaces of a Multimeric Membrane-Spanning Protein. Angewandte Chemie International Edition 2017, 56 (47), 14873–14877. [PubMed: 28960650]

1203. Cecil R; McPhee JR, A kinetic study of the reactions on some disulphides with sodium sulphite. Biochemical Journal 1955, 60 (3), 496–506. [PubMed: 13239586]

1204. Heitmann P, A Model for Sulfhydryl Groups in Proteins. Hydrophobic Interactions of the Cysteine Side Chain in Micelles. European Journal of Biochemistry 1968, 3 (3), 346–350. [PubMed: 5650851]

1205. Means GE; Congdon WI; Bender ML, Reactions of 2,4,6-trinitrobenzenesulfonate ion with amines and hydroxide ion. Biochemistry 1972, 11 (19), 3564–3571. [PubMed: 5053758]

1206. Schirch L; Slagel S; Barra D; Martini F; Bossa F, Evidence for a sulfhydryl group at the active site of serine transhydroxymethylase. Journal of Biological Chemistry 1980, 255 (7), 2986–2989. [PubMed: 7358720]

1207. Mennella C; Visciano M; Napolitano A; Del Castillo MD; Fogliano V, Glycation of lysine-containing dipeptides. Journal of Peptide Science 2006, 12 (4), 291–296. [PubMed: 16180244]

1208. Cornwell O; Bond NJ; Radford SE; Ashcroft AE, Long-Range Conformational Changes in Monoclonal Antibodies Revealed Using FPOP-LC-MS/MS. Analytical Chemistry 2019.

1209. Purushottam L; Adusumalli SR; Singh U; Unnikrishnan VB; Rawale DG; Gujrati M; Mishra RK; Rai V, Single-site glycine-specific labeling of proteins. Nature Communications 2019, 10 (1), 2539.

1210. Osberger TJ; Rogness DC; Kohrt JT; Stepan AF; White MC, Oxidative diversification of amino acids and peptides by small-molecule iron catalysis. Nature 2016, 537 (7619), 214–219. [PubMed: 27479323]

1211. Huang RYC; Garai K; Frieden C; Gross ML, Hydrogen/Deuterium Exchange and Electron-Transfer Dissociation Mass Spectrometry Determine the Interface and Dynamics of Apolipoprotein E Oligomerization. Biochemistry 2011, 50 (43), 9273–9282. [PubMed: 21899263]

1212. Pan Y; Piyadasa H; O'Neil JD; Konermann L, Conformational Dynamics of a Membrane Transport Protein Probed by H/D Exchange and Covalent Labeling: The Glycerol Facilitator. Journal of Molecular Biology 2012, 416 (3), 400–413. [PubMed: 22227391]

1213. Baud A; Gonnet F; Salard I; Le Mignon M; Giuliani A; Mercère P; Sclavi B; Daniel R, Probing the solution structure of Factor H using hydroxyl radical protein footprinting and cross-linking. Biochemical Journal 2016, 473 (12), 1805–1819. [PubMed: 27099340]

1214. Lin M; Krawitz D; Callahan MD; Deperalta G; Wecksler AT, Characterization of ELISA Antibody-Antigen Interaction using Footprinting-Mass Spectrometry and Negative Staining Transmission Electron Microscopy. Journal of The American Society for Mass Spectrometry 2018, 29 (5), 961–971. [PubMed: 29512051]

1215. Shi L; Liu T; Gross ML; Huang Y, Recognition of Human IgG1 by Fcγ Receptors: Structural Insights from Hydrogen–Deuterium Exchange and Fast Photochemical Oxidation of Proteins Coupled with Mass Spectrometry. Biochemistry 2019, 58 (8), 1074–1080. [PubMed: 30666863]

1216. Delahunty C; Yates Iii JR, Protein identification using 2D-LC-MS/MS. Methods 2005, 35 (3), 248–255. [PubMed: 15722221]

1217. Doneanu C; Xenopoulos A; Fadgen K; Murphy J; Skilton SJ; Prentice H; Stapels M; Chen W, Analysis of host-cell proteins in biotherapeutic proteins by comprehensive online two-dimensional liquid chromatography/mass spectrometry. mAbs 2012, 4 (1), 24–44. [PubMed: 22327428]

1218. Garbis SD; Roumeliotis TI; Tyritzis SI; Zorpas KM; Pavlakis K; Constantinides CA, A Novel Multidimensional Protein Identification Technology Approach Combining Protein Size

Exclusion Prefractionation, Peptide Zwitterion–Ion Hydrophilic Interaction Chromatography, and Nano-Ultraperformance RP Chromatography/nESI-MS2 for the in-Depth Analysis of the Serum Proteome and Phosphoproteome: Application to Clinical Sera Derived from Humans with Benign Prostate Hyperplasia. Analytical Chemistry 2011, 83 (3), 708–718. [PubMed: 21174401]

1219. Bouvier ESP; Koza SM, Advances in size-exclusion separations of proteins and polymers by UHPLC. TrAC Trends in Analytical Chemistry 2014, 63, 85–94.

1220. Muneeruddin K; Nazzaro M; Kaltashov IA, Characterization of Intact Protein Conjugates and Biopharmaceuticals Using Ion-Exchange Chromatography with Online Detection by Native Electrospray Ionization Mass Spectrometry and Top-Down Tandem Mass Spectrometry. Analytical Chemistry 2015, 87 (19), 10138–10145. [PubMed: 26360183]

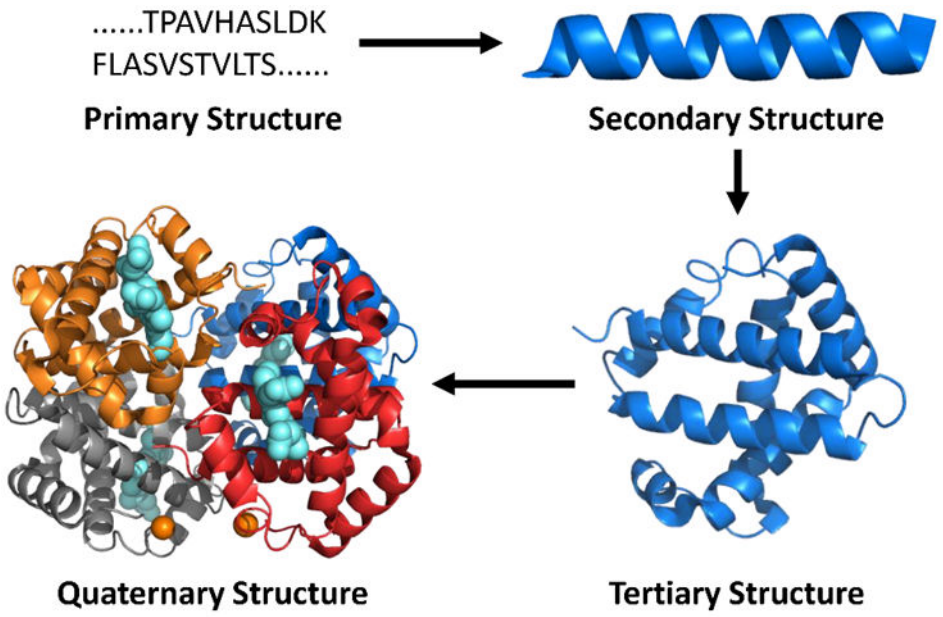

Figure 1.
Four orders of protein structure exemplified by human deoxyhemoglobin (PDB ID 2HHB[3]).

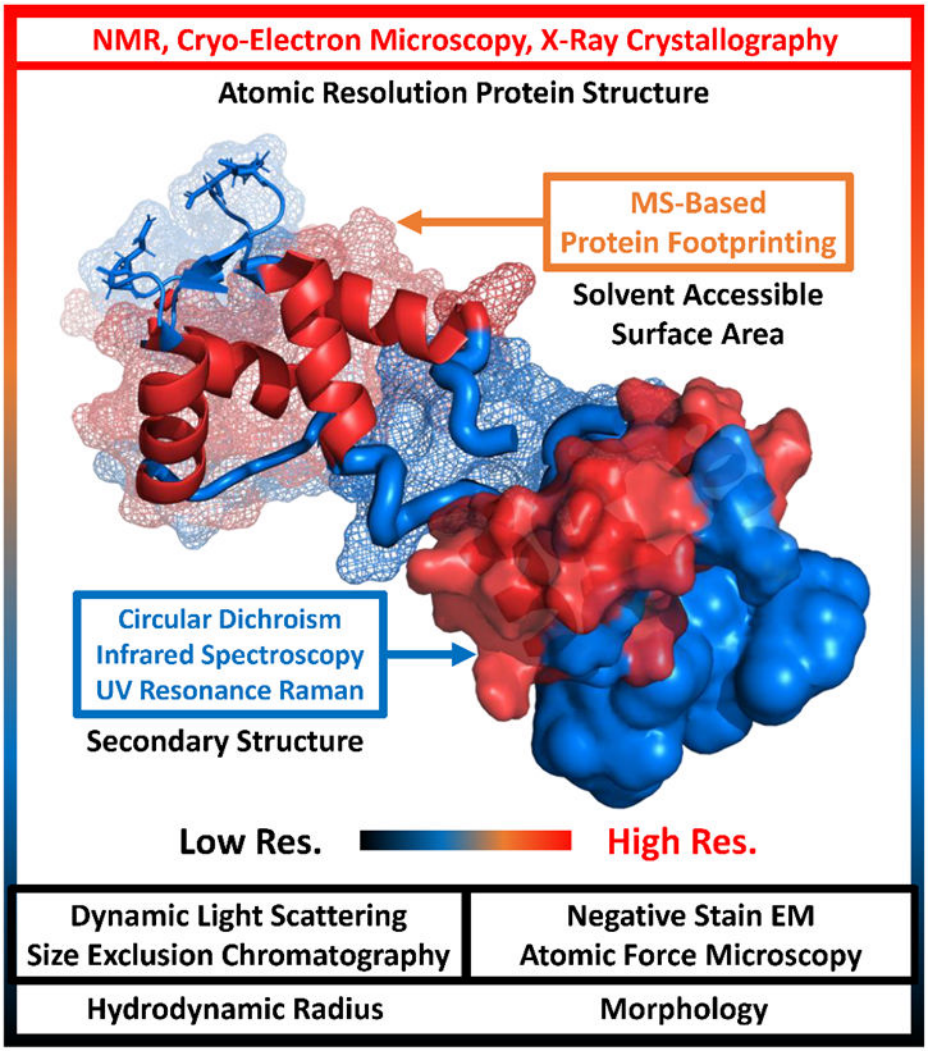

Figure 2.

A summary of commonly used biophysical tools for characterizing protein HOS. Protein structure exemplified by calcium-free bovine calmodulin (PDB ID 1CFD[24])

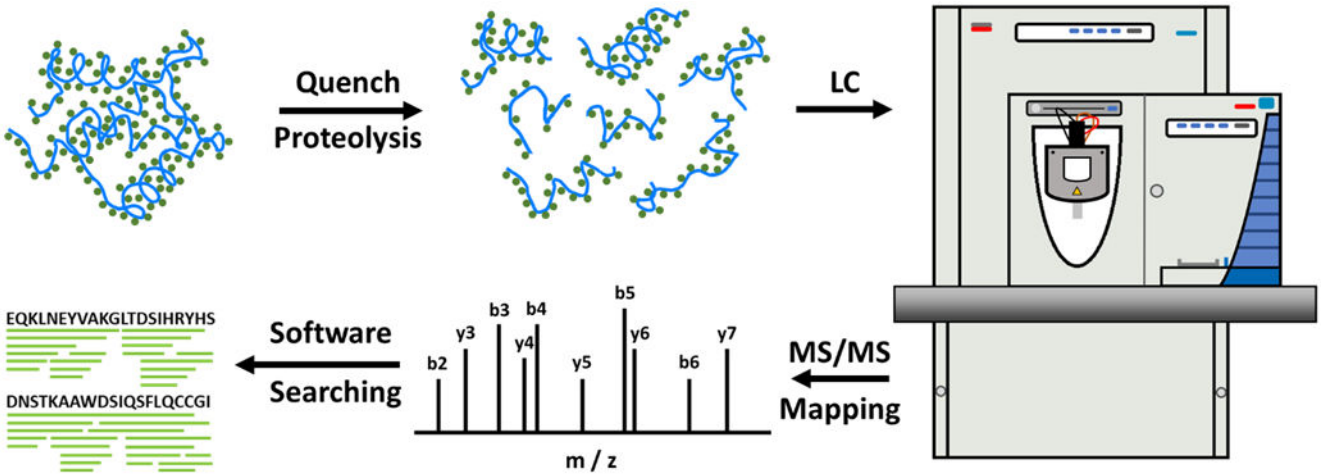

Figure 3.

Schematic illustration of a bottom-up peptide mapping workflow, a necessary step prior to HDX. Green dots in the protein structure indicate hydrogen atoms in the peptide bonds.

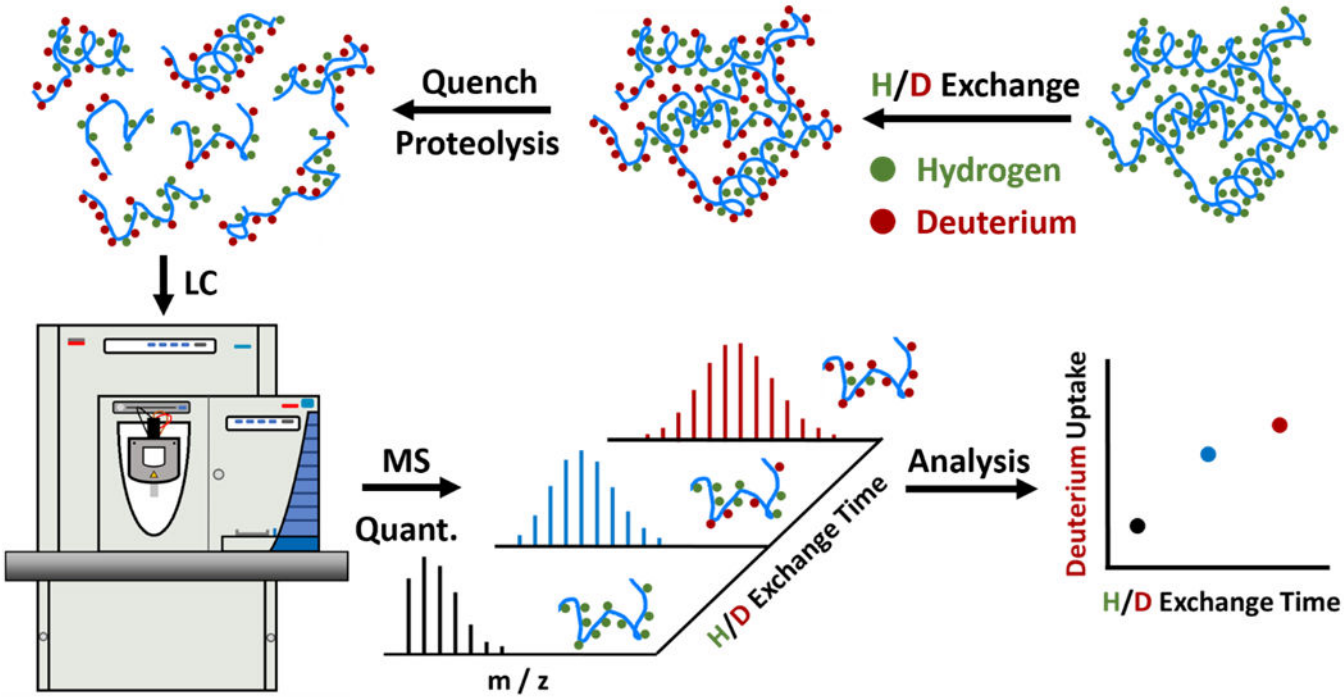

Figure 4.

Schematic illustration of a bottom-up HDX workflow. Green and red dots in the protein structure indicate hydrogen and deuterium atoms in the peptide bonds, respectively.

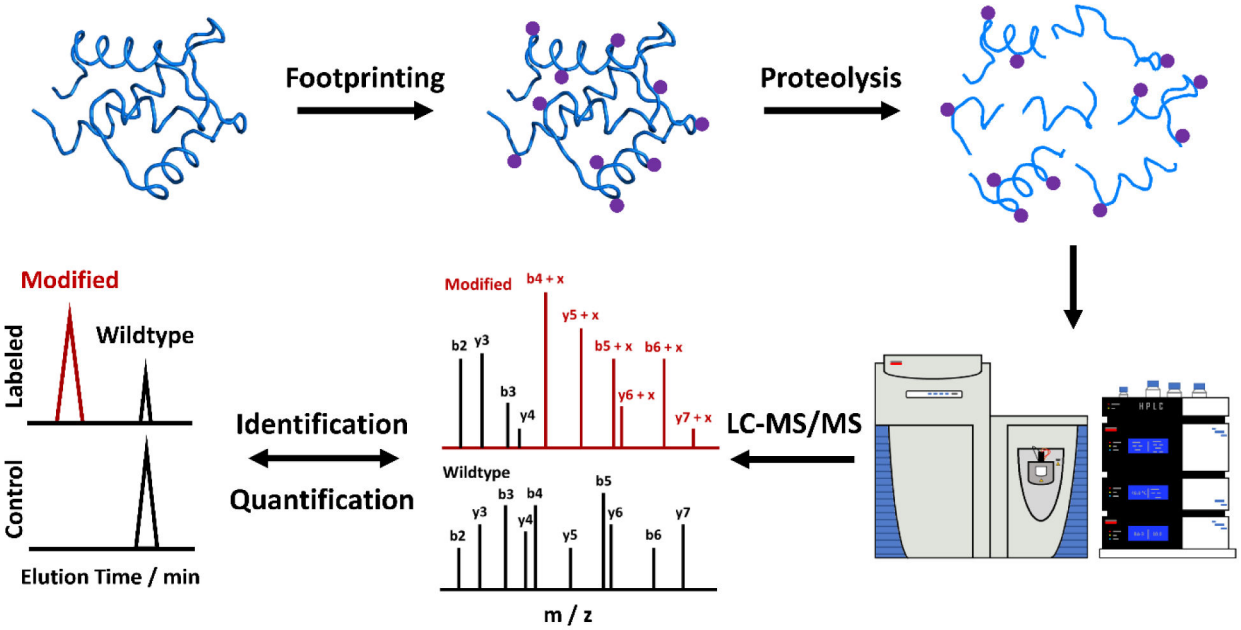

Figure 5.
Schematic illustration of bottom-up protein HOS analysis through irreversible labeling approaches

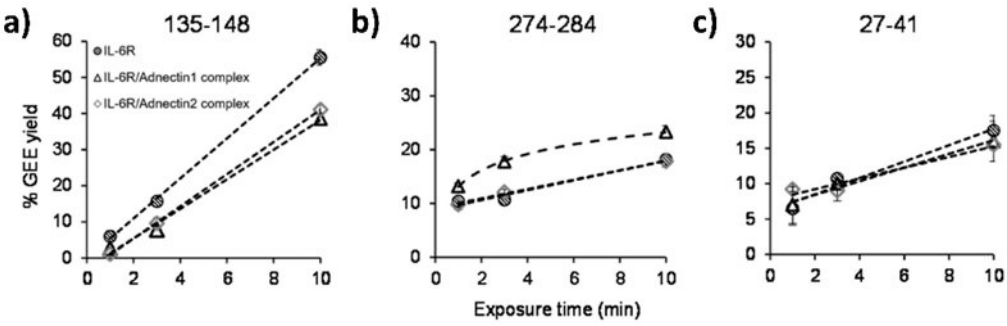

Figure 6.

GEE labeling kinetics for selected IL-6R peptides in the ligand-free (gridded circle), adnectin 1-bound (triangle) and adnectin 2-bound state (diamond) state. (a) Region 135–148 shows decreased GEE incorporation upon adnectin 1/adnectin2 binding, whereas (b) region 274–284 shows increased GEE modification upon adnectin1 binding. (c) Representative peptide region without differentiable GEE modification extent between bound and unbound as a control. Dashed trend curves in (a), (b), and (c) are generated by linear or 2nd-degree polynomial fitting. Figure adopted with permission from Ref. [738]. Copyright 2017 American Chemistry Society.

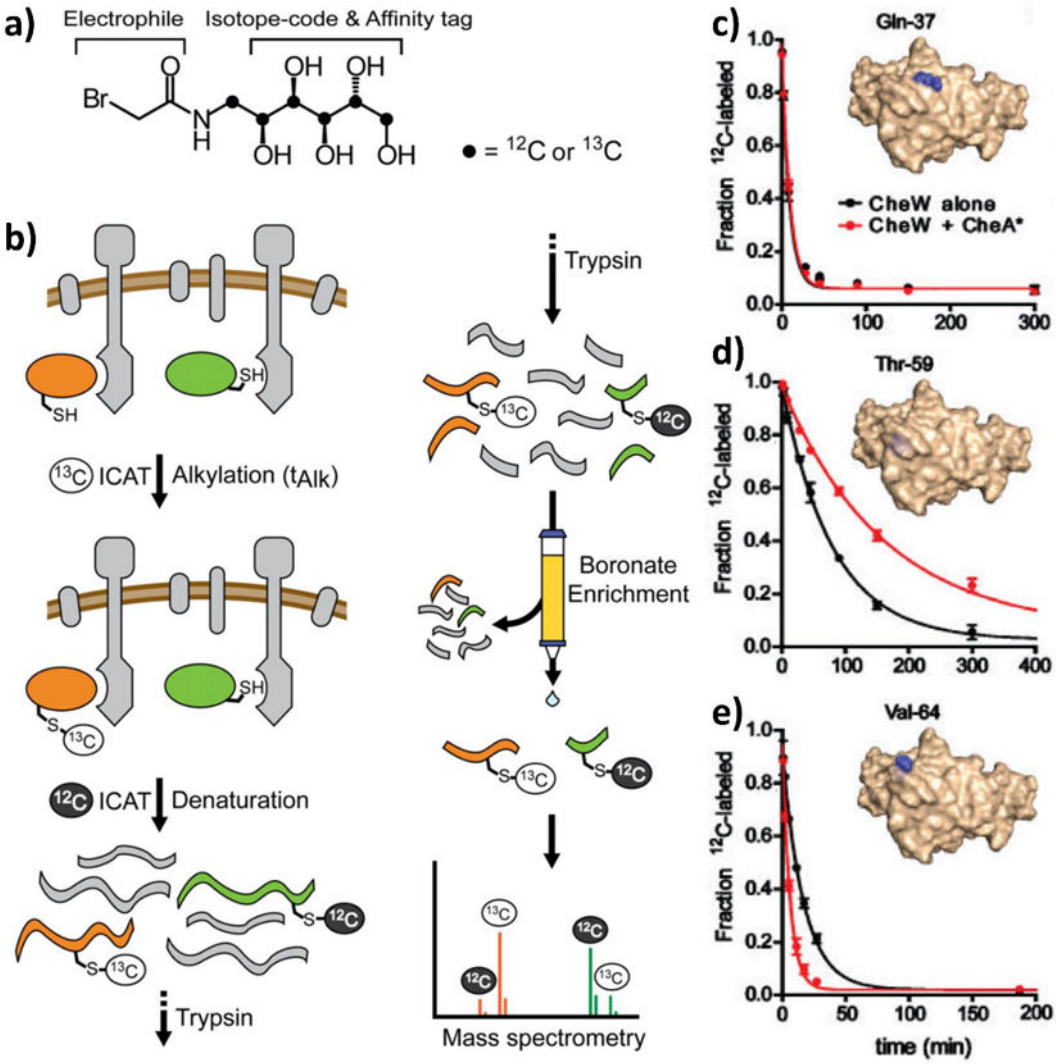

Figure 7.

Overview of Cys footprinting with an ICAT reagent. (a) Structure of bromoacetamide ICAT reagent. Dots represent ^{12}C for light reagent and ^{13}C for heavy reagent. (b) Workflow for alkylation rate determination by ICAT isotope pairs. (c) – (e) Representative alkylation time courses of CheW Cys variants footprinted in the presence (red) or absence (black) of CheA*. Figure adopted with permission from Ref. [744]. Copyright 2011 Elsevier.

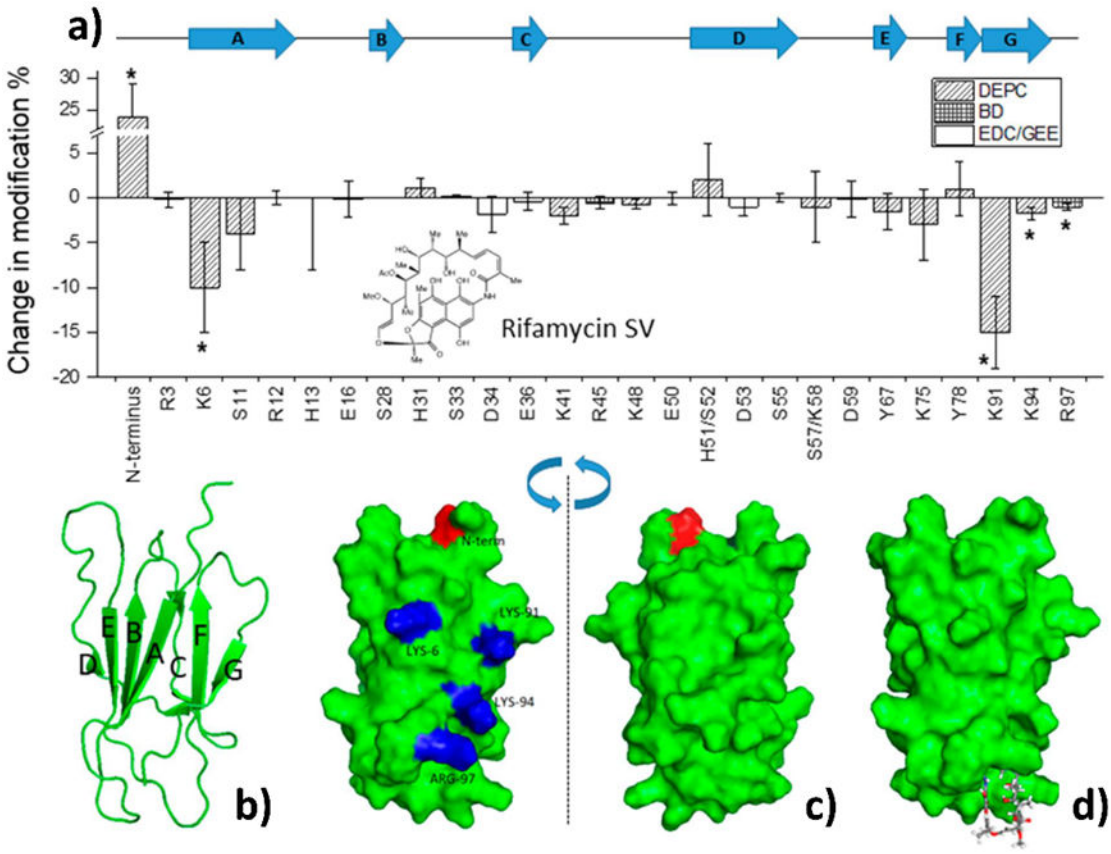

Figure 8.

Covalent labeling results of β2m binding with rifamycin SV. (a) Changes in labeling modification percentages with rifamycin SV bound to the Cu(II)–protein complex. BD is 2,3-butanedione. Error bars represent standard deviations from triplicate measurements. Asterisks above the bars represent the residues that undergo a significant change in modification level at 95% confidence as determined by a two-sample unpaired Student's t test. The arrows at the top of the graph indicate the locations and directions of the seven β strands in β2m. (b) Ribbon structure of β2m, showing the seven β strands labeled A through G. (c) β2m surface structure illustrating the sites undergoing significant changes in covalent labeling induced by rifamycin SV. Sites that increase in labeling are colored red, whereas those that decrease in labeling are colored blue. (d) Protein–ligand docking results for verification. Figure adopted with permission from Ref. [749]. Copyright 2017 American Chemistry Society.

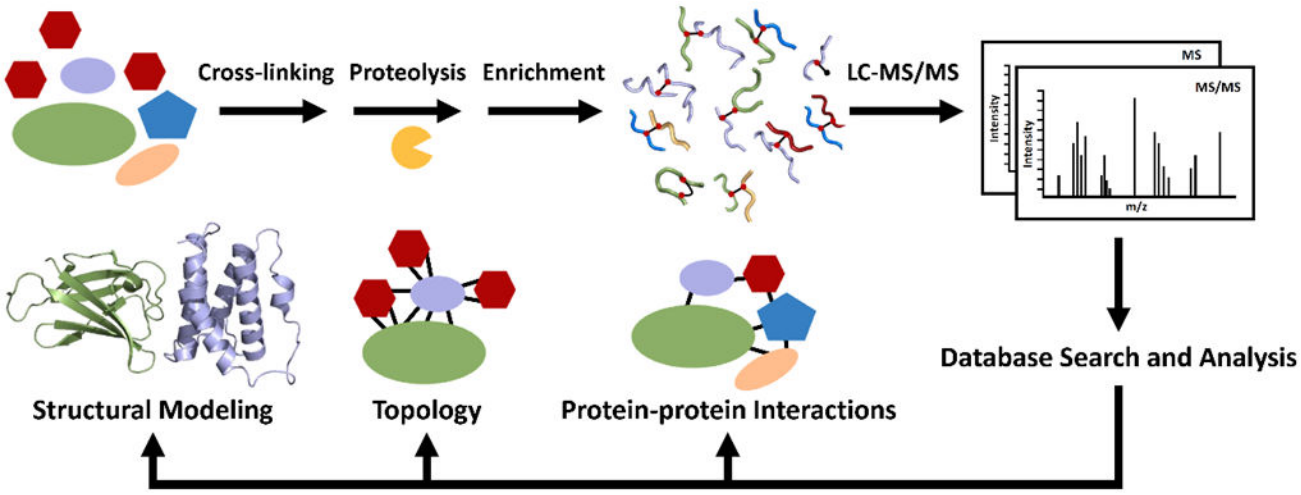

Figure 9.
Workflow of bottom-up cross-linking mass spectrometry

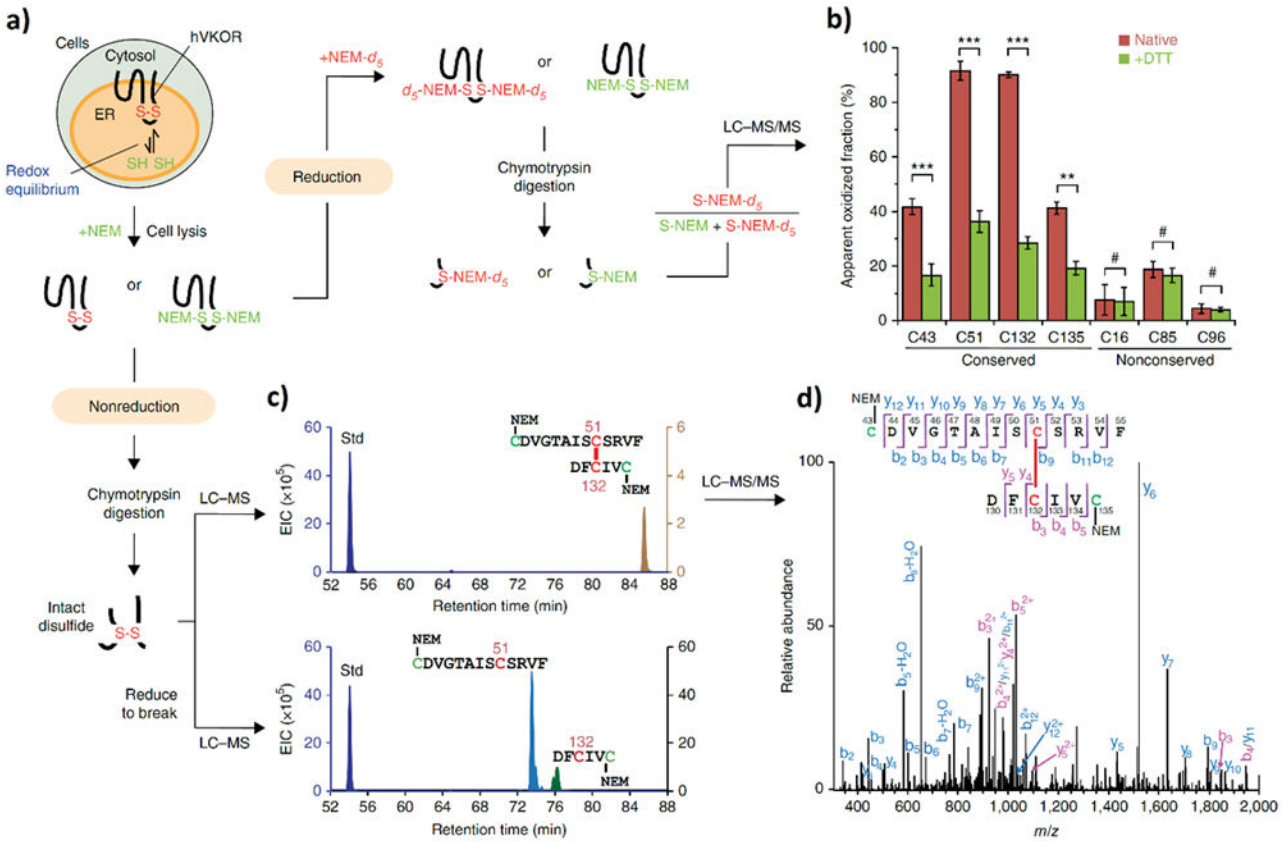

Figure 10.

Schematic illustration of *in vivo* Cys footprinting workflow. (a) Scheme of MS analysis. The redox status of cysteines was quantified by differential isotope footprinting with NEM before and after a reduction step (right). Intact disulfide bonds were detected under nonreducing conditions (bottom). (b) Intracellular cysteine status was determined by quantitative MS before (red) and after DTT reduction (green). Bar graphs show means and errors of multiple peptides from three independent experiments **P < 0.001; ***P < 0.0001; #P > 0.05 by two-tailed Student's t test. (c) Extracted-ion chromatograms showing a Cys51-Cys132 disulfide-linked peptide (top), which separates into two individual peptides (bottom) after reduction of the disulfide. A reference peptide is used as the standard (Std) for peak comparison. (d) MS/MS spectrum of the Cys51-Cys132 linked peptide (from c). Adopted with permission from Ref. [816]. Copyright 2017 Springer Nature.

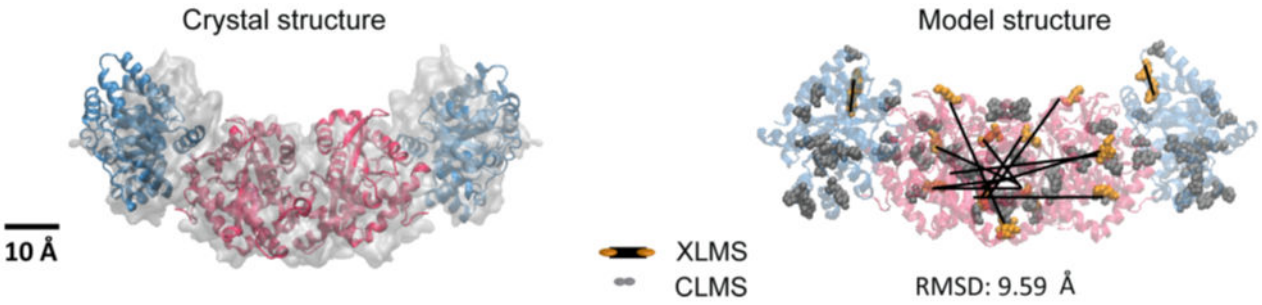

Figure 11.

Representative model of the tetrameric tryptophan synthase and its corresponding crystal structure. Inter-residue proximities (XL-MS) and residue solvent accessibilities (covalent labeling MS, CL-MS) are highlighted. Figure adopted with permission from Ref. [832]. Copyright 2017 American Chemistry Society.

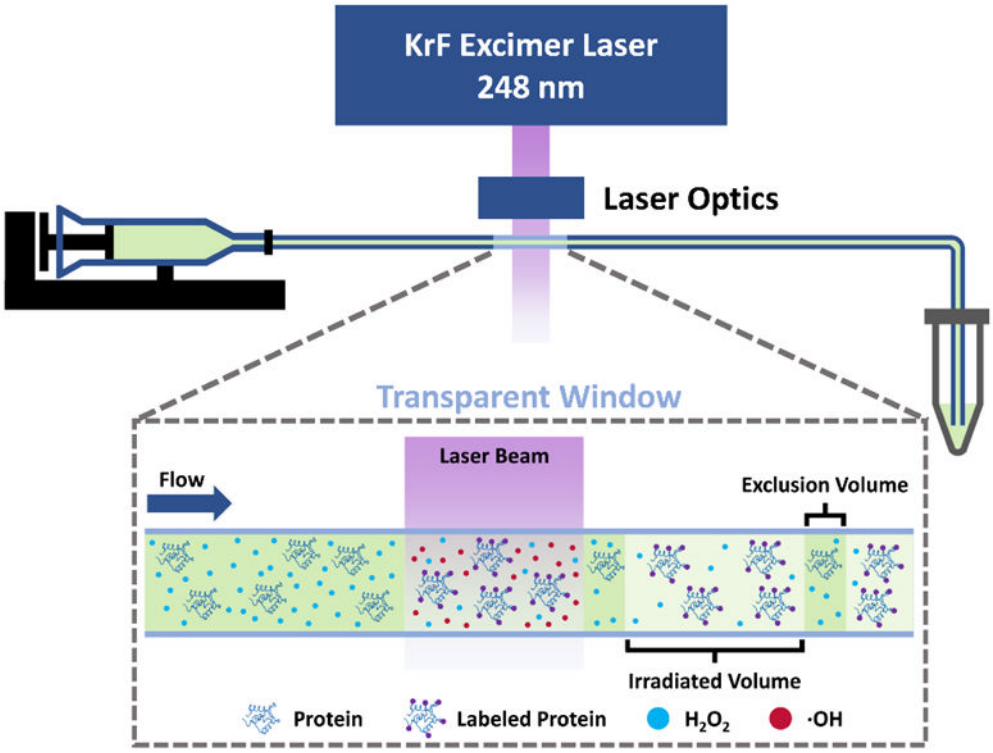

Figure 12.
Schematic illustration of FPOP setup

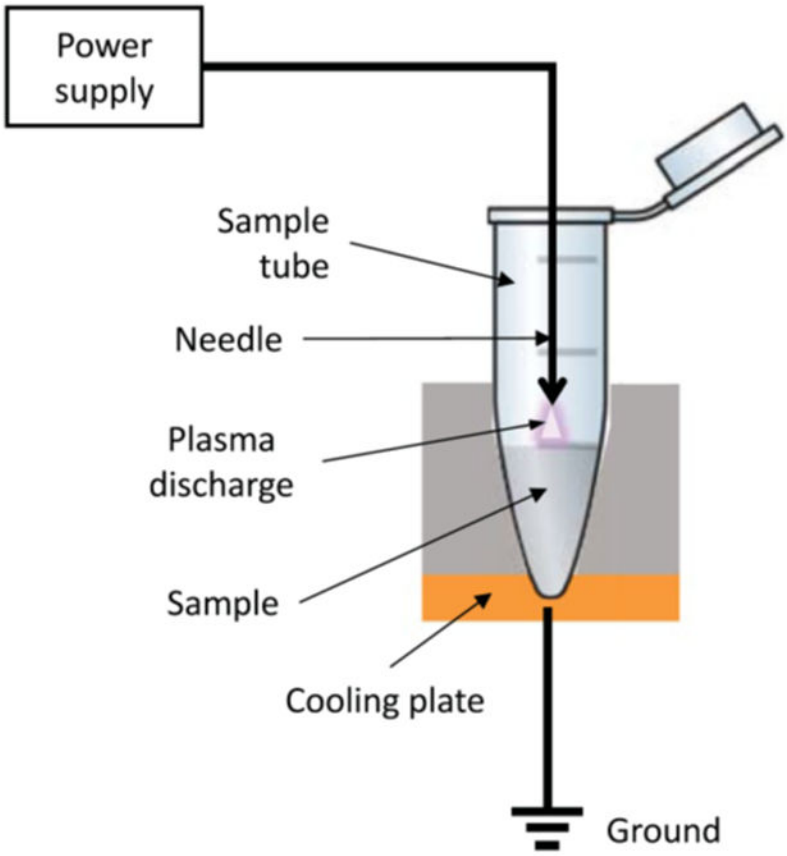

Figure 13.
Schematic illustration of PLIMB setup. Adapted with permission from ref.[907]. Copyright 2017 Springer Nature.

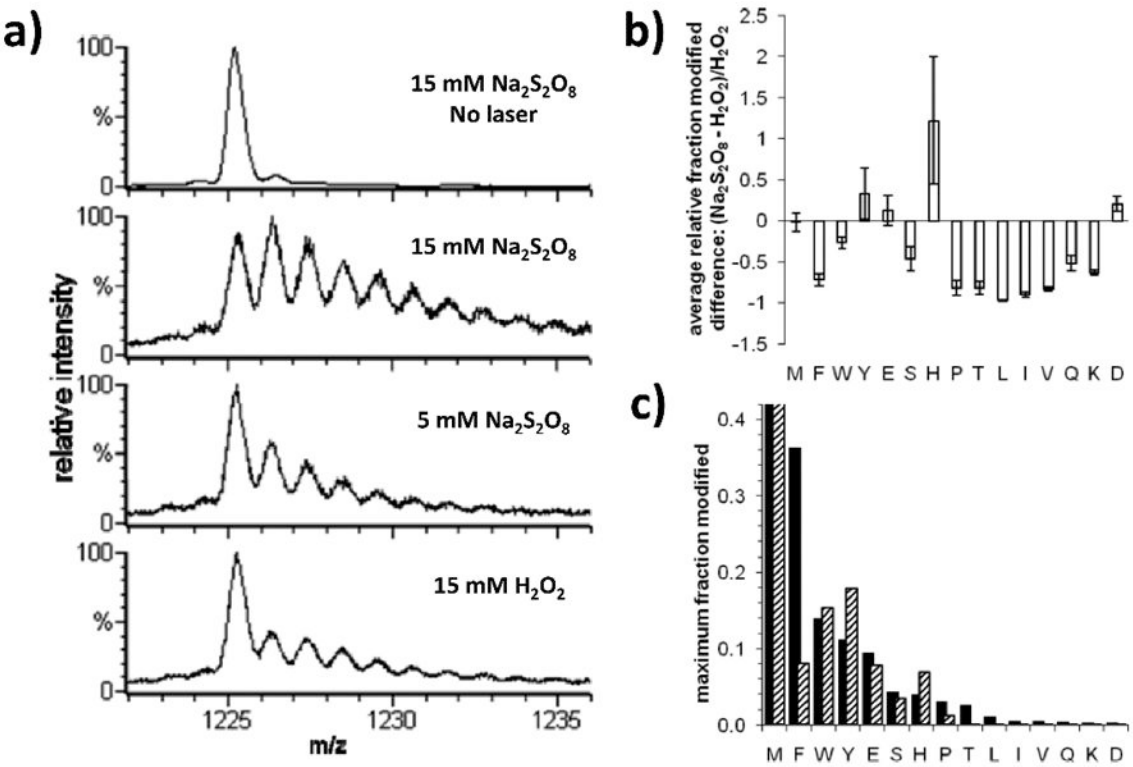

Figure 14.

(a) The ESI-quadrupole time-of-flight mass spectra of the 15th charge state of β-lactoglobulin submitted to different labeling conditions as shown in the figure. (b) The relative difference in fraction modified between persulfate and the H_2O_2 approaches for CaM, aMb, bradykinin, and angiotensin II residues, are averaged per amino acid type. The error bars denote the average pairwise-comparison standard error. (c) The maximum fraction modified among all the same amino acid residues is plotted. Black bars denote H_2O_2 FPOP. Reprinted with permission from Ref.[941] Copyright 2010 American Chemical Society.

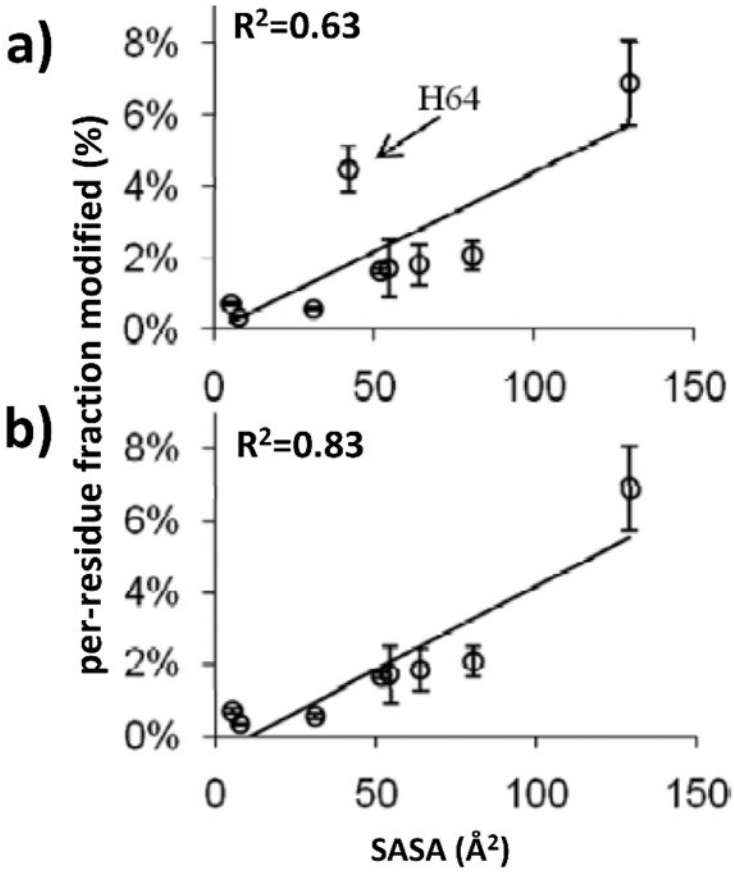

Figure 15.

The modification yields of apomyoglobin His residues, where (a) all histidines were included and (b) His64 was omitted, are plotted against their calculated SASA, shown with least-squares straight-line fits. The SASA values were calculated by using a 1.4 Å probe. Reprinted with permission from Ref.[941] Copyright 2010 American Chemical Society.

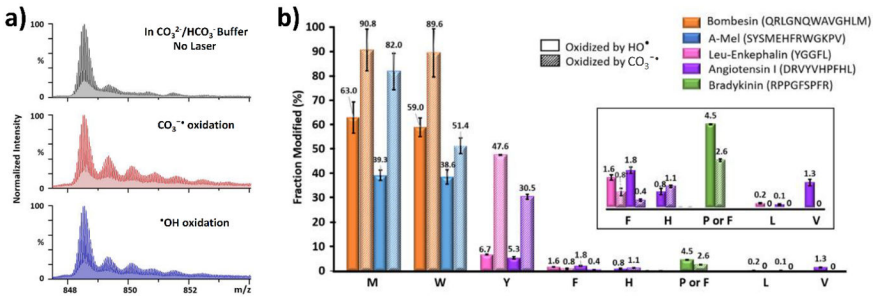

Figure 16.

(a) The quadrupole time-of-flight (QTOF) mass spectra of the + 20 charge state of apo-myoglobin (aMb) under different labeling conditions as given in the figure. (b) Comparison of the residue-level fraction modified (in percentage) of a 'Peptide Cocktail' by $CO_3^{-\bullet}$ and $^{\bullet}$OH. Different colors represent different peptides, and the corresponding sequences are shown. Solid bars denote the $^{\bullet}$OH oxidation extent, and patterned bars denote the $CO_3^{-\bullet}$ oxidation. The data were corrected with respect to a negative control. Error bars are the standard deviations of three independent runs. The inset is an enlarged portion of the figure. For bradykinin, only F undergoes oxidation with $CO_3^{-\bullet}$, whereas F and P are both oxidized by $^{\bullet}$OH but not distinguishable because the chromatograms of the two modified peptides overlap. Reprinted with permission from Ref. [957] Copyright 2019 Elsevier.

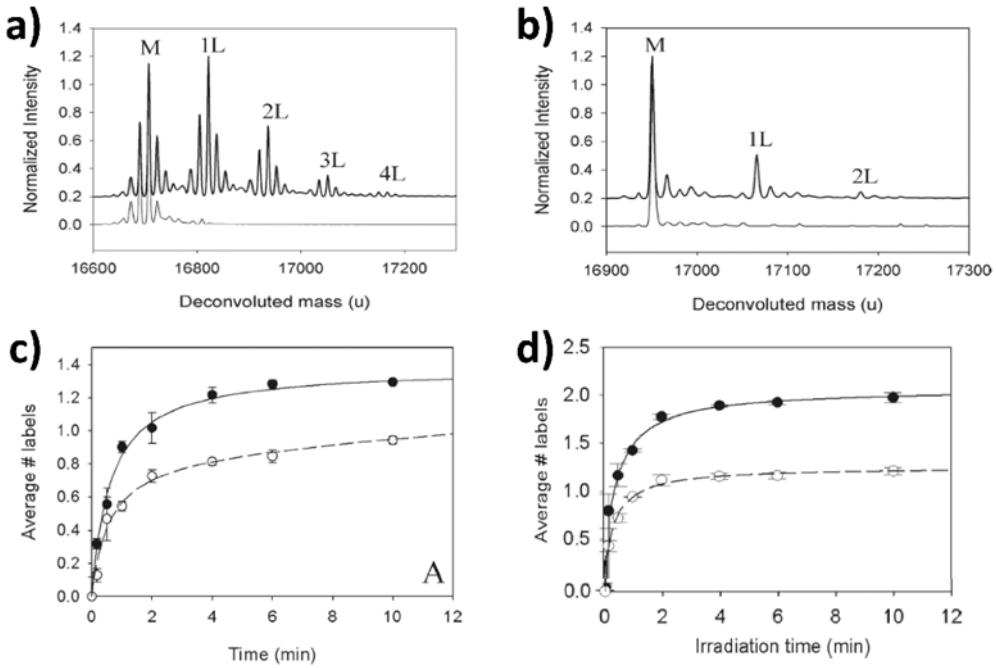

Figure 17.

(a) Deconvoluted mass spectra of myoglobin after footprinting with carbenes. (b) Deconvoluted mass spectra of labeled and unlabeled holo-CaM. (c) Ca^{2+}-binding induces conformational change on calmodulin where apo-calmodulin (closed circles) and holo-calmodulin (open circles) were labeled with 100 mM photoleucine in phosphate buffer and monitored as function of time. (d) Free holo-calmodulin (filled circles) is referenced to M13-bound holo-calmodulin (open circles). Reprinted with permission from Ref. [967]. Copyright 2011 American Chemical Society.

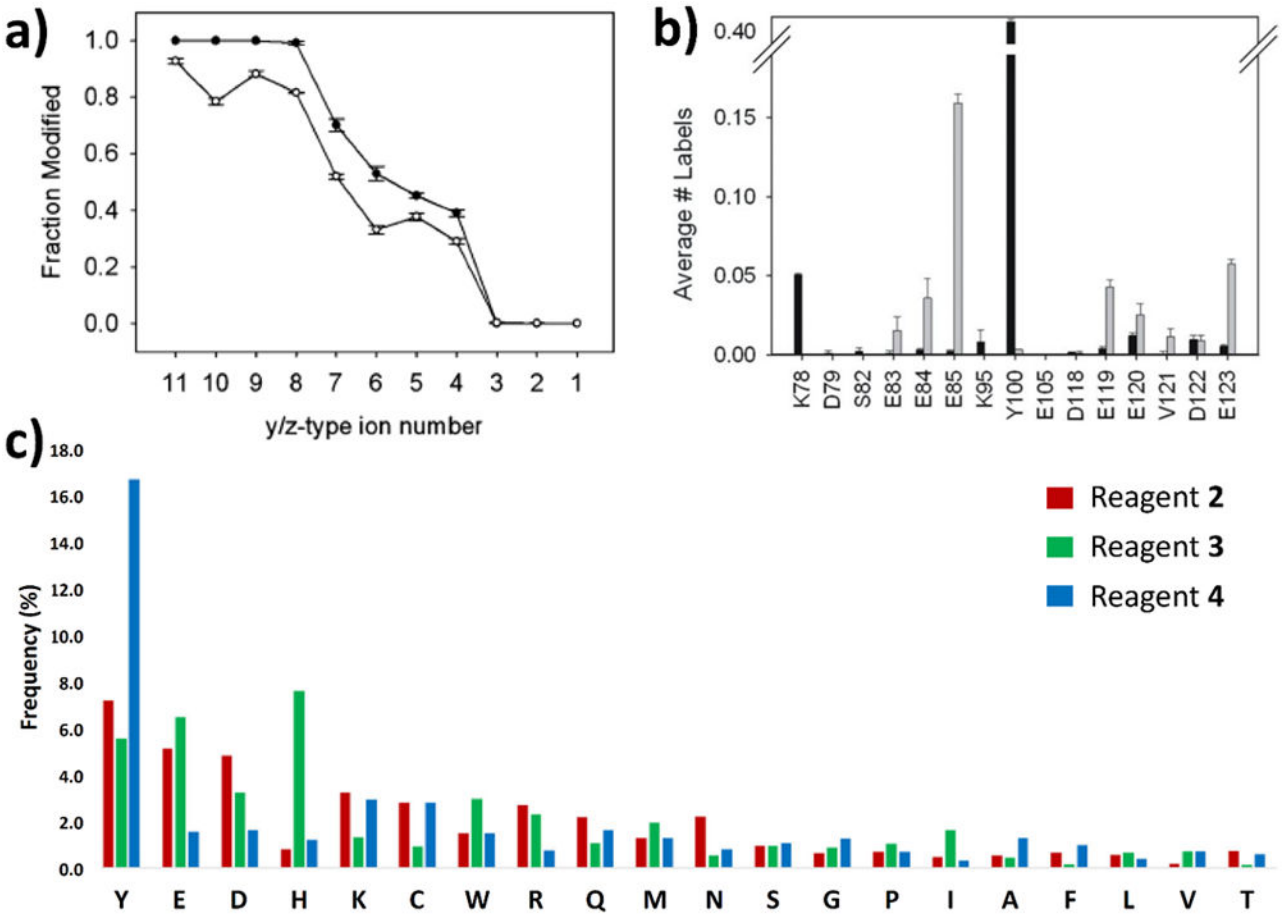

Figure 18.

(a) Fractional distributions of carbene label derived from reagent 1 as determined by ETD (z-ions, filled circles) and HCD (y-ions, open circles) for peptide LTDEEVDEMIR (117–127) in CaM. (b) Residue-level reagent incorporation for select residues, based on ETD fragmentation of MKDTDSEEEIR (77–87), VFDKDGNGYISAAELR (92–107) and LTDEEVDEMIR (117–127) with Reagent 1 (gray bars) and Reagent 2 (black bars). Error bars are ± 1 standard deviation. Reprinted with permission from Ref.[968] Copyright 2012 American Chemical Society. (c) Average frequency of carbene insertion at each residue generated from the photolysis of reagent 2, 3, and 4 in the presence of protein digests (777 peptides). Site of the label insertion was located with MS/MS with a Fusion Lumos with EThcD fragmentation and analyzed with Mass Spec Studio software. Reprinted with permission from Ref.[969]. Copyright 2017 Springer Nature.

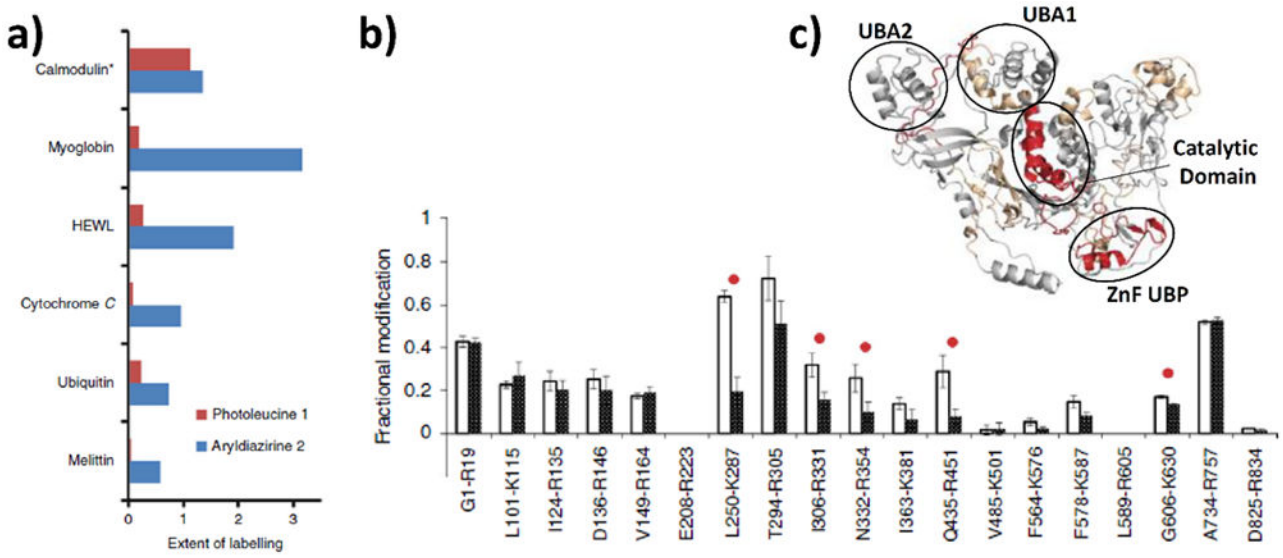

Figure 19.

(a) Extent of labelling of a range of proteins with reagent 1 (100 mM, 16 s irradiation), and reagent 5 (10 mM, 4 s irradiation (*1 s in the case of CaM)). (b) Fractional modification by reagent 5 of USP5 peptides in the presence (black bars) and absence (white bars) of di-ubiquitin. Error bars are ± standard deviations (n = 3) and significant differences (Student's t-test, $p < 0.05$) are highlighted with a red dot. (c) Model of USP5 (based on PDB 3IHP) showing the locations of the five peptides (red) that are masked from labelling by di-ubiquitin binding and their relative locations to the ZnFUBP and catalytic domains. Reprinted with permission from Ref.[974] Copyright 2016 Springer Nature.

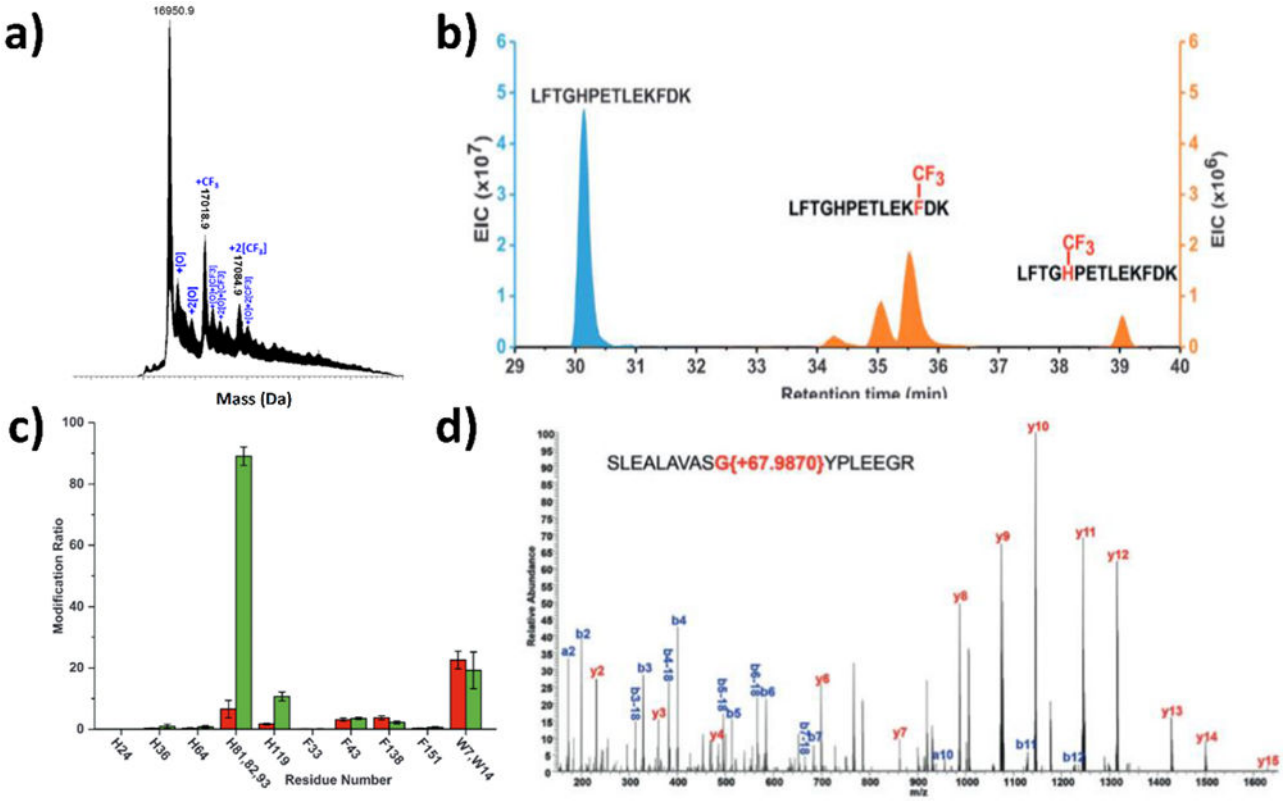

Figure 20.

(a) Deconvoluted mass spectrum of CF_3-modified aMb. (b) EIC of unmodified and CF_3-modified peptide 32–45 of aMb. (c) Comparison of the extent of modification at the residue level for hMb and aMb. (d) A key mass shift of +68 Da is consistent with an unusual Gly labeling, here CF_3 modification on Gly-276 of peptide 267–83, a glycine with large SASA. Reprinted with permission from Ref.[999] Copyright 2017 John Wiley & Sons, Inc.

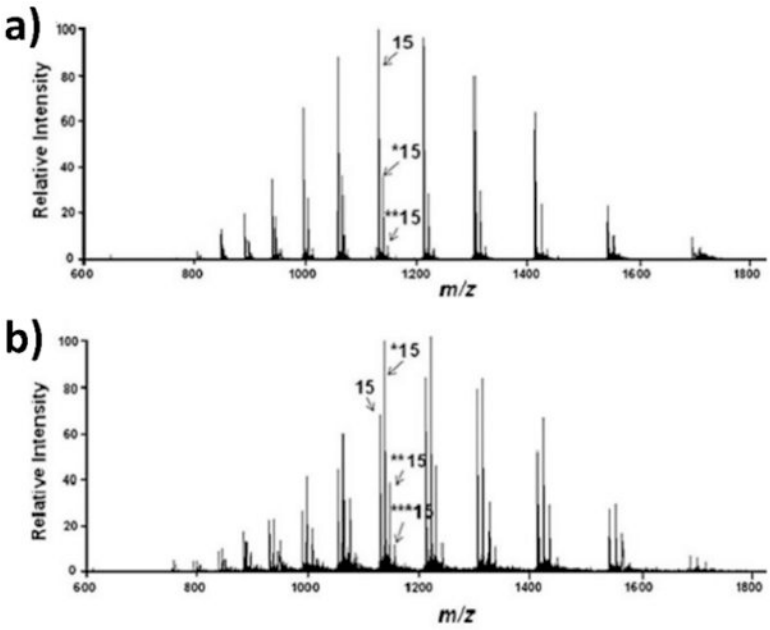

Figure 21.

(a) Full ESI mass spectra of iodinated hMb. (b) Full ESI mass spectrum of iodinated aMb. The unmodified, mono-, di-, and tri-iodinated species of the 15th charge state are indicated by the number of stars. Reprinted with permission from Ref. [181]. Copyright 2012 Springer Nature.

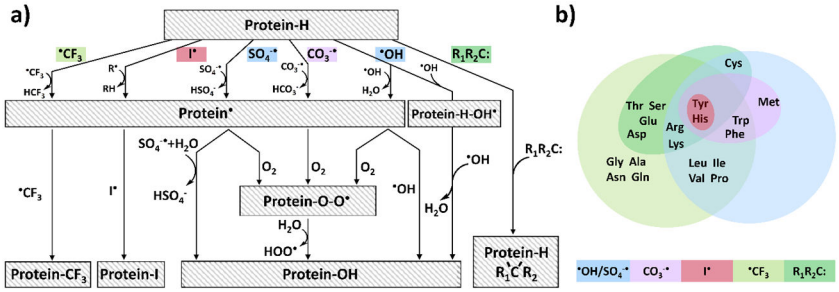

Figure 22.

Summary of radical-based footprinting reagents of (a) proposed pathways and (b) residue specificity.

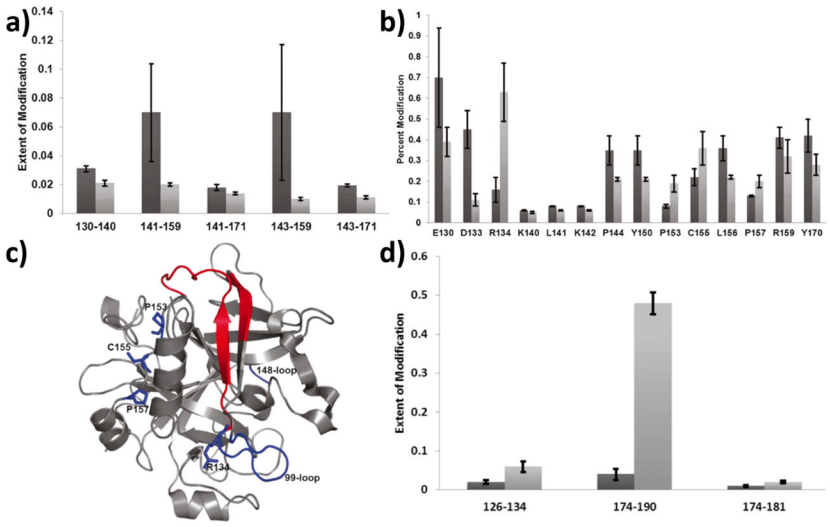

Figure 23.

(a) Extent of modification of thrombin alone (darker bars) and antibody-bound thrombin (lighter bars) for the five peptides that span the 130-171 region. (b) Extent of modification of thrombin alone (darker bars) compared to antibody-bound thrombin (lighter bars) at the residue level. (c) Structural model of thrombin (PDB file 2AFQ[1043]) with the proposed epitope colored in red and the loop regions colored in blue. The individual residues that show increased modification for antibody-bound thrombin are specified. (d) Extent of modification of peptides from thrombin alone (darker bars) and antibody-bound thrombin (lighter bars) show increased solvent accessibility in the antibody-bound form. Reproduced with permission from ref [1044]. Copyright 2011 American Chemical Society.

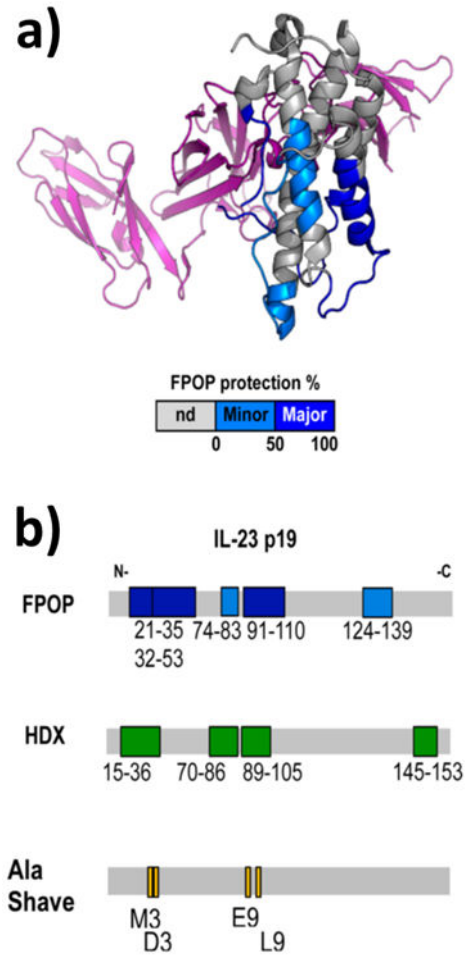

Figure 24.

(a) Epitope regions determined by FPOP mapped on the crystal structure of IL-23 p19 domain. Color code: no significant difference (gray), minor epitope region (cyan), and major epitope region (blue). The p40 subunit is colored in purple. (b) Epitope regions determined by FPOP, HDX, and Ala shave energetics are mapped on the linear sequence of the IL-23 p19 domain. M3, D3, E9, L9 stands for M35A, D36A, E93A, L97A, respectively. Adapted with permission from ref [1048]. Copyright 2011 American Chemical Society.

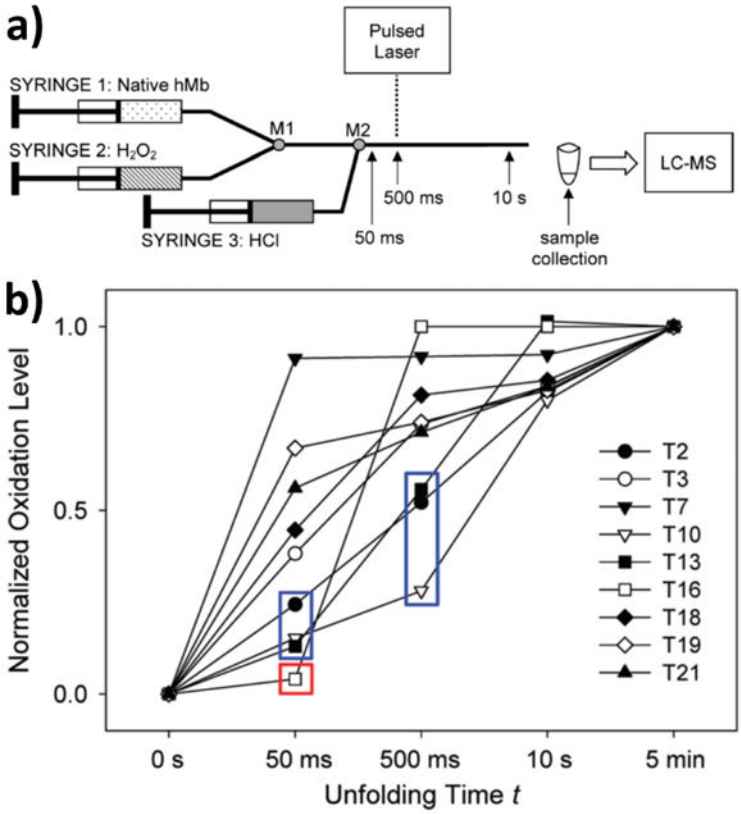

Figure 25.

(a) Schematic illustration of the three-syringe, continuous-flow, rapid mixing setup for oxidative ●OH labeling. (b) Normalized oxidation levels of tryptic peptides plotted as a function of unfolding time *t*. Blue boxes highlight three peptides that retain considerable protection at 50 and 500 ms whereas the peptide highlighted by a red box is protected at 50 ms but not at 500 ms. Adapted with permission from ref [1084]. Copyright 2009 American Chemical Society.

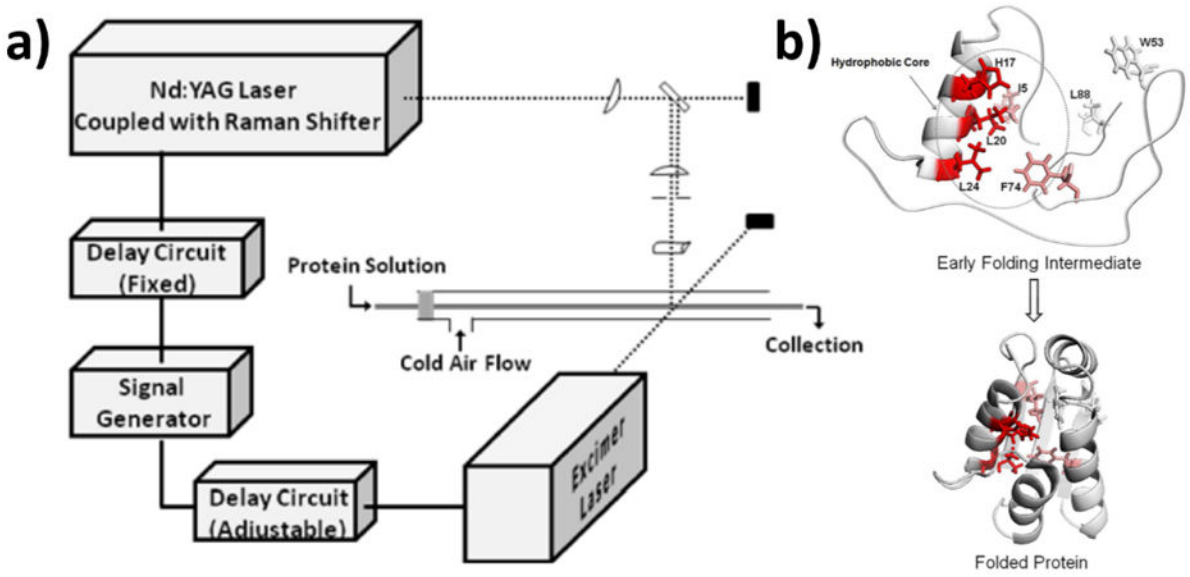

Figure 26.

(a) Schematic illustration of the flow system intersected by two laser beams at a transparent window, as part of a temperature-jump apparatus. Adapted with permission from ref [893]. Copyright 2009 American Chemical Society. (b) Proposed intermediate for barstar early folding. Residues colored in red, pink and gray represent residues that are closely associated with hydrophobic core, weakly associated with hydrophobic core and not involved in early folding intermediate, respectively. Adapted with permission from ref [894]. Copyright 2009 American Chemical Society.

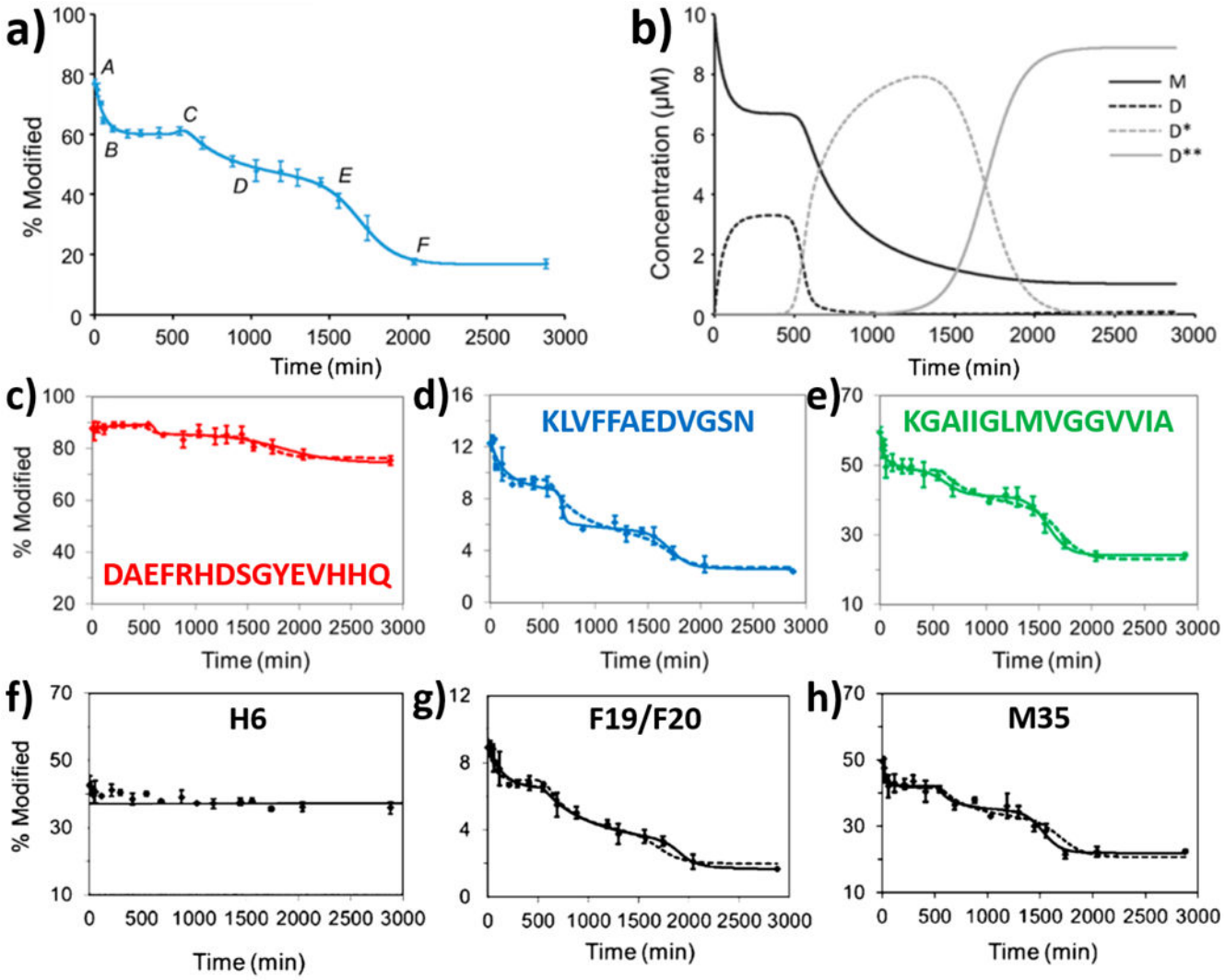

Figure 27.

FPOP and kinetic modeling results for time-dependent aggregation of 42-residue Aβ ($A\beta_{1-42}$) at (a, b) global, peptide and residue levels. (a) Global level results for $A\beta_{1-42}$ aggregation. Solid curve is from a fitting model based on two autocatalytic reactions. (b) Concentrations for representative species (M-monomer, D-paranuclei, D*-protofibrils, D**-fibrils) as a function of incubation time based on kinetic simulation. (c, d, e) Peptide-level results for Lys-N digested $A\beta_{1-42}$, N-terminal region 1-15, middle region 16-27 and C-terminal region 28-42, respectively. (f, g, h) Residue level results for three representative residues, H6, F19/F20 and M35, respectively. Points in each plot represent experimental data (10 μM, pH 7.4, no agitation) and error bars are standard deviations from three independent trials. Solid and dashed lines in (c – h) are model fits independent of or constrained by the global rates, respectively. Adapted with permission from ref [1020]. Copyright 2009 American Chemical Society.

Figure 28.

Schematic illustration LITPOMS workflow. Reprinted with permission from ref. [1129]. Copyright 2019 Springer.

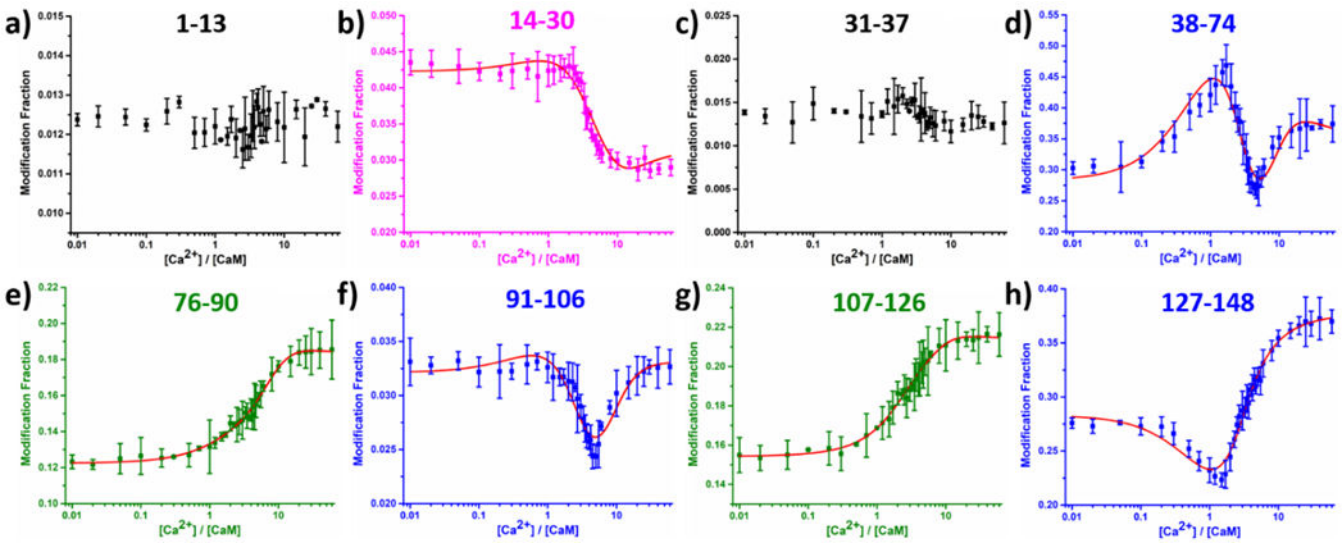

Figure 29.

LITPOMS response of Ca^{2+} - CaM titration at peptide level, where modification fractions were plotted as a function of calcium:calmodulin concentration ratio. Four different classes of behaviors are shown in black (a and c), magenta (b), blue (d, f and h) and olive (e and g). Red solid lines in (b), (d), (e), (f), (g) and (h) are from fitting by a model used in PLIMSTEX. Reprinted with permission from ref [1147]. Copyright 2019 American Chemical Society.

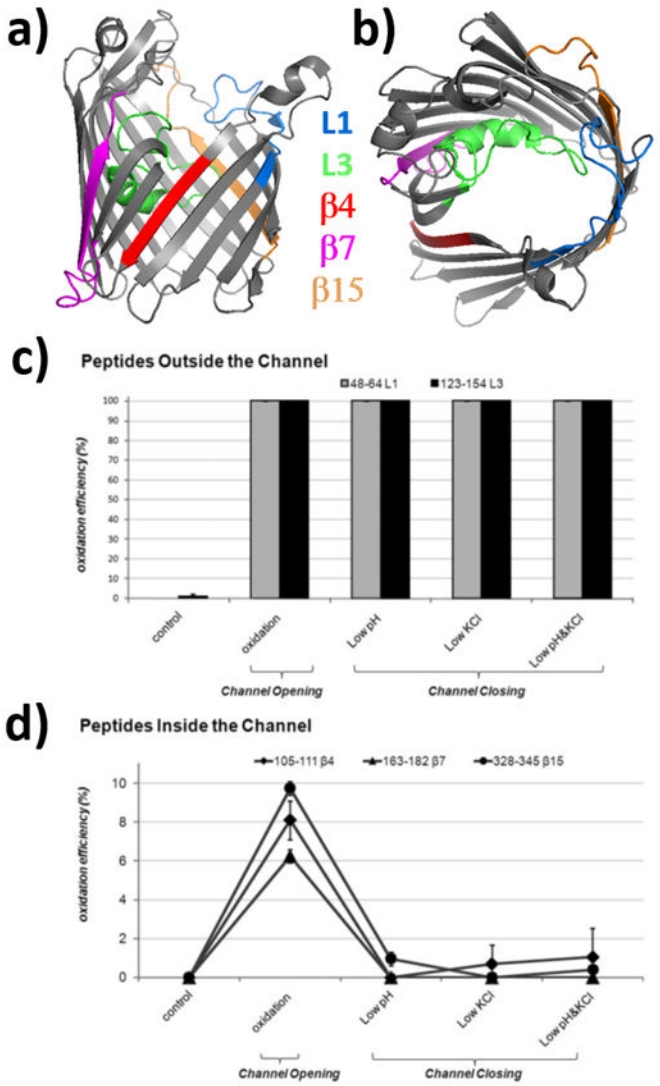

Figure 30.

In vivo labeling of OmpF porin by hydroxyl radicals. 3D structure of OmpF (PDB ID 1OPF) from (a) side view and (b) top view. Structural components of loop 1, 3 and β-sheet 4, 7, 15 are highlighted in blue, green, red, purple and orange, respectively. Oxidation efficiency for (c) loops and (d) β-sheets under different experimental conditions are plotted. Error bars are standard deviations from duplicates. (c) and (d) are reprinted with permission from ref [873]. Copyright 2009 American Society for Biochemistry and Molecular Biology.

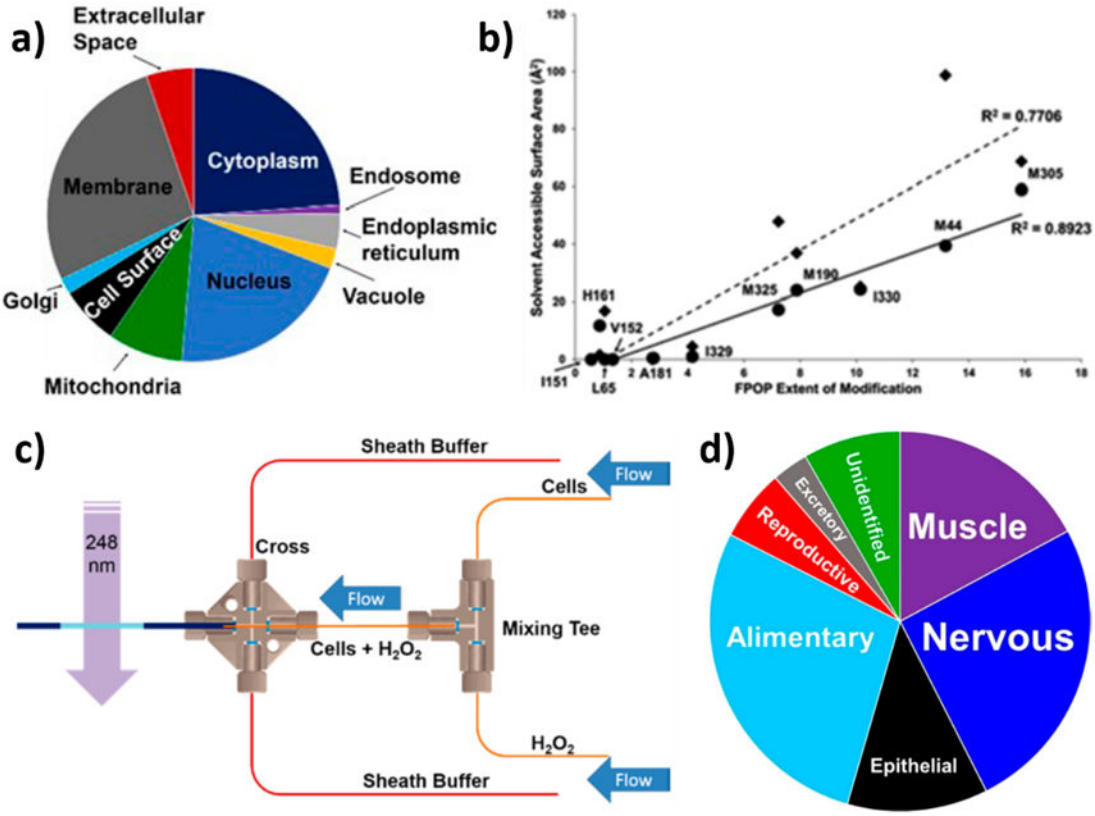

Figure 31.

(a) Pie chart of the subcellular compartment location (African green monkey kidney cell) of oxidized proteins that were identified by LC-MS/MS. Proteins that are present in multiple compartments are represented multiple times. Reprinted with permission from ref [1154]. Copyright 2015 American Chemical Society. (b) Correlation of residue-level FPOP modifications with SASA in the open (circles and solid line) and tight (diamond and dashed line) states of actin. Reprinted with permission from ref[1154]. Copyright 2015 American Chemical Society. (c) Schematic illustration of an improved flow system for *in vivo* FPOP labeling. Blue arrows indicate flow and colored lines represent tubing. Reprinted with permission from ref[1155]. Copyright 2016 American Chemical Society. (d) Pie chart of the oxidatively modified proteins within different body systems of *c. elegans*. Reprinted with permission from ref[1156]. Copyright 2019 American Chemical Society.

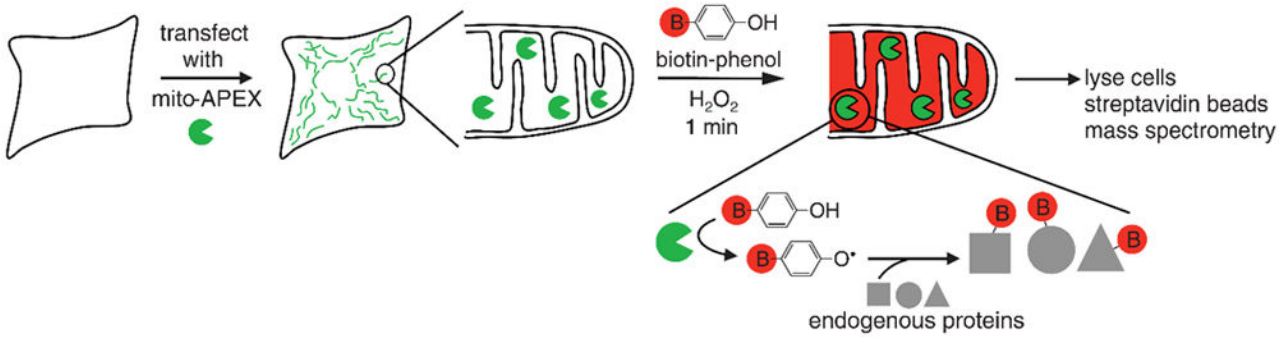

Figure 32.

Schematic illustration of APEX labeling workflow. Reprinted with permission from ref. [1158]. Copyright 2013 American Association for the Advancement of Science.

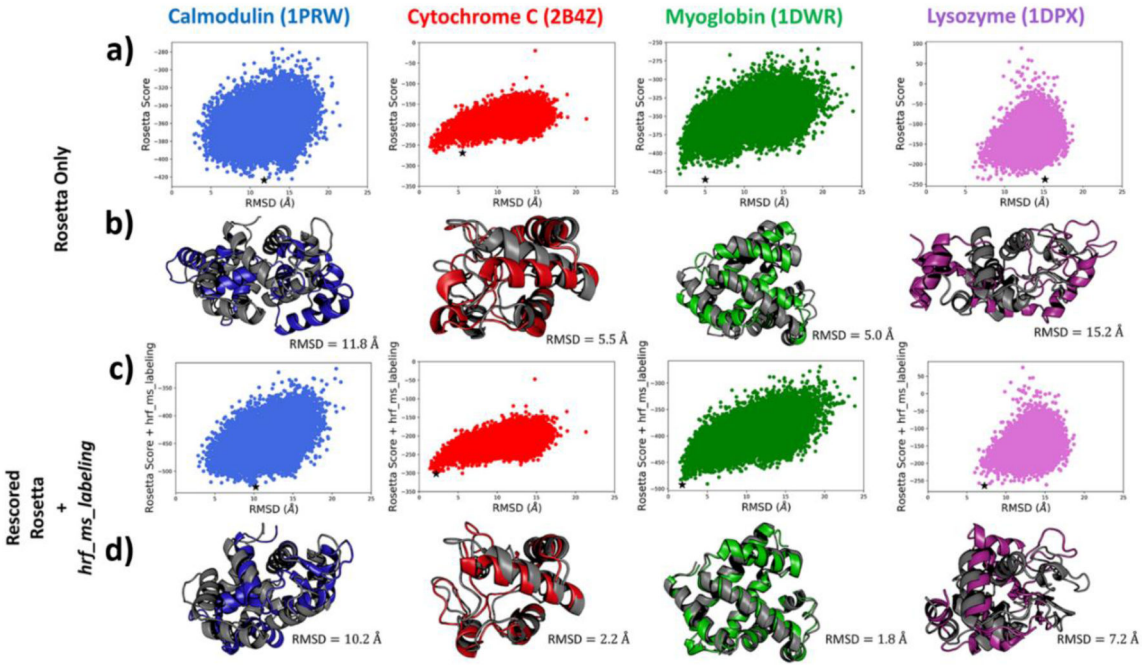

Figure 33.

(a) Rosetta score versus RMSD (with respect to the native structure) plots for 20000 models generated from Rosetta *ab initio* for each of four proteins. Top scoring model is highlighted by a star in each plot. (b) Top scoring models from the Rosetta score versus RMSD distributions in (a) (color) superimposed on the respective native model (gray). PDB ID for these native models are depicted at the top of the figure. (c) Rosetta score + *hrf_ms_labeling* versus RMSD (with respect to the native structure) plots for each of the four proteins after rescoring with the new score term. The top-scoring model is highlighted by a star in each plot. (d) Top scoring models from the Rosetta score + *hrf_ms_labeling* rescoring distributions in (c) (color) superimposed on the respective native model (gray). Reprinted with permission from ref [1175]. Copyright 2018 American Chemical Society.

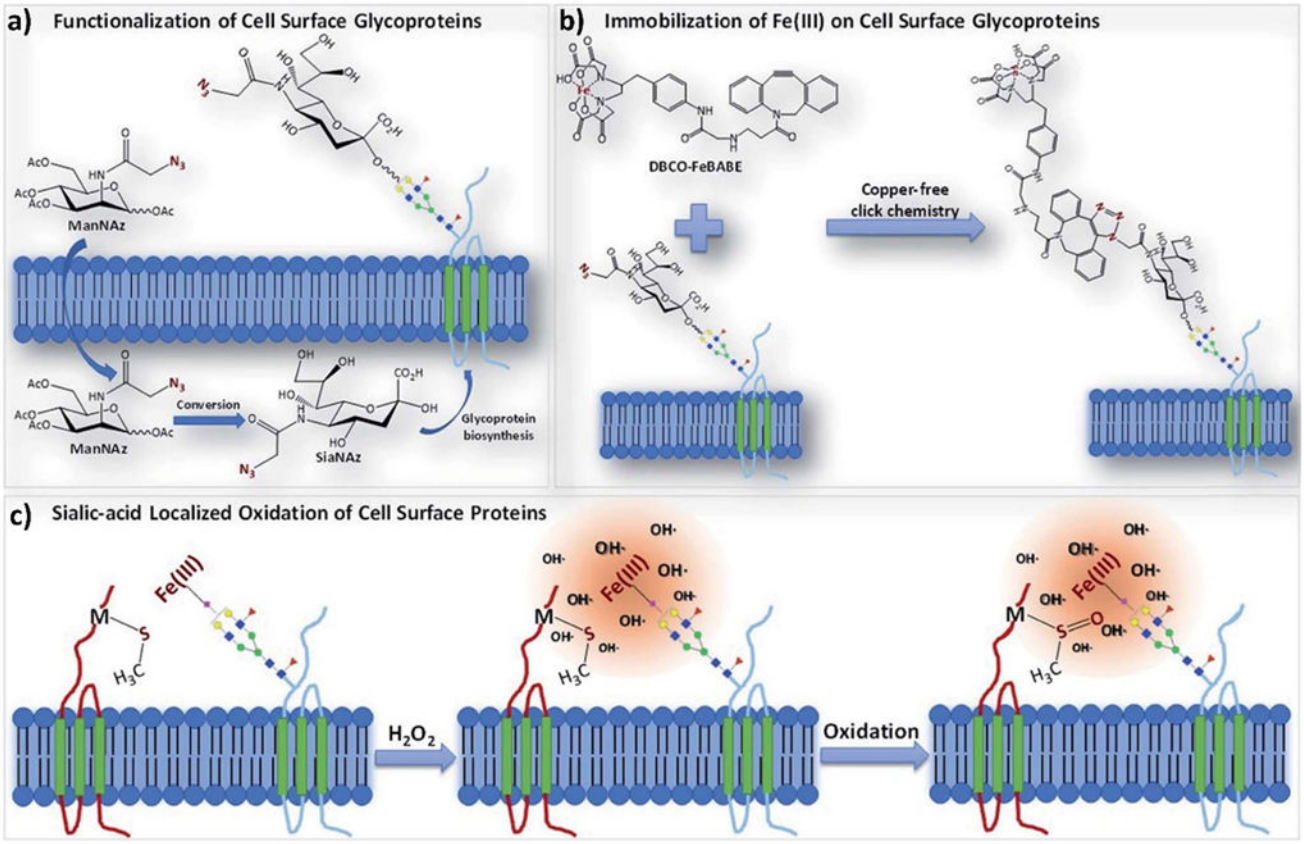

Figure 34.

Schematic illustration of POSE workflow. (a) The incorporation of ManNAz into cell surface glycoproteins as SiaNAz. (b) The bio-orthogonal reaction of the DBCO-FeBABE probe with the SiaNAc group conducted via click-chemistry. (c) The oxidation of proteins in the sialic acid environment by ●OH generated by Fenton Chemistry. Reprinted with permission from ref [872]. Copyright 2019 Royal Society of Chemistry.

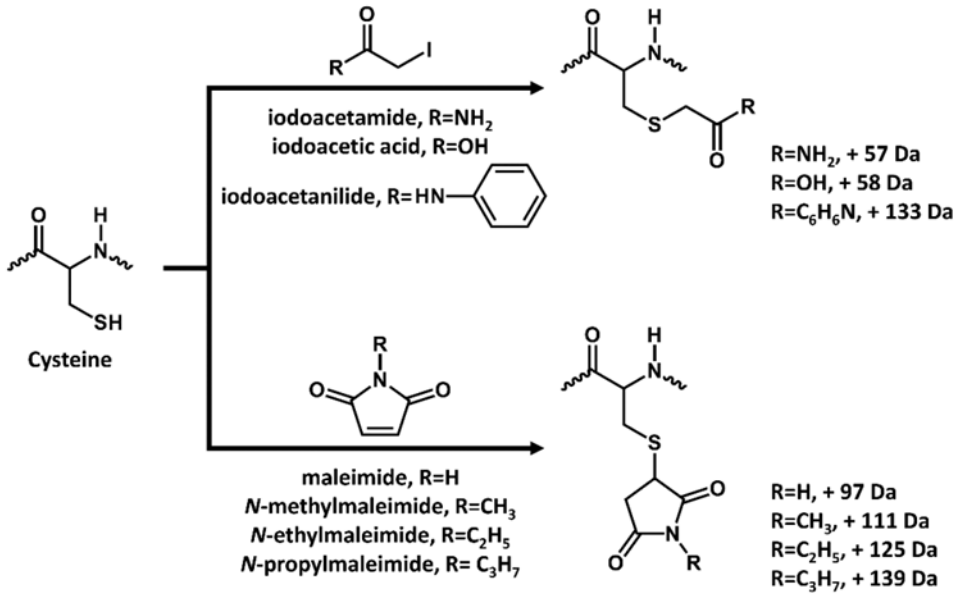

Scheme 1.
Cys labeling pathways with different labeling reagents

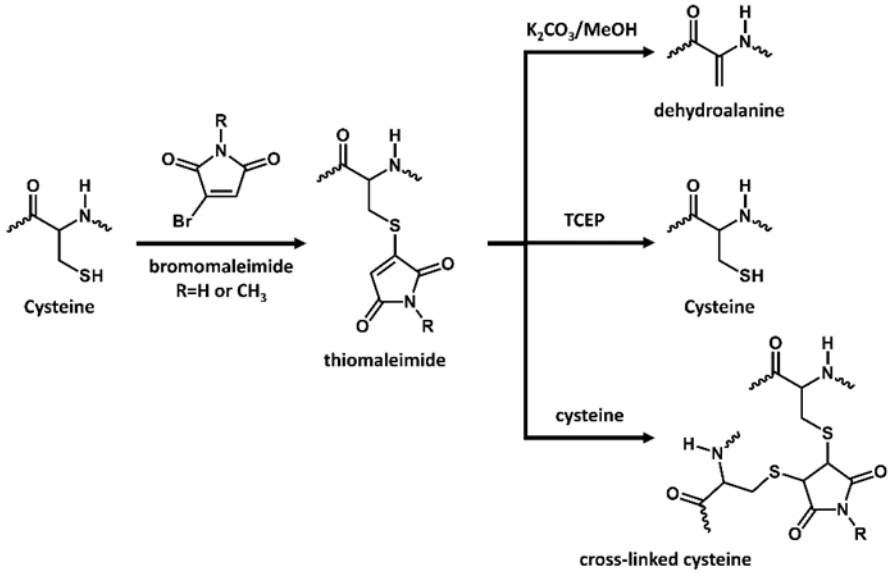

Scheme 2.
Cys labeling pathways with bromomaleimides

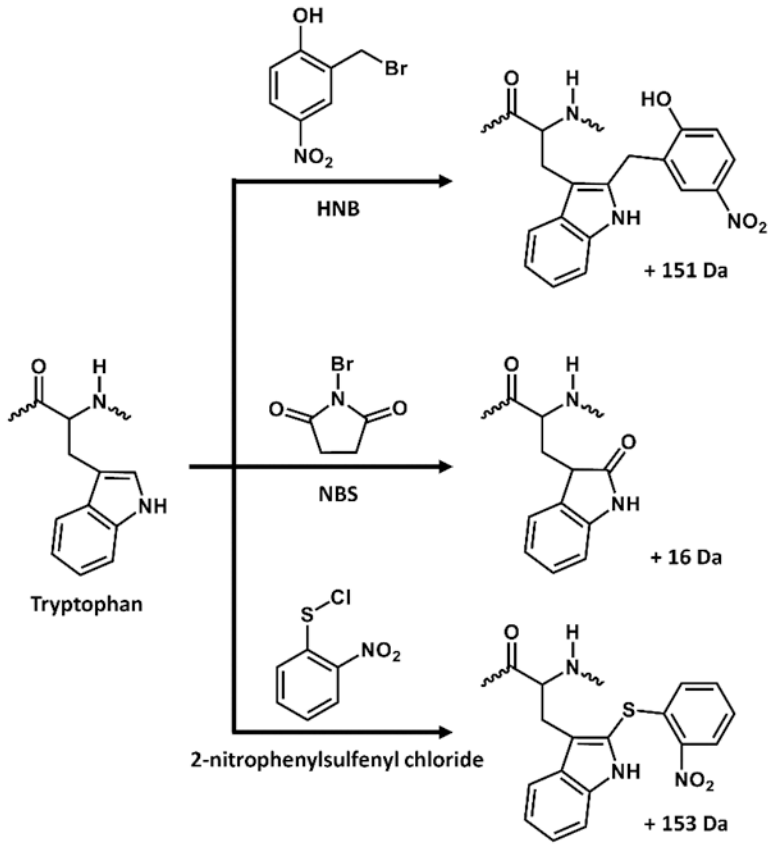

Scheme 3.
Trp labeling pathways with various reagents

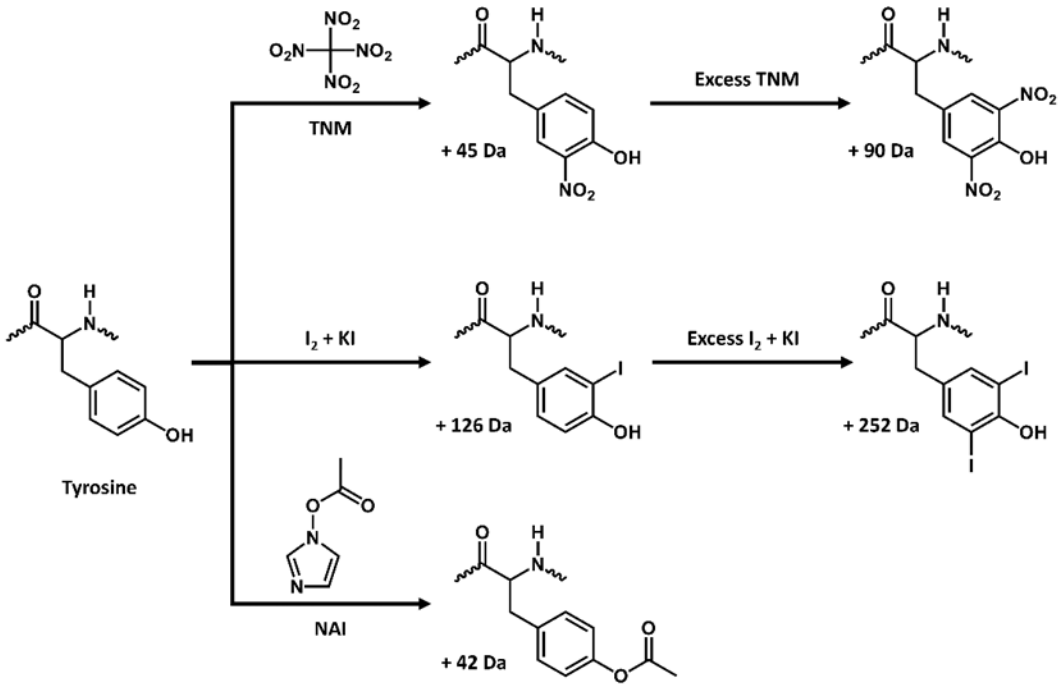

Scheme 4.
Tyr labeling pathways with several reagents

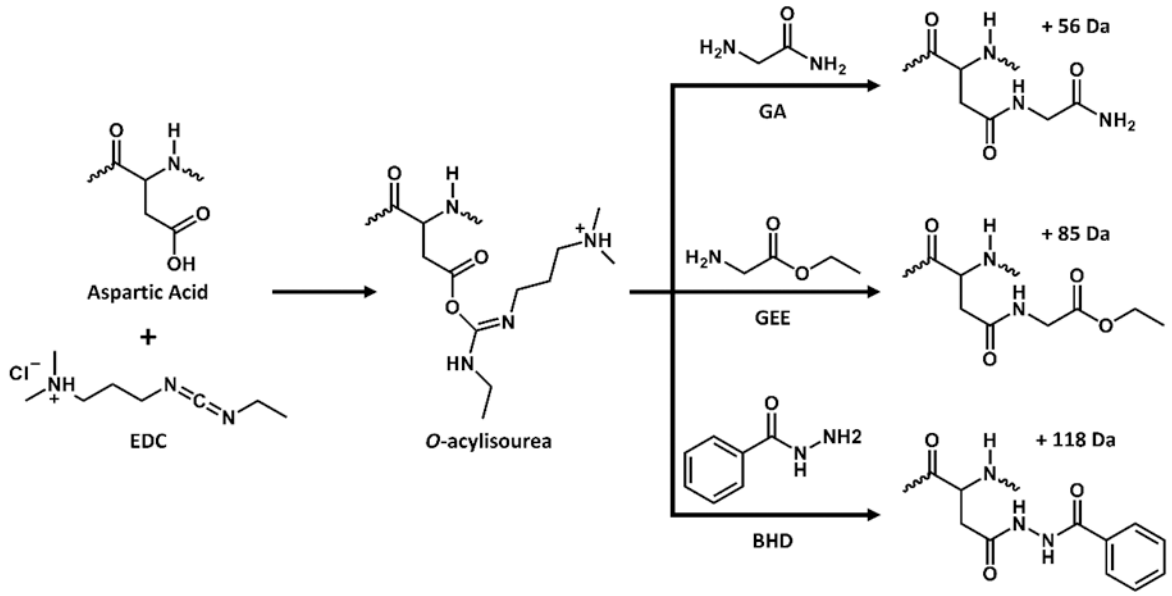

Scheme 5.

Asp and Glu labeling pathways with EDC-activated labeling reagents as demonstrated by Asp

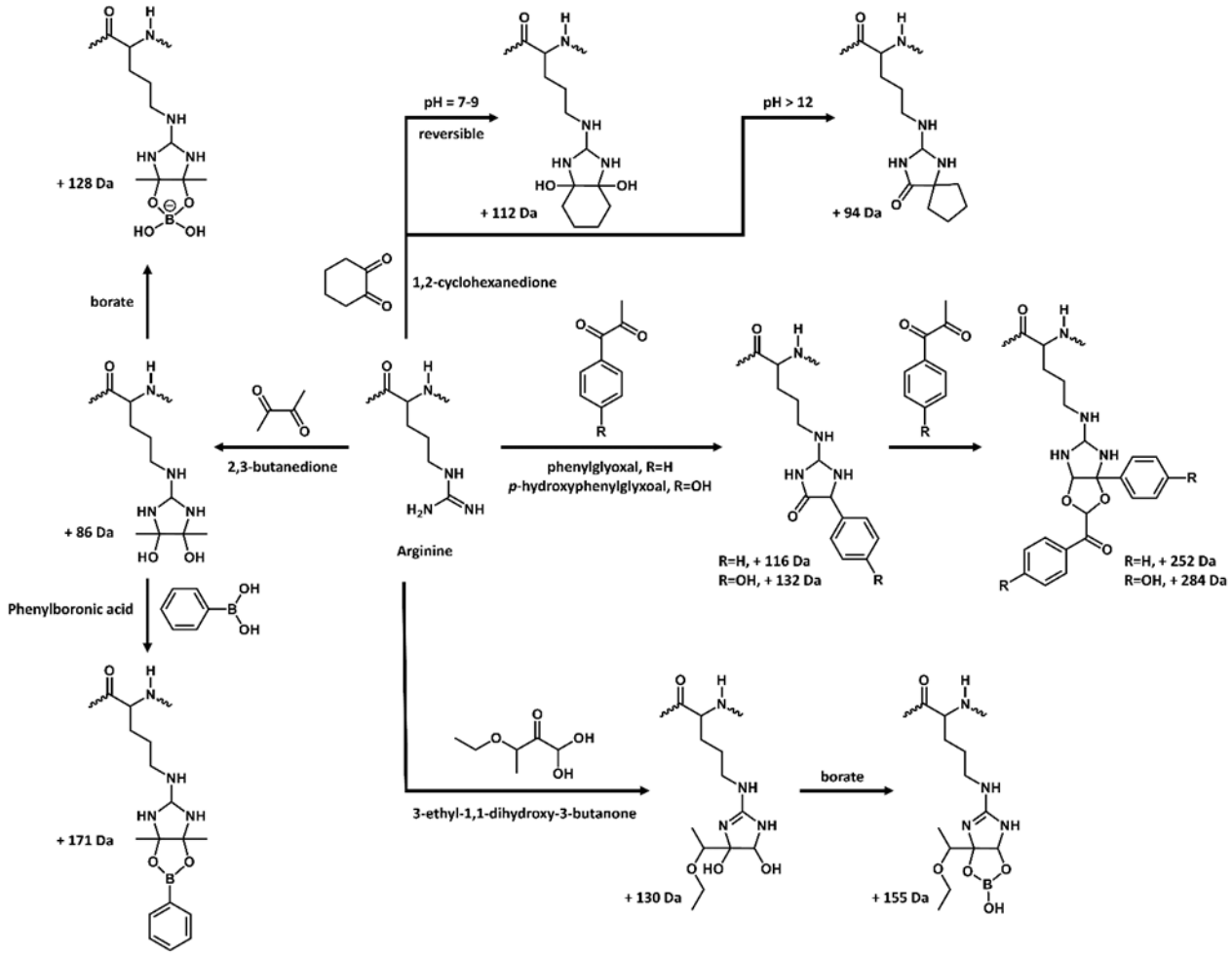

Scheme 6.
Arg labeling pathways with several reagents

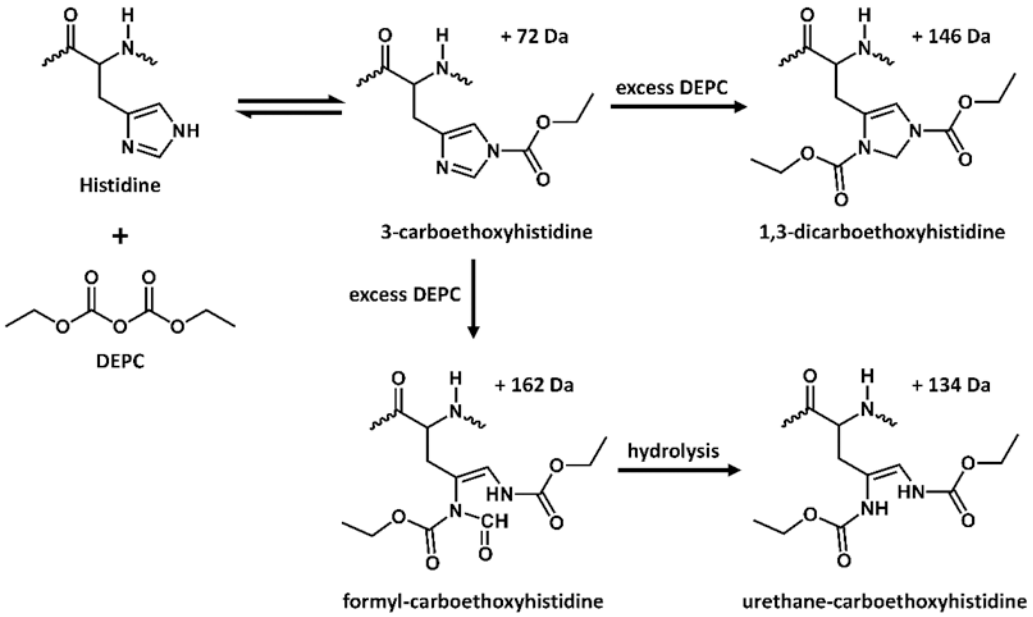

Scheme 7.
His labeling pathways with DEPC

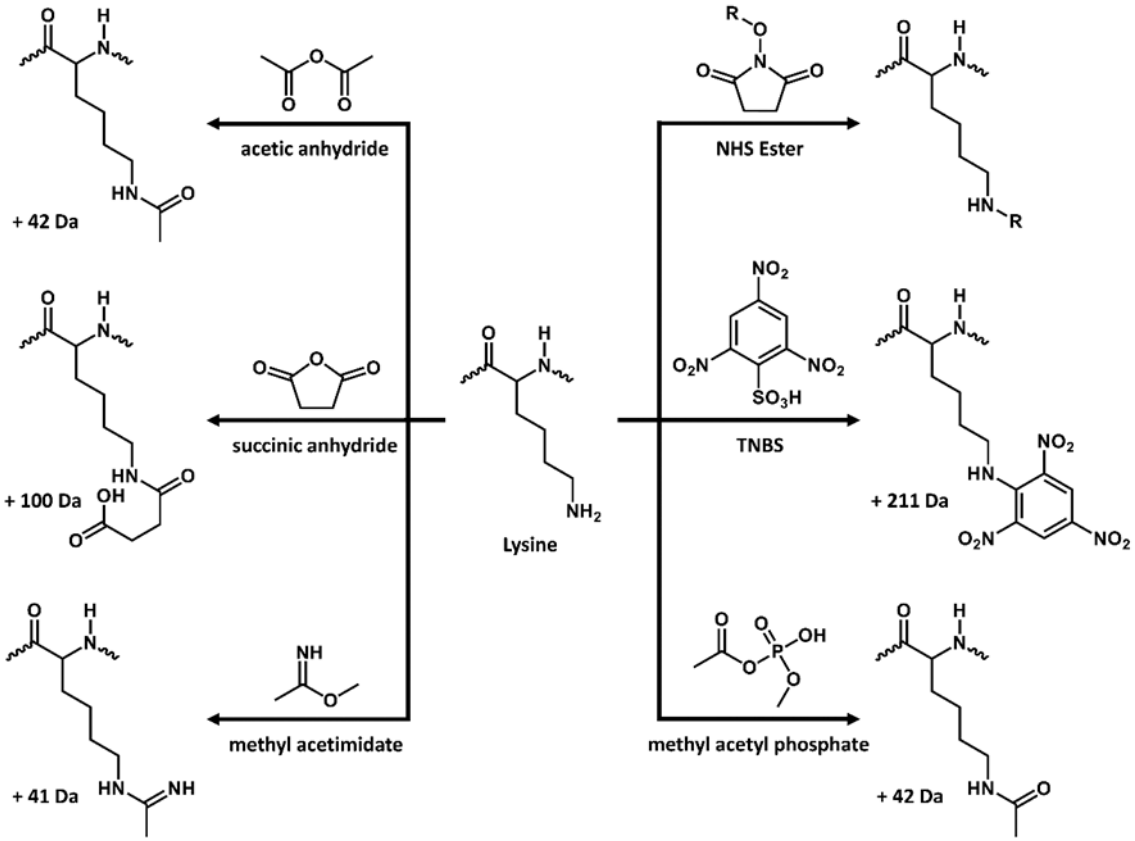

Scheme 8.
Lys labeling pathways with several reagents

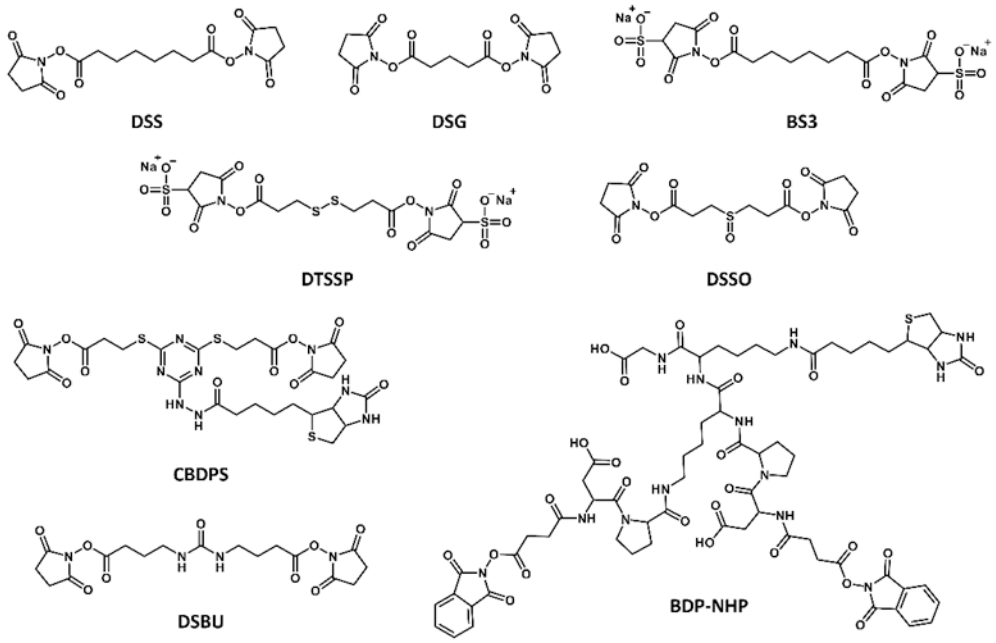

Scheme 9.
Common NHS-ester cross-linkers

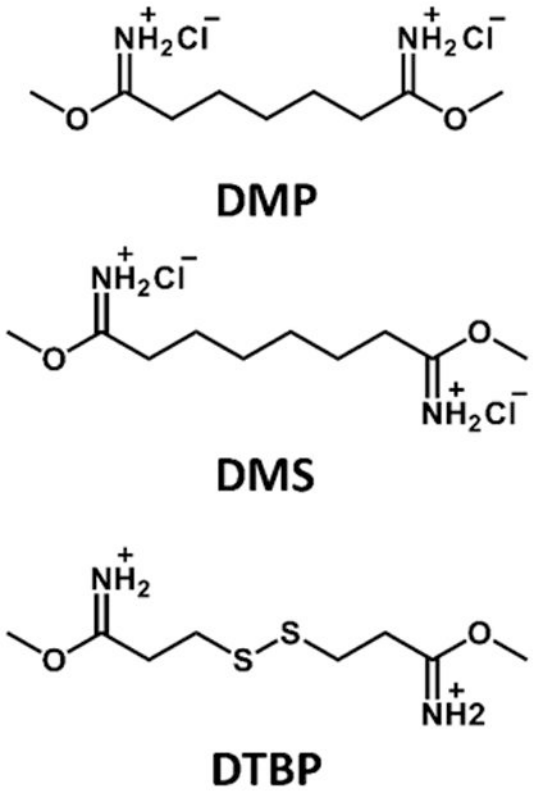

Scheme 10.
Common imidoester cross-linkers

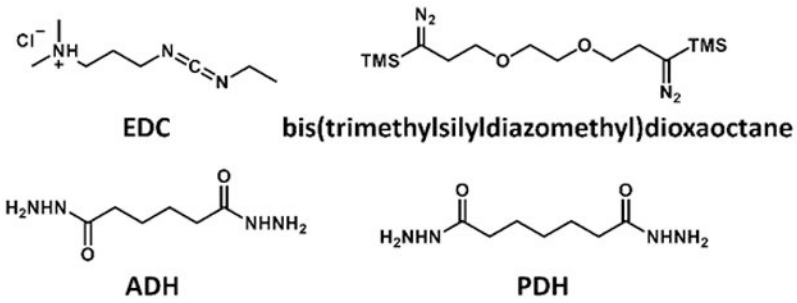

Scheme 11.
Common carbodiimide and dihydrazide cross-linkers

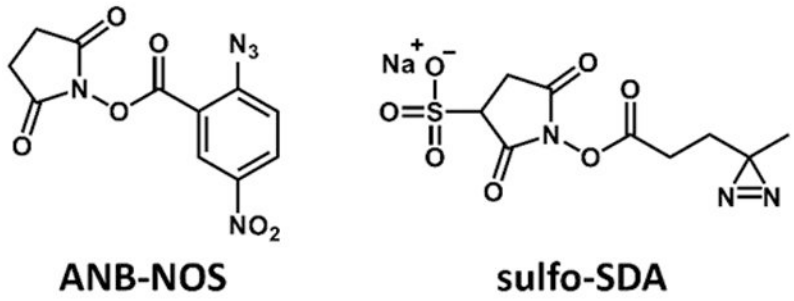

Scheme 12.

Chemical structure of common photoreactive cross-linkers, ANB-NOS and sulfo-SDA

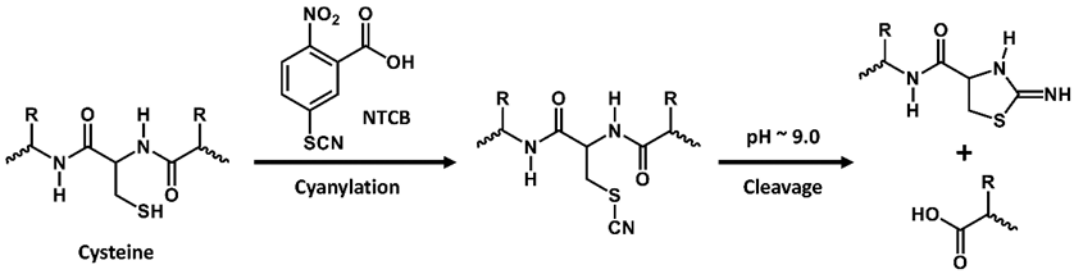

Scheme 13.

Free Cys footprinting by NTCB-mediated cleavage

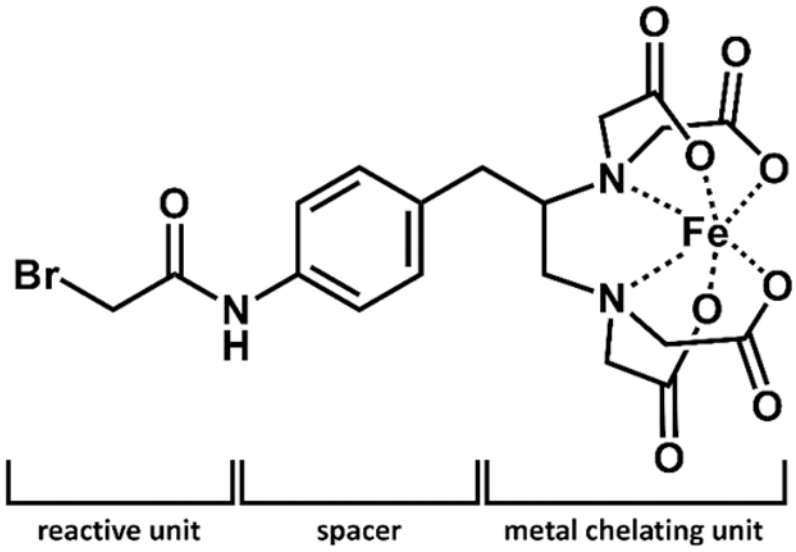

Scheme 14.
Structure of Fe-BABE

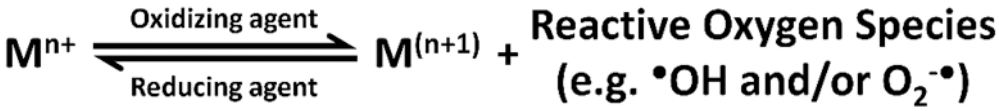

Scheme 15.

General scheme that produces reactive oxygen species during metal-catalyzed oxidation reactions.

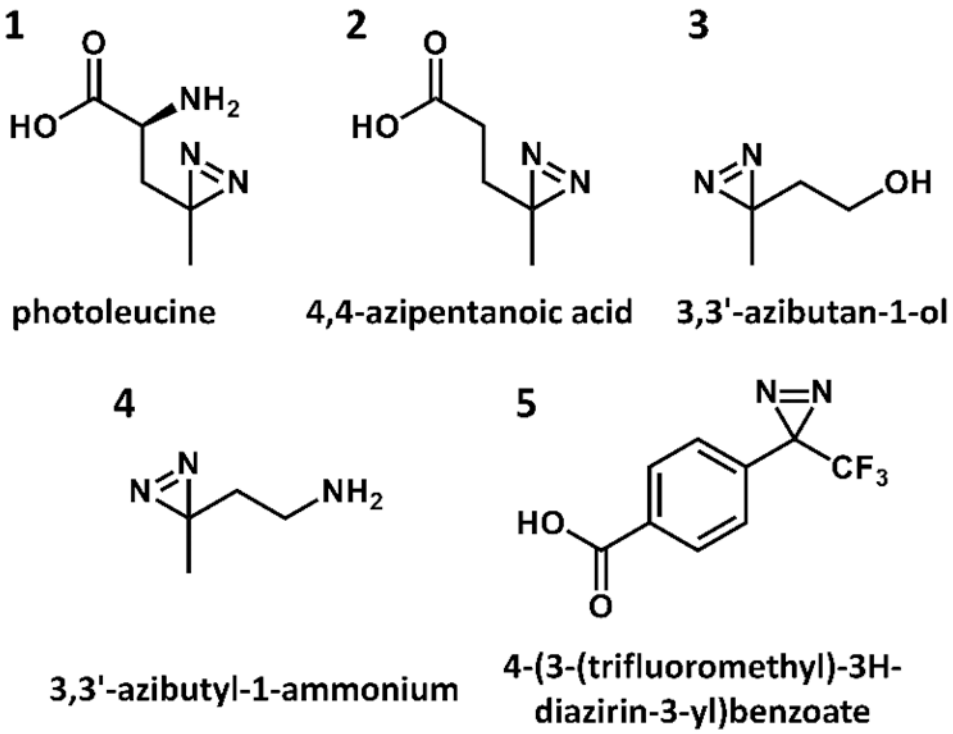

Scheme 16.
Diazirine-based footprinting reagents

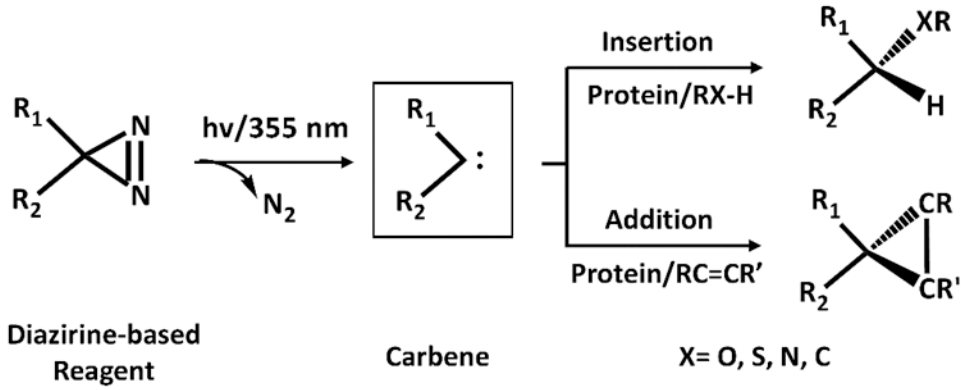

Scheme 17.
Proposed carbene reaction pathway

Table 1.

Rate constants for reactions between amino acids and ●OH[170, 846]

Substrate	Rate Constant ($M^{-1}s^{-1}$)	pH	Substrate	Rate Constant ($M^{-1}s^{-1}$)	pH
Cys	3.5×10^{10}	7.0	Pro	6.5×10^{8}	6.8
Trp	1.3×10^{10}	6.5 – 8.5	Gln	5.4×10^{8}	6.0
Tyr	1.3×10^{10}	7.0	Thr	5.1×10^{8}	6.6
Met	8.5×10^{9}	6 – 7	Lys	3.5×10^{8}	6.6
Phe	6.9×10^{9}	7 – 8	Ser	3.2×10^{8}	~6
His	4.8×10^{9}	7.5	Glu	2.3×10^{8}	6.5
Arg	3.5×10^{9}	6.5 – 7.5	Ala	7.7×10^{7}	5.8
cystine	2.1×10^{9}	6.5	Asp	7.5×10^{7}	6.9
Ile	1.8×10^{9}	6.6	Asn	4.9×10^{7}	6.6
Leu	1.7×10^{9}	~6	Gly	1.7×10^{7}	5.9
Val	8.5×10^{8}	6.9			

Table 2.

Primary oxidation produces (upon ●OH footprinting) and the corresponding mass changes (in reactivity order) for various amino acid residue sidechains.[912]

Sidechain	Modification and Mass Changes
Cys	sulfonic acid (+48), sulfinic acid (+32), hydroxy (−16)
Met	sulfoxide (+16), sulfone (+32), aldehyde (−32)
Trp	hydroxy- (+16, +32, +48, etc.), pyrrol ring-open (+32)
Tyr	hydroxy- (+16, +32, etc.)
Phe	hydroxy- (+16, +32, etc.)
cystine	sulfonic acid (+48+H), sulfinic acid (+32+H)
His	oxo-(+16), ring-open (−22, −10, +5)
Leu	hydroxy- (+16), carbonyl (+14)
Ile	hydroxy- (+16), carbonyl (+14)
Arg	deguanidination (−43), hydroxy- (+16), carbonyl (+14)
Lys	hydroxy- (+16), carbonyl (+14)
Val	hydroxy- (+16), carbonyl (+14)
Ser	hydroxy- (+16), carbonyl (−2, or +16-H2O)
Thr	hydroxy- (+16), carbonyl (−2, or +16-H2O)
Pro	hydroxy- (+16), carbonyl (+14)
Gln	hydroxy- (+16), carbonyl (+14)
Glu	decarboxylation (−30), hydroxy- (+16), carbonyl (+14)
Asp	decarboxylation (−30), hydroxy- (+16)
Asn	hydroxy- (+16)
Ala	hydroxy- (+16)
Gly	N/A

[a] For aliphatic side chains, +14 Da products are normally much less than +16 Da products.

[b] For Ser and Thr, only trivial amount of +16 and −2 Da products were found.